DEVELOPMENT OF DENDRITIC AND POLYMERIC SCAFFOLDS FOR BIOLOGICAL AND CATALYSIS APPLICATIONS

A Dissertation

Presented To

The Academic Faculty

By

Poorva Goyal

In Partial Fulfillment

Of the Requirements for the Degree

Doctor of Philosophy in Chemistry

Georgia Institute of Technology

May 2008

DEVELOPMENT OF DENDRITIC AND POLYMERIC SCAFFOLDS FOR BIOLOGICAL AND CATALYSIS APPLICATIONS

Approved by,

Dr. Marcus Weck, Advisor
Chemistry and Biochemistry
Georgia Institute of Technology

Dr. Robert Dickson
Chemistry and Biochemistry
Georgia Institute of Technology

Dr. Chris Jones
Chemical and Biomolecular Engineering
Georgia Institute of Technology

Dr. Christoph Fahrni
Chemistry and Biochemistry
Georgia Institute of Technology

Dr. Uwe Bunz
Chemistry and Biochemistry
Georgia Institute of Technolgy

Dr. Niren Murthy
Biomedical Engineering
Georgia Institute of Technology

Date Approved: June 2nd 2008

To

‘Om’

ACKNOWLEDGEMENTS

I would like to thank my advisor Prof. Marcus Weck for the invaluable learning experience I have received under his supervision. I am indebted for his constant support and guidance to me throughout the period of my graduate studies. His sharp judgement and understanding has been pivotal in shaping this thesis work. His keen scientific observation, his immense passion for science and his balanced outlook towards life has been very inspiring to me.

I would also like to thank my PhD committee members Prof. Robert Dickson, Prof. Christoph Fahrni, Prof. Uwe Bunz, Prof. Niren Murthy and Prof. Chris Jones for their invaluable insights and their encouragement. I would especially like to thank Prof. Dickson for the benefits I gained through his expert guidance on the NIH collaboration and Prof. Jones for his keen interest and advice during our weekly joint group meetings.

I extend my gratitude to my research collaborators Dr. Kunsang Yoon, Dr. Dulal Senapati and Dr. Xiaolai Zheng. Interaction and working with them has been a great learning experience. I am thankful to Dr. Catia Ornelas for all her help and I am happy that she is carrying on my project. I am also thankful to other past and present Weck group members besides above, especially Warren, Michael, Joel, Amy, Joe, William, Kamlesh, Nandita, Alpay, Caroline, Ashootosh, Trey, Clint and Alex for their camaraderie and help. I greatly enjoyed the coffee sessions with Kamlesh, Nandita and Prerona where we often vented our frustrations with synthetic science and were quite therapeutic. I also thank my other friends for the lighter moments we shared.

Finally, I would like to thank my family who made this journey and others possible for me. I cannot express in words my gratitude and love for my mother Lakshmi Tayal, my father Raj Kumar Tayal and my brother Rahul Tayal. They have unconditionally loved and supported me, strived for me and are the backbone of my strength and aspirations. Lastly, I want to thank my dear husband, Mayur Goyal, for showing belief in me when my own faltered. I thank him for his unflagging support especially when I felt overwhelmed in my research. I am grateful for his daily love and his wonderful companionship.

TABLE OF CONTENTS

LIST OF TABLES

LIST OF FIGURES

LIST OF SCHEMES

LIST OF ABBREVIATIONS

AFM	Atomic force microscopy
CPP	Cell penetrating peptide
CD	Circular dichroism
DTPA	Diethylenetriaminepentaacetic acid
DAB	Diaminobutane
DMSO	Dimethyl sulphoxide
DMF	Dimethyl formamide
DCC	Dicyclohexyl carbodiimide
DIEA	N,N-diisopropyl ethylamine
DMAP	Dimethylaminopyridine
DNA	Deoxyribonucleic acid
DSC	Dynamic light scattering
EDCI	1-ethyl-3-(3'-dimethylaminopropyl) carbodiimide
ESI	Electrospray ionization
FITC	Fluorescein isothiocyanate
FA	Folic acid
G-1	Generation one
G-2	Generation two
G-3	Generation three
GC	Gas chromatography

GPC	Gel permeation chromatography
HKR	Hydrolytic kinetic resolution
HATU	2-(1H-7-azabenzotriazol-1-yl)-1,1,3,3-tetramethyl uronium Hexafluorophosphate
HOBT	1-hydroxy benzotriazole
HPLC	High performance liquid chromatography
MS	Mass spectrometry
MRI	Magnetic resonance imaging
MTX	Methotrexate
PAMAM	Poly(amido amine)
PDI	Poly dispersity index
PPI	Poly(propylene imine)
PEI	Poly(ethylene imine)
PEG	Poly(ethylene glycol)
ROMP	Ring opening metathesis polymerization
RNA	Ribonucleic acid
SFM	Scanning force microscopy
TMS	Trimethyl silyl
THF	Tetrahydrofuran
WAXS	Wide angle X-ray scattering
XRD	X-ray diffraction

SUMMARY

This thesis begins with the introduction of dendrimers and dendritic molecules in the context of polymer science and reviews novel synthetic strategies of dendritic architectures. An explanation of why dendrimers are aptly suited for and how they are increasingly contributing to biological applications is detailed. Despite these accomplishments, there are few reports of post-synthesis tunable architectures as well as functional dendrimer architectures. This thesis hypothesizes that the introduction of facile functional handles on the periphery and cores of dendrimers can lead to novel highly functional dendrimers useful for modular surface modifications of dendrimers with biological units of choice for tunable delivery devices and for high-end imaging applications respectively.

The first functional handles introduced were on the periphery of poly(amide)-based dendrimers. The dendrimers were built by convergent strategies and were equipped with one and/or two selective, robust, and orthogonal functional handles for modular attachment to and transformation of dendrimer surface. By using azides, alkynes and aldehydes as robust functional handles and investigating their orthogonality and activity by high yielding couplings with small organic and biologically significant molecules – a strategy and methodology for development of tunable dendrimer surfaces for numerous future applications was facilitated.

Our second functional handles were introduced in the core of poly(amidoamine) based dendrimers. Raman labels such as triple bonds and carbon-deuterium bonds with

vibrational frequencies in the background free Raman vibrational zone of 1900-2300 cm^{-1} were introduced in the core of dendrimers for scaffold specific labeling. By encapsulationg Ag nanodots within these dendrimers, strong fluorescence and scaffold specific Raman labeling could be achieved. This strategy lays the foundation for the creation of ultrabright, scaffold specific information containing biological labels for studying cell dynamics at single molecule level. Additionally, a dendritic scaffold for studying the molecular weight dependence on cellular uptake is designed and initiated based on above synthetic strategies.

Finally, the use of dendritic frameworks in heterogeneous solid supported catalysis for enhanced cooperativity in reactions involving bimetallic transition states is explored and applied. Prior to this thesis work, heterogeneous resin supported catalysts for HKR reactions suffered from high catalyst loadings and low enantioselectivities induced by the solid support. With the use of flexible linker and dendron framework supporting the catalysts, both of these problems were addressed. This method opens up new routes for creation of highly active heterogeneous solid catalysts involving a bimetallic intermediate.

In the end, the current status of dendritic frameworks is reviewed and methodological extensions to this work are suggested. Conceptions of how our functional dendritic architectures would be useful for future biological and catalytic applications are explored and detailed.

CHAPTER 1

Dendrimers and Dendritic Molecules in Polymer Science

1.1 Abstract

In this chapter, dendrimers, hyperbranched and and dendronized polymers are defined and placed in context of polymer science. The design principles, synthetic strategies and historical evolution of the field of dendritic molecules are reviewed. Emphasis is placed on synthetic strategies and applications of dendrimers and dendronized polymers. A review of these two molecule classes and the goals of this thesis in advancing these two areas is stated.

1.2 Introduction to Dendritic Architectures

Dendritic architecture, which is a perfectly branched macromolecular architecture is one of the most pervasive topologies observed in nature at the macro and micro-dimensional length scales. At the nanoscale or molecular level, the most notable are glycogen and amylopectin, macromolecular hyperbranched structures that nature uses for energy storage. In the polymer field, dendritic topology has now been recognized as a fourth major class of macromolecular architecture[1-3] after Staudinger's 'macromolecular hypothesis' in 1926 that allowed the establishment of the three major polymer architectures with vastly different properties as linear, crosslinked and branched.[4-5] The signature for such a distinction is the unique repertoire of new properties manifested by this class of polymers.[6-10] Presently, this architectural class consists of three dendritic subclasses: (I) dendrons and dendrimers, (II) dendrigraft or dendronized polymers, and (III) randomly hyperbranched polymers and star polymers. The order of this subset,

reflects the relative degree of structural control present in each of these dendritic architectures with dendrimers having the highest level of monodispersity and critical control on nanoscale parameters, such as size, shape, interior and surface functionality. On a comparison with natural systems, evolution has provided well-defined biological building blocks such as proteins, DNA, viruses. Dendritic topology provides a similar platform for systematic constructions in the synthetic nanoscale science world to build molecules of higher complexity and function in an effort to emulate properties of natural molecules and systems. In this chapter and in the following sections, dendritic molecules – primarily dendrimers and dendronized polymers would be defined with emphasis on their early discovery, synthesis and present applications.

1.3 Dendrimers

Dendrimers are the most size-controlled macromolecules in the realm of dendritic architectures as well in the macromolecular architectures along with proteins. Dendrimers are polymers with geometrically restricted structures, and for this reason they are one of the most versatile, compositionally and structurally controlled synthetic nano-scale building blocks available.[1-4] These polymers possess a well-defined and highly branched structure with a high degree of control over their size and shape in three dimensions. Additionally, they have very low polydispersities and allow for a wide variety of functionalization on their multiple functional groups on the exterior as well as interior.[1-4] Dendrimers are produced in an iterative sequence of reaction steps, in which each additional iteration leads to a higher generation material.

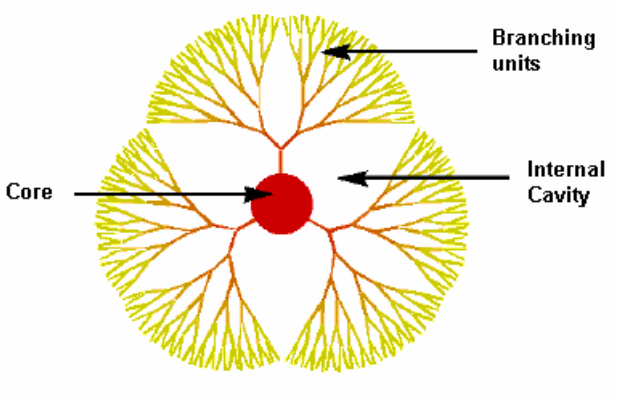

Figure 1.1 Schematic representation of a dendrimer (Taken from http://www.ninger.com/dendrimer/)

1.3.1 History of Dendrimers

In the early 1950's, Flory was among the first to examine the potential role of branched units in macromolecular architectures,[5,11] but it was not until the mid-1980s that methods for the orderly preparation of these polymers had been sufficiently developed to enable their practical study. The first example of an iterative synthetic procedure toward well-defined branched structures was reported by Vögtle,[12] who developed an iterative 'cascade' method for the synthesis of low molecular weight branched amines. A few years later, in the early 1980s, Denkewalter[13-15] patented the synthesis of L-lysine-based dendrimers. The patents describe structures up to high generations; however, except for size exclusion chromatography data,[16] no detailed characteristics of the materials are given. The first dendritic structures that have been thoroughly investigated and that have received wide-spread attention are Tomalia's PAMAM dendrimers[17-18] and Newkome's 'arborol' systems.[19] Using chemistry and conditions less prone to cyclization side-reactions and therefore more suitable for repetitive growth, Tomalia *et al.* disclosed the synthesis and characterization of the first family of dendrimers in 1984-1985 by a divergent strategy.[17-18] Optimization of this

procedure enabled the synthesis of globular poly(amidoamine) (PAMAM) dendrimers on a commercial scale with molecular weights well above 25,000.

Shortly thereafter, in 1985, Newkome reported preliminary results toward a family of trisbranched polyamide 'arborol' dendrimers[19] synthesized divergently, and in 1993, improvements on Vögtle's original synthesis were disclosed by Meijer and Mülhaupt that enabled the production of poly(propylene imine) (PPI) dendrimers.[20,21] In 1989-1998, Hawker and Fréchet introduced the convergent growth approach to dendrimers,[22] the second general route to dendritic structures. Finally, Moore's convergently produced phenylacetylenes dendrimers[23-26] are the last of the major classes of dendrimers described above, reported up to high generations, that are the most studied and known dendrimer classes in the literature. Additionally, many other types of interesting and valuable dendritic systems have been developed[27] and thus, a variety of dendritic scaffolds have become accessible with defined nanoscopic dimensions and discrete numbers of functional end groups.

1.3.2 Structure of Dendrimers

Dendrimers are highly ordered, regularly branched, globular macromolecules prepared by a stepwise iterative approach. Their structure is divided into three distinct architectural regions: (i) a core or focal moiety, (ii) layers of branched repeat units emanating from this core defined as successive generation, and (iii) end groups on the outer layer or periphery (Figure 1.1). Dendrimers are differentiated from other hyperbranched polymers by their structural perfection, leading to an exact number of concentric layers of branching points, often referred to as generations.

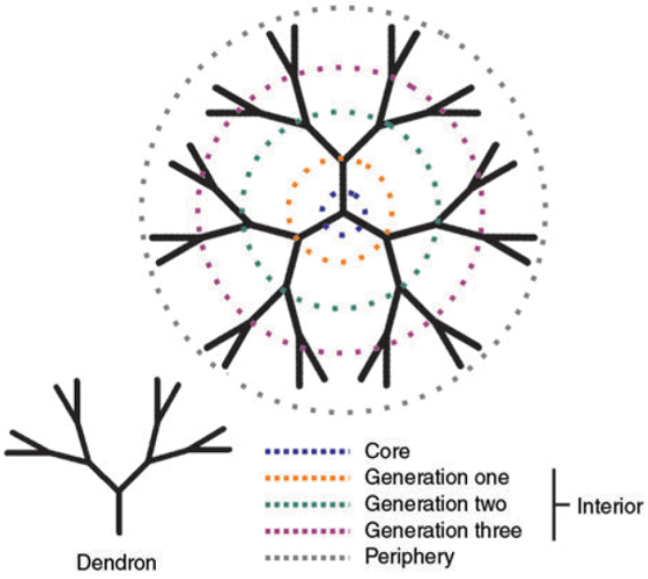

Figure 1.2 Structure of a dendrimer includes core, branched interior layers known as 'generation' and periphery[1] (Adapted image)

Four characteristic features of dendrimers are in sharp contrast to those of traditional linear polymers:

(i) A dendrimer can be isolated as an essentially monodisperse single compound, unlike most linear polymers whose synthesis affords a range of molecular species differing in molecular weight.

(ii) As their molecular weight increases, the properties of dendrimers (e.g., solubility, chemical reactivity, glass transition temperature) are dominated by the nature of the end groups. Unlike linear polymers that contain only two end groups, the number of dendrimer end groups increases exponentially with generation (depending upon the number of arms per branch points) and thereby frequently becoming the primary interface between the dendrimer and its environment.

(iii) In contrast to linear polymer growth that theoretically can continue *ad infinitum*, dendritic growth is mathematically limited. During the growth of a dendrimer,

the number of monomer units increases exponentially with generation, while the volume available to the dendrimer only grows proportionally to the cube of its radius. Hence, dendritic construction is limited by volume rather than by surface. As a result of this physical limitation, dendritic molecules develop a more globular conformation as the generation increases and the dendritic termini turn toward the center to occupy the internal volume (Figure 1.3). At a certain generation a steric limit to regular growth, known as de Gennes dense packing,[28] is reached. Growth may be continued beyond de Gennes dense packing but this leads to irregular dendrimers incorporating structural flaws.

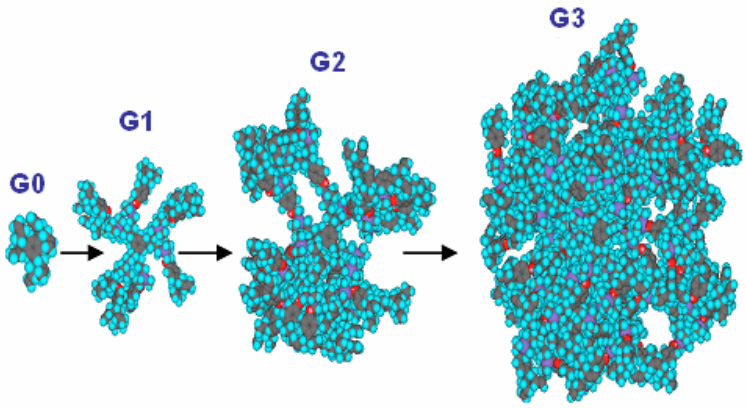

Figure 1.3 Increasing globular conformation with increase in generation of dendrimers

(iv) Rheological behavior and viscosity is another characteristic property of dendrimers which in contrast to linear polymers, exhibits, a decrease in dependence of viscosity with increase in dendrimer generation after a maxima is reached. Hence, Mark-Houwink-type increase in viscosity with molecular mass which is characteristic of traditional polymers shows a maximum in the dependence of viscosity [η] on generation. This unusual property in higher generation dendrimer macromolecules makes them highly desirable

components for preparation of nano-structures and nanodevices, flow modifiers, lubricants, reinforcing agents, blend compatibilizers as well as high viscosity standards.

Thus, dendrimers have a unique combination of properties, with high molecular weights of classic macromolecules, molecular shapes similar to idealized spherical particles, high number of surface functionalities and unique rheological properties. Notably, such combination of molecular and macromolecular properties makes them highly useful entities for a variety of materials applications.

1.3.3 Synthetic Strategies of Dendrimers

Two complementary strategies, divergent and convergent, have been used for the synthesis of dendrimers,[29,30] as shown in Figure 1.4.

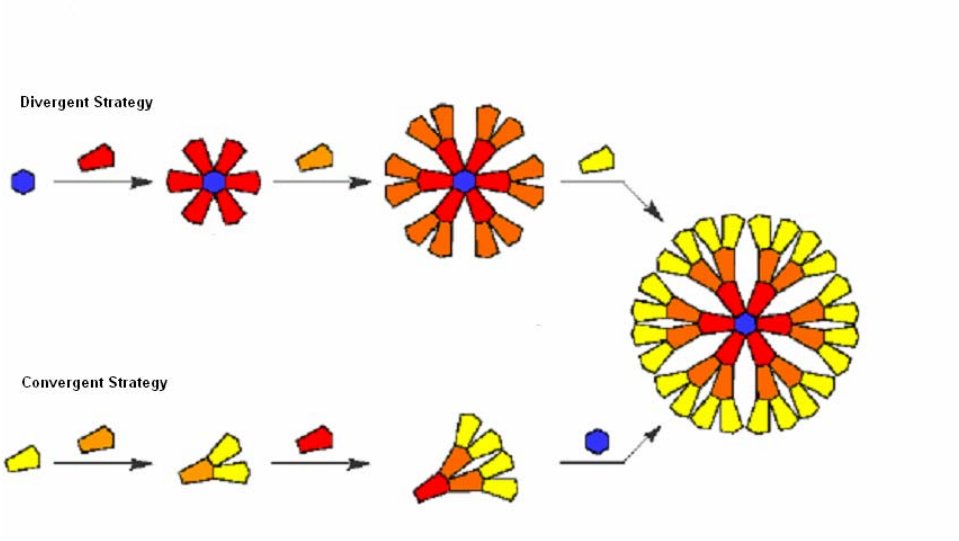

Figure 1.4 Synthetic strategies for dendrimer formation: divergent and convergent (taken from http://www.ninger.com/dendrimer/)

1.3.3.1 Divergent Approach

The divergent approach, arising from the seminal work of Tomalia[17-18] and Newkome,[19] as well as the branched model work of Vögtle,[12] initiates growth from the

core of the dendrimer and continues outward by repetition of coupling and activation steps as shown in Figure 1.5. Reaction of the peripheral functionalities of the core with the complementary reactive groups of the monomer introduces a new latent branch point at each coupling site, resulting in increase in the number of peripheral functionalities. The peripheral functionalities on each monomer are designed to be inert to focal monomer functionality, thereby preventing uncontrolled hyperbranched polymerization. After driving the first coupling reaction to completion, these latent functionalities can be activated to afford a new layer of peripheral groups capable of coupling to additional monomer. Repetition of the coupling and activation steps leads to an exponential increase in the number of reactions at the periphery; therefore, a large excess of reagents is required to drive both reactions to completions. Because of the difference in molecular weight, it may be possible to separate the macromolecule from the excess reagents by a simple distillation, precipitation or ultra-filtration.

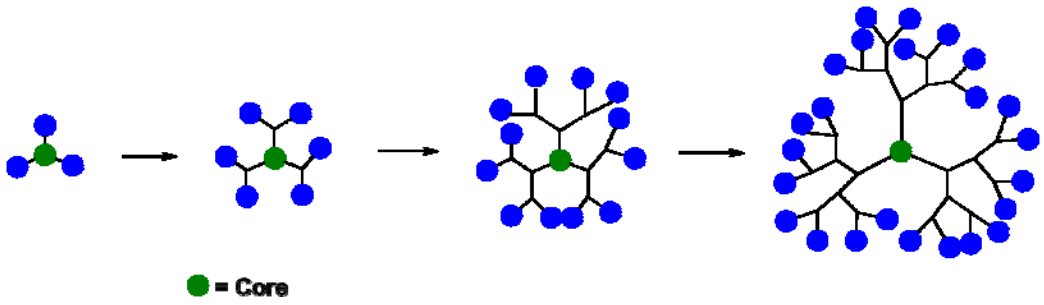

Figure 1.5 Divergent build up of dendrimers

The divergent approach is ideally suited for the large scale preparation of dendrimers as the quantity of dendrimer sample essentially doubles or triples with each generation increment.

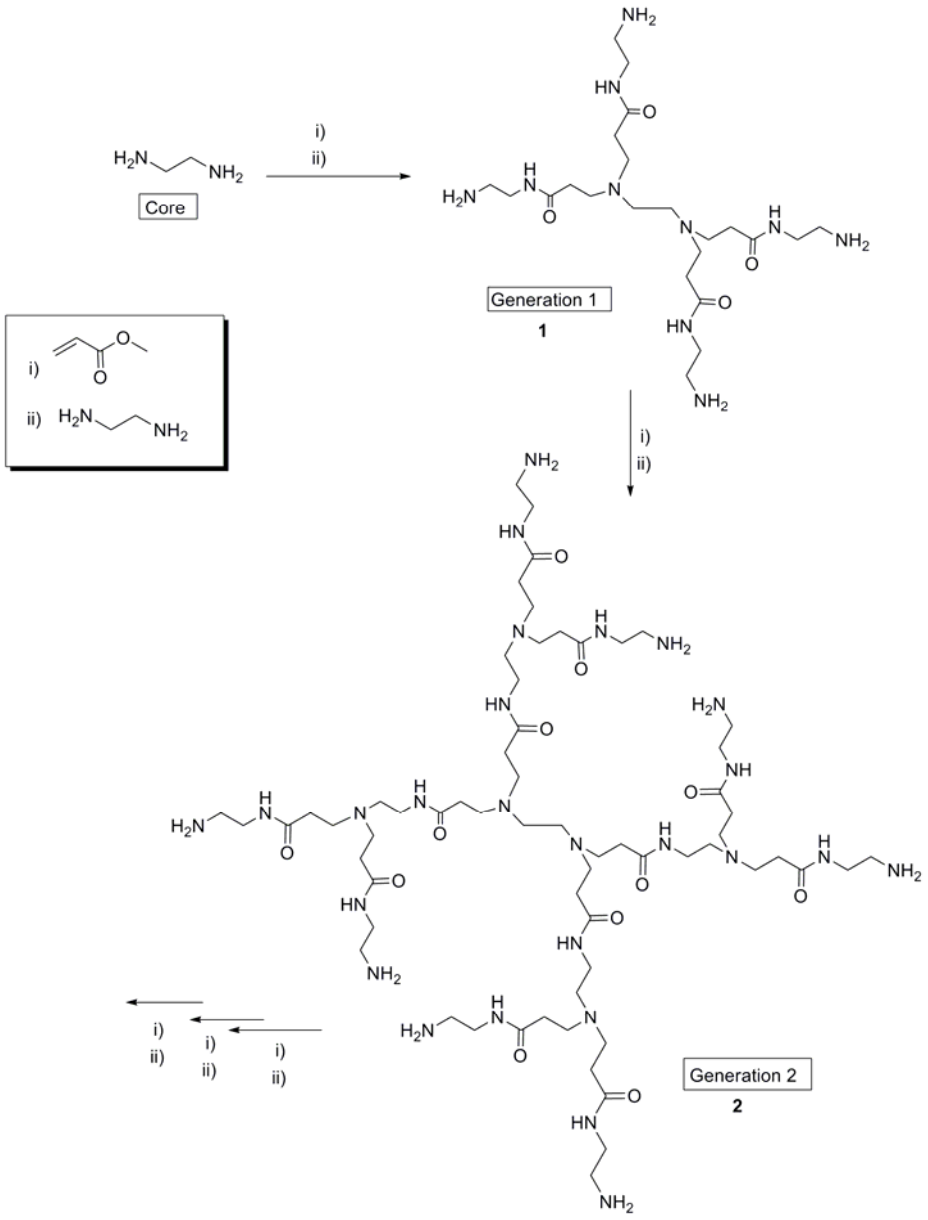

Scheme 1.1 PAMAM dendrimer synthesis reported by Tomalia *et al*[17-18]

However, because the number of coupling reaction increases exponentially with each generation, the likelihood of incomplete functionalization or side reactions increases exponentially as well. Although removal of monomer may be straightforward, any flawed molecules resulting from cyclizations or incomplete reactions cannot be removed easily because of their structural similarity to the desired product. Because of this and

the onset of de Gennes dense packing, high generation dendrimers produced using the divergent approach, though quite monodisperse when compared to narrow polydisperse linear polymers, still contain an appreciable number of structural flaws.

Of the many divergently synthesized dendrimers; PAMAM,[17-18] poly(propylene imine),[21] arborols[19, 31-35] and phosphorous-based dendrimers[36-38] are noteworthy. PAMAM is typically synthesized by using either ethylene diamine, ammonia or cystamine as cores and using an iterative two-step reaction sequence: (a) alkylation of primary amines by Michael addition with methacrylate, and (b) amidation of amplified ester groups with a large excess of ethylenediamine. PAMAM dendrimer synthesis using this iterative protocol was established by Tomalia and coworkers[4,17,18] and is shown in Scheme 1.1 to give G-1 dendrimer **1** and G-2 dendrimer **2**

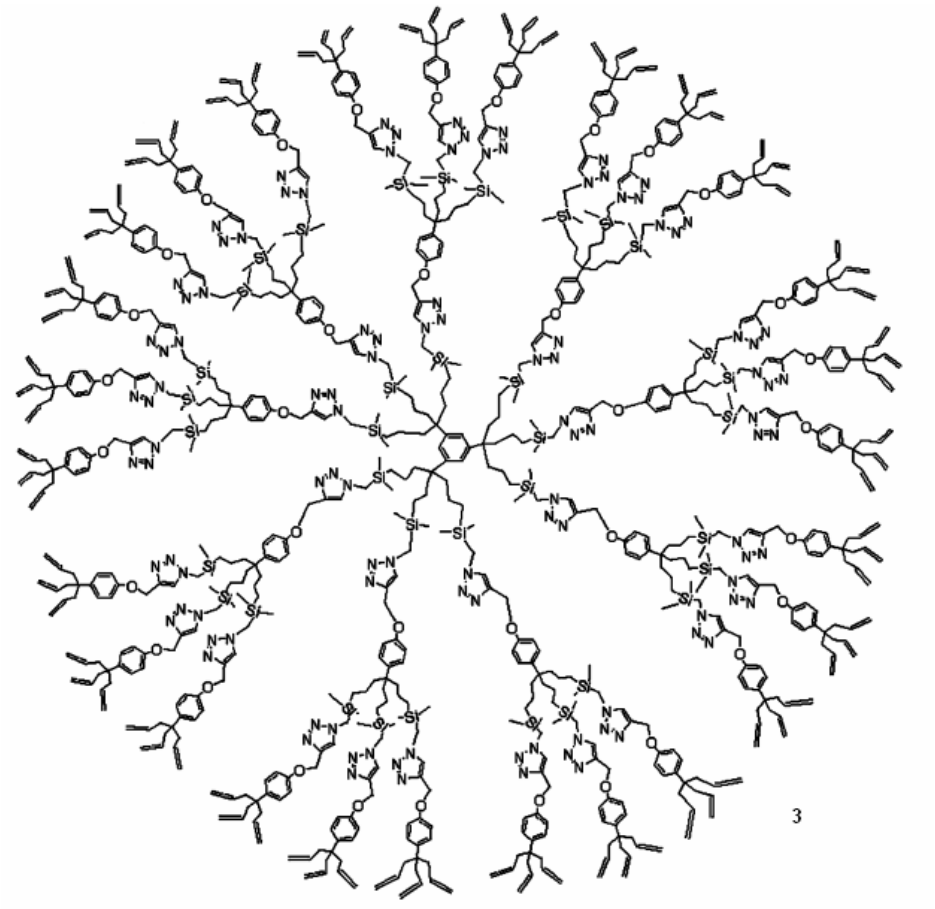

Figure 1.6 Click Dendrimers synthesized by Astruc *et al*. using divergent strategy[39-40] (Adapted image)

Higher generation dendrimers are obtained using the same iterative synthetic protocol. Recently, Astruc and coworkers[39,40] have reported divergently synthesized dendrimers using full 'click assembly'[41,42] or 1,3 dipolar cycloadditions between azides and alkynes. They used Newkome's[19] 1 → 3 C connectivity along with hydrosilylation of terminal olefinic bonds[43] to synthesize the building blocks. The repetition of Cu^{I} - induced click reaction[41-42] between building blocks yielded the G-2 dendrimer **3** as shown in Figure 1.6. They demonstrated an application of these dendrimers with 1,2,3-triazole rings by recognizing, binding and sensing oxo anions and metal cations by clicking ferrocenyl units at the end of the termini.

1.3.2.2 Convergent Approach

The convergent method, initiates growth from the exterior of the molecule and progresses inward by coupling end groups to each branch of the monomer as shown in Figure 1.7. After completion of the coupling, the single functional group located at the focal point of the wedge shaped dendritic fragment, or dendron, can be activated.[29] Coupling of this activated dendron to each of the complementary functionalities on an additional monomer unit affords a higher generation dendron. After sufficient repetition of this process, these dendrons can be attached to a polyfunctional core through their focal point to form a globular multi-dendron dendrimer. Though again an iterative synthesis, the convergent route strongly contrasts its divergent counterpart since it involves only a small number of reactions per molecule during the coupling and activation steps.

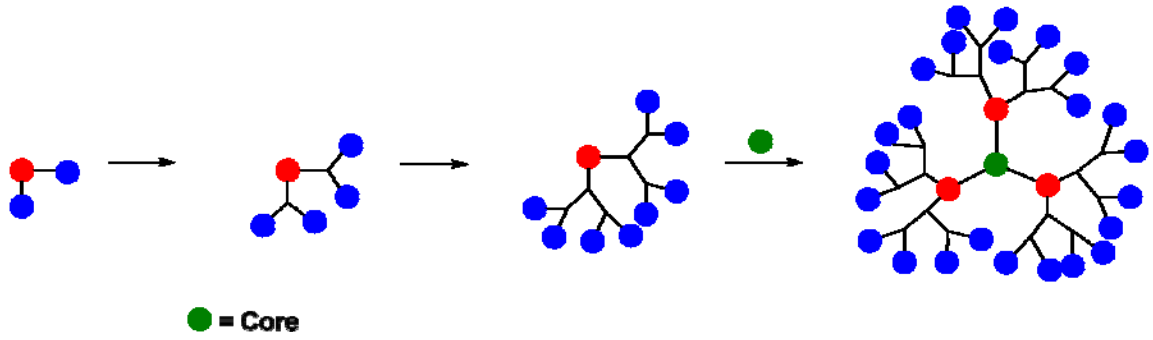

Figure 1.7 Convergent build up of dendrimers

Since the attachment of these dendrons to a polyfunctional core occurs at focal point of the dendron, the preparation of very large dendrimers is not possible due to steric inhibition at the focal point of dendron by its branches. The product purification at each

step of the synthesis is facilitated by the small number of components in the reaction mixture, ensuring that convergent dendrons as purest synthetic macromolecules.

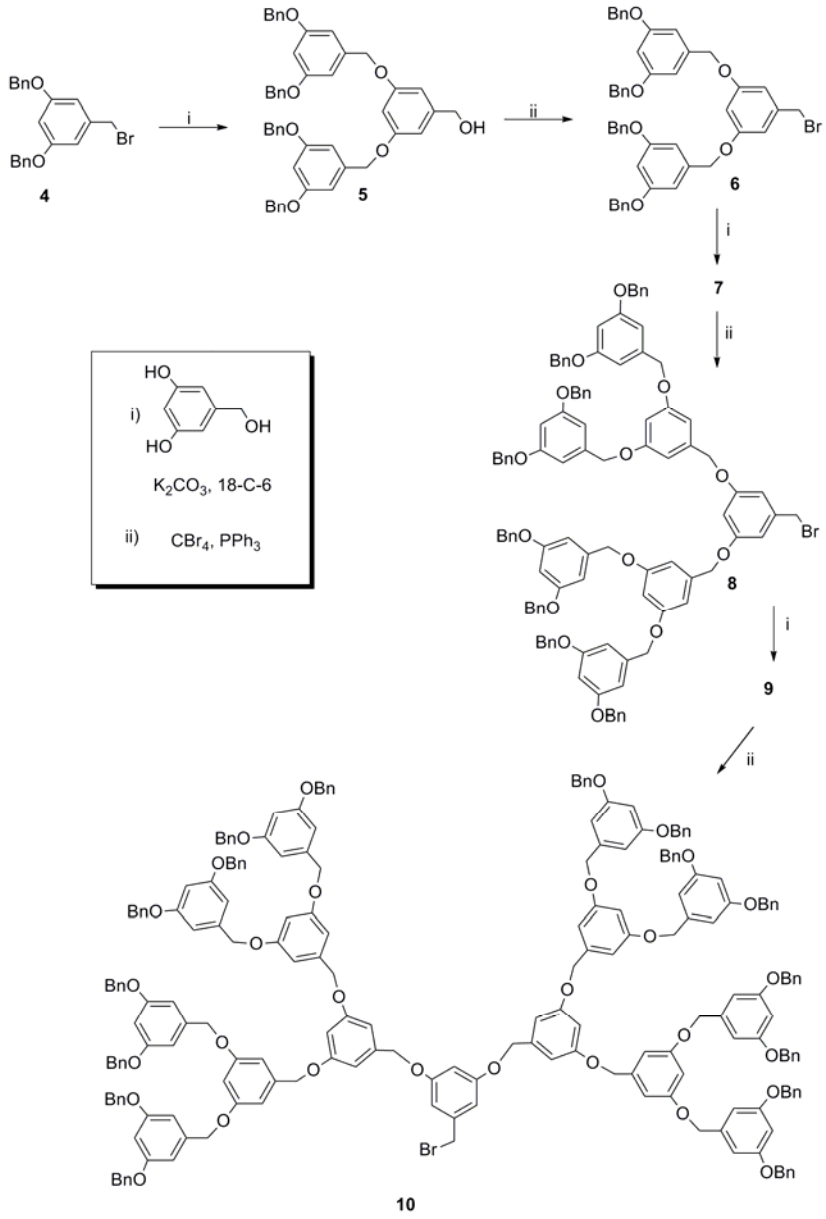

Scheme 1.2 Poly(aryl ether) dendrimer synthesis by Fréchet and Hawker[22,44] (Adapted image)

In 1989-1990, Fréchet and Hawker first developed the synthesis of poly(aryl ether) dendrimers using a convergent strategy.[22,44] The synthesis makes use of 3,5-

dihydroxybenzyl alcohol as the monomer as shown in Scheme 1.2. The phenolic groups of this monomer were coupled to benzylic bromide **4**, producing two new ether linkages of the second generation benzylic alcohol **5**. The focal benzylic alcohol functionality was then activated via bromination to afford dendron **6**. The coupling step was then repeated yielding the third generation benzylic alcohol **7**. Subsequent repetitions of the Williamson coupling and bromination steps enabled the production of the sixth generation dendrons which was subsequently coupled to the core to form the dendrimer.[22,44]

The poly(aryl ether) dendrons are employed frequently and referred to as 'Fréchet-type' dendrons. Other common dendrons[45] used for dendrimer synthesis are 'Percec-type' dendrons and 'Müllen-type' dendrons as shown in Figure 1.8.

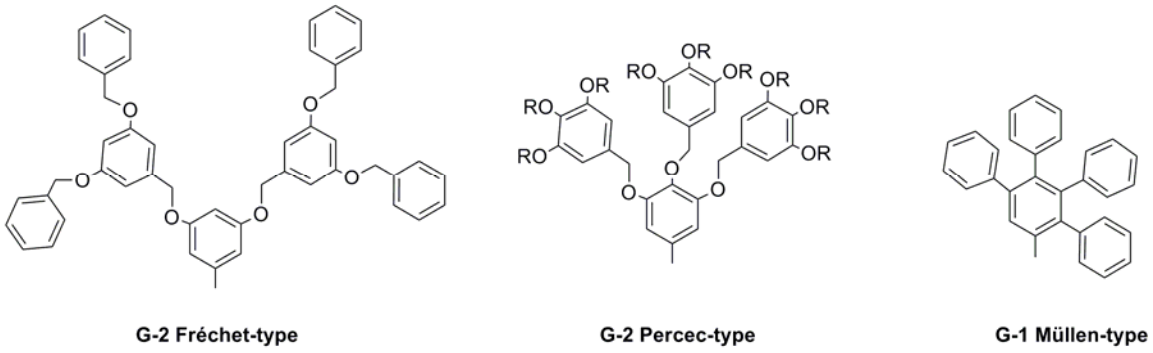

Figure 1.8 Three common dendrons used in dendrimer frameworks

A number of variations have been reported on the original repeat unit **8**. Tyler *et al*. reported the use of 'reversed monomer' **9**, where the building block instead consists of two benzylic alcohols as the latent electrophiles, and one nucleophilic phenol.[46,47] Both Fréchet-type dendrons and the reversed dendrons have proven to be of particular interest in light amplification,[48] and light-harvesting systems,[49-52] because of their complementary

behavior in energy transfer through their molecular frameworks. To investigate the effect of chirality in dendrimers, a number of groups have incorporated chiral spacers into the poly(aryl ether) repeat unit. Chow *et al*.[53-57] modified their dihydroxyphenoxypropanol repeat unit **10** to include the acetonide protected diol spacers: (2R, 3R)- or (2S, 3S)-threitol **11** and **12**. McGrath and coworkers incorporated similar chiral protected diols **13-16** into their studies,[58-62] whereas Seebach and co-workers[63-66] investigated the di- and tribranched chiral monomers **17-19**. To expedite the synthesis of densely packed dendrons, Percec and coworkers[67-71] utilized the triply branched monomer **20** (Figure 1.9).

Two other convergent syntheses including that of a family of poly(1,3,5-phenylene) dendrimers[72,73] were later reported by Miller and Neenan shortly after that of poly(benzyl ether) dendrimers.[22] Preparation of these poly(phenylenes) (Scheme 1.3) and their fluorinated analogues involved the Suzuki coupling of aryl boronic acids **21** or **22** with monomer **23**. Conversion of the trimethylsilyl (TMS) protecting group of products **24** and **25** to the boronic acid functionality in **26** and **27** enabled further coupling to the monomer. This procedure enabled the preparation of dendrons up to the third generation **32-35**. The rigid repeat units of these molecules lead to dendritic structures with well-defined shapes and diameters.

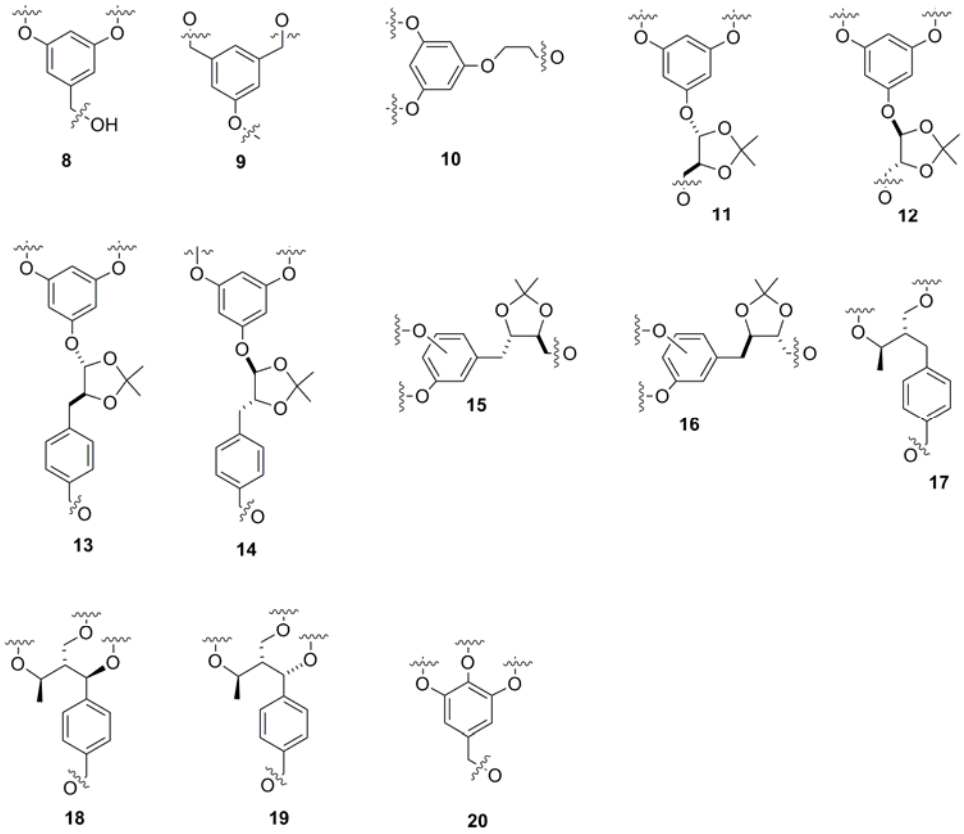

Figure 1.9 Various repeat units rom dendrimers that were synthesized using Fréchet's poly(benzyl ether) dendrimer protocol[46,47]

Recently, poly(aryl alkene) dendrimers were developed by both the Meir and the Burn groups.[74-76] Burn and coworkers[77-78] reported the synthesis of a dendritic framework (Scheme 1.4) via the Heck coupling of a derivatized styrene **36** with the monomer **37**, followed by a Wittig reaction with methyltriphenylphosphonium iodide to produce the activated dendritic styrene **39**. Using this procedure, dendritic materials up to third generation (**41**) could be prepared. Halim *et al*. have studied the photophysical properties of these materials, in particular their application toward light-emitting diode devices.[79-82]

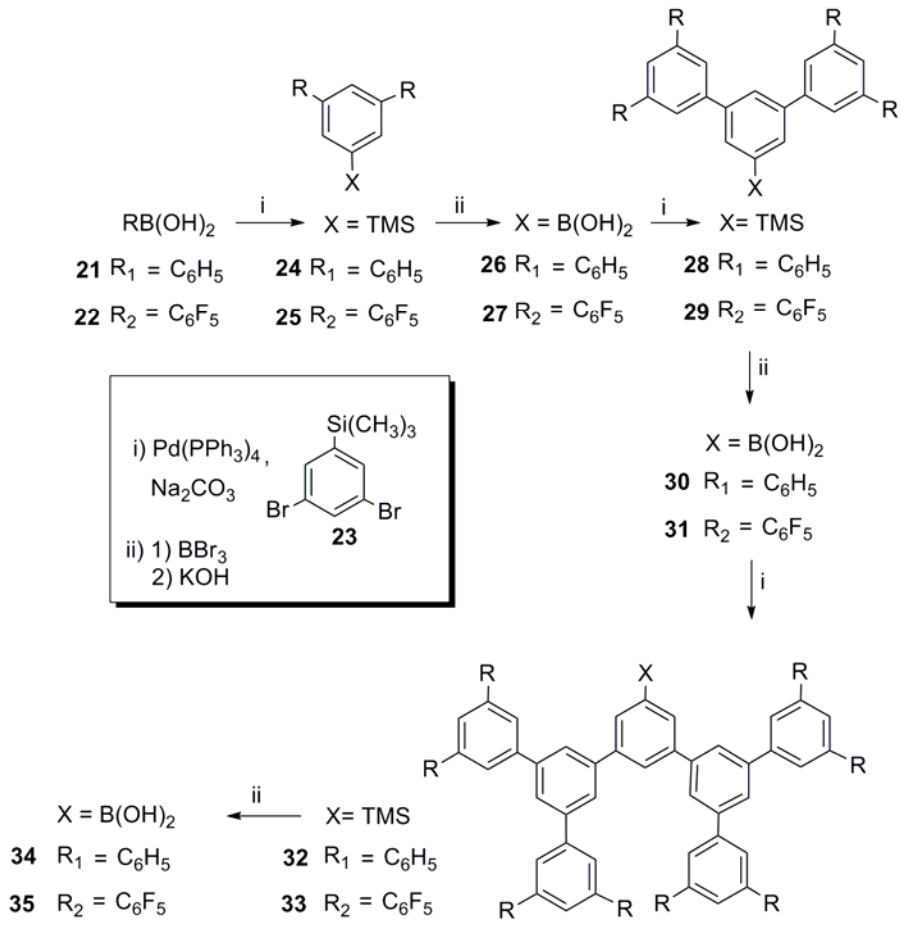

Scheme 1.3 Poly(phenylene) dendrimer synthesis by Miller and Neenan *et al*[72-73] (Adapted image)

Finally, a wide variety of other convergent syntheses have been developed for the preparation of dendritic poly(amides),[83,84] poly(esters),[85,86] poly(urethanes),[87,88] poly(arylethers),[89,90] poly(arylamines),[91,92] poly(arylketones),[93] poly(arylammmonium) salts, [94] poly(thioureas),[95] poly(ether imides),[96] poly(amine ethers),[97] poly(amide ethers),[98,99] poly(saccharides),[100] poly(glycopeptides)[101] and poly(nucleic acids).[102]

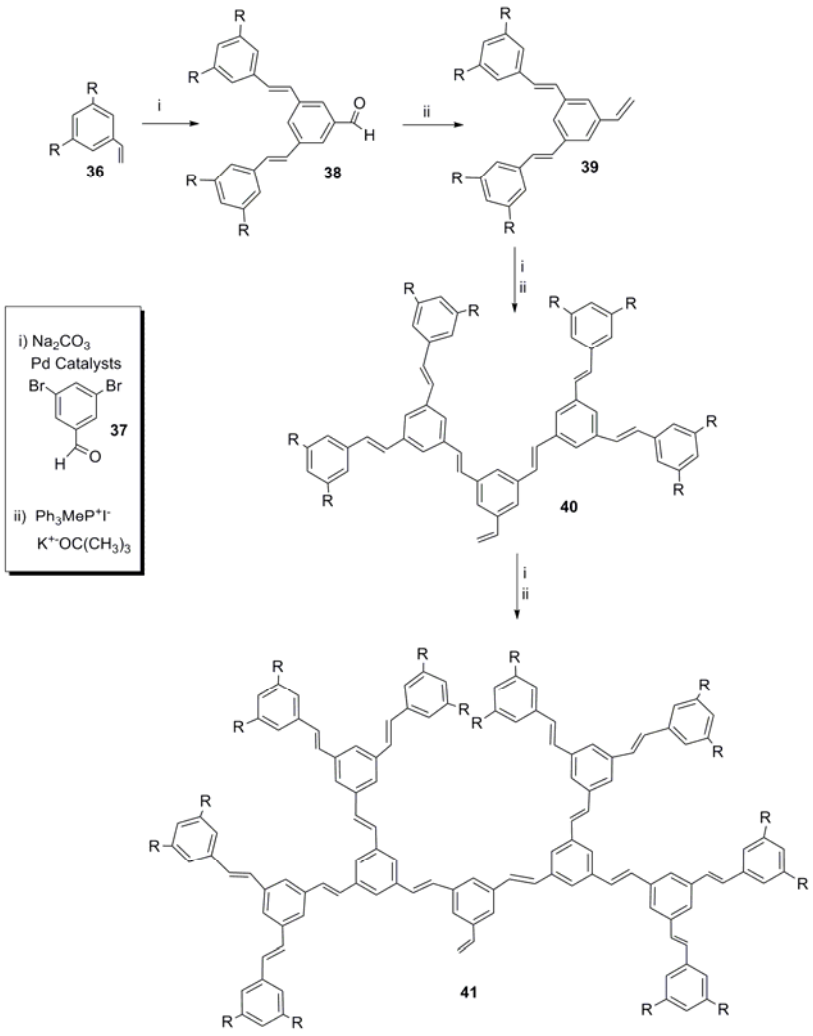

Scheme 1.4 Poly (aryl alkene) dendrimer synthesis by Burn *et al*[77-78] (Adapted image)

Hence, following these guidelines and synthetic protocols for generating dendrimers, synthetic chemists are ardently working to increase the functional performance and complexity of dendrimer architectures.

1.4 Random Hyperbranched Polymers

Another class of dendritic structures is hyperbranched polymers. In contrast to linear random coil polymers, hyperbranched structures such as starch or high-pressure poly(ethylene)s are characterized by more than two terminal groups per molecule which results in substantially smaller volumes and lower intrinsic viscosities compared to their linear polymer counterparts(Figure 1.10).[1] Hyperbranched polymers from poly(isobutylene) are used widely as rheology control agents.[103-104] Typically, hyperbranched polymers are prepared by the polymerization of AB_x monomers.[103-104] When x is 2 or more, polymerization of such monomers gives highly branched polymers as long as A reacts only with B from another molecule. In a similar fashion, copolymerization of A_2 and B_3 in the step growth polymerization or other such polyvalent monomers, can give hyperbranched polymers[105-106] if the polymerization is maintained below the gel point by manipulating monomer stoichiometry or limiting polymer conversion.

Figure 1.10 Schematic representation of a random hyperbranched polymer

Random hyperbranched polymers are generally produced by the one-pot polymerization of AB_x type monomers or macromonomers involving polycondensation, ring-opening, or polyaddition reactions.[1,2] The products usually have broad statistical molecular weight distributions, as observed for traditional polymers. Over the last 10

years, a diverse array of hyperbranched polymers have been reported from these synthetic methodologies including poly(phenylene)s obtained by Suzuki coupling,[107,108] poly(phenylacetylene)s prepared by the Heck reaction,[109] poly(carbosilane)s, poly(carbosiloxane)s,[110] and poly(siloxysilane)s synthesized by hydrosilylation,[111] poly(ether ketone)s by nucleophilic aromatic substitution,[112] and polyesters[113] or polyethers[114] by polycondensations or ring-opening polymerization.[115] These hyperbranched polymers have been useful for a variety of applications including as blend additives and melt modifiers because of their low viscosity and high solubility.[1] However, drawbacks of hyperbranched polymers include broad molecular weight distributions, irregular structure growth and often poor mechanical properties.

1.5 Dendronized Polymers

One of the most interesting class of dendritic architectures is the dendronized polymers. The quest for large size, well-defined macromolecules has led to the extension of dendrimer concepts to dendronized polymers.[116] Dendronized polymers are graft polymers,[10, 117] with the focal point of the dendrons attached to the pending functional group at the repeat units along the polymer backbone (Figure 1.11).

Polymers exist as a random coil, a rigid rod, or a mixture of these two extremes in solution.[10] In case of a rigid rod, polymers have the potential to extend over several nanometers lengthwise, but exhibit a cross-section in the range of only a few Å. Hence, they are not nanometer size object in a strict sense. In case of a random coil, they may exhibit a diameter in the order of a few nanometers in all dimensions. However, due to the conformational flexibility of the polymer backbone, such polymers exhibit structural dynamics.[2] Their average shape in solution is globular and not persistent. As a result, the

presentation of functional groups to the environment is random, and, most importantly, there is no defined interior, exterior, or surface.

Figure 1.11 Schematic representation of a dendronized comb polymer[1] (Adapted image)

Depending on the dendron's structure, size and attachment density along the backbone in a dendronized polymer, conventional polymer backbones such as poly(acrylate) or poly(styrene) can attain conformations all the way from random-coil to a rigid rod or a molecular cylindrical as shown in Figure 1.12, where the polymer backbone is stretched by attaching dendrons of increasing generations and exploiting the steric repulsions between them. This shape control on the backbone can be modulated by several interaction factors such as dendron/dendron, dendron/backbone and solvent/dendron. Hence, by merging both the dendrimer and polymer concepts, molecular cylinders with size ranging from few to several hundred nanometers in diameter and length which differ in chemical constitution, stiffness, surface decoration, backbone properties can be made.[118-120]

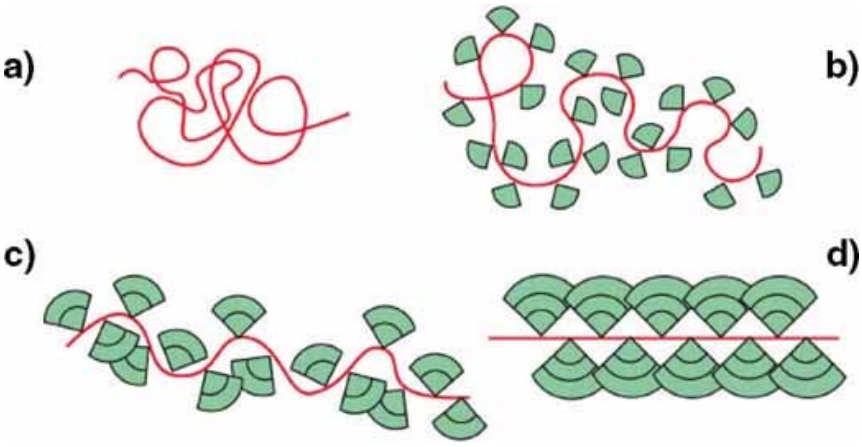

Figure 1.12 Representation of a coiled polymer backbone stretching through the attachment of increasingly sterically demanding dendrons. Polymer backbone with (a) no dendrons; (b) dendrons of the first generation; (c) second generation; (d) third generation[129] (Adapted image)

Dendronized polymers were first established with a patent filed by Tomalia *et al*. in 1987 for the synthesis of large and highly functionalized structures.[7] Fréchet and Hawker were the first to recognize hybrid structures of dendrimers and linear polymers as the next step in molecular architecture and in 1992 attached Fréchet type dendrons to a styrene derivative and copolymerized it with styrene.[122] Percec *et al*. recognized the predominant role of geometry in the self assembly of polymers equipped with 'taper shaped' side-chains.[123-127] Finally, Schlüter *et al*. first established the significance of dendron decoration for the backbone conformation and the overall shape of the obtained macromolecules, rendering them shape persistent, cylindrical nanoscopic objects.[128] Thereafter, dendronized polymers have been used increasingly for a variety of applications such as supported catalysis,[129] energy transfer, light harvesting and electrically conducting materials,[130-134] highly charged polyelectrolytes,[135] drug delivery,[136-138] surface patterning[139-140] and lengthwise phase separated supercylinders.[141] Because of our interest in these materials as supported catalysts and supramolecular

structures for biological applications, some detailed discussion on the synthesis and function of these materials will follow.

1.5.1 Synthetic Methodology of Dendronized Polymers

There are three different synthetic strategies for the synthesis of dendronized polymers:

Graft-To Strategy: In the graft-to strategy, preformed dendrons of desired generation are coupled to the preformed polymer using reactive functional groups along the backbone, as shown in Figure 1.13. The result is a graft polymer rather than a structure perfect comb polymer.[142] Post polymerization reactions towards graft polymers are inherently difficult to achieve with a high degree of conversion, even at low molecular weights. The main reason for the low conversions is a difficulty to access the functional groups along the polymer backbone due to the consequence of random coil conformation of flexible polymer chains. The second reason is the burial of the dendron focal points by dendritic branches in-case of higher generation dendrons. Hence only highly efficient coupling methods will allow for a high degree of dendronization.[125] Another problem with this strategy is the purification of the product. The polymer backbone itself is not monodisperse and exhibits a polydispersity in molecular weight, and possibly tacticity or constitution. Additional structural defects will only add to the polydispersity and increase difficulty in separating different species. Hence, the scope of the graft-to route is limited and most examples of the synthesis through this strategy are limited to G1 or G2 Fréchet-type dendrons.[22]

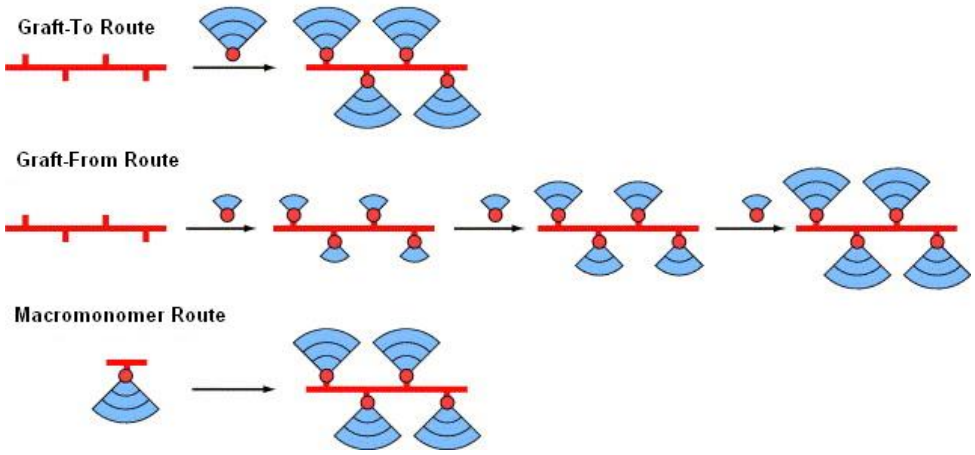

Figure 1.13 Schematic illustration of the three different synthetic strategies towards dendronized polymers[10] (Adapted image)

In a more recent example, Roy *et al.*[143] reported the synthesis of dendronized chitosan **42** in an attempt to improve its solubility and processability.

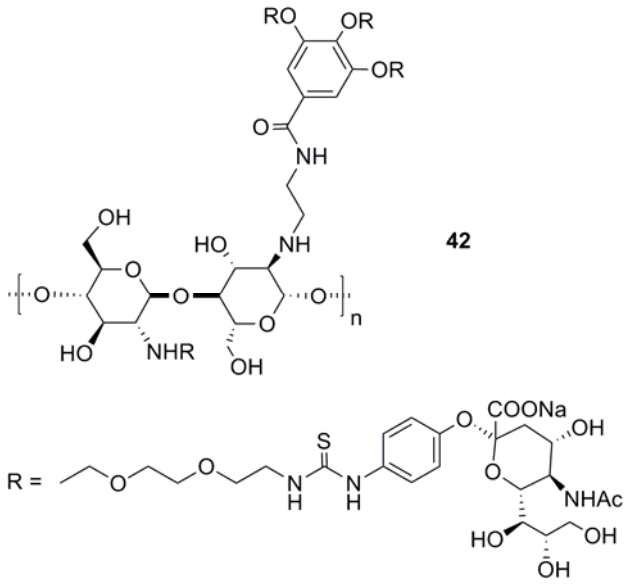

Figure 1.14 Examples of dendronized polymers obtained via a graft-to approach[143]

They used sugar functionalized G1 and G2 dendrons based on gallic acid amide branching units and tri(ethylene)glycol spacers which were peripherally functionalized

with silalic acid moieties. With only 0.15 equivalents of dendrons added per repeating unit, the obtained coverage was 0.13 (87%) for G1 and 0.06 (40%) for G2.

Graft-From Strategy: In the graft-from strategy, generation one dendrons are attached to the preformed polymer, and higher generations are grown successively as shown in Figure 1.13. The resulting dendronized polymer is, again, a graft copolymer rather than a structure perfect comb copolymer,[142] but with the dendritic side-chains grown off or grafted from the polymer backbone. The problems associated with the graft-from strategy are in particular at higher generations, where the required high number of simultaneous coupling events is prone to create defect structures. The resulting defect species are difficult to remove from the desired product because their close similarities, both structurally and size wise. Also, there is a possibility that the successive growth of the polymer side-chains and their increasing steric demand, may provide a pathway for successive unfolding of the backbone. The main problem, however, is the characterization of the products, in particular with respect to the degree of dendron attachment.

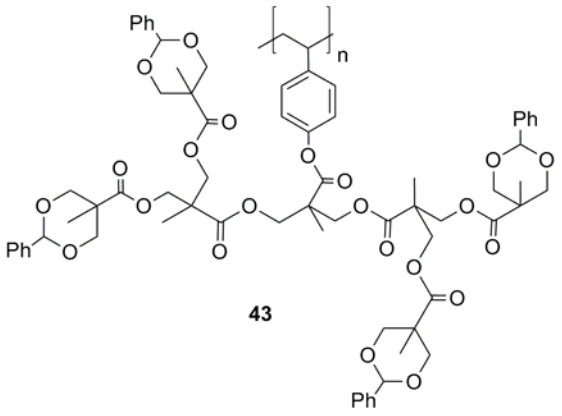

Figure 1.15 Example of poly(styrene) dendronized polymer obtained via a graft-from approach[144]

In a recent example of the graft-from strategy, the authors[144] chose commercially available poly(4-hydroxystyrene) with a polydispersity of 1.1 and molecular weights of 4,000 and 10,000. The polymer was purified after each graft-from reaction step via re-precipitation in methanol. For the lower molecular weight polymer **43**, the build up could be carried out all the way to G-3 dendronized polymer and the polydispersities according to GPC increased only marginally (PDI = 1.17 for G-3). However, in the synthesis starting from higher molecular weight polymer, aggregation had a severe influence, resulting in very low coverage for G-4 dendronized polymer.

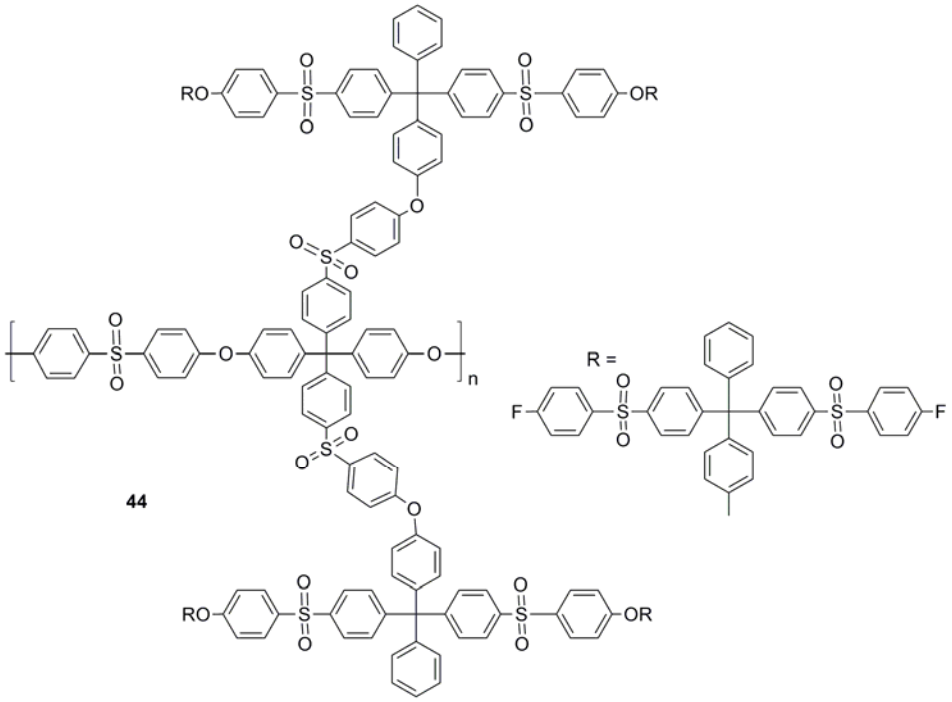

Figure 1.16 Example of a poly(ether sulphone) dendronized polymer synthesized via the graft-from approach[145]

Hay *et al*. demonstrated that, by using more rigid polymer backbones, one can also apply synthetic protocols that are inherently less efficient.[145] They synthesized a linear poly(ether sulphone) **44** equipped with pendant aryl fluoride groups to grow

aromatic ether sulfone based dendrimers up to generation G-3. The isolated yield of the dendronized polymers ranged from 80-90% as characterized by proton NMR.

In a recent example, Rabe[146-147] *et al*. used a poly(styrene) with a G-1 dendron attached bearing peripheral amine groups as the starting polymer and attached activated ester dendrons to build two G-4 dendronized polymers. The surface side-groups on the dendronized polymers were then converted chemically to an azide group and another one to an internal olefin. SFM study of *in-situ* chemical bonding between these peripheral functionalities on cylindrical dendronized polymers by UV decomposition of azides to nitrenes and their addition or insertion to a double bond on second dendronized polymer, established the first 'move-connect-prove' sequence between two individual strands of dendronized polymers as shown in Figure 1.17. This connection was also tested for its mechanical stability.

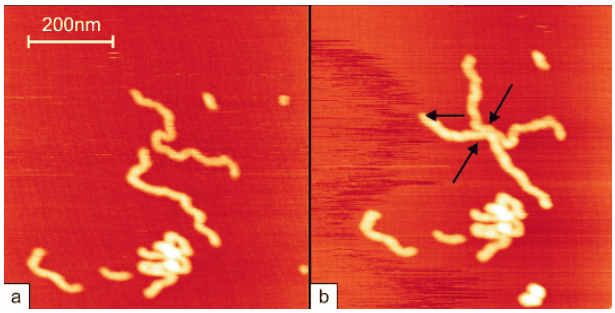

Figure 1.17 Tapping-mode SFM images of (a) two individual dendronized polymers and (b) two individual dendronized polymers after the irradiation with UV light to connect both polymers chemically[146-147] (Adapted image)

Macromonomer Strategy: In the macromonomer strategy, dendrons of the desired generation are attached to a polymerizable group at their focal point to obtain macromonomers which are polymerized subsequently as shown in Figure 1.13. The obvious advantage of this strategy over the other two strategies lies in the fact that it does not involve a post-polymerization reaction. As a result, if a polymerization is feasible,

the resulting polymers must exhibit a quantitative degree of dendron attachment. Hence, they are structurally perfect comb polymers.[142] The macomonomer approach, however has the decisive disadvantage that the steric demand of the dendrons will have a large effect on the kinetics of the polymerization. Steric hindrance may inhibit a polymerization completely or lead to unexpected results such as oligomeric products or very broad polydispersity. Neverthless, the macromonomer route is the most successful approach for obtaining dendronized polymers.[10,125] The different synthetic methods based on polymerization kinetics are categorized into (a) step growth polymerizations; (b) chain growth polymerizations; and (c) living chain growth polymerizations.[148-149]

Step growth polymerizations: In step growth polymerizations, conventional organic reactions between two functional groups A and B are used to build up polymers, usually in the form of polycondensation or polyaddition reactions. Either AB type monomers (with complementary functional groups in one molecule, e.g. α-hydroxyl-ω-carboxylic acid) or pairs of AA-type and BB-type monomers (with the same type of functionality in one molecule, e.g. α,ω-diols or α,ω-dicarboxylic acids) may be used.[10] A problematic aspect in regard to applications is the relatively broad molecular weight distribution of the product as a result of the statistical nature of the step growth process. Despite this, many successful syntheses of dendronized polymers have been reported using this polymerization by tedious optimization of reaction conditions.[150-153]

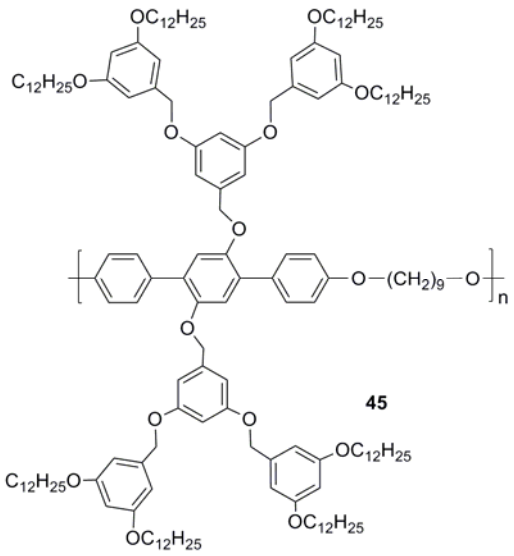

Figure 1.18 Dendronized aromatic-aliphatic polyethers via the macromonomer step-growth approach

In a recent paper,[150] Kallitsis, Pakula *et al*. synthesized dendronized aromatic-aliphatic polyethers **45** (Figure 1.18), using Williamson etherification of G-1 and G-2 dendronized α,ω-dihydroxyterphenyls with α,ω-dibromoalkanes. Thermal and mechanical properties of these materials exhibited phase segregation and two separate melting points for the dendritic side-chains and the main-chain. Preliminary WAXS and 2D X-ray scattering results suggested the presence of hierarchically ordered structures. The authors identified the potential of these rigid-flexible polymers in the synthesis of processable, stable film for polymer based electro-luminescent materials.

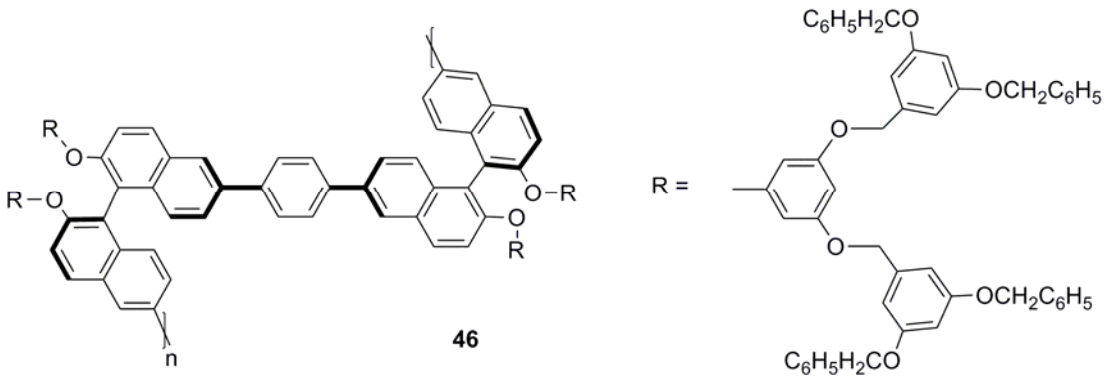

Figure 1.19 Poly(arylene) dendronized polymers obtained using a macromonomer step-growth approach

Xi *et al*.[151] used the Suzuki polycondensation reaction in order to synthesize main chain chiral binaphthyl based poly(arylene)s **46** (Figure 1.19) with pendant Fréchet type dendrons. The obtained polymers had a molecular weight of 239,000 for G-1 as characterized by light scattering. CD spectra showed a strong Cotton effect indicating the presence of a strongly stabilized, chiral helical backbone.

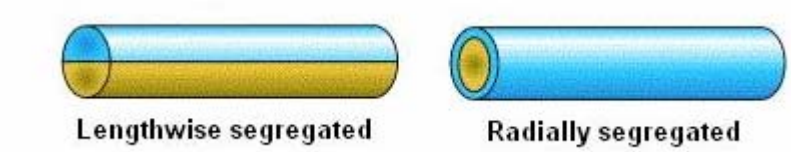

Figure 1.20 Different architectures of amphiphiles derived from dendronized polymers, blockwise and lengthwise segregated cylindrical nanoscopic objects[141,152, 153, 175] (Adapted image)

Schlüter *et al*. used[141,153] Suzuki polycondensation to synthesize rigid-rod like poly(p-phenylene)s having pendant hydrophilic polar dendrons carrying oligo(ethylene) oxide chains along with hydrophobic Fréchet type dendrons. This resulted in the formation of amphiphilic polymeric nanocylinders with a propensity to segregate lengthwise as shown in Figure 1.20. Similarly, radially segregated dendronized polymers have been reported.[152, 175]

Chain growth polymerizations: In chain growth polymerizations, an active center, e.g. a radical, an anion, a cation etc. is generated in the initiation step. With the exception of 'living' chain polymerizations, there is always possibility of active center being quenched. For this reason, chain growth obtained dendronized polymers typically have a PDI of around 2. The main obstacle to obtain high molecular weight material is polymerization kinetics. The propagation rate of polymerization must be fast compared to termination and chain transfer. This may pose a particular problem with dendronized monomers because of their inherent steric demands, which may lead to encapsulation of active center and hence, slow propagation.

The free radical polymerization of dendronized methacrylates and styrenes have been reported extensively by Percec *et al*.[154-157] In one example,[158-159] G2 dendronized units of methacrylates and styrenes, **47** and **48**, were used, which did not have a spacer between the polymerizable unit and the dendron (Figure 1.21).

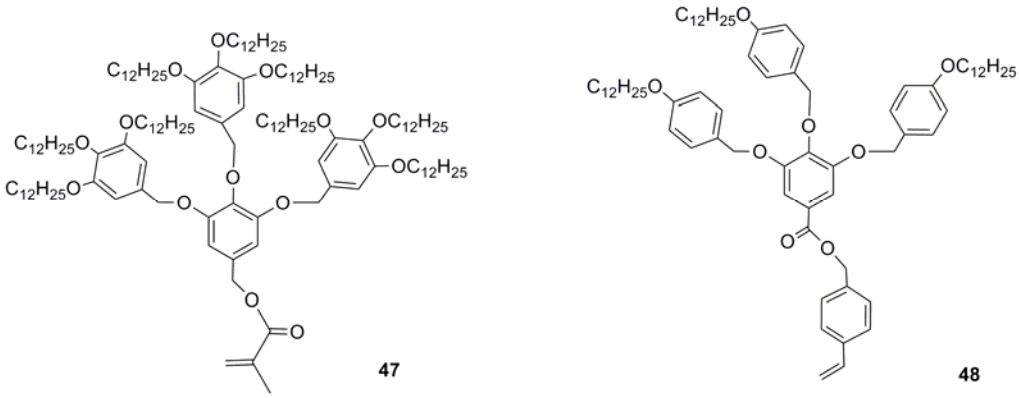

Figure 1.21 Examples of styrenes, methacrylates carrying Percec type dendronized monomers used in free radical polymerization (Adapted image)

Polymerization kinetics of the radical polymerization in the bulk, revealed a complex influence of the molecular and supramolecular structure on the outcome of the polymerization reaction.[158-159] The rate constants observed in the high concentration

regime were more than an order of magnitude higher than those of unsubstituted monomers and high molecular weights of 312,000 were obtained in a short period of time.[158-159] By contrast, in dilute solutions, low molecular weights were obtained. The authors attributed these remarkable findings to the complex self-assembling behavior of dendronized monomers, oligomers and polymers above the critical concentration, giving rise to spherical superstructures and a preorganized supramolecular reactor with enhanced concentration and accessibility of the polymerizable groups (Figure 1.22).

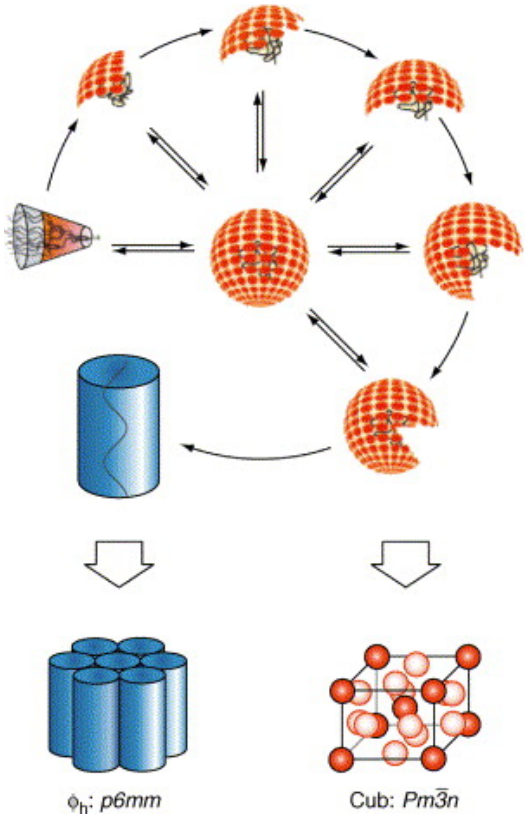

Figure 1.22 Schematic representation of the self-assembly of dendronized polymers into spherical and cylindrical superstructures and corresponding liquid crystalline phases in bulk material as proposed by Percec *et al*[158,160] (Adapted image)

As the polymerization progressed beyond a critical degree, the superstructure is converted to a cylinder that is stabilized by phase segregation and π-π stacking of the aromatic portions of the dendritic wedges. In both cases, the polymerizable groups are

located in a small volume fraction in a high concentration, while the initiator is distributed throughout the whole reaction mixture, and diffusion is low. This reasoning, is consistent with findings on the self-assembly behavior of the dendrons, and model compounds,[159,161] and was further substantiated by DSC and XRD investigations of the obtained dendronized polymers at different degree of polymerization.[160]

Living and controlled chain polymerizations: In living chain polymerizations, both chain transfer and chain termination are absent and initiation is fast in comparison to chain propagation. All polymer chains grow at the same average rate and are never terminated until the reaction is quenched. The molecular weight of the obtained polymers can be adjusted by the stoichiometric ratio of the monomer and the initiator. As a result, the products are usually not contaminated by oligomers, which greatly improves the material properties. In a controlled polymerization, the active species is in a fast equilibrium with a dormant species that does not undergo termination or transfer reaction. While such polymerizations are not strictly 'living' but 'controlled', the obtained polymers exhibit most of the features of living polymerizations. A valuable procedure to obtain well-defined polymers is the ring-opening metathesis polymerization (ROMP)[162-165] of strained cyclic olefins, most often catalyzed by ruthenium complexes such as Grubbs type initiators.[163,166,167] The polymerization is 'living' and is marked by low polydispersities, control over molecular weight by monomer/initiator ratio, the possibility to obtain block copolymers, and control over the chain end functionalizations. Controlled polymerization techniques such as atom transfer radical polymerization[168,169] (ATRP) and reversible addition-fragmentation-transfer[170,171] (RAFT) are increasingly popular since the polymers obtained are almost as well defined as 'living' polymerizations and are very tolerant towards functional groups and impurities.

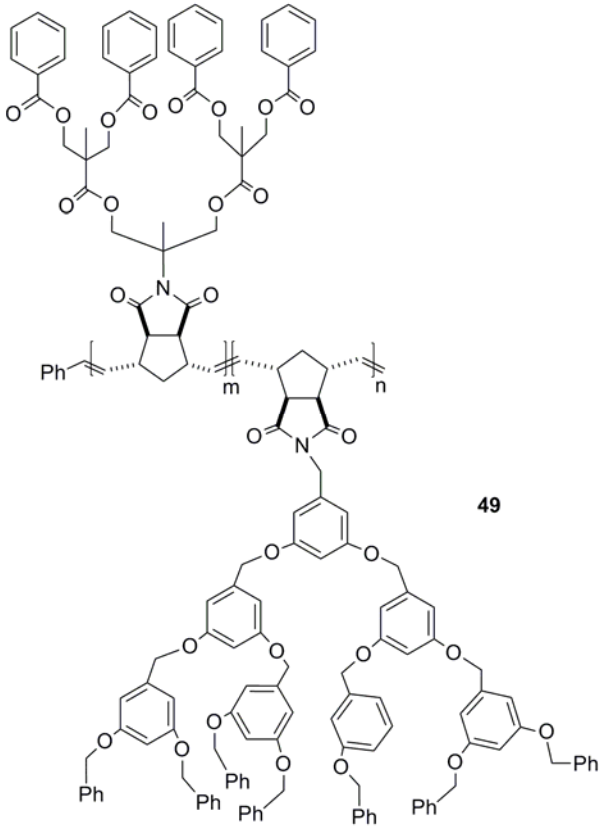

Figure 1.23. Dendronized diblock copolymer by Fréchet *et al.* synthesized by ROMP[172-173] (Adapted image)

Recently reported ROMP by Fréchet *et al*. of G2 to G3 dendronized norbornene monomers, first with a G-2 aliphatic ester dendron and second with sterically demanding G-3 aryl ether dendron, resulted in the formation of di-block copolymer **49** with fully dendronized segments[172-173] using Grubbs third generation initiator (Figure 1.23). AFM visualization of polymer molecules confirmed the diblock structure of the individual dendronized polymer chains as shown in Figure 1.24.

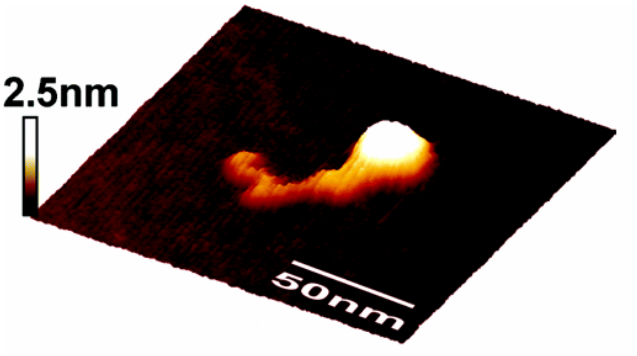

Figure 1.24 Tapping mode AFM image of dendronized diblock copolymers spun cast on mica with an aryl ether dendronized block and a smaller ester dendron block[173] (Adapted image)

Xi *et al*. reported the ATRP of methacrylates carrying G2 Fréchet type and Percec type dendrons.[174] Polydispersities were reasonably low in most cases and block copolymers were synthesized which displayed two glass transition temperatures on DSC. In general, various strategies and synthetic methods for the preparation of dendronized polymers are now well established. Nevertheless, it is still not a trivial task to obtain high molecular weights and high generation dendronized polymers. While some desired structures remain elusive, many interesting materials have become available. Dendronized polymers are now underway with respect to various applications,[2,10,125] including the synthesis of hierarchically structured materials, catalysis, applications in biosciences for drug delivery, ion channel mimics, DNA compactization, as well as optoelectronics applications some of which were detailed above.

1.6 Conclusion

In the last two decades, dendrimers and dendritic molecules have grown from discovery into an ever expanding field of polymer and nanoscience with a wide variety of applications. They are being used in supramolecular polymer chemistry, in medicinal chemistry, in catalysis and in optoelectronics with huge impact. Thanks to the pioneering work by Tomalia, Fréchet, Percec and Newkome, the fundamental principles of these molecules have been established and are well understood. A variety of dendritic molecules with novel, robust structures and function have been reviewed. The current challenge is to increase functional utility of these molecules for facile use in a variety of applications.

The goal of all the projects accomplished in this thesis is to contribute to both the synthetic arena of dendritic molecules elaborated upon and developing new functional molecules that have not been realized so far. The accomplishments of this research will pave way for new materials with better functional properties while establishing methodologies for design of novel materials for applications in biological systems as well as in catalysis.

1.7 References

1. Fréchet, J. M. J.; Tomalia, D. A., Dendrimers and other Dendritic Polymers; John Wiley & Sons: Chichester, UK, 2001.

2. Tomalia, D. A.; Fréchet, J. M. J. Discovery of dendrimers and dendritic polymers: a brief historical perspective. *J. Polym. Sci: Part A: Polym. Chem.* **2002**, *40*, 2719.

3. Tomalia, D. A., Starbust dendrimers – nanoscopic supermolecules according to dendritic rules and principles. *Macromol. Symp.* **1996**, *101*, 243.

4. Tomalia, D. A. Birth of a new macromolecular architecture: dendrimers as quantized building blocks for nanoscale synthetic polymer chemistry. *Prog. Polym. Sci.* **2005**, *30*, 294.

5. Flory, P. J., Principles of Polymer Chemistry; Cornell University Press: Ithaca, NY, 1953.

6. Hecht, S.; Fréchet, J. M. J. Dendritic encapsulation of function: applying nature's site isolation principle from biomimetics to materials science. *Angew. Chem. Int. Ed*. **2001**, *40*, 74.

7. Tomalia, D. A.; Naylor, A. M.; Goddard, W. A. Starbust dendrimers: control of size, shape, surface chemistry, topology and flexibility in the conversion of atoms to macroscopic materials. *Angew. Chem. Int. Ed.* **1990**, *102*, 119.

8. Fischer, M., Vögtle, F. Dendrimers: from design to application – a progress report. *Angew. Chem. Int. Ed.* **1999**, *38*, 885.

9. Matthews, O. A.; Shipway, A. N.; Stoddart, J. F., *Prog. Polym. Sci.* **1998**, *23*, 1.

10. Frauenrath, H. Dendronized polymers-building a new bridge from molecules to nanoscopic objects. *Prog. Polym. Sci.* **2005**, *30*, 325.

11. Flory, P. J. Molecular size distribution in three dimensional polymers. VI. Branched polymer containing A-R-Bf-1-type units. *J. Am. Chem. Soc.* **1952**, *74*, 2718.

12. Buhleier, E; Wehner, W; Vögtle, F. Cascade and nonskid-chain-like syntheses of molecular cavity topologies. *Synthesis* **1978**, 155.

13. Denkewalter, R. G.; Kolc. J.; Lukasavage, W. J., U.S. Pat.4, -289, 872, Sept 15, 1981.

14. Denkewalter, R. G.; Kolc. J.; Lukasavage, W. J. U.S. Pat.4,-360, 646, Nov 23, 1982.

15. Denkewalter, R. G.; Kolc. J.; Lukasavage, W. J. U.S. Pat.4,-410, 688, Oct 18, 1983.

16. Aharoni, S. M.; Crosby, C. R., III; Walsh, E. K. Size and solution properties of globular tert-butyloxycarbonyl-poly(α,ε-L-lysine). Macromolecules **1982**,*15*, 1093.

17. Tomalia, D.A.; Baker, H.; Dewald, J. R.; Hall, M.; Kallos, G.; Martin, S.; Roeck, J.; Ryder, J.; Smith, P. A new class of polymers: starbust-dendritic macromolecules. *Polym. J.* (Tokyo) **1985**, *17*, 117.

18. Tomalia, D.A.; Baker, H.; Dewald, J. R.; Hall, M.; Kallos, G.; Martin, S.; Roeck, J.; Ryder, J.; Smith, P. Dendritic macromolecules: synthesis of starbust dendrimers. *Macromolecules* **1986**, *19*, 2466.

19. Newkome, G. R.; Yao, Z.-Q.; Baker, G. R.; Gupta, K. Micelles. Part 1. Cascade molecules: a new approach to micelles. A [27]-arborol. *J. Org. Chem.* **1985**, *50*, 2003.

20. Wörner, C.; Mülhaupt, R. Polynitrile- and polyamine-functional poly(trimethylene imine) dendrimers. *Angew. Chem., Int. Ed. Engl.* **1993**, *32*, 1306.

21. Brabander-van den Berg, E. M. M.; Meijer, E. W. Poly(propylene imine) dendrimers: large-scale synthesis by heterogeneously catalyzed hydrogenations. *Angew. Chem., Int. Ed. Engl.* **1993**, *32*, 1308.

22. Hawker, C. J. ; Fréchet, J. M. J. Preparation of polymers with controlled molecular architecture. A new convergent approach to dendritic macromolecules. *J. Am. Chem. Soc.* **1990**, *112*, 7638.

23. Moore, J. S. ; Xu, Z. Synthesis of rigid dendritic macromolecules: enlarging the repeat unit size as a function of generation, permitting growth to continue. *Macromolecules* **1991**, *24*, 5893.

24. Xu, Z.; Moore, J. S. Stiff dendritic macromolecules. Rapid formation of large phenylacetylene dendrimers with molecular diameters up to 12.5 nanometers. *Angew. Chem., Int. Ed. Engl.* **1993**, *105,* 1394.

25. Kawaguchi, T.; Walker, K. L.; Wilkins, C. L.; Moore, J. S. Double exponential dendrimer growth. *J. Am. Chem. Soc.* **1995**, *117*, 2159.

26. Moore, J. S. Shape-persistent molecular architectures of nanoscale dimension. *Acc. Chem. Res.* **1997**, *30*, 402.

27. Newkome, G. R.; Moorefield, C. N.; Vögtle, F. Dendritic Molecules: Concepts, Syntheses and Perspectives; VCH: Weinheim, Germany, 1996.

28. De Gennes, P. G.; Hervet, H. Statistics of starburst polymers. *J. Phys. Lett.* **1983**, *44*, 351.

29. Grayson, S. M.; Fréchet, J. M. J. Convergent dendrons and dendrimers: from synthesis to applications. *Chem. Rev.* **2001**, *101*, 3819.

30. Vögtle, F. Dendrimers. *Top. Curr. Chem.* **1998**, 197.

31. Newkome, G. R.; Moorefield, C. N.; Baker, G. R.; Johnson, A. L.; Behera, R. K. Chemistry of micelles. Alkane cascade polymers with a micellar topology: micelle acid derivatives. *Angew. Chem., Int. Ed. Engl.* **1991**, *30*, 1176.

32. Newkome, G. R.; Moorefield, C. N.; Baker, G. R.; Saunders, M. J.; Grossman, S. H. Chemistry of micelles. Monomolecular micelles. *Angew. Chem., Int. Ed. Engl.* **1991**, *103*, 1207.

33. Newkome, G. R.; Behera, R. K.; Moorefield, C. N.; Baker, G. R. Chemistry of micelles. Cascade polymers: synthesis and characterization of one-directional arborols based on adamantane. *J. Org. Chem.* **1991**, *56*, 7162.

34. Newkome, G. R.; Nayak, A.; Behera, R. K.; Moorefield, C. N.; Baker, G. R. Chemistry of micelles series. Cascade polymers: synthesis and characterization of four-directional spherical dendritic macromolecules based on adamantane. *J. Org. Chem.* **1992**, *57*, 358.

35. Newkome, G. R.; Young, J. K.; Baker, G. R.; Potter, R. L.; Audoly, L.; Cooper, D.; Weis, C. D.; Morris, K.; Johnson, C. S. Jr. Cascade polymers. pH dependence of hydrodynamic radii of acid-terminated dendrimers. *Macromolecules* **1993**, *26*, 2394.

36. Launay, N.; Caminade, A. M.; Lahana, R.; Majoral, J-P. General synthetic strategy for neutral phosphorous-containing dendrimers. *Angew. Chem.* **1994**, *106*, 1682.

37. Launay, N.; Caminade, A. M.; Majoral, J-P. Synthesis and reactivity of unusual phosphorous dendrimers. A useful divergent growth approach upto the seventh generation. *J. Am. Chem. Soc.* **1995**, *117*, 3282.

37. Majoral, J. P.; Caminade, A. M. Divergent approaches to phosphorous-containing dendrimers and their functionalization. *Top. Curr. Chem.* **1998**, *197*, 79.

39. Ornelas, C; Aranzaes, J. R.; Cloutet, E.; Alves, S.; Astruc, D. Click assembly of 1,2,3-triazole-linked dendrimers, including ferrocenyl dendrimers, which sense both oxo anions and metal cations. *Angew. Chem. Int. Ed*. **2007**, *46*, 872.

40. Ornelas, C; Salmon, L.; Aranzaes, J. R.; Astruc, D. Catalytically efficient

palladium nanoparticles stabilized by “click” ferrocenyl dendrimers. *Chem. Commun.* **2007**, *46*, 4946.

41. Huisgen, R. Cycloadditions- definition, classification, and characterization. *Angew. Chem. Int. Ed. Engl.*, **1968**, *7*, 321.

42. Kolb, H. C.; Finn, M. G.; Sharpless, K. B. Click chemistry: diverse chemical function from a few good reactions. *Angew. Chem. Int. Ed.* **2001**, *40*, 2004.

43. Van der Made, A. W.; Van Leeuwen, P. W. N. M.; De Wilde, J. C.; Brandes, R. A. C. Dendrimeric silanes. *Adv. Mater.* **1993**, *5*, 466.

44. Hawker, C. J.; Fréchet, J. M. J. A new convergent approach to monodisperse dendritic macromolecules. *J. Chem. Soc., Chem Commun.* **1990**, 1010.

45. Marcos, M; Martin-Rapún, R.; Omenat, A.; Serrano, J. L. Highly congested liquid crystal structures: dendrimers, dendrons, dendronized and hyperbranched polymers. *Chem. Soc. Rev.* **2007**, *36*, 1889.

46. Tyler, T. L.; Hanson, J. E. New approaches to the synthesis of poly(aryl ether) dendrimers. *Polym. Mater. Sci. Eng.* **1995**, *73*, 356.

46. Tyler, T. L.; Hanson, J. E. An efficient synthesis of poly(aryl ether) monodendrons and dendrimers based on 3,5-bis(hydroxymethyl)phenol. *Chem. Mater.* **1999**, *11*, 3452.

48. Kawa, M.; Fréchet, J. M. J., Self-assembled lanthanide-cored dendrimer complexes: enhancement of the luminescence properties of lanthanide ions through site-isolation and antenna effects. *Chem. Mater.* **1998**, *10*, 286.

49. Gilat, S. L.; Adronon, A.; Fréchet, J. M. J. Dye-labeled reversed convergent dendrimers: synthesis and energy transfer. *Polym. Mater. Sci. Eng.* **1997**, *77*, 91.

50. Gilat, S. L.; Adronon, A.; Fréchet, J. M. J. Modular approach to the accelerated convergent growth of laser dye-labeled poly(aryl ether) dendrimers using a novel hypermonomer. *J. Org. Chem.* **1999**, *64*, 7474.

51. Gilat, S. L.; Adronon, A.; Fréchet, J. M. J. Light harvesting and energy transfer in novel convergently constructed dendrimers. *Angew. Chem., Int. Ed.* **1999**, *38*, 1422.

52. Adronov, A.; Malenfant, P. R. L. ; Fréchet, J. M. J. Synthesis and steady-state photophysical properties of dye-labeled dendrimers having novel oligothiophene cores: a comparative study. *Chem. Mater.* **2000**, *12*, 1463.

53. Chow, H. F.; Mak, C. C. Synthesis and structure-optical rotation relationships of homochiral, monodisperse, tartaric acid-based dendrimers. *J. Chem. Soc., Perkin*

Trans. 1 **1994**, 2223.

54. Chow, H. F.; Fok, L. F.; Mak, C. C. Synthesis and characterization of optically active, homochiral dendrimers. *Tetrahedron Lett.* **1994**, *35*, 3547.

55. Chow, H. F.; Mak, C. C. Facile preparation of optically active dendritic fragments containing multiple tartrate-derived chiral units. *Tetrahedron Lett.* **1996**, *37*, 5935.

56. Chow, H. F.; Mak, C. C. Preparation and structure-chiroptical relationships of tartaric acid-based layer-block chiral dendrimers. *J. Chem. Soc., Perkin Trans. I* **1997**, 91.

57. Chow, H. F., Mak, C. C. Synthesis and chiroptical properties of layer-block dendrimers. *Pure Appl. Chem.* **1997**, *69*, 483.

58. McGrath, D. V.; Wu, M. J.; Chaudhry, U. An approach to highly functionalized dendrimers from chiral, non-racemic synthetic monomers. *Tetrahedron Lett.* **1996**, *37*, 6077.

59. McElhanon, J. R.; Wu, M. J.; Escobar, M.; McGrath, D. V. Toward chiral dendrimers with highly functionalized interiors. Dendrons from synthetic AB2 monomers. *Macromolecules* **1996**, *29*, 8979.

60. McElhanon, J. R.; Wu, M. J.; Escobar, M.; Chaudhry, U.; Hu, C. L.; McGrath, D. V. Asymmetric synthesis of a series of chiral AB2 monomers for dendrimer construction. *J. Org. Chem.* **1997**, *62*, 908.

61. McElhanon, J. R.; McGrath, D. V. Constitution, configuration, and the optical activity of chiral dendrimers. *J. Am. Chem. Soc.* **1998**, *120*, 1647.

62. Junge, D. M.; McGrath, D. V. Synthesis of optically active chiral shell dendrons. *Tetrahedron Lett.* **1998**, *39*, 1701.

63. Murer, P.; Seebach, D. Synthesis and properties of first to third generation dendrimers with doubly and triply branched chiral building blocks. *Angew. Chem, Int. Ed. Engl.* **1995**, 34, 2116.

64. Murer, P.; Lapierre, J. M.; Greiveldinger, G.; Seebach, D. Synthesis and properties of first and second generation chiral dendrimers with triply branched units. A spectacular case of diastereoselectivity. *Helv. Chim. Acta.* **1997**, *80*, 1648.

65. Murer, P.; Seebach, D. Synthesis and properties of monodisperse chiral dendrimers (up to fourth generation) with doubly branched building blocks. An intriguing solvent effect. *Helv. Chim. Acta* **1998**, *81*, 603.

66. Greiveldinger, G.; Seebach, D. Second-generation trifluoromethyl-substituted chiral dendrimers containing triply branched building blocks. CF3 as senstitive NMR probe for remote diastereotopicity. *Helv. Chim. Acta* **1998**, *81*, 1003.

67. Hudson, H. D.; Jung, H. T.; Percec, V.; Cho, W. D.; Johansson, G.; Ungar, G.; Balagurusamy, V. S. K. Direct visualization of individual cylindrical and spherical supramolecular dendrimers. *Science* **1997**, *278*, 449.

68. Percec, V.; Ahn, C. H.; Cho, W. D.; Jamieson, A. M.; Kim, J.; Leman, T.; Schmidt, M.; Gerle, M.; Moeller, M.; Prokhorova, S. A.; Sheiko, S. S.; Cheng, S. Z. D.; Zhang, A.; Ungar, G.; Yeardley, D. J. P. Visualizable cylindrical macromolecules with controlled stiffness from backbones containing libraries of self-assembling dendritic side groups. *J. Am. Chem. Soc.* **1998**, *120*, 8619.

69. Percec, V.; Cho, W. D.; Mosier, P. E.; Ungar, G.; Yeardley, D. J. P. Structural analysis of cylindrical and spherical supramolecular dendrimers quantifies the concept of monodendron shape control by generation number. *J. Am. Chem. Soc.* **1998**, *120*, 11061.

70. Percec, V.; Ahn, C. H.; Ungar, G.; Yeardley, D. J. P.; Moller, M.; Sheiko, S. S. Controlling polymer shape through the self-assembly of dendritic side-groups. *Nature* **1998**, *391*, 161.

71. Ungar, G.; Percec, V.; Holerca, M. N.; Johansson, G.; Heck, J. A. Heat-shrinking spherical and columnar supramolecular dendrimers: their interconversion and dependence of their shape on molecular taper angle. *Chem. Eur. J.* **2000**, *6*, 1258.

72. Miller, T. M.; Neenan, T. X. Convergent synthesis of monodisperse dendrimers based upon 1,3,5-trisubstituted benzenes. *Chem. Mater.* **1990**, *2*, 346.

73. Miller, T. M.; Neenan, T. X.; Zayas, R.; Bair, H. E. Synthesis and characterization of a series of monodisperse, 1,3,5-phenylene-based hydrocarbon dendrimers including C276H186 and their fluorinated analogs. *J. Am. Chem. Soc.* 1**992**, *114*, 1018.

74. Meier, H.; Lehmann, M. Stilbenoid dendrimers. *Angew. Chem. Int. Ed.* **1998**, *37*, 643.

75. Lehmann, M.; Schartel, B.; Hennecke, M.; Meier, H. Dendrimers consisting of stilbene or distyrylbenzene building blocks synthesis and stability. *Tetrahedron* **1999**, *55*, 13377.

76. Meier, H.; Lehmann, M.; Kolb, U. Stibenoid dendrimers. *Chem. Eur. J.* **2000**, *6*, 2462.

77. Pillow, J. N. G.; Halim, M.; Lupton, J. M.; Burn, P. L.; Samuel, I. D. W. A facile

iterative procedure for the preparation of dendrimers containing luminescent cores and stilbene dendrons. *Macromolecules* **1999**, *32*, 5985.

78. Pillow, J. N. G.; Burn, P. L.; Samuel, I. D. W.; Halim, M. Synthetic routes to phenylene vinylene dendrimers. *Synth. Met.* **1999**, *102*, 1468.

79. Halim, M.; Samuel, I. D. W.; Pillow, J. N. G.; Monkman, A. P.; Burn, P. L. Control of color and charge injection in conjugated dendrimer/polypyridine bilayer LEDs. *Synth. Met.* **1999**, *102*, 1571.

80. Halim, M.; Samuel, I. D. W.; Pillow, J. N. G.; Burn, P. L. Conjugated dendrimers for LEDs: control of color. *Synth. Met.* **1999**, *102*, 1113.

81. Halim, M.; Pillow, J. N. G.; Samuel, I. D. W.; Burn, P. L. Conjugated dendrimers for light-emitting diodes. Effect of generation. *Adv. Mater.* **1999**, *11*, 371.

82. Halim, M.; Pillow, J. N. G.; Samuel, I. D. W.; Burn, P. L. The effect of dendrimer generation on LED efficiency. *Synth. Met.* **1999**, *102*, 922.

83. Brouwer, A. J.; Mulders, S. J. E.; Liskamp, R. M. J. Convergent synthesis and diversity of amino acid based dendrimers. *Eur. J. Org. Chem.* **2001**, 1903.

84. Ulrich, K. E.; Fréchet, J. M. J. Synthesis of dendritic polyamides via a convergent growth approach. *J. Chem. Soc., Perkin Trans. 1* **1992**, 1623.

85. Miller, T. M.; Kwock, E. W.; Neenan, T. X. Synthesis of four generations of monodisperse aryl ester dendrimers based on 1,3,5-benzenetricarboxylic acid. *Macromolecules* **1992**, *25*, 3143.

86. Kwock, E. W.; Neenan, T. X.; Miller, T. M. Convergent synthesis of monodisperse aryl ester dendrimers. *Chem. Mater.* **1991**, *3*, 775.

87. Taylor, R. T.; Puapaiboon U. Polyurethane dendrimers via curtius reaction. *Tetrahedron Lett.* **1998**, *39*, 8005.

88. Puapaiboon, U.; Taylor, R. T. Characterization and monitoring reaction of polyurethane dendritic wedges and dendrimers using matrix-assisted laser desorption/ionization time-of-flight mass spectrometry. *Rapid Commun. Mass Spectrom.* **1999**, *13*, 508.

89. Chen, Y.-M.; Chen, C.-F.; Liu, W. H.; Xi, F. Synthesis of large building blocks for dendritic polyethers. *Polym. Bull.* **1996**, *37*, 557.

90. Höger, S. Methoxycarbonyl-terminated dendrons via the mitsunobu reaction: an easy way to functionalized hyperbranched building blocks. *Synthesis* **1997**, 20.

91. Kadei, K.; Moors, R.; Vögtle, F. Dendrimers and dendrimer building blocks with trisubstituted benzene and 'hexacyclene' as core units. *Chem. Ber.* **1994**, *127*, 897.

92. Louie, J.; Hartwig, J. F.; Fry, A. J. Discrete high molecular weight triarylamine dendrimers prepared by palladium-catalyzed amination. *J. Am. Chem. Soc.* **1997**, *119*, 11695.

93. Matsuda, K.; Nakamura, N.; Inoue, K.; Koga, N.; Iwamura, H. Toward dendritic two-dimensional polycarbenes: syntheses of 'starbust'-type nona- and dodecadiazo compounds and magnetic study of their photoproducts. *Bull. Chem. Soc. Jpn.* **1996**, *69*, 1483.

94. Stoddart, J. F.;Ashton, P. R.; Shibata, K.; Shipway, A. N. Polycationic dendrimers. *Angew. Chem., Int. Ed. Engl.* **1997**, *36*, 2781.

95. Baussanne, I.; Law, H.; Defaye, J.; Benito, J. M.; Mellet, C. O.; Garcia Fernandez, J. M. Synthesis and comparative lectin-binding affinity of mannosyl-coated β-cyclodextrin-dendrimer constructs. *Chem. Commun.* **2000**, 1489.

96. Leu, C. M.; Chang, Y. T.; Shu, C. F.; Teng, C. F.; Shiea, J. Synthesis and characterization of dendritic poly(ether imide)s. *Macromolecules* **2000**, *33*, 2855.

97. Pan, Y.; Ford, W. T. Dendrimers with alternating amine and ether generations. *J. Org. Chem.* **1999**, *64*, 8588.

98. Ingerl, A.; Neubert, I.; Klopsch, R.; Schlüter, A. D. Hydroxy-functionalized dendritic building block. *Eur. J. Org. Chem.* **1998**, 2551.

99. Klopsch, R.; Koch, S.; Schlüter, A. D. Amino-functionalized, second-generation dendritic building blocks. *Eur. J. Org. Chem.* **1998**, *5*, 1275.

100. Colonna, B.; Harding, V. D.; Nepogodiev, S. A.; Raymo, F. M.; Spencer, N; Stoddart, J. F. Synthetic carbohydrate dendrimers. Part 7. Synthesis of oligosaccharide dendrimers. *Chem. Eur. J.* **1998**, *4*, 1244.

101. Sadalapure, K.; Lindhorst, T. K. A general entry into glycopeptide dendrons. *Angew. Chem., Int. Ed.* **2000**, *39*, 2010.

102. Hudson, R. H. E.; Damha, M. J. Nucleic acid dendrimers: novel biopolymer structures. *J. Am. Chem. Soc.* **1993**, *115*, 2119.

103. Odian, G., Principles of Polymerization; Wiley Interscience: New York, Ed.3, 1991.

104. Rempp, P.; Herz, J. E., Encyclopedia of Polymer Science and Engineering ; Wiley: New York, Ed. 2, 1989.

105. Emrick, T.; Chang, H-T.; Fréchet, J. M. J. The preparation of hyperbranched aromatic and aliphatic polyether epoxides by chloride-catalyzed proton transfer polymerization from ABn and A2 + B3 monomers. *J. Polym. Sci., Part A: Polym. Chem.* **2000**, *38*, 4850.

106. Emrick, T.; Fréchet, J. M. J. Self-assembly of dendritic structures. *Curr. Opin. Colloid Interface Sci.* **1999**, *4*, 15.

107. Kim, Y. H.; Webster, O. W. Hyperbranched polymers. *J. Mol. Sci., Polym. Rev.* **2002**, *C42*, 55.

108. Kim, Y. H.; Webster, O. W. Water soluble hyperbranched polyphenylene: a unimolecular micelle?. *J. Am. Chem. Soc.* **1990**, *112*, 4592.

109. Bharathi, P; Moore, J. S. Solid-supported hyperbranched polymerization: evidence for self-limited growth. *J. Am. Chem. Soc.* **1997**, *119*, 3391.

110. Muzafarov, A. M.; Rebrov, E. A.; Gorbacevich, O. B.; Golly, M.; Gankema, H.; Moller, M. Degradable dendritic polymers – a template for functional pores and nanocavities. *Macromol. Symp.* **1996**, *102*, 35.

111. Miravet, J. F., Fréchet, J. M. J. New hyperbranched poly(siloxysilanes): variation of the branching pattern and end-functionalization. *Macromolecules* **1998**, *31*, 3461.

112. Chu, F.; Hawker, C. J. A versatile synthesis of isomeric hyperbranched poly(ether ketones). *Polym. Bull.* **1993**, *30*, 265.

113. Wooley, K. L.; Hawker, C. J.; Fréchet, J. M. J. One-step synthesis of hyperbranched dendritic polyesters. *J. Am. Chem. Soc.* **1991**, *113*, 4583.

114. Uhrich, K. E.; Hawker, C. J.; Fréchet, J. M. J.; Turner, S. R. One-pot synthesis of hyperbranched polyethers. *Macromolecules* **1992**, *25*, 4583.

115. Liu. M.; Vladimirov, N.; Fréchet, J. M. J. A new approach to hyperbranched polymers by ring opening polymerization of an AB monomer: 4-(2-hydroxyethyl)-ε-caprolactone. *Macromolecules* **1999**, *32*, 6881.

116. Hedrick, J. L.; Magbitang, T.; Connor, E. F.; Glauser, T.; Volksen, W.; Hawker, C. J.; Lee, V. Y.; Miller, R. D. Application of complex macromolecular architectures for advanced microelectronic materials. *Chem. Eur. J.* **2002**, *8*, 3308.

117. Jenkins A. D.; Kratochvil, P.; Stepto, R. F. T.; Suter, U. W. Glossary of

basic terms in polymer science. *Pure Appl. Chem.* **1996**, *68*, 2287.

118. Schlüter, A. D. Dendrimers with polymeric core: toward nanocylinder. *Top. Curr. Chem.* **1998**, *197*, 165.

119. Schlüter, A. D.; Rabe, J. P. Dendronized polymers: synthesis, characterization, assembly at interfaces and manipulation. *Angew. Chem. Int. Ed.* **2000**, *39*, 864.

120. Frey, H. From random coil to extended nanocylinder: dendrimer fragments shape polymer chains. *Angew. Chem. Int. Ed.* **1998**, *37*, 2193.

121. Bosman, A. W.; Janssen, H. M.; Meijer, E. W. About dendrimers: structure, physical properties, and applications. *Chem. Rev.* **1999**, 1665.

122. Hawker, C. J.; Fréchet, J. M. J. The synthesis and polymerization of a hyperbranched polyether macromonomer. *Polymer* **1992**, *33*, 1507.

123. Percec, V.; Heck, J. Liquid crystalline polymers containing mesogenic units based on half-disk and rod-like moieties. Synthesis and characterization of 4-(11-undecan-1-yloxy)-4'-[3,4,5-tri(p-n-dodecan-1-yloxybenzyloxy)benzoate]biphenyl side groups. *J. Polym. Sci., Part A: Polym. Chem.* **1991**, *29*, 591.

124. Percec, V.; Heck, J.; Ungar, G. Liquid crystalline polymers containing mesogenic units based on half-disk and rodlike moieties. Side chain liquid-crystalline poly(methylsiloxanes) containing hemiphasmidic mesogens based on 4-[[3,4,5-tris(alkan-1-yloxy)benzoyl]oxy]-4'-[[p-(propan-1-yloxy)benzoyl]oxy]biphenyl groups. *Macromolecules* **1991**, *24*, 4957.

125. Percec, V.; Lee, M.; Heck, J.; Blackwell, H. E.; Ungar, G.; Alvarez-Castillo, A. Reentrant isotropic phase in a supramolecular disc-like oligomer of 4-[3,4,5-tris(n-dodecyloxy)benzoyloxy]-4'-[(2-vinyloxy)ethoxy]biphenyl. *J. Mater. Chem* **1992**, *2*, 931.

126. Percec, V.; Heck, J.; Lee, M.; Ungar, G.; Alvarez-Castillo, A. Poly[2-vinyloxyethyl 3,4,5-tris[4-(n-dodecanyloxy)benzyloxy]benzoate]: a self assembled supramolecular polymer similar to tobacco mosaic virus. *J. Mater. Chem.* **1992**, *2*, 1033.

127. Percec, V.; Heck, J.; Tomazos, D.; Falkenberg, F.; Blackwell, H. E.; Ungar, G. Self-assembly of taper-shaped monoesters of oligo(ethylene oxide) with 3,4,5-tris(p-dodecyloxybenzyloxy) benzoic acid and their polymethacrylates into tubular supramolecular architectures displaying a columnar mesophase. *J. Chem. Soc. Perkin Trans. 1.* **1993**, *1*, 2799.

128. Freudenberger, R.; Claussen, W.; Schlüter, A. D.; Wallmeier, H. Functionalized rod-like polymers one-dimensional rigid matrixes. *Polymer* **1994**, *35*, 4496.

129. Zhang, A.; Shu, L.; Bo, Z.; Schlüter, A. D. Dendronized polymers: recent progress in synthesis. *Macromol. Chem. Phys.* **2003**, *204*, 328.

130. Sato, T.; Jiang, D –L.; Aida, T. A blue-luminescent dendritic rod: poly(phenyleneethynylene) within a light-harvesting dendritic envelope. *J. Am. Chem. Soc.* **1999**, *121*, 10658.

131. Bao, Z.; Amudson, K. R.; Lovinger, A. J. Poly(phenylenevinylene)s with dendritic side chains: synthesis, self-ordering, and liquid crystalline properties. *Macromolecules* **1998**, *31*, 8647.

132. Jakubiak, R.; Bao, Z.; Rothberg, L. Dendritic side groups as three-dimensional barriers to aggregation quenching of conjugated polymer fluorescence. *Synth. Met.* **2000**, 114, 61.

133. Pogantsch, A.; Wenzl, F. P.; List, E. J. W.; Leising, G.; Grimsdale, A. C.; Müllen, K. Polyfluorenes with dendron side chains as the active materials for polymer light-emitting devices. *Adv. Mater.* **2002**, *14*, 1061.

134. Malenfant, P. R. L.; Fréchet, J. M. J. Dendrimers as solubilizing groups for conducting polymers: preparation and characterization of polythiophene functionalized exclusively with aliphatic ether convergent dendrons. *Macromolecules* **2000**, *33*, 3634.

135. Goessl, I.; Shu, L.; Schlüter, A. D.; Rabe, J. P. Molecular structure of single DNA complexes with positively charged dendronized polymers. *J. Am. Chem. Soc.* **2002**, *124*, 6860.

136. Lee, C. C.; Yoshida, M.; Fréchet, J. M. J.; Dy, E. E.; Szoka, F. C. In vitro and in vivo evaluation of hydrophilic dendronized linear polymers. *Bioconjugate Chem.* **2005**, *16*, 535.

137. Lee, C. C.; Grayson, S. M.; Fréchet, J. M. J. Synthesis of narrow-polydispersity degradable dendronized aliphatic polyesters. *J. Polym. Sci., Part A: Polym. Chem.* **2004**, *42*, 3563.

138. Al-Jamal, K. T.; Ramaswamy, C.; Florence, A. T. Supramolecular structures from dendrons and dendrimers. *Adv. Drug Delivery Rev.* **2005**, *57*, 2238.

139. Stocker, W.; Karakaya, B.; Schürmann, B. L.; Rabe, J. P.; Schlüter, A. D. Ordered dendritic nanorods with a poly(p-phenylene) backbone. *J. Am. Chem. Soc.* **1998**, *120*, 7691.

140. Stocker, W.; Schürmann, B. L.; Rabe, J. P.; Förster, S.; Lindner, P.; Neubert, I.; Schlüter, A. D. A dendritic nanocylinder. Shape control through implementation of steric strain. *Adv. Mater.* **1998**, *10*, 793.

141. Bo, Z.; Rabe, J. P.; Schlüter, A. D. A poly(para-phenylene) with hydrophobic and hydrophilic dendrons: prototype of an amphiphilic cylinder with the potential to segregate lengthwise. *Angew. Chem. Int. Ed.* **1999**, *38*, 2370.

142. Jenkins, A. D.; Kratochvil, P.; Stepto, R. F. T.; Suter, U. W. Glossary of basic terms in polymer science. *Pure Appl. Chem.* **1996**, *68*, 2287.

143. Sashiwa, H.; Shigemasa, Y.; Roy, R. Chemical modification of chitosan. 10. Synthesis of dendronized chitosan-sialic acid hybrid using convergent grafting of preassembled dendrons built on gallic acid and tri(ethylene glycol) backbone. *Macromolecules* **2001**, *34*, 3905.

144. Grayson, S. M.; Fréchet, J. M. J. Divergent synthesis of dendronized poly(p-hydroxystyrene) *Macromolecules* **2001**, *34*, 6542.

145. Martinez, C. A.; Hay, A. S. Synthesis of dendritic poly(arylene ether)s from a linear polymer core. *Polymer* **2002**, *43*, 3843.

146. Shu, L.; Schlüter, A. D.; Ecker, C.; Severin, N.; Rabe, J. P. Extremely long dendronized polymers: synthesis, quantification of structure perfection, individualization, and SFM manipulation. *Angew. Chem. Int. Ed.* **2001**, *40*, 4666.

147. Barner, J.; Mallwitz, F.; Shu, L.; Schlüter, A. D.; Rabe, J. P. Covalent connection of two individual polymer chains on a surface: an elementary step towards molecular nanoconstructions. *Angew. Chem. Int. Ed.* **2003**, *42*, 1932.

148. Mita, I.; Stepto, R. F. T.; Suter, U. W. Basic classification and definitions of polymerization reactions. *Pure Appl. Chem.* **1994**, *66*, 2483.

149. Penczek, S. Terminology of kinetics, thermodynamics, and mechanisms of polymerization. *J. Polym. Sci, Part A : Polym. Chem.* **2002**, *40*, 1665.

150. Andreopoulou, A. K.; Carbonnier, B.; Kallitsis, J. K.; Pakula, T. Dendronized rigid-flexible macromolecular architectures: syntheses, structure, and properties in bulk. *Macromolecules* **2004**, *37*, 3576.

151. Jiang, J.; Liu, H-W.; Zhao, Y-L.; Chen, C-F.; Xi, F. Synthesis of dendronized, chiral conjugated polymers with appendant Fréchet-type dendrons. *J. Polym. Sci, Part A : Polym. Chem.* **2002**, *40*, 1167.

152. Kim, Y.; Mayer, M. F.; Zimmerman, S. C. A new route to organic nanotubes from porphyrin dendrimers. Angew. Chem. Int. Ed. **2003**, *42*, 1121.

153. Bo, Z.; Zhang, C.; Severin, N.; Rabe, J. P.; Schlüter, A. D. Synthesis of amphiphilic poly(para-phenylene)s with pendant dendrons and linear chains. *Macromolecules* **2000**, *33*, 2688.

154. Kwon, Y. K.; Chvalun, S.; Schneider, A-I.; Blackwell, J.; Percec, V.; Heck, J. A. Supramolecular tubular structures of a polymethacrylate with tapered side groups in aligned hexagonal phases. *Macromolecules* **1994**, *27*, 6129.

155. Kwon, Y. K.; Chvalun, S.; Blackwell, J.; Percec, V.; Heck, J. A. Effect of temperature on the supramolecular tubular structure in oriented fibers of a poly(methacrylate) with tapered side groups. *Macromolecules* **1995**, *28*, 1552.

156. Percec, V.; Schlueter, A. D.; Kwon, Y. K.; Blackwell, J.; Möller, M.; Slangen, P. J. Dramatic stabilization of a hexagonal columnar mesophase generated from supramolecular and macromolecular columns by the semifluorination of the alkyl groups of their tapered building blocks. *Macromolecules* **1995**, *28*, 8807.

157. Percec, V.; Schlueter, D.; Ungar, G.; Cheng, S. Z. D.; Zhang, A. Hierarchical control of internal superstructure, diameter, and stability of supramolecular and macromolecular columns generated from tapered monodendritic building blocks. *Macromolecules* **1998**, *31*, 1745.

158. Percec, V.; Ahn, C. H.; Barboiu, B. Self-encapsulation, acceleration and control in the radical polymerization of monodendritic monomers via self-assembly. *J. Am. Chem. Soc.* **1997**, *119*, 12978.

159. Balagurusamy, V. S. K.; Ungar, G.; Percec, V.; Johannson, G. Rational design of the first spherical supramolecular dendrimers self-organized in a novel thermotropic cubic liquid-crystalline phase and the determination of their shape by X-ray analysis. *J. Am. Chem. Soc.* **1997**, *119*, 1539.

160. Percec, V.; Ahn, C. H.; Ungar, G.; Yeardley, D. J. P.; Möller, M.; Sheiko, S. S. Controlling polymer shape through the self-assembly of dendritic side-groups. *Nature* **1998**, *391*, 161.

161. Hudon, S. D.; Jung, H. T.; Percec, V.; Cho, W. D.; Johannson, G.; Ungar, G. Direct visualization of individual cylindrical and spherical supramolecular dendrimers. *Science* **1997**, *278*, 449.

162. Schrock, R. R. Olefin metathesis by well-defined complexes of molybdenum and tungsten. *Topics Organomet. Chem.* **1998**, *1*, 1.

163. Trnka, T. M.; Grubbs, R. H. The development of L2X2Ru:CHR olefin metathesis catalysts: an organometallic success story. *Acc. Chem. Res.* **2001**, *34*, 18.

164. Fürstner, A. Olefin metathesis and beyond. *Angew. Chem. Int. Ed.* **2000**, *39*, 3012.

165. Grubbs, R. H. Olefin metathesis. *Tetrahedron* **2004**, *60*, 7117.

166. Weck, M.; Schwab, P.; Grubbs, R. H. Synthesis of ABA triblock copolymers of

norbornenes and 7-oxanorbornenes via living ring-opening metathesis polymerization using well-defined, bimetallic ruthenium catalysts. *Macromolecules* **1996**, *29*, 1789.

167. Love, J. A.; Morgan, J. P.; Trnka, T. M.; Grubbs, R. H. A practical and highly active ruthenium-based catalyst that effects the cross metathesis of acrylonitrile. *Angew. Chem. Int. Ed.* **2002**, *41*, 4035.

168. Matyjaszewski, K.; Xia, J. Atom transfer radical polymerization. *Chem. Rev.* **2001**, *101*, 2921.

169. Kamigaito, M.; Ando, T.; Sawamoto, M. Metal-catalyzed living radical polymerization. *Chem. Rev.* **2001**, *101*, 3689.

170. Chong, Y. K.; Krstina, J.; Le, T. P. T. ; Moad, G. ; Postma, A.; Rizzardo, E.; Thang, S. H. Thiocarbonylthio compounds (S:C(Ph)S-R) in free radical polymerization with reversible addition-fragmentation chain transfer (RAFT polymerization). Effect of the free radical leaving group R. *Macromolecules* **2003**, *36*, 2256.

171. Chiefari, J.; Mayadunne, R. T. A.; Moad, C. L.; Moad, G.; Rizzardo, E.; Postma, A.; Skidmore, M. A.; Thang, S. H. Thiocarbonylthio compounds (S:C(Z)S-R) in free radical polymerization with reversible addition-fragmentation chain transfer (RAFT polymerization). Effect of the activating group Z. *Macromolecules* **2003**, *36*, 2273.

172. Ball, Z. T.; Sivula, K.; Fréchet, J. M. J. Well-defined fullerene-containing homopolymers and diblock copolymers with high fullerene content and their use for solution-phase and bulk organization. *Macromolecules* **2006**, *39*, 70.

173. Rajaram, S.; Choi, T-L.; Rolandi, M.; Fréchet, J. M. J. Synthesis of dendronized diblock copolymers via ring-opening metathesis polymerization and their visualization using atomic force microscopy. *J. Am. Chem. Soc.* **2007**, *129*, 9619.

174. Cheng, C. X.; Tang, R. P.; Zhao, Y. L.; Xi, F. Synthesis of dendronized poly(methacrylates) and their diblock copolymers by atom transfer radical polymerization. *J. Appl. Poly. Sci.* **2004**, *91*, 2733.

175. Percec, V.; Bera, T. K.; Glodde, M.; Fu, Q.; Balagurusamy, V. S. K.; Heiney, P. A. Hierarchical self-assembly, co-assembly, and self-organization of novel crystalline lattices and superlattices from a twin-tapered dendritic benzamide and its four-cylinder-bundle supramolecular polymer. *Chem. Eur. J.* **2003**, *9*, 921.

CHAPTER 2

Biological Applications of Dendrimers

2.1 Abstract

In this chapter, biological applications that rely on dendrimers are introduced. An overview of successes and limitations of present dendritic scaffolds is presented. Furthermore, the advantages of dendrimers for biological applications as well as the challenges prerequisite to its development and implementation in biological systems are addressed. Finally, a brief description of how dendrimers would be used for this thesis research is given.

2.2 Dendrimer Architecture for Medicine

The objective of bio-macromolecular constructs for medicine is to design controlled scaffolds on the nanoscale that allow for a deeper understanding of human ills and diseases as well as allow for the use of such scaffolds in treating such diseases. A technology platform that provides a wide range of synthetic nanostructures that may be controlled as a function of size, shape and surface chemistry and can be scaled comparable to the biological nano-materials such as DNA, RNA, proteins, viruses, cellular receptor sites will be critical. Many of these critical parameters can be addressed through the use of dendrimers and include the following:

(a) Monodisperse and smaller hydrodynamic volume compared to other polymers.

(b) Nanoscale sizes for passive targeting mediated by EPR (enhanced permeability retention) effect.

(c) Mathematically defined number of terminal surface groups suitable for conjugation of drugs, signaling groups, targeting moieties, biocompatible or cell-permeable groups that can be optimized as a function of generation level (Scheme 2.1).

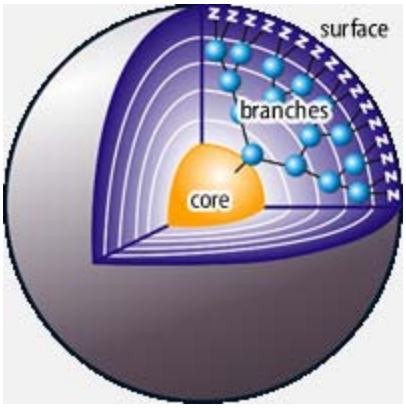

Figure 2.1 Schematic representation of a higher generation dendrimer depicting core, interior and surface[77] (Adapted image)

(d) Well-defined interior void space within the dendrimer suitable for encapsulation or isolation of small-molecule drugs, metals or signaling groups. Incarceration in this void space reduces drug toxicity and allows controlled release. The nature (hydrophobic versus hydrophilic) and size (increases with generation) of interior can be modulated.

2.3 Biocompatibility of Dendrimers

2.3.1 *In vitro* Toxicity

Dendrimers with cationic surface groups: Cationic macromolecules in general cause destabilization of the cell membrane resulting in cell lysis.[1] The exact mechanism of cytotoxicity caused by polycationic structures has not been fully revealed, although it is suggested[2] to be due to favored interactions between the negatively charged cell

membrane and, for dendrimers, the positively charged dendrimer surface, enabling adherence to cell membrane and its lysis. Earlier, comparative toxicity studies on different cell-lines concluded that amino-terminated G-5 poly-amidoamine (PAMAM) dendrimers had lower toxicity than lysine based dendrimers.[3] However, later, *in vitro* toxicity by IC_{50} measurements (concentration where 50% inhibition of mitochondrial dehydrogenase activity is measured) on amino-terminated PAMAM dendrimers showed significant toxicity on human intestinal adenocarcinoma Caco-2 cells.[4,5] In addition, cytotoxicity was shown to be generation dependent for amino terminated PAMAM, with higher generation dendrimers being the most cytotoxic.[4,6,7] For amino terminated poly-propyleneimine (PPI) dendrimers, a similar generation dependent increase in cytotoxicity has been found, with the higher generation dendrimers being the most cytotoxic (IC_{50}< 5 μg mL^{-1} for G-5 PPI).[8] Also, haematotoxicity studies using amino terminated PAMAM and PPI dendrimers concluded that dendrimers have a haemolytic effect on a solution of rat blood cells which increases with increasing dendrimer generation.[9] In summary, amino-terminated dendrimers were shown to be generally cytotoxic.[9]

Dendrimers with anionic and neutral surface groups: Recent toxicity studies of anionic carboxyl terminated 'half generation' PAMAM at lower generations showed neither haematotoxicity nor cytotoxicity compared to amine terminated PAMAM at the same generation.[4,9] However, the biocompatibility of dendrimers is not determined by the nature of surface groups. Dendrimers based on aromatic polyether skeletons having anionic carboxylate groups on surface were shown to be haemolytic, suggested by the aromatic interior of dendrimer causing haemolysis through hydrophobic membrane contact.[9]

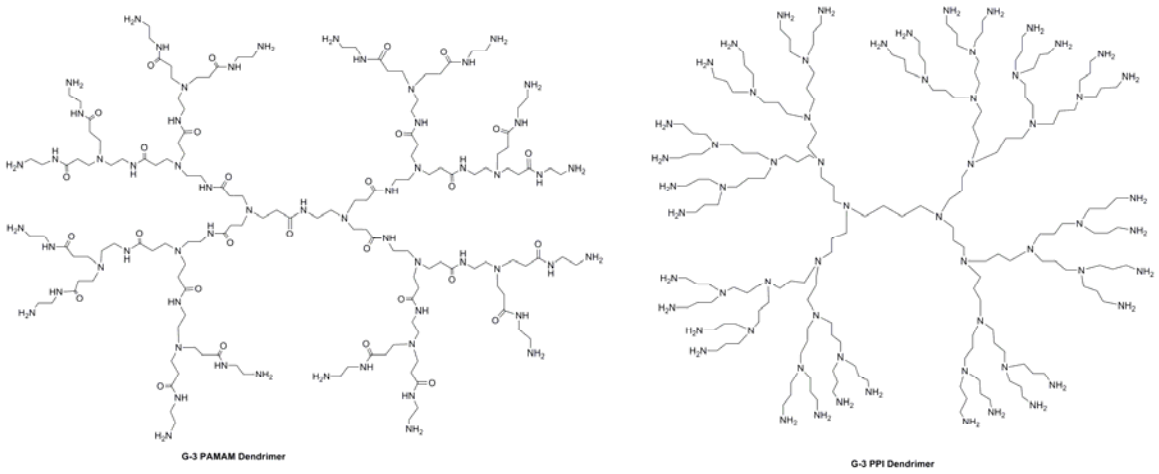

Figure 2.2 Common commercially available dendrimers: polyamidoamine (PAMAM) dendrimer and polypropylene imine (PPI) dendrimer (Adapted image)

Upon partial derivitization of PAMAM dendrimer surface amines with chemically inert functionalities like poly(ethylene glycol) (PEG) or fatty acids or aliphatic ethers, the cytotoxicity towards Caco-2 cells was reduced significantly (from IC_{50} ~0.13 mM to > 1 mM). However, introduction of large number of lipid chains increased the cytotoxicity of the system, due to cell lysis by hydrophobic interactions.[4] In summary, positive biocompatibility patterns were associated with lower generations (G1- G4), anionic or neutral polar terminal surface groups compared with higher generations neutral apolar and cationic surface groups.[2,4,10-12] Non/low-immunogenicity properties for dendrimers were induced by surface functionalization with PEG groups.[2,4,13]

2.3.2 *In vivo* Toxicity

Injections into mice with 10 mg ml^{-1} concentrations of PAMAM dendrimers did not appear to be cytotoxic, independent of whether they were modified or unmodified at the dendrimer surface.[6,14] Recently, hydroxyl- or methoxy-terminated dendrimers based on a polyester scaffold were shown to be non toxic both *in vitro* and *in vivo*.[12, 15] At very

high concentrations (40 mg mL^{-1}) these polyesters dendrimers induced some inhibition of cell growth *in vitro* but no increase in cell death was observed upon injection in mice.

2.4 Dendrimers as Nanoscale Scaffold

2.4.1 Dendrimers as Imaging Agents

Among the most common biological applications of dendrimers is their use as imaging agents or imaging agent carrier.[2] This part of thesis will introduce the use of dendrimers for magnetic resonance imaging. Paramagnetic metal chelates such Gd(III)-N,N´´,N´´´,N´´´´-tetracarboxymethyl-1,4,7,10-tetraazacyclododecane (Gd(III)-DOTA), Gd(III)-diethylenetriamine pentaacetic acid (Gd(III)-DTPA), and their derivatives increase the relaxation rate of surrounding water protons and are used as contrast agents for magnetic resonance imaging (MRI).[16-17] However, shortcomings of these low molecular weight contrast agents are short circulation times within the body and inefficient discrimination between diseased and normal tissue. As early as 1990, Lauterbur, Wiener and Tomalia pioneered the use of functionalized dendrimer scaffolds as MRI contrast agents by reporting some of the highest known relaxivities for these agents.[18-19] The extraordinary properties of dendrimers as MRI agents have been studied extensively *in vivo* during the last decade by Kobayashi and Brechbiel.[20-25] Dendrimer based MRI contrast agents have found to be effective at a 100 fold lower concentration of Gadolinium ions in comparison to the concentration of iodine atoms required for CT imaging.

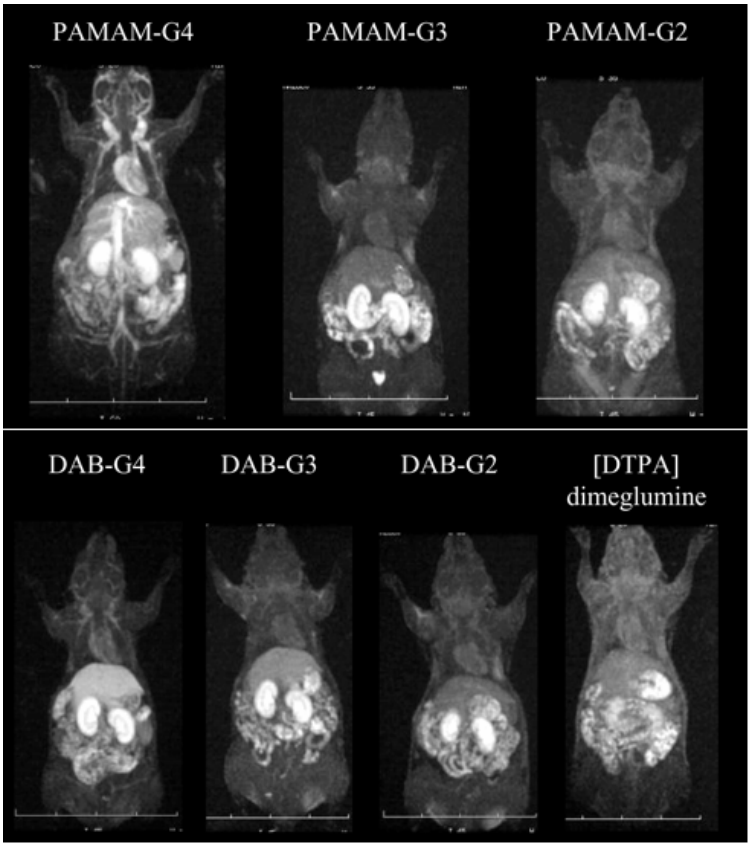

Figure 2.3 Whole body 3D-micro-MR imaging of a mouse injected with 0.03 mmol Gd/ kg of a dendrimer-Gd (DTPA) conjugate[21] (Adapted image)

These contrast enhancements using dendrimers appear to result from a combination of the geometrical amplifications of chelated gadolinium that is attached on a dendrimer surface and higher rotational correlation times with minimal segmental rotational motion that are intrinsic to the dendrimer conjugates.

A linear increase in the relaxivity as a function of molecular weight or generation were found in one study utilizing G-3 and G-5 PAMAM dendrimer chelates.[26] A less desired feature of these MRI dendrimers was the retention of up to 40% of the larger derivatives in the liver, even seven days after administration. This problem was addressed by the incorporation of PEG subunits into Gd(III)-chelated PAMAM dendrimers, reducing liver retention to 1-8%.[27] Another study used six small PAMAM

and diaminobutane (DAB) dendrimers for intravenous injection of 0.03 mmol Gd/kg of dendrimer.[21] Dynamic MRI found that brighter liver and kidney images were obtained with DAB based agents than PAMAM based agents or Gd-[DTPA]-dimeglumine alone. The blood signal–intensity values were significantly higher with G-4 PAMAM based agents than DAB based agents (Figure 2.3). It was also found that DAB based agents are cleared more rapidly from the body than PAMAM based agents with the same number of surface groups, identifying G-2 PAMAM and G-2, G-3 DAB dendrimers as potential contrast agents for clinical use.[21] More recently, it was found that the molecular size of dendrimer based MRI agents altered the route of excretion.[25] Contrast agents with molecular weights less than 60 kDa were excreted through the kidney resulting in these agents being potentially suitable as functional renal contrast agents. Hydrophilic and larger sized contrast agents were found better suited for use as blood pool contrast agents.[25] Finally, contrast agents conjugated to either monoclonal antibodies[28] or cyclic-RGD peptide[29] were able to function as tumor specific contrasts. The potential of these dendrimer based MRI agents has resulted in several commercial developments such as Gadomer-17.[13, 30,78]

Another tool for *in vivo* imaging using dendrimers is photonic oxygen sensing. Because the concentration of oxygen in certain tumors can indicate whether the tumor will respond to treatment, methods to accurately determine this parameter are desirable.[31] By encapsulating hydrophobic metalloporphyrins in the cores of variously sized poly(glutamic acid) (Figure 2.4), poly(aryl ether) or poly(ether amide) dendrimers, Vinogradov and co-workers[32-34] have prepared water-soluble oxygen sensors whose phosphorescence is quenched upon collision with dissolved oxygen.

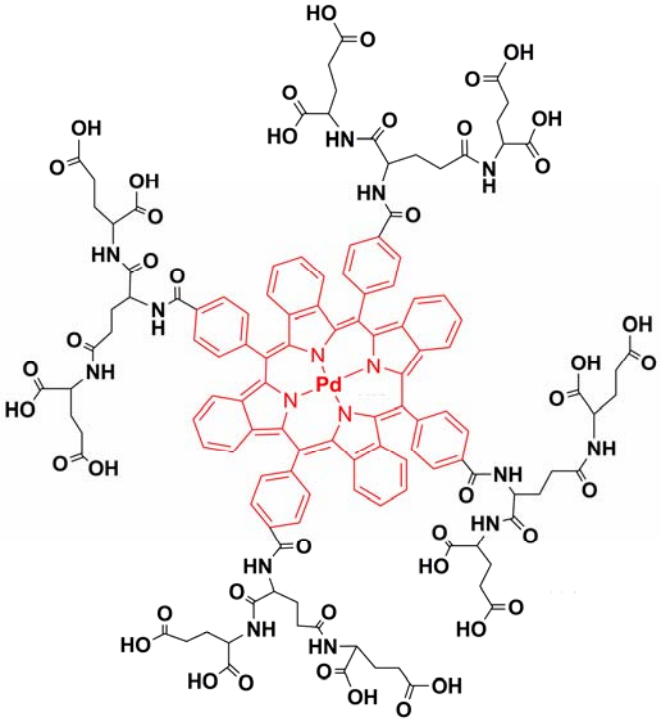

Figure 2.4 G-2 poly(glutamic acid) dendrimer with a tetra-benzoporphyrin core[33] (Adapted image)

Once present in the tissue of interest, the dendrimer sensor can be induced to phosphoresce by irradiating it with visible light or multiple photons of near infra-red light.[33, 34] The phosphorescence lifetime of the dendrimers is inversely related to the oxygen concentration and can be measured both *in vitro* and *in vivo*.[31] The metalloporphyrin, such as palladium-complexes of tetrabenzoporphyrins (Figure 2.4), has to be water soluble and protected from interactions with serum-borne macromolecules such as albumin. With improvement in current photophysical technology, the solubilizing and steric stabilizing core-shell architecture provided by dendrimers will be essential for accurate optical imaging.

2.4.2 Dendrimers as Delivery Devices

The surface of dendrimers provides an excellent platform for the attachment of cell-specific ligands, solubility modifiers, stealth molecules and imaging tags. The ability to attach any or all of these molecules in a well-defined manner onto a robust dendritic surface clearly differentiates dendrimers from other carriers such as micelles, liposomes, emulsion droplets, and engineered particles.

One example of cell-specific dendritic carriers is a dendrimer modified with folic acid.[35-39] Folate binding proteins are overexpressed on the surface of a variety of cancer cells. Baker and coworkers[35-37] and others[38-39] have carried out extensive studies with folate-dendrimer conjugates and shown them to be well-suited for targeted, cancer-specific drug delivery of cytotoxic substances. In one study,[40] the *in vitro* targeting and cell uptake properties of a G-5 PAMAM dendrimer conjugate to which folic acid, methotrexate (a widely used chemotherapeutic drug) and fluorescein isothiocyanate (FI) were coupled, was used (Figure 2.5). The surface amines of G-5 PAMAM were acetylated with acetic anhydride to reduce nonspecific binding of the dendrimer. The cell uptake of dendrimers was measured in KB cells that express a high cell surface folic acid receptor. Confocal microscopy demonstrated cellular internalization of this trifunctional dendrimer (as shown in Figure 2.6), and an induced time and dose dependent inhibition of cell growth in KB cells.[40] Recently, folate-PAMAM dendrimers have been used successfully as carriers of boron isotopes in boron neutron-capture treatment of cancer tumors.[41]

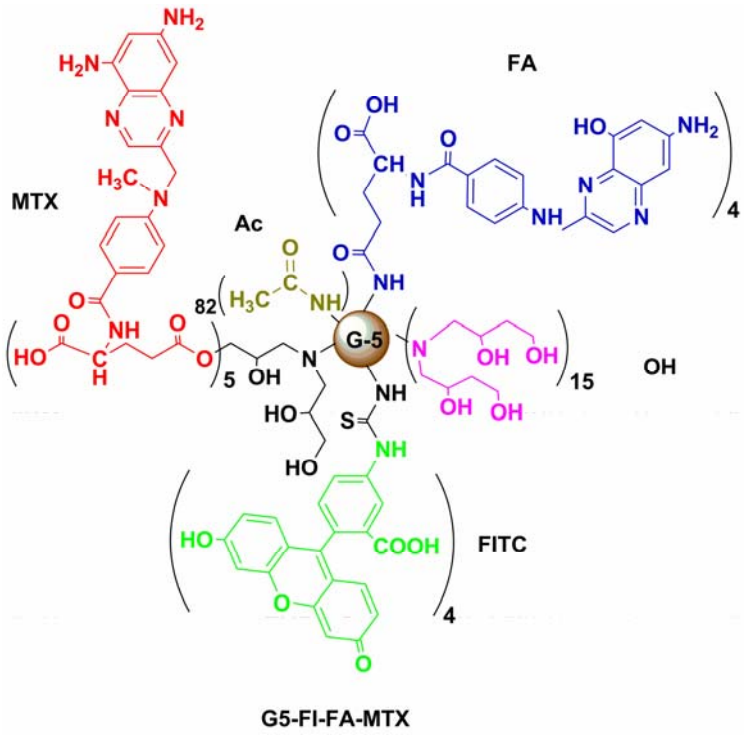

Figure 2.5 Schematic representation of a G-5 PAMAM dendrimer surface-functionalized with FITC, FA and MTX by Baker and coworkers[40] (Adapted image)

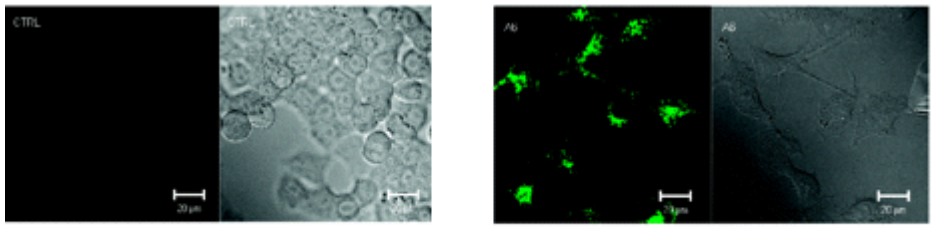

Figure 2.6 Confocal microscopy of KB cells incubated with 250 nM of dendrimer conjugate[40] for 24 h (Adapted image)

Carbohydrates constitute another important class of biological recognition molecules, displaying a wide variety of spatial structures due to their branching possibility and anomericity. To achieve sufficiently high binding affinities between mono- and oligosaccharide ligands and cell membrane receptors, these ligands have to be presented to receptors in a multivalent or cluster fashion.[42-44]

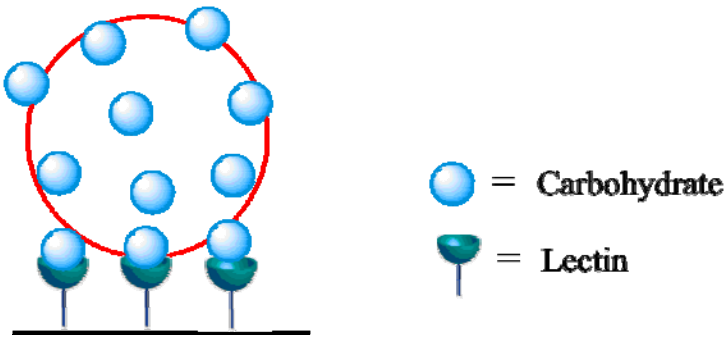

Figure 2.7 Multivalent carbohydrate binding of a glycodendrimer to lectin[44-50]

Numerous studies have shown that glycosylated dendrimers show multivalency and proximity effects in binding with natural carbohydrate proteins such as lectin (Figure 2.7).[44-50] The design and use of glycodendrimers for biomedical applications as vaccines has been investigated extensively.[44-50] In one study, glycodendrimers which have been prepared from the coupling of multibranched lysine dendrimers with mannose isothiocyanate showed enhancement of binding affinity towards macrophage/monocyte localized mannose-specific lectin. In particular, 300-400 times increase in affinity for the octameric adduct was observed compared to the monosaccharide.[45] In a recent study,[51] anionic PAMAM dendrimers (G-3.5) were conjugated to D(+)-glucoseamine and D(+)-glucoseamine 6-sulphate. These water-soluble conjugates not only revealed antiangiogenic properties but synergistically prevented scar tissue formation after glaucoma surgery. In a clinically relevant rabbit study, the long-term success of surgery by prevention of scar tissue formation was increased from 30% to 80%, using these dendrimer conjugates.[51]

Recently,[52] antibodies specific to CD14[53] and PSMA (prostrate specific membrane antigen)[55] were conjugated to a G-5 PAMAM dendrimer, bearing a fluorescein isothiocyanate (FI) imaging tag. Cell binding and internalization of the antibody-conjugated dendrimers to antigen expressing cells were evaluated by flow cytometry and confocal microscopy. It was found that the conjugates bind specifically to antigen expressing cells in a time- and dose-dependent fashion with an affinity similar to that of free antibody. Confocal microscopy indicated cellular internalization of the dendrimer conjugate (Figure 2.8).[52] Targeting of the dendrimers by attaching growth factors such as VEGF (Vascular endothelial growth factor) has also been investigated which showed binding of the dendrimer-VEGF conjugate to VEGF receptors comparable to native VEGF.[56]

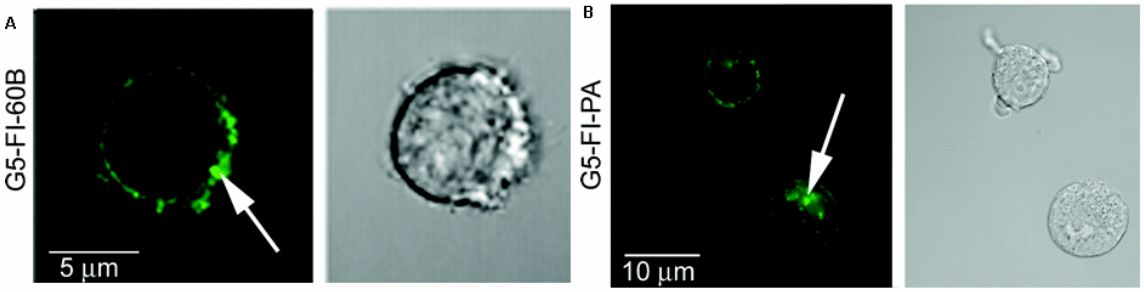

Figure 2.8 Confocal microscopic analysis of G5-FI-Antibody treated cells.[52] (A) HL-60 cells incubated with 12.5 nM G5-FI-Antibody 60 bca[54] for 1 h at 4 ˚C and then rinsed and image taken. Arrow indicates the binding of the conjugate on the cell surface. (B) Confocal image of LNCaP cells treated with 50 nm of G5-Fluorescein-Antibody PA[55] for 1 h at room temperature and then rinsed and image taken. Arrow indicates internalization of the conjugate at room temperature (Adapted image)

Numerous reports have been published on the possible use of amino terminated PAMAM and PPI dendrimers as non-viral gene transfer agents, enhancing the transfection of DNA into the cell nucleus.[57-61] The exact structure of these binding motifs

has not been determined in detail, but it is suggested to be based on acid-base interactions between the anionic phosphate moieties in the DNA backbone and the primary and tertiary amines in the dendrimer, which are positively charged under physiological conditions.[2] The synthesis of L-arginine grafted G-4 PAMAM has been reported recently.[62] By this surface modification by grafting L-arginine (Figure 2.9), the gene delivery efficiency is greatly enhanced in comparison to unmodified G-4 PAMAM, as shown in Figure 2.10. This transfection efficiency is better than that of PEI or lipofectamine, making PAMAM-Arg a promising non-viral vector.[62] In comparison to intact dendrimers, partially degraded dendrimers with more flexible structure have been found to have enhanced transfection efficiency for gene delivery by endocytic pathway.[63] The more flexible higher generation PPI dendrimers are found to be too cytotoxic for use as non-viral gene vectors, however lower generations are well suited for gene-delivery.[8]

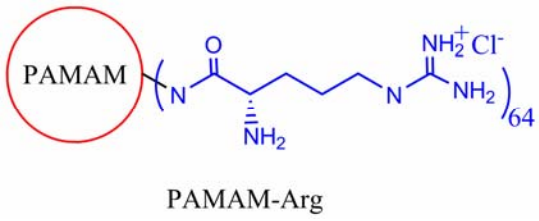

PAMAM-Arg

Figure 2.9 G-4 PAMAM dendrimer modified with L-arginine on its surface[62]

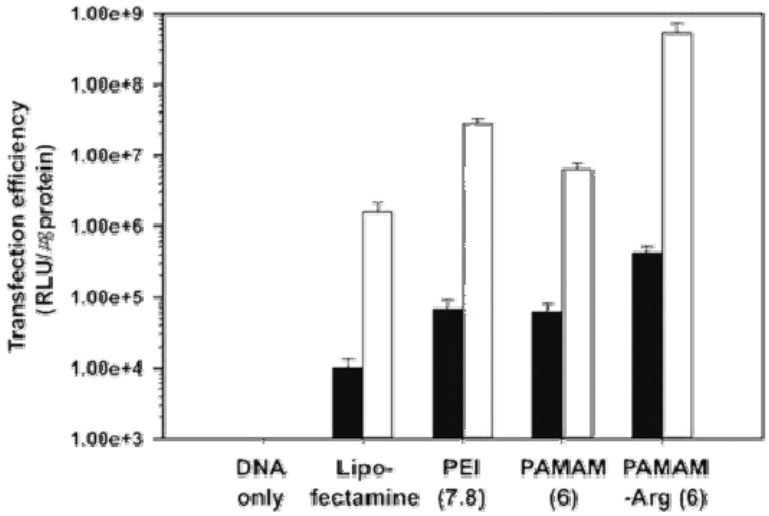

Figure 2.10 Transfection efficiency for Neuro 2A cell lines. Amount of DNA was 0.2 (black) and 1.0 μg (white). Values in parenthesis represent the charge ratio of the dendrimer/plasmid DNA complexes[62] (Adapted image)

2.5 Dendrimers as Nanocontainers

The interior of dendrimers is well-suited for the encapsulation of guest molecules and host-guest interactions. Tomalia demonstrated by electron microscopy that sodium carboxylated PAMAM dendrimers possess topologies of classical micelles.[64] The unimolecular micelle reported by the Fréchet group is based on a polyaryl ether dendrimeric network having carboxylate surface group, and capable of dissolving apolar guest molecules, such as pyrene.[65] The host guest binding is assumed to be mediated through π-π interactions between the electron rich aryl ether and the aromatic guest.[66] Dendrimers specifically tailored to bind hydrophobic guests to the core have been created by Diederich *et al.* under the name of 'dendrophanes'.[67-68] The water soluble dendrophanes are centered around a 'cyclophane' core and can bind aromatic compounds via π-π interactions. These dendritic structures were shown to be excellent carriers of steroids (Figure 2.11).[67-68] In one study, encapsulation of the well-known anticancer drug

cis-platinum within PAMAM dendrimers gave conjugates that exhibited slower release and higher accumulation in solid tumors along with lower toxicity compared to free cisplatin.[69] Similarly, encapsulation of silver salts within PAMAM dendrimers produced conjugates exhibiting slower silver release rates and antimicrobial activity against various Gram positive bacteria.[70]

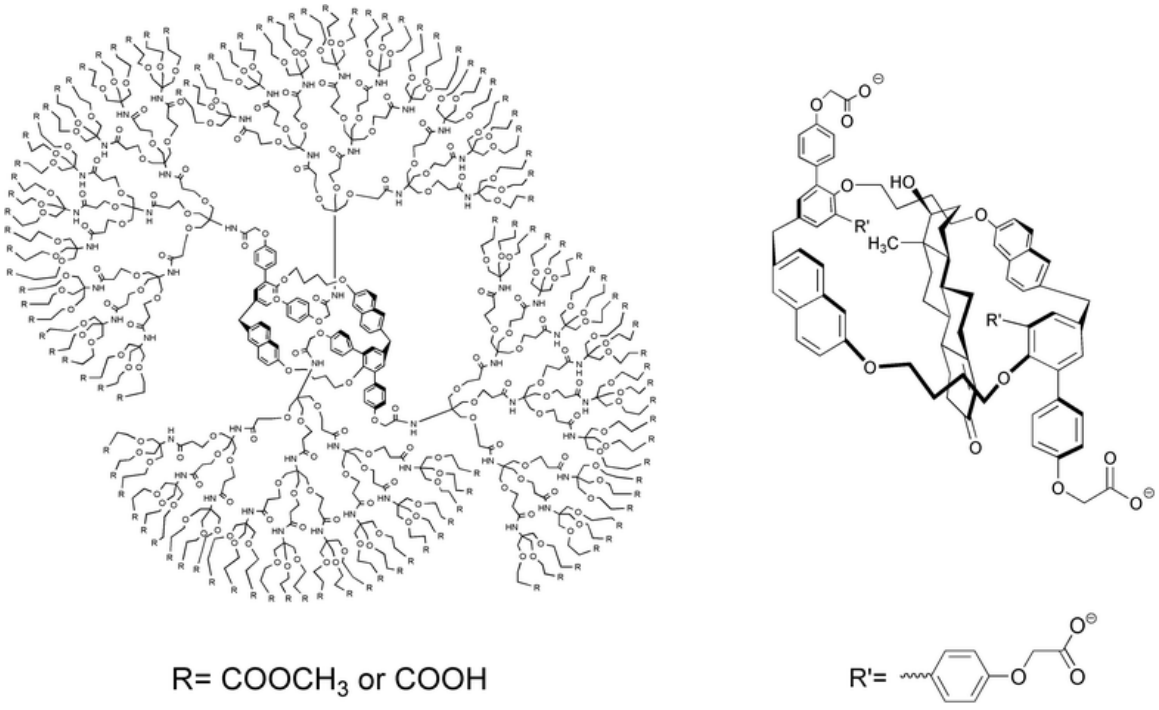

Figure 2.11 Left: G-3 Dendrophane for the encapsulation of steroids. Right: Host-guest binding motif upon complexation with testostorone[67-68] (Adapted image)

In another study, poly(ethyleneglycol) monomethyl ether chains with molecular weights around 550 and 2000 Da were attached to G3 and G4 PAMAM dendrimers.[71] The encapsulation behavior of these dendrimers (Figure 2.12) for the anticancer drug methotrexate was studied.[71,72] The highest encapsulation efficiency was found for G-4

PAMAM terminated with PEG_{2000} chains and the drug release from this dendrimer was slow at low ionic strength but fast in isotonic solution.[71]

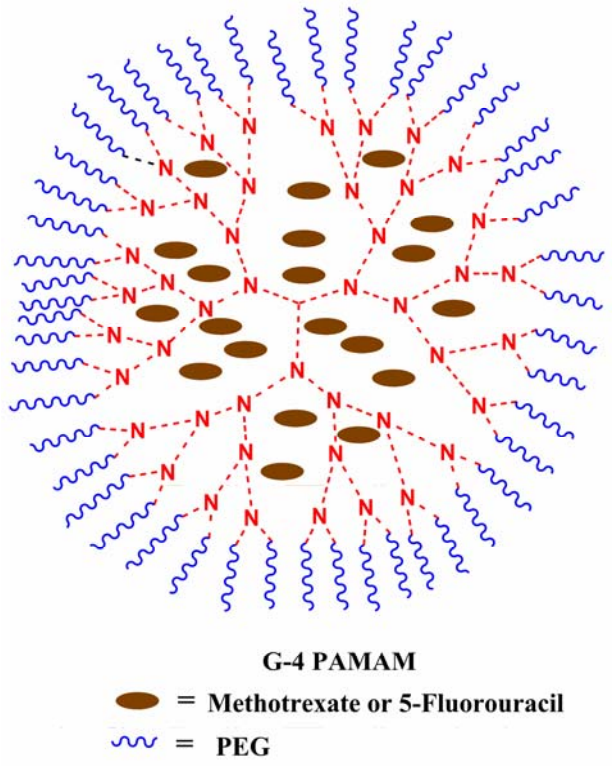

Figure 2.12 Schematic presentation of the encapsulation of anticancer drugs methotrexate or 5-fluorouracil into PEGylated G-4 PAMAM dendrimer[71,72]

The anticancer drug 5-fluorouracil encapsulated into G-4 PAMAM dendrimer with PEG_{5000} surface chains (Figure 2.12), revealed reduced release rate and hemolytic toxicity compared to non-PEGylated dendrimer.[72] Recent studies using Caco-2 cell lines have suggested that low generation PAMAM dendrimers cross cell membranes through combination of paracellular transport and absorptive endocytosis.[73]

2.6 Challenges, Design Elements and Perspectives

Several dendrimer types such as PAMAM, PEI that are commercially available have already found use as drug candidates for receptor-ligand interactions, drug carriers

for solubility and non-toxicity, membrane permeability as well as targeting as described above. Furthermore, dendrimers are increasingly finding use as scaffolds in the design of biosensors, imprinting and artificial receptors. Methods and strategies for synthesizing, modifying and derivatizing present or new dendrimers, for enabling specific tailoring of binding moieties need to be continually evolved to obtain higher degree of tunability for biological applications as well as creating entirely new class of bioactive substances based on dendrimers. However, the shortcomings of present systems remain the lack of easy derivatization of dendrimers with functional units of choice, non-selective and statistical functionalizations of present scaffolds for generating function.

After defining dendrimers and dendritic molecules and reviewing literature on their design, current functional utility and use in biological applications, several design elements and function need to be addressed and developed for the realization of the potential utility of dendrimers for biological and materials applications.

Specifically, these important areas include:

(i) The design and synthesis of selective functional motifs on the dendrimer surface for the generation of tunable dendritic materials for an array of biological or materials application via fast and efficient post-synthetic functionalization with desired functional unit.

(ii) The evaluation of these functional motifs along the dendrimer surface since they must adhere to several stringent design criteria including i) rapid and quantitative coupling yields with its complementary partner, ii) ability to operate independent of and in presence of another orthogonal functional handle, and iii) biocompatibility.

(iii) Development of other robust techniques for the characterization of dendrimers besides NMR and mass spectrometry. These techniques should pave the way and allow for unambiguous tracking of dendrimers as components of materials and biological scaffolds.

(iv) Development of biological labels which are dendrimer based and show no photobleaching, are extremely bright and biocompatible and allow for unambiguous scaffold specific information.

(v) Evaluation of cellular uptake of dendritic materials and its dependence on molecular weight to elucidate molecular transporter/translocator molecules and methodology.

(vi) As a secondary goal, the development of dendritic materials with enhanced functional utility and activity for use in catalysis.

Once addressed, the above-mentioned challenges, design elements and objectives would allow for realization of the final goal: the development of versatile functional dendritic architectures for biological and catalytic applications. The accomplishments of this research will pave the way for use of these materials and methodologies for building superior functional architectures for *in vitro* and *in vivo* applications in biology and for applications in catalysis.

The remaining thesis focuses on the experimental steps taken during the development and realization of dendritic architectures for the above-mentioned goals. The major strides made follow three major landmark achievements: (i) the design and synthesis of dendrimers with high degree of control over selective surface

functionalization methodologies and their orthogonal functional transformations (Chapter 3), (ii) the synthesis of dendrimers with Raman labels for scaffold specific characterization of dendrimers and as highly fluorescent noble-metal containing ultrabright biolabels (Chapter 4), (iii) the design and synthesis of dendritic molecules for studying cell transport and translocation methodology (Chapter 5), (iv) the synthesis and application of dendronized polymers for improved catalytic properties in heterogeneous systems (Chapter 6), and a detailed discussion on the potential future applications either already initiated such as for the development of a targeted *in vivo* self assembling delivery vehicle or suggested, which would bring in the full realization of the impact of this thesis work (Chapter 7).

2.7 References

1. Rittner, K.; Benavente, A.; Bompard, S.; Heitz, F.; Divita, G.; Brasseur, R.; Jacobs, E. New basic membrane destabilizing peptides for plasmid-based gene delivery in vitro and in vivo. *Mol. Therapy* **2002**, *5*, 104.

2. Boas, U.; Heegaard, M. H. Dendrimers in drug research. *Chem. Soc. Rev.* **2004**, *33*, 43.

3. Haensler, J.; Szoka Jr, F. C. Polyamidoamine cascade polymers mediate efficient transfection of cells in cluture. *Bioconjugate Chem.* **1993**, *4*, 372.

4. Jevprasesphant, R.; Penny, J.; Jalal, R.; Attwood, D.; Mckeown, N. B.; D'Emanuele, A. The influence of surface modification on the cytotoxicity of PAMAM dendrimers. *Int. J. Pharm.* **2003**, *252*, 263.

5. El Sayed, M.; Ginski, M.; Rhodes, C.; Ghandehari, H. Transepithelial transport of poly(amidoamine) dendrimers across Caco-2 cell monolayers. *J. Controlled Release* **2002**, *81*, 355.

6. Roberts, J. C.; Bhalgat, M. K.; Zera, R. T. Preliminary biological evaluation of polyamidoamine (PAMAM) starbust dendrimers. *J. Biomed. Mater. Res.* **1996**, *30*, 53.

7. Fischer, D.; Li, Y.; Ahlemeyer, B.; Krieglstein, J.; Kissel, T. In vitro cytotoxicity testing of polycations: influence of polymer structure on cell viability and hemolysis. *Biomaterials* **2003**, *24*, 1121.

8. Zinselmeyer, B. H.; Mackay, S. P.; Schatzlein, A. G.; Uchegbu, I. F. The lower-generation polypropyleneimine dendrimers are effective gene-transfer agents. *Pharmacol. Res.* **2002**, *19*, 960.

9. Malik, N.; Wiwattanapatapee, R.; Klopsch, R.; Lorenz, K.; Frey, H.; Weener, J. W.; Meijer, E. W.; Paulus, W.; Duncan, R. Dendrimers: Relationship between structure and biocompatibility in vitro, and preliminary studies on the biodistribution of ^{125}I-labelled polyamidoamine dendrimers in vivo. *J. Controlled Release* **2000**, *65*, 133.

10. Kolhe, P.; Khandare, J.; Pillai, O.; Kannan, S.; Lieh-Lai, M.; Kannan, R. M. Preparation, cellular transport, and activity of polyamidoamine-based dendritic nanodevices with a high drug payload. *Biomaterials* **2006**, *27*, 660.

11. Kannan, S.; Kolhe, P.; Raykova, V.; Glibatec, M.; Kannan, R. M., Leih-Lai, M.; Bassett, D. Dynamics of cellular entry and drug delivery by dendritic polymers into human lung epithelial carcinoma cells. *J. Biomater. Sci. Polymer Edn.* **2004**, *15*, 311.

12. Padilla De Jesús, O. L.; Ihre, H. R.; Gagne, L.; Fréchet, J. M. J. ; Szoka, F. C. Polyester dendritic systems for drug delivery applications: in vitro and in vivo evaluation. *Bioconjugate Chem.* **2002**, *13*, 453.

13. Svenson, S.; Tomalia, D. A. Dendrimers in biomedical applications- reflections on the field. *Adv. Drug Deliv. Rev.* **2005**, *57*, 2106.

14. Bourne, N.; Stanberry, L. R.; Kern, E. R.; Holan, G.; Matthews, B.; Bernstein, D. I. Dendrimers, a new class of candidate topical microbiocides with activity against herpes simplex virus infection. *Antimicrob. Agents Chemother.* **2000**, *44*, 2471.

15. Ihre, H. R.; Padilla, D.; Szoka, F. C.; Fréchet, J. M. J. Polyester dendritic systems for drug delivery applications: design, synthesis, and characterization. *Bioconjugate Chem.* **2002**, *13*, 443.

16. Hay, B. P.; Werner, E. J.; Raymond, K. N. Estimating the number of bound waters in Gd(III) complexes revisited. Improved methods for the prediction of *q*-values. *Bioconjugate Chem.* **2004**, *15*, 1496.

17. Doubrovin, M.; Serganova, I.; Mayer-Kuckuk, P.; Ponomarev, V.; Blasberg, R. G. Multimodality in vivo molecular-genetic imaging. *Bioconjugate Chem.* **2004**, *15*, 1376.

18. Wiener, E. C.; Brechbiel, M. W.; Brothers, H.; Magin, R. L.; Gansow, O. A.; Tomalia, D. A.; Lauterbur, P. C. Dendrimer-based metal chelates: a new class of magnetic resonance imaging contrast agents. *Magn. Reson. Med.* **1994**, *31*, 1.

19. Konda, S. D.; Aref, M.; Wang, S.; Brechbiel, M.; Wiener, E. C. Specific targeting of folate-dendrimer MRI contrast agents to the high affinity folate receptor expressed in ovarian tumor xenografts. *Magn. Reson. Mat.* **2001**, *12*, 104.

20. Kobayashi, H.; Brechbiel, M. W. Nano-sized MRI contrast agents with dendrimer cores. *Adv. Drug Deliv. Rev.* **2005**, *57*, 2271.

21. Kobayashi, H.; Kawamoto, S.; Jo, S-K.; Bryant, H. L.; Brechbiel, M. W.; Star, R. A. Macromolecular MRI contrast agents with small dendrimers: pharmacokinetic differences between sizes and cores. *Bioconjugate Chem.* **2003**, *14*, 388.

22. Talanov, V. S.; Regino, C. A. S.; Kobayashi, H.; Bernardo, M.; Choyke, P. L.; Brechbiel, M. W. Dendrimer-based nanoprobe for dual modality magnetic resonance and fluorescence imaging. *Nano Lett.* **2006**, *6*, 1459.

23. Kobayashi, H.; Kawamoto, S.; Choyke, P. L.; Sato, N.; Knopp, M. V.; Star, R. A.; Waldmann, T. A.; Tagaya, Y.; Brechbiel, M. W. Comparison of dendrimer-based macromolecular contrast agents for dynamic micro-magnetic resonance lymphangiography. *Magn. Reson. Med.* **2003**, *50*, 758.

24. Kobayashi, H.; Kawamoto, S.; Star, R. A.; Waldmann, T. A.; Tagaya, Y.; Brechbiel, M. W. Micro-magnetic resonance lymphangiography in mice using a novel dendrimer-based magnetic resonance imaging contrast agent. *Cancer Res.* **2003**, *63*, 271.

25. Kobayashi, H.; Brechbiel, M. W. Dendrimer-based macromolecular MRI contrast agents: characteristics and application. *Mol. Imaging* **2003**, *2*, 1.

26. Bryant, L. H.; Brechbiel, M. W.; Wu, C.; Bulte, J. W. M.; Herynek, V.; Frank, J. A. Synthesis and relaxometry of high generation (G = 5, 7, 9, and 10) PAMAM-dendrimer-DOTA-gadolinium chelates. *J. Magn. Reson. Imaging* **1999**, *9*, 348.

27. Margerum, L. D.; Campion, B. K.; Koo, M.; Shargill, N.; Lai, J. J.; Marumoto, A.; Sontum, P. C. Gadolinium (III) DO3A macrocycles and polyethylene glycol coupled to dendrimers. Effect of molecular weight on physical and biological properties of macromolecular magnetic resonance imaging contrast agents. *J. Alloys Compd.* **1997**, *249*, 185.

28. Kobayashi, H.; Sato, N.; Saga, T.; Nakamoto, Y.; Ishimori, T.; Toyama, S.; Togashi, K.; Konishi, J.; Brechbiel, M. W. Monoclonal antibody-dendrimer conjugates enable radiolabeling of antibody with markedly high specific activity with minimal loss of immunoreactivity. *Eur. J. Nuclear Med.* **2000**, *27*, 1334.

29. Dijkgraaf, I.; Rijnders, A. Y.; Soede, A.; Dechesne, A. C.; Wilma van Esse, G.; Brouwer, A. J.; Corstens, F. H. M.; Boerman, O. C.; Rijkers, D. T. S.; Liskaml, R. M. J. Synthesis of DOTA-conjugated multivalent cyclic-RGD peptide dendrimers via 1,3 dipolar cycloaddition and their biological evaluation: implications for tumor targeting and tumor imaging purposes. *Org. Biomol. Chem.* **2007**, *5*, 935.

30. Roberts, H. C.; Saeed, M.; Roberts, T. P. L.; Mühler, A.; Brasch, R. C. MRI of acute myocardial ischemia: comparing a new contrast agent, Gd-DTPA-24-cascade-polymer, with Gd-DTPA. *J. Magn. Reson. Imaging* **1999**, *9*, 204.

31. Ziemer, L. S.; Lee, W. M. F.; Vinogradov, S. A.; Sehgal, C.; Wilson, D. F. Oxygen distribution in murine tumors: characterization using oxygen-dependent quenching of phosphorescence. *J. Appl. Physiol.* **2005**, *98*, 1503.

32. Rozhkov, V.; Wilson, D.; Vinogradov, S. Phosphorescent Pd Porphyrin-dendrimers: tuning core accessibility by varying the hydrophobicity of the dendritic matrix. *Macromolecules* **2002**, *35*, 1991.

33. Dunphy, I.; Vinogradov, S. A.; Wilson, D. F. Oxyphor R2 and G2: phosphors for measuring oxygen by oxygen-dependent quenching of phosphorescence. *Anal. Biochem.* **2002**, *310*, 191.

34. Briñas, R. P.; Troxler, T.; Hochstrasser, R. M.; Vinogradov, S. A. Phosphorescent oxygen sensor with dendritic protection and two-photon absorbing antenna. *J. Am. Chem. Soc.* **2005**, *127*, 11851.

35. Quintana, A.; Raczka, E.; Piehler, L.; Lee, I.; Mye, A.; Majoras, I.; Patri, A. K.; Thomas, T.; Mule, J.; Baker Jr., J. R. Design and function of a dendrimer-based therapeutic nanodevice targeted to tumor cells through the folate receptor. *Pharm. Res.* **2002**, *19*, 1310.

36. Hong, S.; Bielinska, A. U.; Mecke, A.; Keszler, B.; Beals, J. L.; Shi, X.; Balogh, L.; Orr, B. G.; Baker Jr., J. R. Interaction of poly(amidoamine) dendrimers with supported lipid bilayers and cells: hole formation and the relation to transport. *Bioconjugate Chem.* **2004**, *15*, 774.

37. Majoras, I. J.; Myc, A.; Thomas, T.; Mehta, C. B.; Baker Jr., J. R. PAMAM dendrimer-based multifunctional conjugate for cancer therapy: synthesis, characterization, and functionality. *Biomacromolecules* **2006**, *7*, 572.

38. Ross, J. F.; Chaudhuri, P. K.; Ratnam, M. Differential regulation of folate receptor isoforms in normal and malignant tissues in vivo and in established cell lines. Physiologic and clinical implications. *Cancer* **1994**, *73*, 2432.

39. Kono, K.; Liu, M., Fréchet, J. M. J. Design of dendritic macromolecules containing folate or methotrexate residues. *Bioconjugate Chem.* **1999**, *10*, 1115.

40. Thomas, T. P.; Majoras, I. J.; Kotlyar, A.; Kukowska-Latallo, J. F.; Bielinska, A.; Myc, A.; Baker Jr., J. R. Targeting and inhibition of cell growth by an engineered dendritic nanodevice. *J. Med. Chem.* **2005**, *48*, 3729.

41. Shukla, S.; Wu, G.; Chatterjee, M.; Yang, W.; Sekido, M.; Diop, L. A.; Muller, R.; Sudimack, J. J.; Lee, R. J.; Barth, R. F.; Tjarks, W. Synthesis and biological evaluation of folate receptor-targeted boronated PAMAM dendrimers as potential agents for neutron capture therapy. *Bioconjugate Chem.* **2003**, *14*, 158.

42. Lundquist, J. J.; Toone, E. J. The cluster glycoside effect. *Chem. Rev.* **2002**, *102*, 555.

43. Zanini, D.; Roy, R. Synthesis of new *α*-thiosialodendrimers and their binding properties to the sialic acid specific lectin from *limax flavus*. *J. Am. Chem. Soc.* **1997**, *119*, 2088.

44. Bezouska, K. Design, functional evaluation and biomedical applications of carbohydrate dendrimers (glycodendrimers). *Rev. Mol. Biotechnol.* **2002**, *90*, 269.

45. Roy, R. Syntheses and some applications of chemically defined multivalent

glycoconjugates. *Curr. Opin. Struc. Biol.* **1996**, *6*, 692.

46. Lindhorst, T. K. Artificial multivalent sugar ligands to understand and manipulate carbohydrate-protein interactions. *Top. Curr. Chem.* **2002**, *218*, 201.

47. Rockendorf, N.; Lindhorst, T. K. Glycodendrimers. *Top. Curr. Chem.* **2001**, *217*, 201.

48. Veprek, P.; Jezek, J. Peptide and glycopeptide dendrimers. Part II. *J. Pept. Sci.* **1999**, *5*, 203.

49. Andre, S.; Pieters, R. J.; Vrasidas, I.; Kaltner, H.; Kuwabara, I.; Liu, F. T.; Liskamp, R. M.; Gabius, H. J. Wedgelike glycodendrimers as inhibitors of binding of mammalian galectins to glycoproteins, lactose maxiclusters, and cell surface glycoconjugates. *ChemBiochem.* **2001**, *2*, 822.

50. Pieters, R. J. Interference with lectin binding and bacterial adhesion by multivalent carbohydrates and peptidic carbohydrate mimics. *Trends Glycosci. Glycotechnol.* **2004**, 16, 243.

51. Shaunak, S.; Thomas, S.; Gianasi, E.; Godwin, A.; Jones, E.; Teo, I.; Mireskandari, K.; Luthert, P.; Duncan, R.; Patterson, S.; Khaw, P.; Brocchini, S. Polyvalent dendrimer glucosamine conjugates prevent scar tissue formation. *Nat. Biotechnol.* **2004**, *22*, 977.

52. Thomas, T. P.; Patri, A. K.; Myc, A.; Myaing, M. T.; Ye, J. Y.; Norris, T. B.; Baker Jr., J. R. In vitro targeting of synthesized antibody-conjugated dendrimer nanoparticles. *Biomacromolecules* **2004**, *5*, 2269.

53. Marcinkowska, E. Evidence that activation of MEK1,2/erk1,2 signal transduction pathway is necessary for calcitriol-induced differentiation of HL-60 cells. *Anticancer Res.* **2001**, *21*, 499.

54. Antal-Szalmas, P.; Strijp, P. J.; Weersink, A. J.; Verhoef, J.; Van Kessel, K. P. Quantitation of surface CD14 on human monocytes and neutrophils. *J. Leukocyte Biol.* **1997**, *61*, 721.

55. Bander, N. H.; Nanus, D. M.; Milowsky, M. I.; Kostakoglu, L.; Vallabahajosula, S.; Goldsmith, S. J., Targeted systemic therapy of prostrate cancer with a monoclonal antibody to prostrate-specific membrane antigen. *Semin. Oncol.* **2003**, *30*, 667.

56. Backer, M. V.; Gaynutdinov, T. I.; Patel, V.; Bandyopadhyaya, A.; Thirmumamagal, B. T. S.; Tjarks, W.; Barth, R. F.; Claffey, K.; Backer, J. M. Vascular endothelial growth factor selectively targets boronated dendrimers to tumor vasculature. *Mol. Cancer Ther.* **2005**, *4*, 1423.

57. Hughes, J. A.; Aronsohn, A. I.; Avrutskaya, A. V.; Juliano, R. L. Evaluation of adjuvants that enhance the effectiveness of antisense oligodeoxynucleotides. *Pharm. Res.* **1996**, *13*, 404.

58. Yoo, H.; Sazani, P.; Juliano, R. L. PAMAM dendrimers as delivery agents for antisense oligonucleotides. *Pharm. Res.* **1999**, *16*, 1799.

59. Lebedeva, I.; Benimetskaya, L.; Stein, C. A.; Vilenchik, M. Cellular delivery of antisense oligonucleotides. *Eur. J. Pharm. Biopharm.* **2000**, *50*, 101.

60. Jaaskelainen, I.; Peltola, S.; Honkakoski, P.; Monkkonen, J.; Urtti, A. A lipid carrier with a membrane active component and a small complex size are required for efficient cellular delivery of anti-sense phosphorothioate oligonucleotides. *Eur. J. Pharm. Sci.* **2000**, *10*, 187.

61. Dass, C. R. Vehicles for oligonucleotide delivery to tumors. *J. Pharm. Pharmacol.* **2002**, *54*, 3.

62. Choi, J. S.; Nam, K.; Park, J.; Kim, J. B.; Lee, J. K.; Park, J. Enhanced transfection efficiency of PAMAM dendrimer by surface modification with L-arginine. *J. Controlled Release* **2004**, *99*, 445.

63. Dennig, J.; Duncan, E. Gene transfer into eukaryotic cells using activated polyamidoamine dendrimers. *Rev. Mol. Biotechnol.* **2002**, *90*, 339.

64. Tomalia, D. A. Birth of a new macromolecular architecture: dendrimers as quantized building blocks for nanoscale synthetic organic chemistry. *Aldrichimica Acta* **2004**, *37*, 39.

65. Hawker, C. J.; Fréchet, J. M. J. Preparation of polymers with controlled molecular architecture. A new convergent approach to dendritic macromolecules. *J. Am. Chem. Soc.* **1990**, *112*, 7638.

66. Hawker, C. J.; Wooley, K. L.; Fréchet, J. M. J. Unimolecular micelles and globular amphiphiles: dendritic macromolecules as novel recyclable solubilization agents. *J. Chem. Soc., Perkin Trans.* **1993**, *1*, 1287.

67. Wallimann, P.; Marti, T.; Furer, A.; Diederich, F. Steroids in molecular recognition. *Chem. Rev.* **1997**, *97*, 1567.

68. Wallimann, P.; Seiler, P.; Diederich, F. Dendrophanes: novel steroid-recognizing dendritic receptors. *Helv. Chim. Acta.* **1996**, *79*, 779.

69. Malik, N.; Evagorou, E. G.; Duncan, R. Dendrimer-platinate: a novel approach to cancer chemotherapy. *Anticancer Drugs* **1999**, *10*, 767.

70. Balogh, L.; Swanson, D. R.; Tomalia, D. A.; Hagnauer, G. L.; McManus, A. T. Dendrimer-silver complexes and nanocomposites as antimicrobial agents. *Nano Lett.* **2001**, *1*, 18.

71. Kojima, C.; Kono, K.; Maruyama, K.; Takagishi, T. Synthesis of polyamidoamine dendrimers having poly(ethyleneglycol) grafts and their ability to encapsulate anticancer drugs. *Bioconjugate Chem.* **2000**, *11*, 910.

72. Bhadra, D.; Bhadra, S.; Jain, S.; Jain, N. K. A PEGylated dendritic nanoparticulate carrier of fluorouracil. *Int. J. Pharm.* **2003**, *257*, 111.

73. El-Sayed, M.; Rhodes, C. A.; Ginski, M.; Ghandehari, H. Transport mechanisms of poly(amidoamine) dendrimers across Caco-2 cell monolayers. *Int. J. Pharm.* **2003**, *265*, 151.

74. Tomalia, D. A.; Reyna, L. A.; Svenson, S. Dendrimers as multi-purpose nanodevices for oncology drug delivery and diagnostic imaging. *Biochem. Soc. Trans.* **2007**, *35*, 61.

75. Lee, C. C.; Mackay, J. A.; Fréchet, J. M. J., Szoka, F. C. Designing dendrimers for biological applications. *Nature Biotechnol.* **2005**, *23*, 1517.

76. Paleos, C. M.; Tsiourvas, D.; Sideratou, Z. Molecular engineering of dendritic polymers and their application as drug and gene delivery systems. *Mol. Pharm.* **2007**, *4*, 169.

77. http://dnanotech.com/images/dendrimerPurpleWeb-200.jpg

78. Gadomer 17 is produced by Schering AG, Berlin (Germany).

CHAPTER 3

Development of Mono- and Bifunctionalized Dendrimers with Selective Orthogonal Surface Sites for Biological Applications

3.1 Abstract

This chapter describes the methodology for the synthesis of four multifunctionalized dendrimers based on an orthogonal, functionalization strategy. This methodology was developed since reports of dendrimers with unique sites on the surface for post-synthetic manipulations are scarce and such dendritic synthons with one or two robust, reactive groups might have potential impact in targeted biological delivery and imaging. Polyamide based dendrimers possessing either a single aldehyde, a single azide, a single alkyne or both, azide and aldehyde moieties, on their periphery were synthesized using a convergent synthetic strategy. These dendrimers were functionalized quantitatively with small organic and biological molecules containing complementary functionalities to those on dendrimers, such as hydrazide, alkyne and azide groups, with complete specificity of each functional moiety for its complementary motif. This orthogonal functionalization methodology has the potential to develop and use these multifunctional dendritic synthons for a variety of applications ranging from targeted delivery vehicles for biological applications to optical materials

3.2 Introduction

The ability to directly import therapeutic agents into target cells and tissues and to direct them to specific organelles would greatly enhance their functional efficacy and remains a major goal in drug delivery. The available spectrum of cell penetrating peptide-based import signals[1-4] and intracellular routing signals might provide practical solutions towards achieving a guided or vectorial delivery of molecules. Nonviral chemical delivery techniques involving cationic lipids[5] and liposomes,[6,7] peptides,[8] dendrimers[9-11] and controlled release polymers[12] have mainly focused on the transport of therapeutic agents or plasmids across the eukaryotic cellular membrane into the cytoplasm. For further advances in tissue targeting, work on surface modification of such vehicles with antibodies,[13-14] proteins[15] or ligands[16-18] recognized by specific cell type or organelle is ongoing.

While significant progress has been made in targeted delivery, the development of alternate templates that favor the optimal presentation of functional signals and have a capacity for encapsulation is desirable. Through the use of dendrimers, one might be able to design well-defined, three-dimensional architectures, which are amenable to post synthetic surface manipulations, thereby creating biologically relevant and versatile materials. Here, we present a step towards this goal, the synthesis of selective orthogonal moieties on dendrimers and their recognition by complementary units on small biologically relevant and organic molecules.

In the burgeoning field of dendrimer chemistry, dendrimers terminated with either latent or reactive surface groups are common,[19-22] but these molecules cannot be manipulated to generate single or well-defined patterns of multiple functional groups.[23-26] Few examples in the literature, have dendrimers with different function on or in close

proximity to the periphery.[27-36] However, the development of dendrimers that have unique sites for surface manipulation[37-40] or orthogonal surface functional groups[41-44] for multifunctionalization has been scarce. Engineering fewer sites for manipulation greatly increases the synthetic challenge. The complexity of the targets varies significantly in both the number and arrangement of groups.

The earliest example of a dendrimer displaying a single latent group for post synthetic manipulation was reported in 1990 by Fréchet and Hawker.[43, 45] Hawker employed convergent approaches to prepare a dendrimer incorporating one, two or three cyano functionalities on their periphery, as shown in Figure 3.1. While this was neither orthogonal nor trivial in execution, it remained the solitary example of a selectively functionalized dendrimer for 10 years. Schlüter and coworkers in 2000, reported[39] dendrimers using Hawker's original strategy to display an aromatic bromide in three different positions, including one near the surface, as shown in Figure 3.2. Schlüter was the first to show further functionalization of these selectively present aryl bromide groups by cross-coupling with 4-tert-butylphenylboronic acids under Suzuki conditions. Simanek and coworkers, thereafter, used the melamine based dendrimers to construct dendritic structures with one or two boc-protected amine sites on the surface.[46] While the synthesis of Hawker and Schlüter using Fréchet type dendrimers exploited statistical reactions biased by sterics to obtain asymmetry, Simanek used the differential temperature reactivity of triazines to obtain asymmetry.

Thayumanavan and coworkers in 2002 reported a benzyl ether based dendrimer with two protected phenolic functional groups on its periphery.[47] This chapter reports the first study of dendrimers containing one or two robust, reactive and orthogonal functional groups on their periphery and their post-synthetic high yielding manipulations with small

organic and biomolecules.[48-49] These dendrimers allow easy coupling to a host of chemical moieties bearing complementary functionalities for development of versatile next-generation dendritic materials.

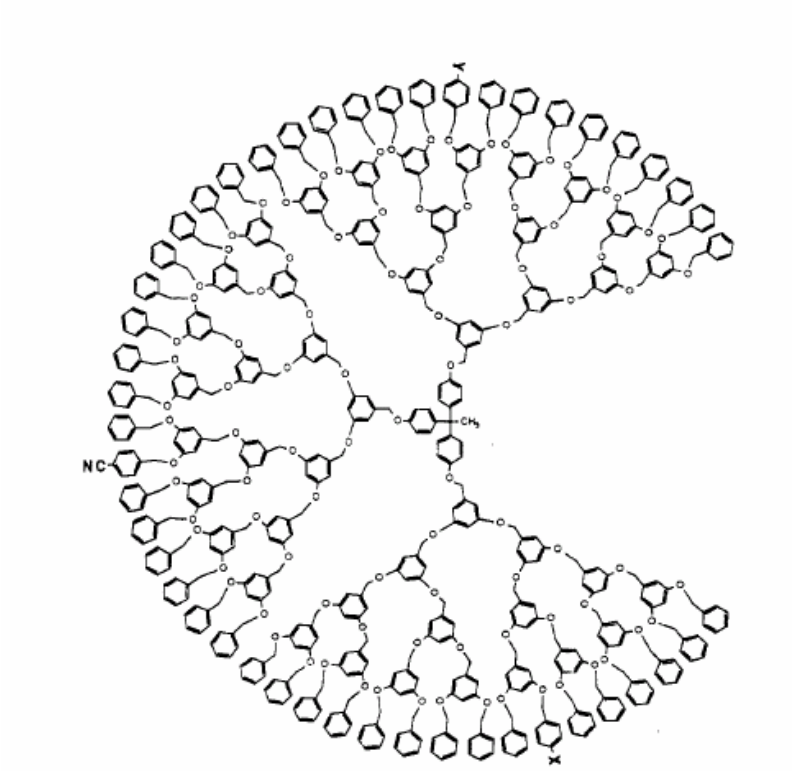

Figure 3.1 Fréchet's dendritic macromolecule containing varying number of cyano functionalities with X= H, Y=CN and X=Y=CN [43,45] (Adapted figure)

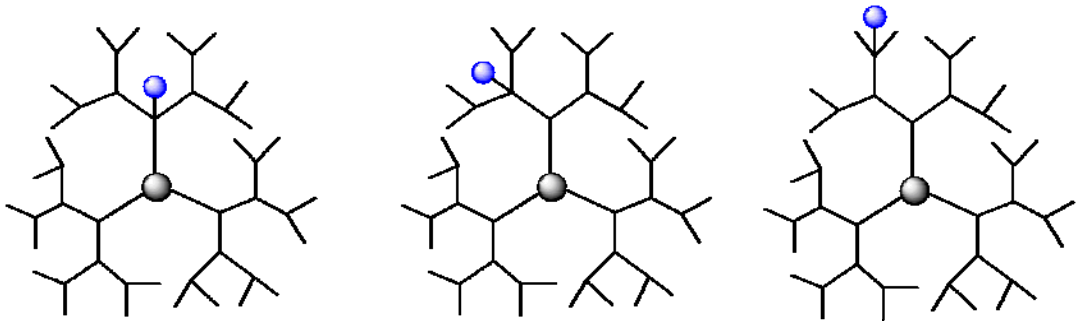

Figure 3.2 Schematic representation of Schlüter's aryl ether based dendrimer construction displaying an aryl bromide functional group (blue) in first, second and third generation[39] (Adapted figure)

For our purpose, we used Newkome's[50-52] non-functionalized dendron (Figure 3.3B and 3.3D), mono-functionalized 1→ (2+1) *C*-branching dendron (Figure 3.3C) and modified mono-functionalized 1→ (2+1) *C*-branching dendron (Figure 3.3E) for the introduction of selective functionalities on the dendrimers.

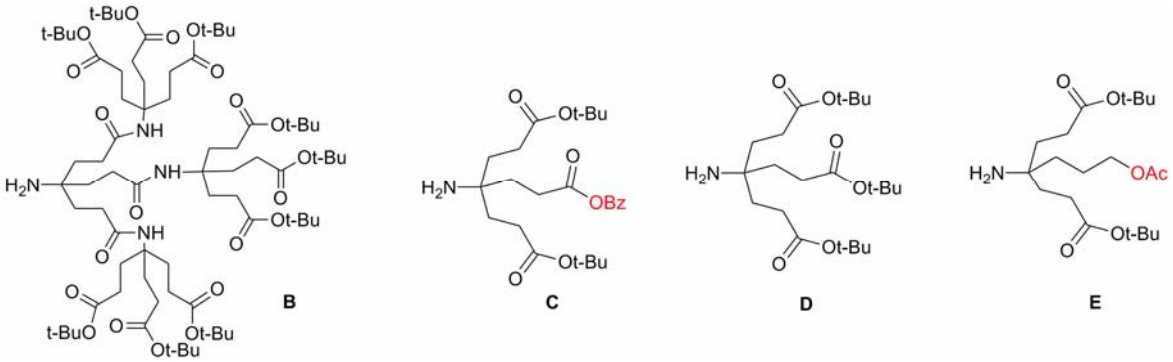

Figure 3.3 Newkome's nonfunctionalized (**B**, **D**) and monofunctionalized (**C, E**) branching units[50-52]

In this chapter, the development of mono and bi-functionalized dendritic scaffolds containing distinct, robust and highly selective orthogonal functional motifs along the dendrimer surface is presented which was accomplished in collaboration with Dr. Kunsang Yoon. The three functionalities utilized in this study are i) an aldehyde group

that allows for biocompatible addition of hydrazide or semicarbazide[53] and ii) an azide group and (iii) and an alkyne group that can be employed in 1,3-dipolar cycloadditions.[54-57] In particular, four classes of dendrimers having single alkyne, single azide, single aldehyde and both azide and aldehyde functionalities on the periphery were synthesized and investigated, as shown in Figure 3.4. Each of these four polyamide based dendrimers lead to either a monofunctionalized or bifunctionalized dendrimer having selectively present orthogonal functional moieties. We also investigated the capability of dendrimers **1**-**4** to couple with small organic and biological molecules. The couplings occurred quantitatively and the products were isolated in high yields. Ultimately this detailed study allowed us to develop novel multifunctionalized dendrimers that allow for either a one step post synthetic chemospecific multifunctionalization or a one step single dendrimer functionalization to construct tunable materials with unprecedented complexity.

3.3 Results and Discussion

3.3.1 Synthesis of Monofunctionalized and Bifunctionalized Dendrimers

The key building block in our design that introduces single and dual functionalities onto the dendrimer surface is dendron **A** (Scheme 3.2) which is obtained by a series of convergent steps from dendrons **7**, **C** and **D**.

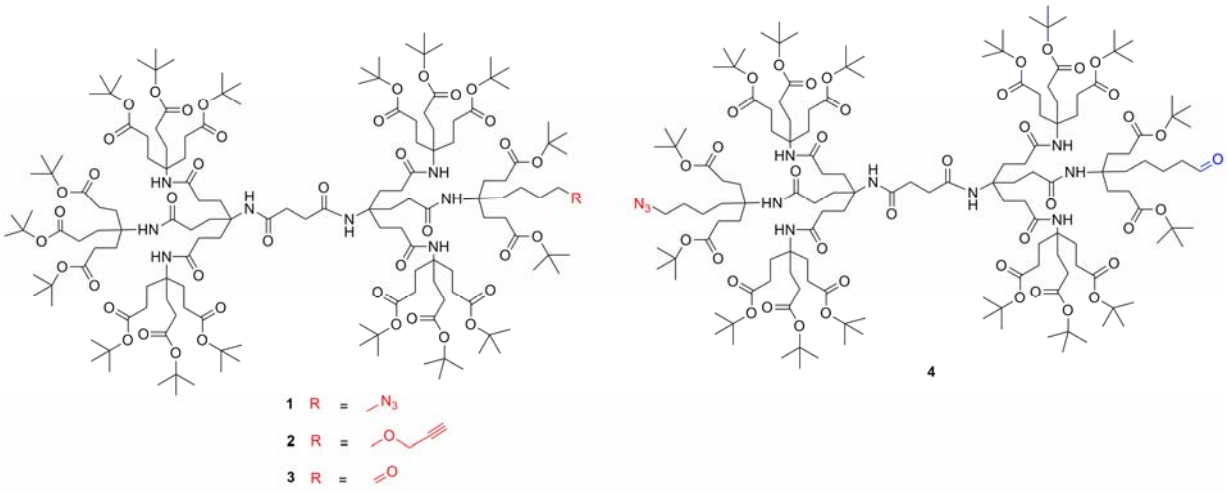

Figure 3.4 Synthesized dendritic scaffolds containing single azide **1**, alkyne **2**, aldehyde **3** and both azide and aldehyde **4** functionality on its periphery

Dendron **7** was obtained by Michael type addition of 6-nitrohexanol[58] to *t*-butyl acrylate in the presence of Triton B to provide monomer **5** in 55% yield. Subsequent acylation of the alcohol using acetic anhydride in pyridine followed by the catalytic reduction of the nitro group of **6** with H_2 under 60 psi in ethanol afforded **7** in 98% yields (Scheme 3.1).

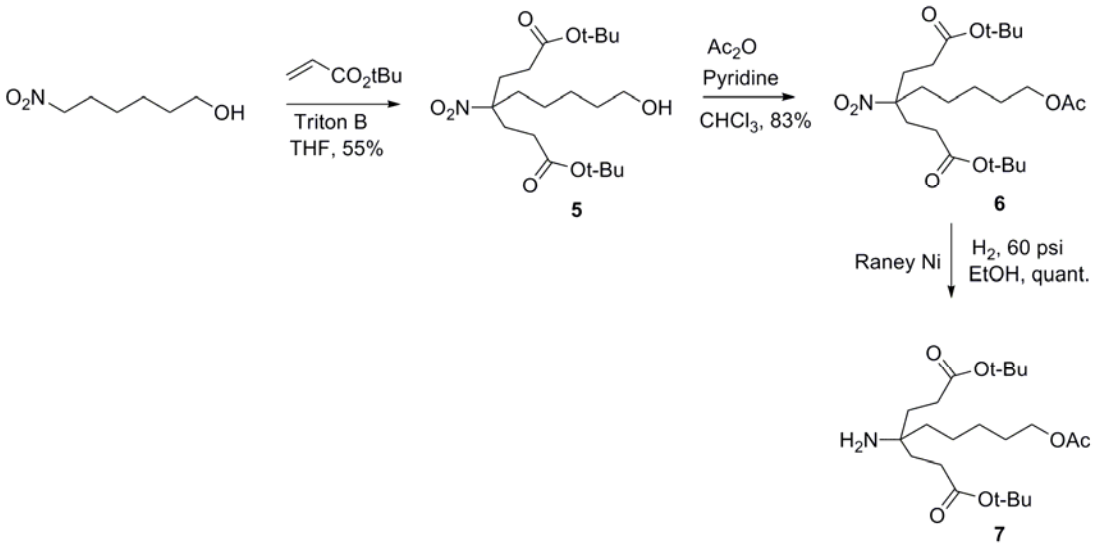

Scheme 3.1 Synthesis of the monofunctional first generation dendron **7**

The quantitative reduction of the nitro group to the amine was supported by a change in the ^{13}C chemical shift in the NMR spectra of the nitro-carbon from 92.8 ppm to 52.6 ppm for the amine-carbon. Other building blocks (**B**, **C, D)** were synthesized as reported by Newkome and coworkers.[50] A convenient route to **B** was published recently.[59]

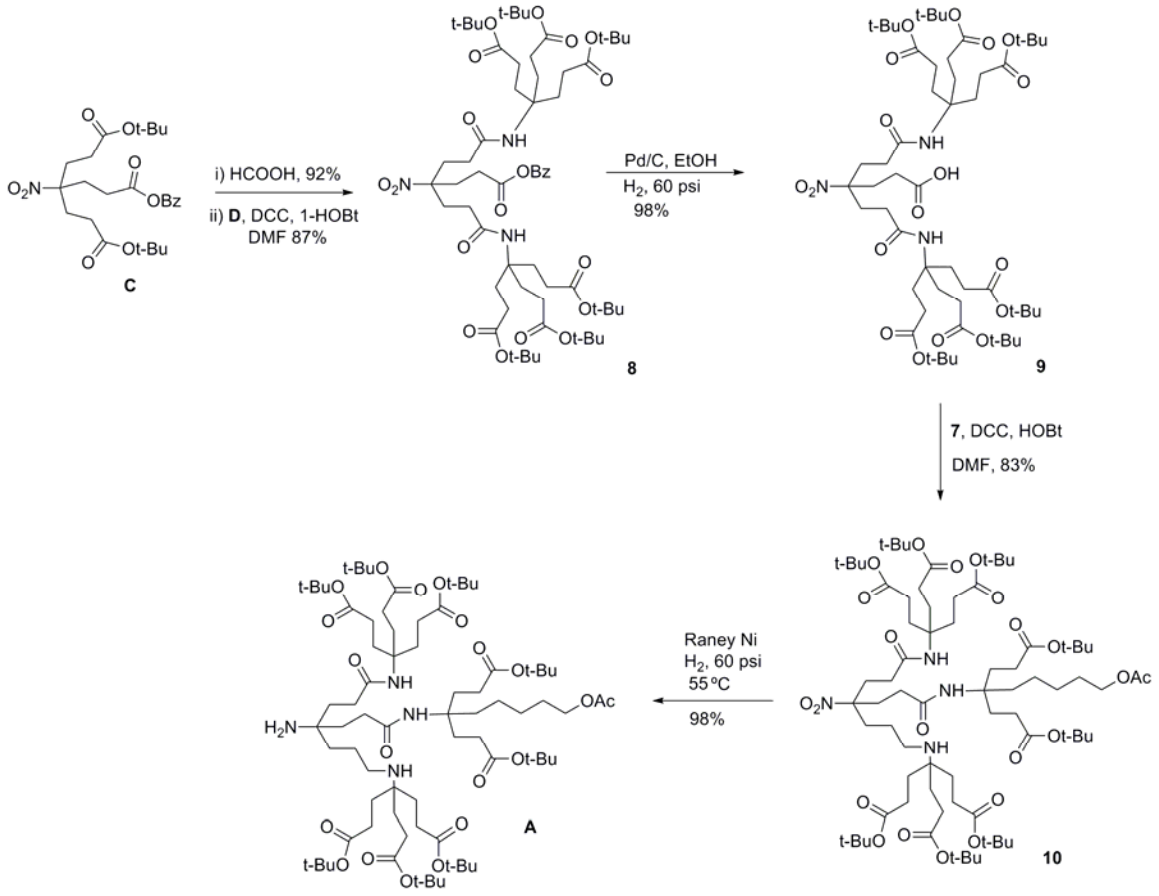

Scheme 3.2 Synthesis of the monofunctional second generation dendron **A**

With these basic monomers in hand, the second generation acetyl-protected monofunctional dendron **A** was prepared by the series of chemical transformations as shown in Scheme 3.2. Deprotection of the *t*-butyl groups on monomer **C** followed by the DCC and 1-HOBT promoted coupling with two equivalents of **D** afforded compound **8** in

87% yield. Removal of the benzyl ester group on **8** using Pd/C under 60 psi of H_2 gave **9** in 98% yield. Dendron **9** was then coupled to **7** using DCC and 1-HOBT to afford **10** in 83% isolated yields. Reduction of the nitro group on **10** by Raney Ni at 55 ºC under 60 psi H_2 provided the second generation target dendron **A** in 98% yield which was identified by a change in the ^{13}C chemical shift of $C^{4°}$ moiety in the NMR spectra from 92.5 ppm to 52.6 ppm as well as the molecular ion peak in the mass spectrum (ESI-MS) at m/z 1439.945 $[M + H]^+$. The overall yield of dendron **A** from its building blocks was 68%.

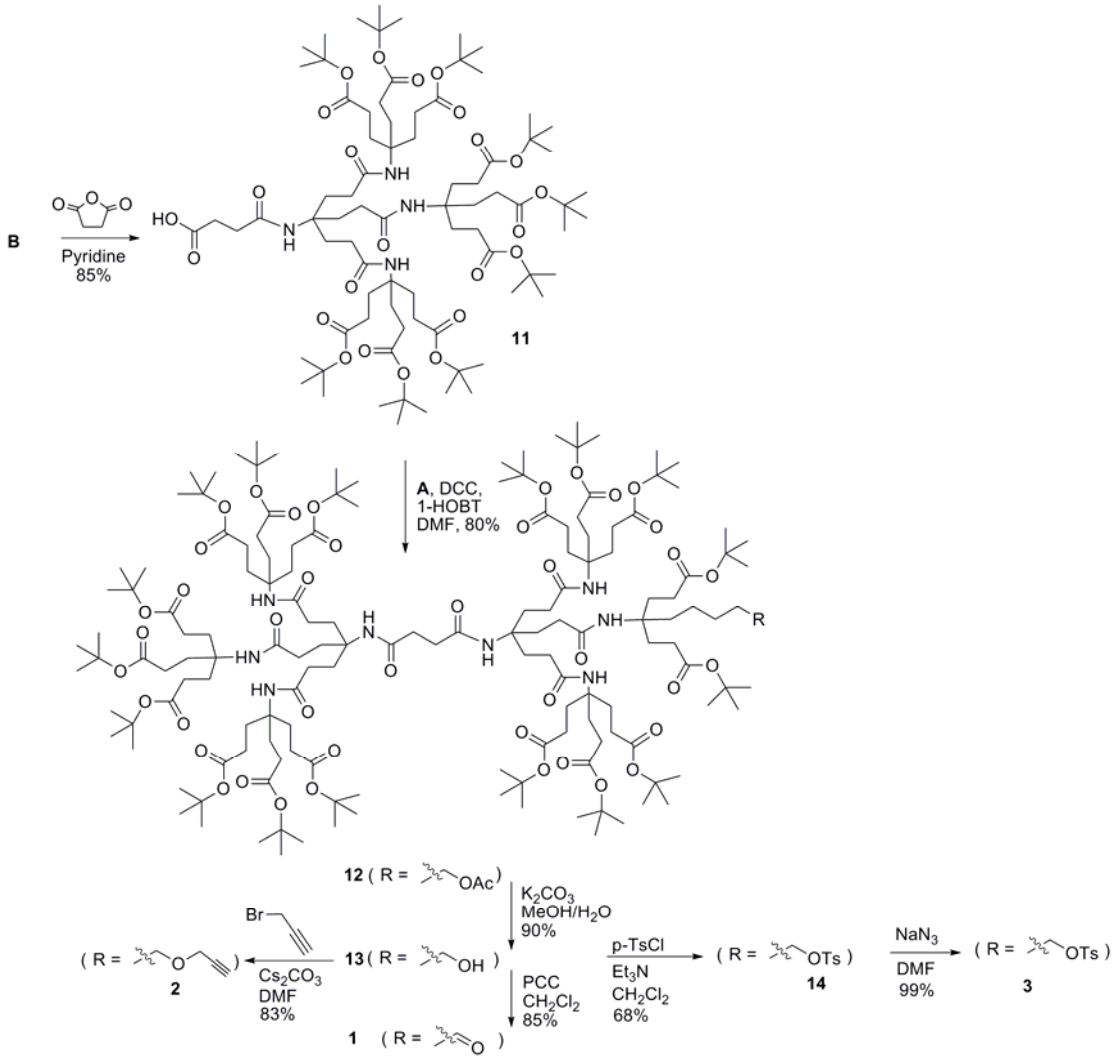

Scheme 3.3 Synthesis of monofunctional dendrimers **1**, **2** and **3**

Monofunctional target dendrimers **1**, **2** and **3** were then obtained by the stepwise incorporation of **B** and **A** onto the core molecule, as shown in Scheme 3.3. Dendron **B** was treated with succinic anhydride in the presence of pyridine to yield **11** in 85% yields. Dendron **11** was then coupled to **A** using DCC and 1-HOBT to yield the protected monofunctionalized dendrimer **12** in 80% yield which was deprotected using K_2CO_3 to provide dendrimer **13** in 90% yields. The formation of the product was confirmed by the disappearance of the proton signal of the acetyl group in the ^{1}H NMR spectra and a change in the chemical shift for the -C*H*$_2$OH moiety from 4.01 ppm to 3.60 ppm. The alcohol **13** was oxidized to an aldehyde using PCC to afford dendrimer **1** in 85% yields which was confirmed by the appearance of a new aldehyde proton signal in the ^{1}H NMR spectra at 9.61 ppm and a new ^{13}C NMR signal at 201.4 ppm for the newly formed carbonyl carbon. To obtain the alkyne functionalized monofunctional dendrimer, dendrimer **13** was treated with propargyl bromide in the presence of Cs_2CO_3 in DMF at 80 °C for three days to afford the desired acetylene dendrimer **2** in 83% isolated yield. The transformation was demonstrated by the observation of a new ^{1}H NMR signal at 2.54 ppm for the terminal acetylene proton and two new ^{13}C NMR signals at 75.7 and 77.8 ppm for acetylene carbons. To obtain the target azide dendrimer **3**, **13** was tosylated and subsequently treated with sodium azide in DMF to give **3** in quantitative yields. The conversions were confirmed by the observation of the chemical shift change (^{1}H NMR) for the methylene protons (C*H*$_2$R) from 3.60 ppm (R = OH) to 3.97 ppm (R = OTs) and 3.26 ppm (R = N_3).

The bifunctional dendrimers can be obtained in close analogy to the procedure described above for the monofunctionalized dendrimers by the stepwise incorporation of acetyl protected dendron **A** to the core molecule, deprotection and conversion of the

alcohol moiety into the desired aldehyde functionality followed by the coupling of another acetyl functionalized dendron molecule **A** to the core, deprotection and finally the transformation of the terminal alcohol group into a tosylate and then an azide moiety as shown in Scheme 3.4. Using this synthetic protocol with all transformations being carried out in good to excellent isolated yields, dendrimer **4** was synthesized in 35% overall yields.

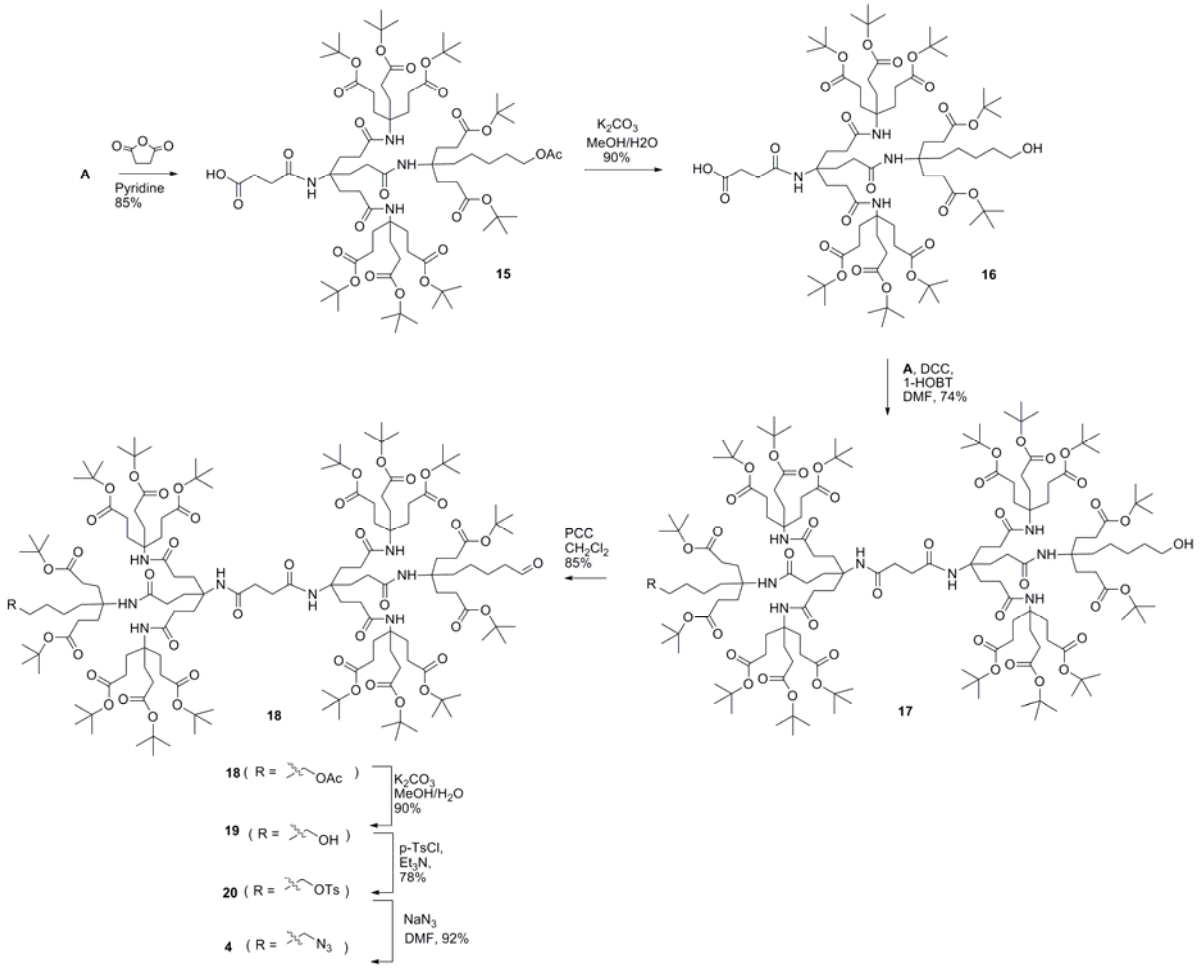

Scheme 3.4 Synthesis of bifunctional dendrimer **4**

3.3.2 Functionalizations on Monofunctionalized Dendrimers

Essential for the success of our multifunctionalizable dendritic scaffolds bearing one or two orthogonal groups on the surface is that i) the chemical transformations take

place in high yields and ii) the functional groups retain their orthogonality, i.e. during the chemical transformations they show no interference with each other or with the rest of dendrimer backbone. Therefore, we investigated the orthogonality by coupling small organic and biological relevant molecules on **1**, **2**, **3** and **4**. Initially, we investigated the chemical transformations on the single aldehyde group of dendrimer **1**. The aldehyde group can be used for Schiff base couplings with molecules bearing hydrazides, semicarbazides and aminoxy moieties.[53] As an example of these transformations, we investigated the hydrazide based couplings of **1** to phenyl hydrazine, anisic hydrazine and biotin hydrazide. All couplings were carried out in ethanol or DMSO for 16 hours and the results are presented in Table 3.1. In all cases, we observed quantitative conversions of the aldehyde to the corresponding Schiff base products which were characterized by the disappearance of the singlet in the ^{1}H NMR spectra for the aldehyde proton at 9.61 ppm and the appearance of a new triplet for the methine proton (–C*H*=N-NH-R) at 7.48-7.50 ppm depending upon the R group. The final products were obtained in 97-98% isolated yields and identified by ^{1}H and ^{13}C NMR spectroscopy and MALDI-TOF mass spectroscopy.

Thereafter, we investigated the functionalization of dendrimers **2** and **3** using 1,3 dipolar cycloadditions between an azide and an alkyne moiety. Unlike the typical 1,3 dipolar cycloaddition conditions at moderate temperature, our preliminary study using acetylene dendrimer **2** and benzyl azide under the 'typical' reaction conditions showed incomplete conversions and temperatures of 80 °C for 20 h were needed to obtain quantitative yields. To reduce the reaction time and to have less harsh reaction conditions, we investigated the microwave assisted 1,3 dipolar cycloaddition-based functionalization of our dendrimers.

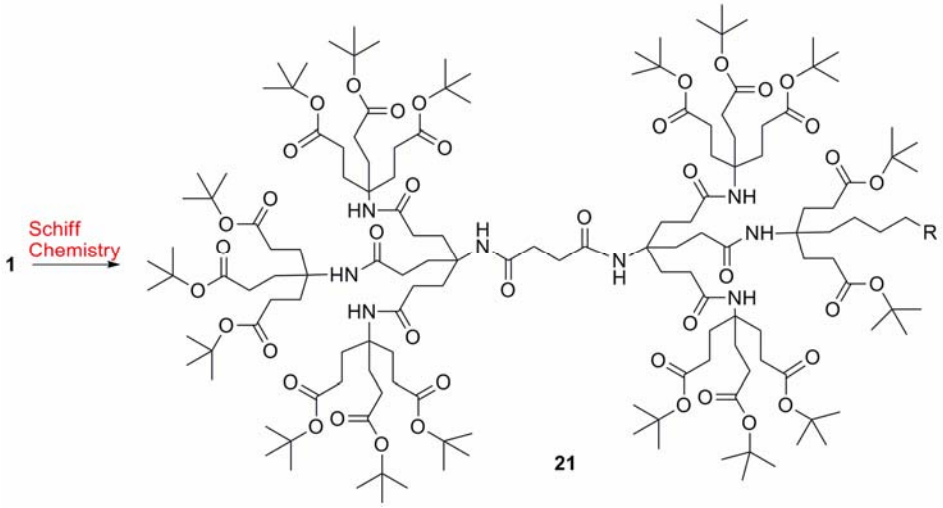

Reactants	Product 21 (R=)	^{1}H NMR(δ)[b] / yield
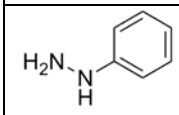	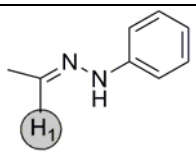 **21a**	H_1 = 7.50 ppm 98%
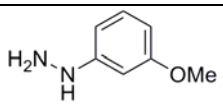	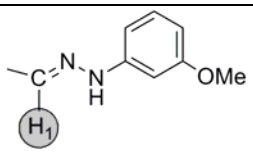 **21b**	H_1 = 7.50 ppm 98%
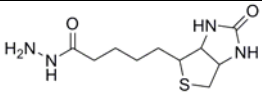	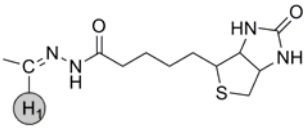 **21c**	H_1 = 7.48 ppm 97%

Table 3.1 Schiff base couplings of molecules on dendrimer **1**[a]
[a] Reaction conditions: Ethanol (**21a** and **21b**) or DMSO (**21c**), rt, 16 hrs. [b]Chemical shift for the newly formed Schiff product proton H_1.

1,3 Dipolar cycloadditions can be assisted by microwave irradiation to reduce the reaction time significantly and to provide near perfect regioselectivity.[60] The microwave

assisted 1,3 dipolar cycloadditon has been utilized for biological systems including the attachment of peptides onto a dendritic molecules[61] and the conjugation of oligonucleotides and carbohydrates.[62] For the microwave experiments, **2** was treated with benzyl azide under typical 1,3 dipolar cycloaddition conditions using Na ascorbate and $CuSO_4 \cdot 5H_2O$ in a 1:1 mixture of *t*-BuOH and H_2O in a sealed glass vial.

The microwave reactor was set-up using the power-time control method at 100 W irradiation power and a shut-off temperature of 100 °C. The reaction was terminated after 10 minutes to afford the desired triazole product in high yields. While the yields are similar to the ones described above using conventional heating methods, the microwave irradiation significantly cuts down the reaction time from hours to minutes. Table 3.2 summarizes the microwave assisted 1,3 dipolar cycloaddition reactions that were carried out on dendrimers **2** and **3**. For all reactions studied under microwave conditions, we obtained excellent isolated yields (95-98%). Furthermore, when comparing the alkyne functionalized dendrimer (**2**) with the azide functionalized one (**3**), we did not detect any significant reactivity differences.

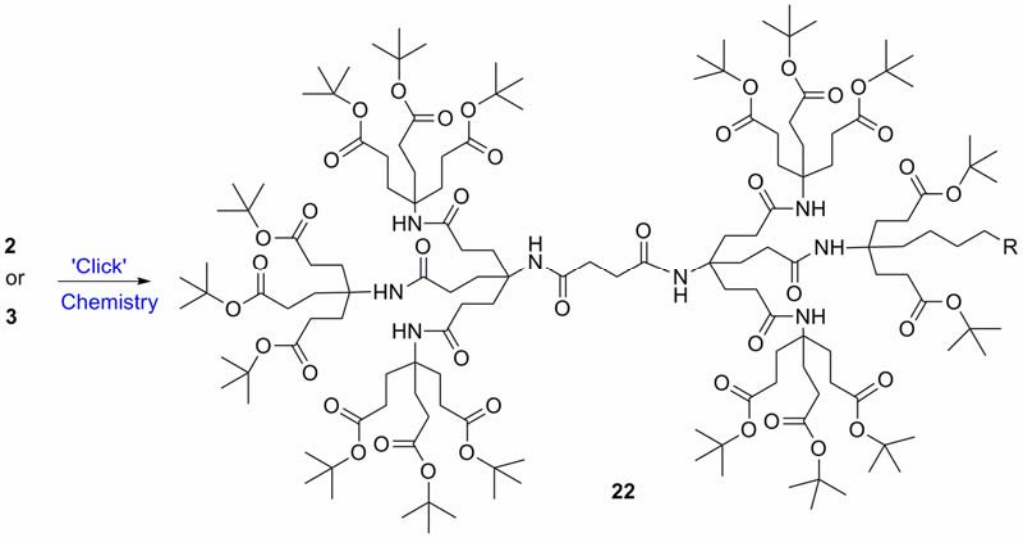

Dendrimer	Reactant	Product **22** (R=)	Yield / ^{1}H NMR (δ)[b]
2	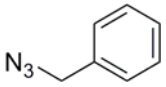	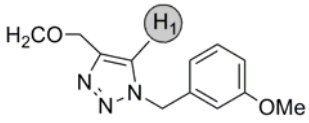 **22a**	H_1 = 7.62 ppm 98%
2	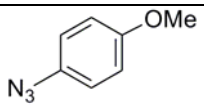	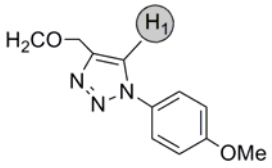 **22b**	H_1 = 8.07 ppm 95%
3	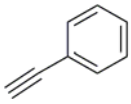	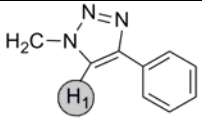 **22c**	H_1 = 7.93 ppm 98%
3	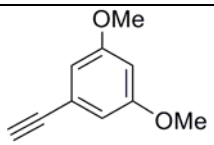	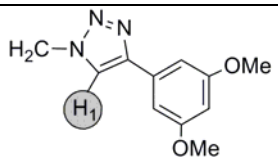 **22d**	H_1 = 7.87 ppm 97%

Table 3.2 Microwave assisted 1,3 dipolar cycloadditions on **2** and **3**[a]
[a]Reaction conditions: *t*-BuOH:H_2O (1:1), 10 mol % Na ascorbate, 5 mol % $CuSO_4 \cdot 5H_2O$. Microwave setting: Power-time control method, 100W, 10 min, P_{max}= 65 psi, and T_{max}= 100°C. [b] Chemical shift for the newly formed triazole protons.

3.3.3 Functionalizations on Bifunctionalized Dendrimers

Amino acids and peptides are the simplest mimics of proteins and polymer surfaces functionalized with them have been investigated for generating materials for drug delivery, protein surface recognition and asymmetric catalysis.[63-65] Another important biological moiety is biotin because of its high binding affinity for the protein streptavidin. This ligand-receptor interaction is used widely in biosensing, purification, and drug delivery.[66-68] Applications utilizing protein recognition of biotinylated species such as polymers, small molecules, and nanoparticles have been utilized as model systems to study and mimic the multivalent interactions occuring in protein cell recognition.[66-68] Given the high application potential and fundamental significance of biotinylated and amino acid functionalized species, the functionalization of dendrimer **4** with these molecules was undertaken.

Dendrimer **4** is equipped with two single orthogonal functionalities on the surface, namely an aldehyde group for schiff base couplings and an azide for 'click' and staudinger ligations. To demonstrate the possibilities of this multifunctionalization concept for biomaterials applications, we used **4** for couplings with two representative biological molecules–propargyl glycine and biotin hydrazide, both bearing complementary functional groups to that on the dendritic scaffold. Dendrimer **4** was treated with biotin hydrazide in ethanol overnight to obtain a biotin functionalized dendrimer **23** in 96% isolated yields characterized by the disappearance of the singlet at 9.61 ppm for the aldehyde proton and the appearance of a new triplet for the methine

proton (-C*H*=N-) at 7.48 ppm in the ^{1}H NMR spectra and a diagnostic shift to 154.3 ppm for the carbon (-*C*H=N-) from 200.2 ppm in the ^{13}C NMR spectra. After successful aldehyde functionalization, dendrimer **23** was treated with propargyl glycine under typical 'click' conditions using sodium ascorbate and $CuSO_4 \bullet 5H_2O$ in a 1:1 mixture of *t*-BuOH and H_2O in a sealed glass vial in a microwave reactor. The reaction was completed in 10 minutes to afford the triazole product **24** in 97% isolated yield. The conversion was confirmed by ^{1}H NMR spectroscopy by the newly formed signal at 7.57 ppm for the proton on the triazol moiety. Both of these functional group conversions, 'click' chemistry and Schiff base transformation, are fully tolerant of each other and any functional groups present in dendrimers **1**, **2, 3** and **4**. No changes in the chemical nature of the dendrimer scaffold were observed after each transformation. These studies clearly demonstrate that the orthogonality of the functional groups on the surface of mono- and bifunctional dendrimers is preserved.

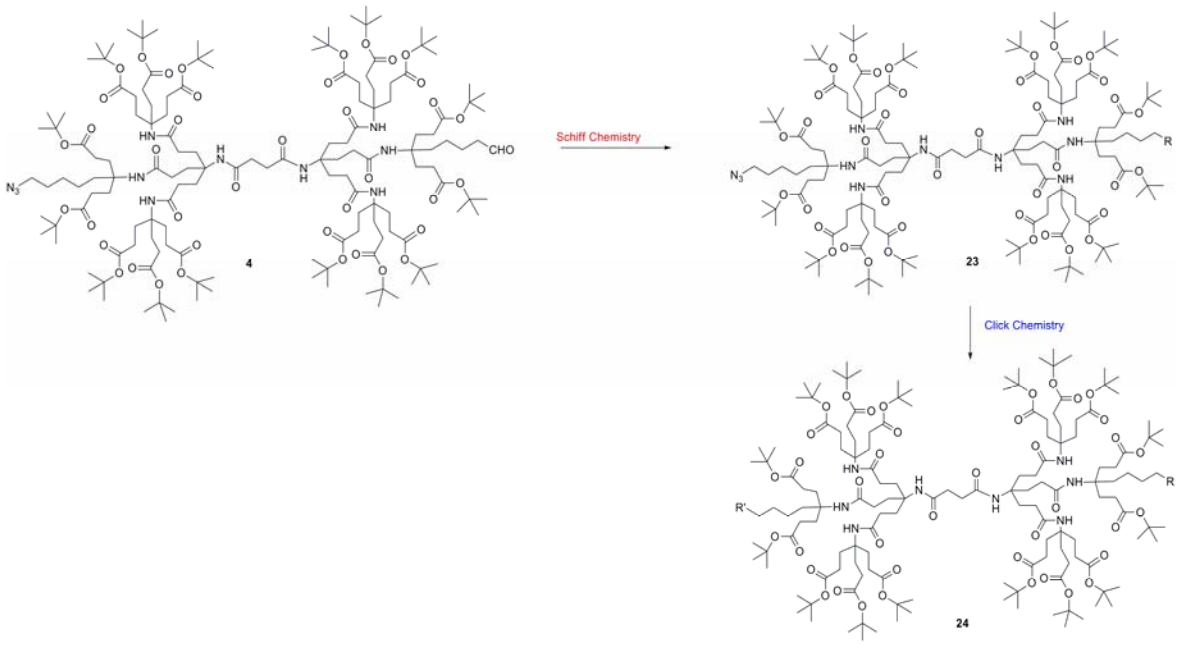

Dendrimer	**Reactants**	**Products** (R =)	**^{1}H NMR (δ)[b] / yields**
4	Biotin Hydrazide	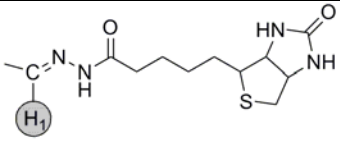 **23**	H_1 = 7.48 ppm 96%
23	Propargyl Glycine	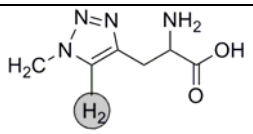 **24**	H_2 = 7.57 ppm 97%

Table 3.3 Schiff base and click couplings on Dendrimer **4**[a]
[a]Reaction conditions: 1) Schiff base coupling: DMSO, rt, 16 hrs; 2) 'Click' coupling: *t*-BuOH:H_2O (1:1), 10 mol% Na ascorbate, 5 mol% $CuSO_4 \cdot 5H_2O$. [b]Chemical shift for the newly formed Schiff base product proton H_1 and triazole proton H_2.

3.4 Conclusion

The synthesis of dendrimers containing orthogonal functional groups on the surfaces for derivatization with biological moieties will be crucial for further developments in targeted delivery, molecular imaging and materials applications. The goal of the research reported in this chapter was the fabrication of such a dendrimer, which equipped with selective surface handles allows for modular transformation to and attachment of biological units of choice for tunable delivery devices and imaging applications in biology.

Towards this end, the research described in this chapter has demonstrated the first successful synthesis of a second generation polyamide based dendrimer bearing one or two orthogonal functional handles on its surface. In particular, dendrimers containing single azide, single aldehyde, single alkyne and both azide and aldehyde moieties were synthesized. Most importantly, targeted and quantitative functionalization of these chemical handles with small organic and biologically-relavant molecules was demonstrated.

This study accomplishes our goal of introduction of functional handles on the periphery of dendrimers and their easy functionalizations. The described approach allows for the chemoselective conjugation of any desired molecules that is tolerant to 'click' and/or Schiff-base coupling conditions to our polyamide based dendritic scaffolds. Therefore, because of their ready tunability, these mono and bi-functionalized dendrimers should provide guidelines for the development of synthetic multivalent frameworks for many applications in chemical biology.

3.5 Experimental

Materials and Methods:

Propargyl glycine was purchased from ChemImpex. Tetrahydrofuran (THF) was distilled from sodium benzophenone ketyl, dichloromethane and pyridine were distilled from calcium hydride. Dry DMF stored over 4 Å molecular sieves was used. NMR spectra were acquired with a Varian Mercury 400 (^{1}H, 400.0 Hz; ^{13}C, 100.6 MHz) or a Varian Mercury 300 (^{1}H, 300.0 MHz; ^{13}C, 75.5 MHz) spectrometer. Chemical shifts are reported in ppm and referenced to the residual nuclei in the corresponding deuterated solvents. Abbreviations used include singlet (s), doublet (d), triplet (t), quartet (q), and unresolved multiplet (m). Mass spectral analyses were provided by the Georgia Tech Mass Spectrometry Facility on a VG-70se spectrometer using ESI or FAB, and on ABI 4700 Proteomics Analyzer for matrix assisted laser desorption ionization (MALDI) tandem time-of-flight (TOF). Elemental analyses were performed using Perkin Elmer Series II CHNS/O Analyzer 2400. All microwave irradiation experiments were carried out in a CEM Focused Microwave™ Synthesis System, Model Discover.

Di-tert-butyl 4-(5-hydroxypentyl)-4-nitroheptanedioate (5): To a solution of 6-nitrohexanol (16.3 g, 110 mmol) and tert-butyl acrylate (35.3 mL, 244 mmol) in THF (220 mL) was added Triton-B (5.50 mL, 40 wt % solution in MeOH) at room temperature over 2 hours. After stirring for 15 hours at room temperature, all the volatiles were removed *in vacuo* to give a dark yellowish residue, which was dissolved in diethyl ether, washed with 5% aqueous HCl, 10% aqueous $NaHCO_3$, and saturated NaCl solution, and then dried over $MgSO_4$. After filtration, the organic mixture was

concentrated *in vacuo*. The residue was purified by silica gel column chromatography eluting with EtOAc/hexanes (1:1) to give target compound **5** as a white solid (24.4 g, 55%). ^{1}H NMR (300 MHz, [D]$CHCl_3$, TMS): δ = 1.25 (m, 2H), 1.38 (m, 2H), 1.44 (s, 18H), 1.56 (m, 3H), 1.88 (t, *J* = 7.8 Hz, 2H), 2.19 (m, 8H), 3.63 (t, *J* = 6.3 Hz, 2H). ^{13}C NMR (75.5 MHz, $CDCl_3$, TMS): δ = 23.3, 25.7, 27.9, 29.8, 30.3, 32.1, 35.3, 62.3, 81.0, 92.9, 171.2. MALDI-TOF: $[M + H]^+$ calcd for $C_{20}H_{38}NO_7$, 404.2648; found, 404.2661. Elemental analysis.calcd (%) for $C_{20}H_{37}NO_7$: C 59.53; H 9.24; N 3.47. found C 59.40; H 9.32; N 3.48.

Di-tert-butyl 4-(5-acetoxypentyl)-4-nitroheptanedioate (6): To a solution of **3** (21.8 g, 54.1 mmol) and pyridine (5.25 mL, 64.9 mmol) in $CHCl_3$ (180 mL) was added Ac_2O (6.09 mL, 64.9 mmol) at 0 °C. The mixture was warmed up to room temperature slowly and stirred for 15 hours. The mixture was washed with water, dried over $MgSO_4$, filtered, and concentrated *in vacuo*. The crude product was purified by silica gel column chromatography eluting with EtOAc/hexanes (1:3) to give compound **6** as a white solid (19.9 g, 83%). ^{1}H NMR (300 MHz, [D]$CHCl_3$, TMS): δ = 1.25 (m, 2H), 1.37 (m, 2H), 1.43 (s, 18H), 1.63 (m, 2H), 1.88 (t, *J* = 8.1 Hz, 2H), 2.19 (m, 8H), 2.04 (s, 3H), 4.04 (t, *J* = 6.6 Hz, 2H). ^{13}C NMR (75.5 MHz, $CDCl_3$, TMS): δ = 20.9, 23.3, 26.0, 28.0, 28.3, 29.8, 30.3, 35.3, 64.2, 81.1, 92.8, 171.1, 171.2. HRMS MALDI-TOF: $[M + H]^+$ calcd for $C_{22}H_{40}NO_8$, 446.2754; Found, 446.2776. Elemental analysis. calcd (%) for $C_{22}H_{39}NO_8$: C 59.31; H 8.82; N 3.14. Found C 59.20; H 8.80; N 3.36.

Di-tert-butyl 4-(5-acetoxypentyl)-4-aminoheptanedioate (7): To a solution of **6** (7.00 g, 15.7 mmol) in absolute EtOH (160 mL) was added Raney-Ni (6.28 g). Then the

reaction mixture was stirred under 60 psi of H_2 for 12 hours at room temperature. The catalyst was removed by filtration through celite and the filtrate was concentrated *in vacuo* to afford amine **7** as a colorless oil (6.39 g, 98%). ^{1}H NMR (300 MHz, [D]$CHCl_3$, TMS): δ = 1.24 (m, 6H), 1.38 (s, 18H), 1.57 (m, 6H), 1.99 (s, 3H), 2.17 (t, *J* = 8.2 Hz, 4H), 3.99 (t, *J* = 6.6 Hz, 2H) ^{13}C NMR (75.5 MHz, $CDCl_3$, TMS): δ = 20.9, 23.0, 26.5, 28.0, 28.5, 29.9, 34.5, 39.4, 52.5, 64.4, 80.1, 171.0, 173.1. HRMS MALDI-TOF: $[M + H]^+$ calcd for $C_{22}H_{42}NO_6$, 416.3012; Found, 416.3017.

Nitro dendron 8: C (33.8 g, 70.6 mmol) was dissolved in HCO_2H (266 mL) and stirred for 6 hours at room temperature. The mixture was concentrated *in vacuo* to afford diacid as a white solid (23.8g, 92 %). ^{1}H NMR (300 MHz, [D]$CHCl_3$, TMS): δ = 2.26 (m, 6H), 2.36 (m, 6H), 5.11 (s, 2H), 7.34 (m, 5H). ^{13}C NMR (75.5 MHz, $CDCl_3$, TMS): δ = 28.4, 28.5, 29.3, 30.6, 67.0, 91.8, 128.3, 128.5, 128.6, 135.2, 171.8, 178.0. HRMS MALDI-TOF: $[M + H]^+$ calcd for $C_{17}H_{22}NO_8$, 368.1345; Found, 368.1367. Elemental analysis.calcd (%) for $C_{17}H_{21}NO_8$: C 55.58; H 5.76; N 3.81. Found C 55.36; H 5.62; N 3.81.

To a solution of the above described diacid monomer (3.93 g, 10.7 mmol) in DMF (120 mL) were added DCC (4.96 g, 24.1 mmol) and 1-HOBT (3.25 g, 24.1 mmol) at room temperature. After the mixture was stirred for 2 hours, dendron **D** (10.00 g, 24.1 mmol) was added and then the resulting mixture was stirred for 3 days at room temperature. After filtration, the filtrate was concentrated *in vacuo*. The residue was dissolved in CH_2Cl_2 and washed with a saturated aqueous solution of $NaHCO_3$ (2×) and then saturated NaCl solution. The organic phase was dried over $MgSO_4$, filtered, concentrated *in vacuo*, and purified by silica gel column chromatography eluting with EtOAc/hexanes

(2:3) to afford dendron **8** as a white solid (10.9 g, 87%). ^{1}H NMR (300 MHz, [D]$CHCl_3$, TMS): δ = 1.39 (s, 54H), 1.91 (m, 12H), 2.06 (m, 4H), 2.17 (m, 18H), 2.35 (m, 2H), 5.08 (s, 2H), 6.16 (s, 2H), 7.31 (m, 5H). ^{13}C NMR (75.5 MHz, $CDCl_3$, TMS): δ = 28.0, 28.6, 29.8, 29.9, 31.2, 31.3, 57.6, 66.7, 80.7, 92.3, 128.3, 128.3, 128.5, 135.5, 170.1, 171.8, 172.8. HRMS MALDI-TOF: $[M + Na]^+$ calcd for $C_{61}H_{99}N_3O_{18}Na$, 1184.6821; Found, 1184.6507. Elemental analysis.calcd (%) for $C_{61}H_{99}N_3O_{18}$: C 63.03; H 8.58; N 3.61. Found C 63.08; H 9.02; N 3.73.

Nitro dendron 9: In the presence of 10% Pd on activated carbon (1.20 g), a solution of dendron **8** in absolute EtOH (110 mL) was hydrogenated at 60 psi of H_2 at room temperature for 12 hours. The solution was filtered through Celite and the solvent was removed *in vacuo* to afford monoacid dendron **9** as a white solid (6.11 g, 98%). ^{1}H NMR (300 MHz, [D]$CHCl_3$, TMS): δ = 1.42 (s, 54H), 1.92 (m, 12H), 2.10 (m, 4H), 2.20 (m, 16H), 2.31 (m, 4H), 6.14 (s, 2H). ^{13}C NMR (75.5 MHz, $CDCl_3$, TMS): δ = 28.0, 28.3, 28.9, 29.8, 30.0, 31.1, 31.3, 57.5, 80.9, 92.5, 170.7, 173.1, 174.7. HRMS MALDI-TOF: $[M + Na]^+$ calcd for $C_{54}H_{93}N_3O_{18}Na$, 1094.6351; Found, 1094.6018. Elemental analysis.calcd (%) for $C_{54}H_{93}N_3O_{18}$: C 60.48; H 8.74; N 3.92. Found C 60.45; H 8.97; N 4.04.

Nitro dendron 10: To a solution of nitro dendron **9** (6.11 g, 5.70 mmol) in DMF (60 mL) were added DCC (1.41 g, 6.84 mmol) and 1-HOBT (0.924 g, 6.84 mmol) at room temperature. After the mixture was stirred for 2 hours, a solution of amine dendron **5** (2.84 g, 6.84 mmol) in DMF (20 mL) was added and then the resulting mixture was stirred for 3 days at room temperature. After filtration, the filtrate was concentrated *in*

vacuo to give a white residue, which was dissolved in CH_2Cl_2 (30 mL) and washed with a saturated aqueous solution of $NaHCO_3$ (2×) and then saturated NaCl solution. The organic phase was dried over $MgSO_4$, filtered, concentrated *in vacuo*, and purified by silica gel column chromatography eluting with EtOAc/hexanes (1:1) to afford dendron **10** as a white solid (6.94 g, 83%). ^{1}H NMR (300 MHz, [D]$CHCl_3$, TMS): δ = 1.27 (m, 4H), 1.43 (s, 72H), 1.65 (m, 4H), 1.94 (m, 16H), 2.04 (s, 3H), 2.10 (m, 4H), 2.20 (m, 24H), 4.03 (t, *J* = 6.6 Hz, 2H), 5.77 (s, 1H), 6.08 (s, 2H). ^{13}C NMR (75.5 MHz, $CDCl_3$, TMS): δ = 21.0, 22.7, 26.0, 28.0, 28.3, 29.7, 29.8, 30.0, 31.2, 34.8, 57.5, 58.0, 64.3, 80.6, 92.5, 170.3, 170.4, 171.3, 172.7, 172.9. HRMS MALDI-TOF: $[M + Na]^+$ calcd for $C_{76}H_{132}N_4O_{23}Na$, 1491.9180; Found, 1491.8817. Elemental analysis calcd (%) for $C_{76}H_{132}N_4O_{23}$: C 62.10; H 9.05; N 3.81. Found C 62.09; H 9.07; N 4.05.

Amine dendron A: To a solution of **10** (7.03 g, 4.95 mmol) in absolute EtOH (50 mL) was added Raney-Ni (2.00 g). The reaction mixture was stirred under 60 psi of H_2 for 24 hours at 55 °C. The catalyst was removed by filtration on celite and the filtrate was concentrated *in vacuo* to afford amine dendron **A** as a white solid (6.98 g, 98%). ^{1}H NMR (300 MHz, [D]$CHCl_3$, TMS): δ = 1.26 (m, 4H), 1.42 (s, 72H), 1.61 (m, 10H), 1.92 (m, 16H), 2.03 (s, 3H), 2.16 (m, 22H), 4.01 (t, *J* = 6.6 Hz, 2H), 5.86 (s, 1H), 6.14 (s, 2H). ^{13}C NMR (75.5 MHz, $CDCl_3$, TMS): δ = 21.0, 22.7, 26.1, 28.0, 28.3, 29.8, 30.0, 31.5, 31.6, 34.7, 35.2, 52.6, 57.3, 57.7, 64.4, 80.6, 171.3, 172.5, 172.6, 172.7, 172.9. ESI-MS (m/z): $[M + H]^+$ calcd for $C_{76}H_{135}N_4O_{21}$, 1439.9; Found, 1439.9. Elemental analysis calcd (%) for $C_{76}H_{134}N_4O_{21}$: C 63.39; H 9.38; N 3.89. Found C 62.93; H 9.35; N 4.06.

Dendron 11: A solution of the second generation amine dendron **B** (1.56 g, 1.08 mmol) and succinic anhydride (0.164 g, 1.63 mmol) in pyridine (22 mL) was stirred at room temperature for 48 hours. The solution was concentrated under reduced pressure and the residue was dissolved in $CHCl_3$ and washed with an aqueous solution of 10% HCl (2×). The organic layer was dried over $MgSO_4$, filtered, and concentrated to dryness. The crude material was purified by silica gel column chromatography eluting with EtOAc/hexanes (2:1) to afford dendron **11** as a white solid (1.39 g, 85%). ^{1}H NMR (300 MHz, [D]$CHCl_3$, TMS): δ = 1.43 (s, 81H), 1.92 (m, 24H), 2.15 (m, 24H), 2.37 (m, 2H), 2.64 (m, 2H), 6.05 (s, 3H), 7.24 (s, 1H). ^{13}C NMR (75.5 MHz, $CDCl_3$, TMS): δ = 28.0, 29.8, 30.0, 31.6, 31.7, 57.2, 57.3, 80.7, 171.3, 173.1, 175.3. ESI-MS (m/z): $[M + H]^+$ calcd for $C_{80}H_{139}N_4O_{24}$, 1540.0; Found, 1539.8. Elemental analysis calcd (%) for $C_{80}H_{138}N_4O_{24}$: C 62.39; H 9.03; N 3.64. Found C 62.34; H 9.11; N 3.91.

Dendrimer 12: To a solution of dendron **11** (1.34 g, 0.870 mmol) in DMF (9 mL) were added DCC (0.197 g, 0.957 mmol) and 1-HOBT (0.129 g, 0.957 mmol) at room temperature. After the mixture was stirred for 2 hours, amine dendron **A** (2.84 g, 0.957 mmol) was added and then the resulting mixture was stirred for 3 days at room temperature. After filtration, the filtrate was concentrated *in vacuo* to give a white residue, which was dissolved in CH_2Cl_2 (20 mL) and washed with a saturated aqueous solution of $NaHCO_3$ (2×) and then saturated NaCl solution. The organic phase was dried over $MgSO_4$, filtered, concentrated *in vacuo*, and purified by silica gel column chromatography eluting with EtOAc/hexanes (3:2) to afford dendrimer **12** as a white solid (2.17 g, 80%). ^{1}H NMR (300 MHz, [D]$CHCl_3$, TMS): δ = 1.25 (m, 4H), 1.44 (s,

153H), 1.60 (m, 4H), 1.92 (m, 46H), 2.01(s, 3H), 2.03 (m, 46H), 2.40 (s, 4H), 4.01 (t, J = 6.8 Hz, 2H), 6.23 (s, 1H), 6.38 (s, 5H), 7.24 (s, 1H), 7.30 (s, 1H). ^{13}C NMR (75.5 MHz, $CDCl_3$, TMS): δ = 21.0, 26.1, 28.0, 28.1, 29.7, 31.4, 32.8, 52.2, 57.6, 57.7, 64.5, 80.3, 171.8, 172.7, 172.8, 172.9. MALDI-TOF: $[M + Na]^+$ calcd for $C_{156}H_{270}N_8O_{44}Na$, 2983.9; Found, 2983.2. Elemental analysis calcd (%) for $C_{156}H_{270}N_8O_{44}$: C 63.26; H 9.19; N 3.78. Found C 63.04; H 9.35; N 4.13.

Dendrimer 13: To a solution of dendrimer **11** (1.61 g, 0.544 mmol) in MeOH (20 mL) was added a solution of K_2CO_3 (0.150 g, 1.09 mmol) in H_2O (2 mL) at room temperature. After stirring for 2 hours, the mixture was diluted with CH_2Cl_2 (80 mL) and then quenched with H_2O (20 mL). The resulting solution was extracted with CH_2Cl_2 (3 × 40 mL). The combined organic layers were washed with saturated NaCl solution, dried over $MgSO_4$, filtered, concentrated *in vacuo*, and purified by silica gel column chromatography eluting with EtOAc/hexanes (2:1) to afford dendrimer **13** as a white solid (1.46 g, 90%). ^{1}H NMR (300 MHz, [D]$CHCl_3$, TMS): δ = 1.26 (m, 4H), 1.43 (s, 153H), 1.63 (m, 4H), 1.94 (m, 46H), 2.03 (m, 46H), 2.40 (s, 4H), 3.60 (t, J = 6.2 Hz, 2H), 6.34 (s, 2H), 6.41 (s, 1H), 6.44 (s, 3H), 7.44 (s, 2H). ^{13}C NMR (75.5 MHz, $CDCl_3$, TMS): δ = 28.1, 29.8, 31.5, 32.2, 32.8, 52.2, 57.3, 57.3, 57.7, 57.8, 62.3, 80.4, 172.7, 172.8, 172.9, 173.0. MALDI-TOF: $[M + Na]^+$ calcd for $C_{154}H_{268}N_8O_{43}Na$, 2941.9; Found, 2942.4. Elemental analysis.calcd (%) for $C_{154}H_{268}N_8O_{43}$: C 63.35; H 9.25; N 3.84. Found C 62.82; H 9.19; N 4.30.

Dendrimer 1: To a suspension of PCC (14.6 mg, 0.0678 mmol) in CH_2Cl_2 (6 mL) was added dendrimer **13** (0.165 g, 0.0565 mmol). After stirring for three hours at room

temperature the mixture was diluted with CH_2Cl_2 and filtered through celite. The filtrate was concentrated *in vacuo* and purified by silica gel column chromatography eluting with EtOAc/hexanes (7:3) to afford dendrimer **1** as a yellow solid (12.4 mg, 85%). ^{1}H NMR (300 MHz, [D]$CHCl_3$, TMS): δ = 1.26 (m, 2H), 1.43 (s, 153H), 1.63 (m, 4H), 1.94 (m, 46H), 2.03 (m, 46H), 2.40 (m, 6H), 6.41 (s, 2H), 6.44 (s, 3H), 7.32 (s, 1H), 7.41 (s, 2H), 9.61 (s, 1H). ^{13}C NMR (75.5 MHz, $CDCl_3$, TMS): δ = 28.1, 29.8, 31.5, 32.2, 32.8, 52.2, 57.3, 57.3, 57.7, 57.8, 80.4, 172.1, 172.7, 172.8, 173.2, 201.4. MALDI-TOF: $[M + Na]^+$ calcd for $C_{154}H_{266}N_8O_{43}Na$, 2938.8; Found, 2939.3. Elemental analysis calcd (%) for $C_{154}H_{266}N_8O_{43}$: C 63.39; H 9.19; N 3.84. Found C 62.88; H 9.11; N 3.54.

Dendrimer 2: (Synthesis done by Dr. Yoon)

To a solution of **13** (0.202 g, 0.0691 mmol) in DMF (7 mL) were added Cs_2CO_3 (0.113 g, 0.346 mmol) and propargyl bromide (0.082 g, 0.691 mmol). After heating at 80 °C for 3 days, the mixture was cooled to room temperature, filtered, and concentrated *in vacuo*, and purified by silica gel column chromatography eluting with EtOAc/hexanes (2:1) to give 0.170 g of dendrimer **2** as a white solid in 83% yield. ^{1}H NMR ($CDCl_3$, 300 MHz): δ 1.09 (m, 4H), 1.41 (s, 153H), 1.65 (m, 4H), 1.93 (m, 46H), 2.15 (m, 46H), 2.38 (bs, 4H), 2.54 (s, 1H), 4.13 (t, J = 4.7 Hz, 2H), 4.70 (s, 2H), 6.32 (s, 1H), 6.46 (s, 5H), 7.17 (bs, 1H), 7.21 (bs, 1H). ^{13}C NMR ($CDCl_3$, 75.5 MHz): δ 25.0, 25.7, 26.0, 28.2, 28.6, 29.9, 31.6, 34.0, 34.6, 55.1, 57.3, 57.7, 57.8, 68.6, 75.7, 77.8, 80.4, 171.7, 172.5, 172.7, 172.8. Elemental analysis.calcd (%) for $C_{157}H_{270}N_8O_{43}$: C, 63.75; H, 9.20; N, 3.79. found C, 63.30; H, 9.15; N, 4.20.

Dendrimer 14: To a solution of **13** (0.120 g, 0.041 mmol) in CH_2Cl_2 (2 mL) were added NEt_3 (0.017 mL, 0.123 mmol) and p-TsCl (0.031 g, 0.164 mmol) at 0 °C. After stirring for 1 hour at 0 °C, the mixture was warmed to room temperature and stirred for 15 hours. The mixture was quenched with H_2O and then extracted twice with CH_2Cl_2. The combined organic layers were washed with brine, dried over Na_2SO_4, concentrated *in vacuo*, and purified by silica gel column chromatography eluting with EtOAc/hexanes (2:1) to give 0.086 g of dendrimer **14** as a yellow solid in 68% yield. ^{1}H NMR ($CDCl_3$, 400 MHz): δ 1.19 (m, 4H), 1.39 (s, 153H), 1.60 (m, 4H), 1.92 (m, 46H), 2.16 (m, 46H), 2.37 (br s, 4H), 2.41 (s, 3H), 3.97 (t, J = 6.4 Hz, 2H), 6.25 (s, 1H), 6.38 (s, 5H), 7.21 (br s, 2H), 7.32 (d, J = 8.1 Hz, 2H), 7.75 (d, J = 8.1 Hz, 2H). ^{13}C NMR ($CDCl_3$, 100 MHz): δ 21.6, 24.6, 25.6, 27.1, 28.0, 28.3, 28.7, 29.7, 31.4, 32.4, 32.9, 36.6, 57.2, 57.6, 57.7, 70.6, 80.3, 127.8, 129.8, 133.0, 144.6, 171.9, 172.7, 172.8, 172.9. LRMS MALDI-TOF: $[M + Na]^+$ calcd for $C_{161}H_{274}N_8O_{45}SNa$, 3095.9; found, 3095.4. Elemental analysis.calcd (%) for $C_{161}H_{274}N_8O_{45}S$: C, 62.91; H, 8.98; N, 3.65. found C, 62.65; H, 9.21; N, 3.67.

Dendrimer 3: (Synthesis done by Dr. Yoon)

To a solution of **14** (0.087 g, 0.0283 mmol) in DMF was added NaN_3 (0.00276 g, 0.0424 mmol). The resulting mixture was stirred at 80 °C for 2 days. After the mixture was cooled to room temperature, H_2O was added and the resulting solution was extracted three times with CH_2Cl_2. The combined organic layers were washed with H_2O and then brine, dried over Na_2SO_4, filtered, and concentrated *in vacuo* to give 0.082 g of dendrimer **3** as a yellow solid in 99% yield. ^{1}H NMR ($CDCl_3$, 300 MHz): δ 1.20 (m,

4H), 1.40 (s, 153H), 1.61 (m, 4H), 1.92 (m, 46H), 2.18 (m, 46H), 2.38 (br s, 4H), 3.26 (t, J = 6.9 Hz, 2H), 6.25 (s, 1H), 6.36 (s, 5H), 7.30 (s, 2H). ^{13}C NMR ($CDCl_3$, 75.5 MHz): δ 27.0, 28.1, 28.8, 29.2, 29.7, 31.4, 51.4, 57.3, 57.7, 80.4, 172.7, 172.9. LRMS MALDI-TOF: $[M + Na]^+$ calcd for $C_{154}H_{267}N_{11}O_{42}Na$, 2966.9; found, 2966.2. Elemental analysis.calcd (%) for $C_{154}H_{267}N_{11}O_{42}$: C, 62.81; H, 9.14; N, 5.23. found C, 62.50; H, 9.47; N, 4.98.

Dendron 15: A solution of the second generation amine dendron **A** (0.654 g, 0.454 mmol) and succinic anhydride (0.0953 g, 0.953 mmol) in pyridine (15 mL) was stirred at room temperature for 48 hours. The solution was concentrated under reduced pressure and the residue was dissolved in $CHCl_3$ and washed with an aqueous solution of 10% HCl (2×). The organic layer was dried over $MgSO_4$, filtered, and concentrated to dryness. The crude material was purified by silica gel column chromatography eluting with EtOAc/hexanes (2:1) to afford dendron **15** as a white solid (0.60 g, 85%). ^{1}H NMR (300 MHz, [D]$CHCl_3$, TMS): δ = 1.26 (m, 4H), 1.43 (s, 72H), 1.61 (m, 10H), 1.92 (m, 16H), 2.03 (s, 3H), 2.15 (m, 22H), 2.40 (m, 2H), 2.62 (m, 2H), 4.01(t, J = 6.6 Hz, 2H), 5.82(s, 1H), 6.08 (s, 2H), 7.31(s, 1H). ^{13}C NMR (75.5 MHz, $CDCl_3$, TMS): δ = 21.0, 24.2, 26.1, 28.5, 29.8, 30.1, 39.0, 40.1, 41.7, 64.6, 80.4, 170.3, 172.8, 173.2. ESI-MS (m/z): $[M + H]^+$ calcd for $C_{80}H_{139}N_4O_{24}$, 1540.9; Found, 1541.6. Elemental analysis calcd (%) for $C_{80}H_{138}N_4O_{24}$: C 62.39; H 9.03; N 3.64. Found C 62.34; H 8.99; N 3.41.

Dendron 16: To a solution of dendron **15** (0.713 g, 0.463 mmol) in MeOH (8 mL) was added a solution of K_2CO_3 (0.127 g, 0.925 mmol) in H_2O (1 mL) at room temperature.

After stirring for 2 hours, the mixture was diluted with CH_2Cl_2 (30 mL) and then quenched with H_2O (8 mL). The resulting solution was extracted with CH_2Cl_2 (3 × 30 mL). The combined organic layers were washed with saturated NaCl solution, dried over $MgSO_4$, filtered, concentrated *in vacuo*, and purified by silica gel column chromatography eluting with EtOAc/hexanes (2:1) to afford dendron **16** as a white solid (0.626 g, 90%). ^{1}H NMR (300 MHz, [D]$CHCl_3$, TMS): δ = 1.26(m, 4H), 1.44 (s, 72H), 1.62(m, 10H), 1.92 (m, 16H), 2.15 (m, 22H), 2.40 (m, 2H), 2.62 (m, 2H), 3.60 (t, *J* = 6.2 Hz, 2H), 6.08 (s, 2H), 6.12 (s, 1H), 7.31 (s, 1H). ^{13}C NMR (75.5 MHz, $CDCl_3$, TMS): δ = 21.0, 24.7, 25.9, 27.2, 28.3, 29.8, 30.0, 32.1, 40.1, 41.7, 62.5, 81.4, 172.1, 172.8, 173.2. ESI-MS (m/z): $[M + H]^+$ calcd for $C_{78}H_{137}N_4O_{23}$, 1498.9; Found, 1497.8. Elemental analysis calcd (%) for $C_{78}H_{136}N_4O_{23}$: C 62.54; H 9.15; N 3.74. Found C 62.52; H 9.02; N 3.65.

Dendrimer 17: To a solution of dendron **16** (0.236 g, 0.157 mmol) in DMF (9 mL) were added DCC (0.039 g, 0.189 mmol) and 1-HOBT (0.026 g, 0.189 mmol) at room temperature. After the mixture was stirred for 2 hours, amine dendron **A** (0.272 g, 0.189 mmol) was added and the resulting mixture was stirred for three days at room temperature. After filtration, the filtrate was concentrated *in vacuo* to give a yellow residue, which was dissolved in CH_2Cl_2 and washed with a saturated aqueous solution of $NaHCO_3$ (2×) and then saturated NaCl solution. The organic phase was dried over $MgSO_4$, filtered, concentrated *in vacuo*, and purified by silica gel column chromatography eluting with EtOAc/hexanes (1:1) to afford dendrimer **17** as a white solid (0.338 g, 74%). ^{1}H NMR (300 MHz, [D]$CHCl_3$, TMS): δ = 1.24 (m, 4H), 1.44 (s, 144H), 1.53(m, 2H), 1.60 (m, 2H), 1.92 (m, 48H), 2.03 (s, 3H), 2.10 (m, 48H), 2.40 (s,

4H), 3.60 (m, 2H), 4.00 (t, J = 6.8 Hz, 2H), 6.23 (s, 1H), 6.32 (s, 5H), 6.41 (s, 1H), 7.30 (s, 1H). ^{13}C NMR (75.5 MHz, $CDCl_3$, TMS): δ = 20.1, 21.0, 24.3, 26.1, 28.0, 28.6, 29.7, 32.4, 38.8, 40.3, 42.1, 62.6, 64.7, 80.9, 170.8, 171.8, 172.0, 173.0. MALDI-TOF: $[M + Na]^+$ calcd for $C_{154}H_{268}N_8O_{43}Na$, 2942.7; Found, 2942.4. Elemental analysis calcd (%) for $C_{154}H_{268}N_8O_{43}$: C 63.35; H 9.25; N 3.84. Found C 63.18; H 9.23; N 3.62.

Dendrimer 18: To the solution of PCC (0.0128 g, 0.0595 mmol) suspended in CH_2Cl_2 (5 mL) was added dendrimer **17** (0.145 g, 0.0496 mmol). After stirring for 3 hours at room temperature, the mixture was diluted with CH_2Cl_2 (15 mL) and filtered through celite. The filtrate was concentrated *in vacuo* and purified by preparatory thin layer chromatography with EtOAc/hexanes (2:1) as solvent system to afford dendrimer **18** as a yellow solid (0.122 g, 85%). ^{1}H NMR (300 MHz, [D]$CHCl_3$, TMS): δ = 1.24 (m, 4H), 1.44 (s, 144H), 1.60 (m, 2H), 1.92 (m, 48H), 2.03 (s, 3H), 2.10 (m, 48H), 2.40 (m, 6H), 4.00 (t, J = 6.8 Hz, 2H), 6.23 (s, 1H), 6.32 (s, 5H), 6.41 (s, 1H), 7.30 (s, 1H), 9.61 (s, 1H). ^{13}C NMR (75.5 MHz, $CDCl_3$, TMS): δ = 20.1, 21.0, 24.3, 28.0, 28.1, 28.6, 29.7, 38.8, 40.3, 42.1, 43.3, 64.7, 80.9, 170.8, 171.8, 172.0, 173.0, 200.2. MALDI-TOF: $[M + Na]^+$ calcd for $C_{154}H_{266}N_8O_{43}Na$, 2940.7; Found, 2941.6. Elemental analysis calcd (%) for $C_{154}H_{266}N_8O_{43}$: C 63.39; H 9.19; N 3.84. Found C 63.34; H 9.11; N 3.68.

Dendrimer 19: To a solution of dendrimer 15 (0.128 g, 0.0438 mmol) in MeOH (8 mL) was added a solution of K_2CO_3 (12.1 mg, 0.0877 mmol) in H_2O (1 mL) at room temperature. After stirring for two hours, the mixture was diluted with CH_2Cl_2 (40 mL) and then quenched with H_2O (8 mL). The resulting solution was extracted with CH_2Cl_2 (3 × 30 mL). The combined organic layers were washed with saturated NaCl solution,

dried over $MgSO_4$, filtered, concentrated *in vacuo* to afford dendrimer **19** as a yellow solid (0.114 g, 90%). ^{1}H NMR (300 MHz, [D]$CHCl_3$, TMS): δ = 1.24 (m, 4H), 1.44 (s, 144H), 1.60 (m, 2H), 1.92 (m, 48H), 2.10 (m, 48H), 2.40 (m, 6H), 3.62 (t, *J* = 6.4 Hz, 2H), 6.23 (s, 1H), 6.32 (s, 5H), 6.41 (s, 1H), 7.30 (s, 1H), 9.61 (s, 1H). ^{13}C NMR (75.5 MHz, $CDCl_3$, TMS): δ = 20.1, 24.3, 25.6, 28.0, 28.1, 28.6, 29.7, 32.0, 38.8, 40.3, 42.1, 43.3, 63.1, 80.9, 171.8, 172.0, 173.0, 200.2. MALDI-TOF: $[M + Na]^+$ calcd for $C_{152}H_{264}N_8O_{42}Na$, 2896.8; Found, 2897.5. Elemental analysis calcd (%) for $C_{152}H_{264}N_8O_{42}$: C 63.48; H 9.25; N 3.90. Found C 63.02; H 9.21; N 3.82.

Dendrimer 20: To a solution of **19** (0.126 g, 0.0438 mmol) in CH_2Cl_2 (2 mL) were added Et_3N (0.016 mL, 0.131 mmol) and p-TsCl (0.025 g, 0.131 mmol) at 0 °C. After stirring for one hour at 0 °C, the mixture was warmed up to room temperature and stirred for 20 hours. The mixture was quenched with H_2O and then extracted with CH_2Cl_2 (2 × 15 mL). The combined organic layers were washed with saturated NaCl, dried over $MgSO_4$, concentrated *in vacuo*, and purified by preparatory thin layer chromatography with EtOAc to afford dendrimer **20** as a yellow solid (0.103 g, 78%). ^{1}H NMR (300 MHz, [D]$CHCl_3$, TMS): δ = 1.24 (m, 4H), 1.44 (s, 144H), 1.60 (m, 2H), 1.92 (m, 48H), 2.10 (m, 48H), 2.40 (m, 9H), 3.97 (t, *J* = 6.0 Hz, 2H), 6.23 (s, 1H), 6.32 (s, 5H), 6.41 (s, 1H), 7.30 (s, 1H), 7.44 (d, *J* = 5.8 Hz, 2H), 7.62 (d, *J* = 6.1 Hz, 2H), 9.61 (s, 1H). ^{13}C NMR (75.5 MHz, $CDCl_3$, TMS): δ = 20.1, 21.2, 24.3, 25.6, 28.0, 28.1, 28.6, 28.7, 29.7, 38.8, 40.3, 42.1, 43.3, 69.7, 80.9, 128.0, 130.6, 140.3, 144.3, 171.8, 172.0, 173.0, 200.2. MALDI-TOF: $[M + Na]^+$ calcd for $C_{159}H_{270}N_8O_{44}SNa$, 3050.8; Found, 3051.2.

Elemental analysis calcd (%) for $C_{159}H_{270}N_8O_{44}S$: C 63.03; H 8.98; N 3.70. Found C 62.91; H 8.82; N 3.70.

Dendrimer 4: To a solution of **20** (0.065 g, 0.0215 mmol) in DMF was added NaN_3 (0.0021 g, 0.0323 mmol). The reaction mixture was stirred at 80 °C for 2 days. After the mixture was cooled down to room temperature, H_2O was added and the resulting solution was extracted with CH_2Cl_2 (3 × 15 mL). The combined organic layers were washed with H_2O and then saturated NaCl solution, dried over $MgSO_4$, concentrated *in vacuo* and purified by preparatory thin layer chromatography with EtOAc to afford compound **4** as a yellow solid (0.057 g, 92%). ^{1}H NMR (300 MHz, [D]$CHCl_3$, TMS): δ = 1.24 (m, 2H), 1.31 (m, 2H), 1.44 (s, 144H), 1.60 (m, 2H), 1.92 (m, 48H), 2.10 (m, 48H), 2.40 (m, 6H), 3.26 (m, 2H), 6.23 (s, 1H), 6.32 (s, 5H), 6.98 (s, 1H), 7.20 (s, 1H), 9.61 (s, 1H). ^{13}C NMR (75.5 MHz, $CDCl_3$, TMS): δ = 20.1, 24.3, 25.6, 28.0, 28.1, 28.6, 29.7, 30.0, 38.8, 40.3, 42.1, 43.3, 49.7, 80.9, 171.8, 172.0, 173.0, 200.2. MALDI-TOF: $[M + Na]^+$ calcd for $C_{152}H_{263}N_{11}O_{41}Na$, 2921.8; Found, 2921.7. Elemental analysis calcd (%) for $C_{152}H_{263}N_{11}O_{41}$: C 62.94; H 9.14; N 5.31. Found C 62.81 ; H 9.10 ; N 5.34

General procedure for Schiff base couplings: To a solution of the dendrimer-aldehyde **1** in ethanol (for **21a** and **21b**) or DMSO (for **21c**) was added the appropriate hydrazide and the reaction was stirred for 16 hrs at room temperature. The reaction mixture was concentrated *in vacuo*, re-dissolved in CH_2Cl_2 and washed with H_2O and brine, dried over $MgSO_4$, and filtered. The solvent was removed *in vacuo* to give the target compound.

Compound 21a: Aldehyde dendrimer **1** (50.0 mg, 0.017 mmol) was treated with phenyl hydrazine (1.85 mg, 0.017 mmol) to afford compound **21a** as a yellowish solid (50.1 mg, 98%). ^{1}H NMR (300 MHz, [D]$CHCl_3$, TMS): δ = 1.26 (m, 2H), 1.31 (m, 2H), 1.43 (s, 153H), 1.63 (m, 4H), 1.94 (m, 46H), 2.17 (m, 46H), 2.40 (s, 4H), 6.41 (s, 2H), 6.44 (s, 5H), 6.91 (d, *J* = 8.2 Hz, 1H), 7.25 (d, *J* = 6.2 Hz, 2H), 7.32 (s, 1H), 7.34 (d, *J* = 5.6 Hz, 2H), 7.50 (t, *J* = 5.8 Hz, 1H), 10.73 (s, 1H). ^{13}C NMR (75.5 MHz, $CDCl_3$, TMS): δ = 28.1, 29.8, 31.5, 32.2, 32.8, 52.2, 57.3, 57.3, 57.7, 57.8, 80.4, 115.4, 130.1, 142.8, 159.2, 172.1, 172.7, 172.8, 173.2. MALDI-TOF: $[M + Na]^+$ calcd for $C_{160}H_{272}N_{10}O_{42}Na$, 3030.9; Found, 3031.6.

Compound 21b: Aldehyde dendrimer **1** (12.0 mg, 0.004 mmol) was treated with anisic hydrazine (0.68 mg, 0.004 mmol) to afford compound **21b** as a yellowish solid (12.4 mg, 98%). ^{1}H NMR (300 MHz, [D]$CHCl_3$, TMS): δ = 1.26 (m, 2H), 1.31 (m, 2H), 1.43 (s, 153H), 1.63 (m, 4H), 1.94 (m, 46H), 2.17 (m, 46H), 2.40 (s, 4H), 3.82 (s, 3H), 6.16 (s, 1H), 6.37 (d, *J* = 6.4 Hz, 1H), 6.41 (s, 2H), 6.44 (s, 5H), 6.91 (d, *J* = 8.2 Hz, 1H), 7.14 (m, 1H), 7.32 (s, 1H), 7.50 (t, *J* = 5.8 Hz, 1H), 10.72 (s, 1H). ^{13}C NMR (75.5 MHz, $CDCl_3$, TMS): δ = 28.1, 29.8, 31.5, 32.2, 32.8, 52.2, 55.4, 57.2, 57.3, 57.7, 57.8, 80.4, 98.6, 106.1, 130.3, 143.6, 159.2, 161.5, 172.1, 172.7, 172.8, 173.2. MALDI-TOF: $[M + Na]^+$ calcd for $C_{161}H_{274}N_{10}O_{43}Na$, 3060.9; Found, 3059.5.

Compound 21c: Aldehyde dendrimer **1** (16.0 mg, 0.005 mmol) was treated with biotin hydrazide (1.41 mg, 0.005 mmol) to afford compound **21c** as a yellowish solid (16.2 mg, 97%). ^{1}H NMR (300 MHz, [D]$CHCl_3$, TMS): δ = 1.24 (m, 2H), 1.26 (m, 2H), 1.31 (m,

2H), 1.43 (s, 153H), 1.52 (m, 2H), 1.63 (m, 6H), 1.94 (m, 46H), 2.17 (m, 46H), 2.32 (m, 2H), 2.40 (s, 4H), 2.83 (d, J = 5.2 Hz, 2H), 3.27 (m, 1H), 4.62 (t, J = 6.5 Hz, 1H), 4.91 (d, J = 7.0 Hz, 1H), 6.22 (s, 2H), 6.41 (s, 2H), 6.44 (s, 5H), 7.32 (s, 1H), 7.48 (t, J = 6.2 Hz, 1H), 10.52 (s, 1H). ^{13}C NMR (75.5 MHz, $CDCl_3$, TMS): δ = 28.1, 29.8, 31.5, 32.2, 32.8, 38.8, 52.2, 55.1, 57.2, 57.3, 57.7, 57.8, 63.9, 80.4, 154.3, 166.2, 169.2, 172.1, 172.7, 172.8, 173.2. MALDI-TOF: $[M + Na]^+$ calcd for $C_{164}H_{282}N_{12}O_{44}SNa$, 3181.8; Found, 3181.2.

Compound 22a: (Synthesis done by Dr. Yoon)

Acetylenyl dendrimer **2** (20.0 mg, 0.0067 mmol) was treated with benzyl azide (0.89 mg, 0.0067 mmol) to give 20.2 mg of compound **22a** as a yellowish solid in 98% yield. ^{1}H NMR ($CDCl_3$, 400 MHz): δ 1.26 (m, 4H), 1.42 (s, 153H), 1.64 (m, 4H), 1.94 (m, 46H), 2.19 (m, 46H), 2.39 (bs, 4H), 4.12 (t, J = 6.6 Hz, 2H), 5.54 (s, 2H), 6.25 (s, 1H), 6.40 (s, 5H), 7.20 (s, 1H), 7.24 (s, 1H), 7.32 (m, 2H), 7.36 (m, 3H), 7.62 (s, 1H). ^{13}C NMR ($CDCl_3$, 100 MHz): δ 25.0, 25.7, 28.2, 28.7, 29.9, 31.6, 33.0, 34.0, 49.2, 54.3, 57.3, 57.7, 57.8, 80.4, 128.5, 129.1, 129.3, 137.0, 142.8, 157.3, 171.6, 172.5, 172.7, 172.8.

Compound 22b: (Synthesis done by Dr. Yoon)

Acetylenyl dendrimer **2** (25.0 mg, 0.0084 mmol) was treated with 4-methoxy phenyl azide (1.25 mg, 0.0084 mmol) to give 24.7 mg of the compound **22b** as a yellowish solid in 95% yield. ^{1}H NMR ($CDCl_3$, 400 MHz): δ 1.10 (m, 4H), 1.39 (s, 153H), 1.67 (m, 4H), 1.94 (m, 46H), 2.17 (m, 46H), 2.39 (bs, 4H), 3.86 (s, 3H), 4.14 (t, *J* = 6.6 Hz, 2H), 5.34 (s, 2H), 6.39 (s, 5H), 6.47 (s, 1H), 7.01 (d, *J* = 6.9 Hz, 2H), 7.21 (s, 1H), 7.25 (s, 1H), 7.64 (d, *J* = 6.6 Hz, 2H), 8.06 (s, 1H). ^{13}C NMR ($CDCl_3$, 100 MHz): δ 25.0, 25.7, 28.2, 28.7, 29.9, 31.3, 31.6, 33.0, 34.0, 34.7, 49.2, 55.7, 57.3, 57.7, 57.8, 60.8, 68.4, 80.4, 114.7, 122.2, 134.5, 142.8, 153.7, 161.5, 171.6, 172.5, 172.7, 172.8.

Compound 22c: (Synthesis dony by Dr. Yoon)

Azide dendrimer **3** (30.0 mg, 0.010 mmol) was treated with phenyl acetylene (1.03 mg, 0.010 mmol) to give 30.1 mg of the compound **22c** as a yellowish solid in 98% yield. ^{1}H NMR ($CDCl_3$, 400 MHz): δ 1.26 (m, 4H), 1.42 (s, 153H), 1.69 (m, 4H), 1.95 (m, 46H), 2.16 (m, 46H), 2.38 (bs, 4H), 4.42 (t, *J* = 7.2 Hz, 2H), 5.30 (s, 2H), 6.37 (s, 3H), 6.41 (s, 3H), 7.20 (s, 1H), 7.25 (s, 1H), 7.33 (d, *J* = 7.1 Hz, 1H), 7.42 (t, *J* = 7.1 Hz, 2H), 7.85 (d, *J* = 7.1 Hz, 2H), 7.95 (s, 1H). ^{13}C NMR ($CDCl_3$, 100 MHz): δ 25.4, 25.9, 26.8, 28.2, 29.8, 31.4, 32.2, 47.7, 57.4, 57.7, 57.8, 80.4, 120.0, 125.6, 127.9, 128.4, 133.9, 147.5, 171.6, 172.5, 172.7. HRMS MALDI-TOF: $[M + Na]^+$ calcd for $C_{162}H_{273}N_{11}O_{42}Na$, 3067.9462; found, 3067.9694.

Compound 22d: (Synthesis done by Dr. Yoon)

Azide dendrimer **3** (30.0 mg, 0.010 mmol) was treated with 1-ethynyl-3,5-dimethoxy benzene (1.64 mg, 0.010 mmol) to give 30.5 mg of the compound **22d** as a yellowish solid in 97% yield. ^{1}H NMR ($CDCl_3$, 400 MHz): δ 1.32 (m, 4H), 1.41 (s, 153H), 1.65 (m, 4H), 1.94 (m, 46H), 2.18 (m, 46H), 2.37 (bs, 4H), 3.83 (s, 6H), 4.39 (t, *J* = 7.2 Hz, 2H), 6.36 (s, 3H), 6.39 (s, 3H), 6.43 (t, *J* = 2.2 Hz, 1H), 7.01 (d, *J* = 2.2 Hz, 2H), 7.20 (s, 1H), 7.28 (s, 1H), 7.87 (s, 1H). ^{13}C NMR ($CDCl_3$, 100 MHz): δ 25.0, 25.7, 26.8, 28.2, 29.9, 30.3, 31.4, 31.5, 33.0, 50.3, 55.5, 57.3, 57.7, 57.8, 80.4, 100.4, 103.6, 120.1, 132.4, 147.3, 160.9, 171.6, 172.5, 172.7. HRMS MALDI-TOF: $[M + Na]^+$ calcd for $C_{164}H_{277}N_{11}O_{44}Na$, 3127.9674; found, 3127.9781.

Compound 23: Bifunctional dendrimer **4** (22.0 mg, 0.007 mmol) was treated with biotin hydrazide (1.9 mg, 0.007 mmol) to afford compound **23** as a yellowish solid (22.8 mg, 96%). ^{1}H NMR (300 MHz, [D]$CHCl_3$, TMS): δ = 1.23 (m, 2H), 1.24 (m, 2H), 1.31 (m, 6H), 1.44 (s, 144H), 1.52 (m, 2H), 1.60 (m, 2H), 1.92 (m, 48H), 2.10 (m, 48H), 2.32 (m, 2H), 2.40 (m, 4H), 2.83 (d, *J* = 5.4 Hz, 2H), 3.26 (m, 2H), 3.27 (m, 1H), 4.62 (t, *J* = 6.1 Hz, 1H), 4.91 (d, *J* = 7.3 Hz, 1H), 6.23 (s, 3H), 6.32 (s, 5H), 6.98 (s, 1H), 7.20 (s, 1H), 7.48 (t, *J* = 7.2 Hz, 1H), 10.51 (s, 1H). ^{13}C NMR (75.5 MHz, $CDCl_3$, TMS): δ = 20.1, 24.3, 25.6, 26.2, 28.0, 28.1, 28.6, 29.7, 30.0, 38.2, 38.8, 40.3, 42.1, 49.7, 55.2, 63.9, 80.9, 154.3, 166.3, 169.2, 171.8, 172.0, 173.0. MALDI-TOF: $[M + Na]^+$ calcd for $C_{162}H_{279}N_{15}O_{42}SNa$, 3164.1; Found, 3164.4.

Compound 24: To a solution of compound **23** (22.8 mg, 0.007 mmol) and propargyl glycine (0.82 mg, 0.007 mmol) in a 1:1 mixture of water and t-BuOH (1 mL each) in a 10

mL glass vial equipped with a small magnetic stir bar were added sodium ascorbate (10 mol%) and $CuSO_4 \cdot 5H_2O$ (5 mol%). After the vial was tightly sealed with an aluminum/Teflon® crimp top, the mixture was irradiated for 10 minutes using the power-time control method at 100 W irradiation power and 100 °C as the maximum temperature. During the reaction, the maximum temperature reached 91 ºC. After the completion of the reaction, the mixture was cooled down to room temperature and then diluted with CH_2Cl_2 (10 mL). The resulting solution was washed with water twice and the combined organic layers were dried over $MgSO_4$, filtered, and concentrated *in vacuo* to afford compound **24** as a yellowish solid (22.9 mg, 97%). ^{1}H NMR (300 MHz, [D]$CHCl_3$, TMS): δ = 1.23 (m, 2H), 1.24 (m, 2H), 1.31 (m, 6H), 1.44 (s, 144H), 1.52 (m, 2H), 1.60 (m, 2H), 1.92 (m, 48H), 2.10 (m, 48H), 2.32(m, 2H), 2.40 (m, 4H), 2.83 (d, *J* = 5.4 Hz, 2H), 3.21(d, *J* = 5.1 Hz, 2H), 3.27 (m, 1H), 4.22 (m, 1H), 4.42 (d, *J* = 5.7 Hz, 2H), 4.62 (t, *J* = 6.1 Hz, 1H), 4.91 (d, *J* = 7.3 Hz, 1H), 6.23 (s, 3H), 6.32 (s, 5H), 6.98 (s, 1H), 7.20 (s, 1H), 7.48 (t, *J* = 7.2 Hz, 1H), 7.57 (s, 1H), 10.51 (s, 1H), 12.47 (bs, 1H). ^{13}C NMR (75.5 MHz, $CDCl_3$, TMS): δ = 20.1, 24.3, 25.6, 26.2, 28.0, 28.1, 28.6, 29.7, 30.0, 38.2, 38.8, 40.3, 42.1, 49.7, 55.2, 63.9, 80.9, 154.3, 166.3, 169.2, 171.8, 172.0, 173.0. MALDI-TOF: $[M + Na]^+$ calcd for $C_{167}H_{286}N_{16}O_{44}SNa$, 3277.1; Found, 3276.4 .

3.6 References

1. Mitchell, D. J.; Kim, D. T.; Steinman, L.; Fathman, C. G.; Rothbard, J. B. Polyarginine enters cells more efficiently than other polycationic homopolymers. *J. Peptide Res.* **2000**, *56*, 318.

2. Derossi, D.; Joliot, A. H.; Chassaing, G.; Prochiantz, A. The third helix of the antennapedia homeodomain translocates through biological membranes. *J. Biol. Chem.* **1994**, *269*, 10444.

3. Vidal, P.; Chaloin, L.; Heitz, A.; Van Mau, N.; Mery, J.; Divita, G.; Heitz, F. Interactions of primary amphipathic vector peptides with membranes. Conformational consequences and influence on cellular localization. *J. Membr. Biol.* **1998**, *162*, 259.

4. Vives, E.; Brodin, P.; Lebleu, B. A truncated HIV-1 Tat protein basic domain rapidly translocates through the plasma membrane and accumulates in the cell nucleus. *J. Biol. Chem.* **1997**, *272*, 16010.

5. Mahato, R. I. Water insoluble and soluble lipids for gene delivery. *Adv. Drug Delivery Rev.* **2005**, *57*, 699.

6. Kaneda, Y. Virosomes: evolution of the liposome as a targeted drug delivery system. *Adv. Drug Delivery Rev.* **2000**, *43*, 197.

7. Brown, M. D.; Schatzlein, A. G.; Uchegbu, I. F. Gene delivery with synthetic (non viral) carriers. *Int. J. Pharm.* **2001**, *229*, 1.

8. England, B. P.; Balasubramanian, P.; Uings, I.; Bethell, S.; Chen, M. -J.; Schatz, P. J.; Yin, Q.; Chen, Y. -F.; Whitehorn, E. A.; Tsavaler, A.; Martens, C. L.; Barrett, R. W.; McKinnon, M. A potent dimeric peptide antagonist of interlukin-5 that binds two interlukin-5 receptor alpha chains. *Proc. Natl. Acad. Sci. U. S. A.* **2000**, *97*, 6862.

9. Hussain, M.; Shchepinov, M.; Sohail, M.; Benter, I. F.; Hollins, A. J.; Southern, E. M.; Akhtar, S. A novel anionic dendrimer for improved cellular delivery of antisense oligonucleotides. *J. Controlled Release* **2004**, *99*, 139.

10. Manunta, M.; Tan, P. H.; Sagoo, P.; Kashefi, K.; George, A. J. T. Gene delivery by dendrimers operates via a cholesterol dependent pathway. *Nucleic Acids Res.* **2004**, *32*, 2730.

11. Quintana, A.; Raczka, E.; Piehler, L.; Lee, I.; Myc, A.; Majoros, I.; Patri, A. K.; Thomas, T.; Mule, J.; Baker, Jr., J. R. Design and function of a dendrimer-based therapeutic nanodevice targeted to tumor cells through the folate receptor. *Pharm. Res.* **2002**, *19*, 1310.

12. Rosler, A.; Vandermeulen, G. W. M.; Klok, H. -A. Advanced drug delivery devices via self-assembly of amphiphilic block copolymers. *Adv. Drug Delivery Rev.* **2001**, *53*, 95.

13. Patri, A. K.; Myc, A.; Beals, J.; Thomas, T. P.; Bander, N. H.; Baker, Jr., J. R. Synthesis and in vitro testing of J591 antibody-dendrimer conjugates for targeted prostate cancer therapy. *Bioconjugate Chem.* **2004**, *15*, 1174.

14. Torchilin, V. P.; Levchenko, T. S.; Lukyanov, A. N.; Khaw, B. A.; Klibanov, A. L.; Rammohan, R.; Samokhin, G. P.; Whiteman, K. R. p-Nitrophenylcarbonyl-PEG-PE-liposomes: fast and simple attachment of specific ligands, including monoclonal antibodies, to distal ends of PEG chains via p-nitrophenylcarbonyl groups. *Biochim. Biophys. Acta, Biomembranes* **2001**, *1511*, 397.

15. Meier, W.; Nardin, C.; Winterhalter, M. Reconstitution of channel proteins in (polymerized) ABA triblock copolymer membranes. *Angew. Chem. Int. Ed.* **2000**, *39*, 4599.

16. Singh, D.; Kiarash, R.; Kawamura, K.; LaCasse, E. C.; Gariepy, J. Penetration and intracellular routing of nucleus-directed peptide-based shuttles (loligomers) in eukaryotic cells. *Biochemistry* **1998**, *37*, 5798.

17. Sheldon, K.; Liu, D.; Ferguson, J.; Gariepy, J. Loligomers: design of de novo peptide-based intracellular vehicles. *Proc. Natl. Acad. Sci. U. S. A.* **1995**, *92*, 2056.

18. Brokx, R. D.; Bisland, S. K.; Gariepy, J. Designing peptide-based scaffolds as drug delivery vehicles. *J. Controlled Release* **2002**, *78*, 115.

19. Lee, C. C.; MacKay, J. A.; Fréchet, J. M. J.; Szoka, F. C. Designing dendrimers for biological applications. *Nature Biotechnology* **2005**, *23*, 1517.

20. Choi, Y.; Thomas, T.; Kotlyar, A.; Islam, M. T.; Baker, Jr., J. R. Synthesis and functional evaluation of DNA-assembled polyamidoamine dendrimer clusters for cancer cell -specific targeting. *Chemistry & Biology* **2005**, *12*, 35.

21. Chen, H. -T.; Neerman, M. F.; Parrish, A. R.; Simanek, E. E. Cytotoxicity, hemolysis, and acute in vivo toxicity of dendrimers based on melamine, candidate vehicles for drug delivery. *J. Am. Chem. Soc.* **2004**, *126*, 10044.

22. Bosman, A. W.; Janssen, H. M.; Meijer, E. W. About dendrimers: structure, physical properties, and applications. *Chem. Rev.* **1999**, *99*, 1665.

23. Newkome, G. R.; Weis, C. D.; Moorefield, C. N.; Baker, G. R.; Childs, B. J.; Epperson, J. Isocyanate-based dendritic building blocks: combinatorial tier construction and macromolecular-property modification. *Angew. Chem. Int. Ed.* **1998**, *37*, 307.

24. Leon, J. W.; Kawa, M.; Fréchet, J. M. J. Isophthalate ester-terminated dendrimers: versatile nanoscopic building blocks with readily modifiable surface functionalities. *J. Am. Chem. Soc.* **1996**, *118*, 8847.

25. Grayson, S; Fréchet, J. M. J. Synthesis and surface functionalization of aliphatic polyether dendrons. *J. Am. Chem. Soc.* **2000**, *122*, 10335.

26. Freeman, A. W.; Chrisstoffels, L. A. J.; Fréchet, J. M. J. A simple method for controlling dendritic architecture and diversity: a parallel monomer combination approach. *J.Org. Chem.* **2000**, *65*, 7612.

27. Weil, T.; Wiesler, U. M.; Herrmann, A.; Bauer, R.; Hofkens, J.; De Schryver, F. C.; Müllen, K. Polyphenylene dendrimers with different fluorescent chromophores asymmetrically distributed at the periphery. *J. Am. Chem. Soc.* **2001**, *123*, 8101.

28. Leon, J. W.; Fréchet, J. M. J. Analysis of aromatic polyether dendrimers and dendrimer-linear block copolymers by matrix-assisted laser desorption ionization mass spectrometry. *Polym. Bull. (Berlin)* **1995**, *35*, 449.

29. Freeman, A. W.; Chrisstoffels, L. A. J.; Fréchet, J. M. J. A simple method for controlling dendritic architecture and diversity: a parallel monomer combination approach. *J. Org. Chem.* **2000**, *65*, 7612.

30. Maraval, V.; Laurent, R.; Donnadieu, B.; Mauzac, M.; Caminade, A. -M.; Majoral, J. -P. Rapid synthesis of phosphorous-containing dendrimers with controlled molecular architectures: first example of surface-block, layer-block, and segment-block dendrimers issued from the same dendron. *J. Am. Chem. Soc.* **2000**, *122*, 2499.

31. Larre, C.; Bressolles, D.; Turrin, C.; Donnadieu, B.; Caminade, A. -M.; Majoral, J. -P. Chemistry within megamolecules: regiospecific functionalization after construction of phosphorous dendrimers. *J. Am. Chem. Soc.* **1998**, *120*, 13070.

32. Li, W. -S.; Kim Kil, S.; D.-L. Jiang, D. -L.; Tanaka, H.; T. Kawai, T.; Kwon Jung, H.; Kim, D.; Aida, T. Construction of segregated arrays of multiple donor and acceptor units using a dendritic scaffold: remarkable dendrimer effects on photoinduced charge separation. *J. Am. Chem. Soc.* **2006**, *128*, 10527.

33. Dichtel, W. R.; Hecht, S.; Fréchet, J. M. J. Functionally layered dendrimers: a new building block and its application to the synthesis of multichromophoric light-harvesting systems. *Org. Lett.* **2005**, *7*, 4451.

34. Gillies, E. R.; Fréchet J. M. J. Designing macromolecules for therapeutic applications: polyester dendrimer-poly(ethylene oxide) 'bow-tie' hybrids with tunable molecular wieght and architecture. *J. Am. Chem. Soc.* **2002**, *124*, 14137.

35. Chen, Y.; Ambade, A. V.; Vutukuri, D. R.; Thayumanavan, S. Self-assembly of

facially amphiphilic dendrimers on surfaces. *J. Am. Chem. Soc.* **2006**, *128*, 14760.

36. Vutukuri, D. R.; Basu, S.; Thayumanavan, S. Dendrimers with both polar and apolar nanocontainers characteristics. *J. Am. Chem. Soc.* **2004**, *126*, 15636.

37. Zhang, W.; Nowlan, III, D. T.; Thomson, L. M.; Lackowski, W. M.; Simanek, E. E. Orthogonal, convergent synthesis of dendrimers based on melamine with one or two unique surface sites for manipulation. *J. Am. Chem. Soc.* **2001**, *123*, 8914.

38. Majoros, I. J.; Thomas, T. P.; Mehta, C. B.; Baker, Jr., J. R. Poly(amidoamine) dendrimer-based multifunctional engineered nanodevice for cancer therapy. *J. Med. Chem.* **2005**, *48*, 5892.

39. Bo, Z.; Schäefer, A.; Franke, P.; Schlüter, A. D. A facile synthetic route to a third-generation dendrimer with generation-specific functional aryl bromides. *Org. Lett.* **2000**, *2*, 1645.

40. Wu, P.; Malkoch, M.; Hunt, J. N.; Vestberg, R.; Kaltgrad, E.; Finn, M. G.; Fokin, V. V.; Sharpless, K. B.; Hawker, C. J. Multivalent, bifunctional dendrimers prepared by click chemistry. *Chem. Commun.* **2005**, 5775.

41. Lim, J.; Simanek, E. E. Toward the next-generation drug delivery vehicle: synthesis of a dendrimer with four orthogonally reactive groups. *Mol. Pharm.* **2005**, *2*, 273.

42. Steffensen, M. B.; Simanek, E. E. Synthesis and manipulation of orthogonally protected dendrimers: building blocks for library synthesis. *Angew. Chem. Int. Ed.* **2004**, *43*, 5178.

43. Hawker, C. J.; Fréchet, J. M. J. Control of surface functionality in the synthesis of dendritic macromolecules using the convergent-growth approach. *Macromolecules* **1990**, *23*, 4726.

44. Herrmann, A.; Mihov, G.; Vandermeulen, G. W. M.; Klok, H. -A.; Mullen, K. Peptide-functionalized polyphenylene dendrimers. *Tetrahedron* **2003**, *59*, 3925.

45. Wooley, K. L.; Hawker, C. J.; Fréchet, J. M. J. Polymers with controlled molecular architecture: control of surface functionality in the synthesis of dendritic hyperbranched macromolecules using the convergent approach. *J. Chem. Soc., Perkins Trans. 1* **1991**, 1059.

46. Zhang, W; Simanek, E. E. Dendrimers based on melamine. Divergent and orthogonal, convergent syntheses of a G3 dendrimer. *Org. Lett.* **2000**, *2*, 843.

47. Ganesh, R. N.; Shraberg, J.; Sheridan P. G.; Thayumanavan, S. Synthesis of difunctionalized dendrimers: an approach to main-chain poly(dendrimers). *Tetrahedron Lett.* **2002**, *43*, 7217.

48. Yoon, K.; Goyal, P.; Weck, M. Monofunctionalization of dendrimers with use of microwave-assisted 1,3-dipolar cycloadditions. *Org. Lett.* **2007**, *9*, 2051.

49. Goyal, P.; Yoon, K.; Weck, M. Multifunctionalization of dendrimers through orthogonal transformations. *Chem Eur. J.* **2007**, *13*, 8801.

50. Newkome, G. R.; Kim, H. J.; Moorefield, C. N.; Maddi, H.; Yoo, K. -S. Synthesis of new 1→ (2 +1) C-branched monomers for the construction of multifunctional dendrimers. *Macromolecules* **2003**, *36*, 4345.

51. Newkome, G. R.; Nayak, A.; Behera, R. K.; Moorefield, C. N.; Baker, G. R. Chemistry of micelles series. Cascade polymers: synthesis and characterization of four-directional spherical dendritic macromolecules based on adamantane. *J. Org. Chem.* **1992**, *57*, 358.

52. Newkome, G. R.; Kotta, K. K.; Moorefield, C. N. Design, synthesis, and characterization of conifer-shaped dendritic architectures. *Chem. Eur. J.* **2006**, *12*, 3726.

53. Rodriguez, E. C.; Marcaurelle, L. A.; Bertozzi, C. R. Aminooxy-, hydrazide-, and thiosemicarbazide-functionalized saccharides: versatile reagents for glycoconjugate synthesis. *J. Org. Chem.* **1998**, *63*, 7134.

54. Lee Lac, V.; Mitchell Michael, L.; Huang, S.-J.; Fokin Valery, V.; Sharpless, K. B.; Wong, C.-H. A potent and highly selective inhibitor of human α-1,3-fucosyltransferase via click chemistry. *J. Am. Chem. Soc.* **2003**, *125*, 9588.

55. Helms, B; Mynar, J. L.; Hawker, C. J.; Fréchet, J. M. J. Dendronized linear polymers via 'click chemistry'. *J. Am. Chem. Soc.* **2004**, *126*, 15020.

56. Hoogenboom, R.; Moore, B. C.; Schubert, U. S. Synthesis of star-shaped poly(vepsiln-caprolactone) via 'click' chemistry and 'supramolecular click' chemistry. *Chem. Commun.* **2006**, *38*, 4010.

57. Wang, X-Y.; Kimyonok, A.; Weck, M. Functionalization of polymers with phosphorescent iridium complexes via click chemistry. *Chem. Commun.* **2006**, *37*, 3933.

58. Ballini, R.; Petrini, M.; Rosini, G. New and efficient synthesis of ω-nitro alcohols and spiroketals by chemo- and regioselective reductive cleavage of 2-nitro cycloalkanones. *Tetrahedron* **1990**, *46*, 7531.

59. Newkome, G. R.; Kotta, K. K.; Moorefield, C. N. *J. Org. Chem.* **2005**, *70*, 4893.

60. Appukkuttan, P; Dehaen, W; Fokin, V. V.; Van der Eycken, E. A microwave-assisted click chemistry synthesis of 1,4-disubstituted 1,2,3-triazoles via a copper (I)-catalyzed three-component reaction. *Org. Lett.* **2004**, *6*, 4223.

61. Rijkers, D. T. S.; van Esse, G. W.; Merkx, R.; Brouwer, A. J.; Jacobs, H. J. F.; Pieters, R. J.; Liskamp, R. M. J. Efficient microwave-assisted synthesis of multivalent dendrimeric peptides using cycloaddition reaction (click) chemistry. *Chem Commun.* **2005**, 4581.

62. Bouillon, C.; Meyer, A.; Vidal, S.; Jochum, A.; Chevolot, Y.; Cloarec, J. -J.; Praly, J. -P.; Vasseur, J. -J.; Morvan, F. Microwave assisted 'click' chemistry for the synthesis of multiple labeled-carbohydrate oligonucleotides on solid support. *J. Org. Chem.* **2006**, *71*, 4700.

63. Hopkins, T. E.; Wagener, K. B. Amino acid and dipeptide functionalized polyolefins. *Macromolecules* **2003**, *36*, 2206.

64. Maynard, H. D.; Okada, S. Y.; Grubbs, R. H. Inhibition of cell adhesion to fibronectin by oligopeptide-substituted polynorbornenes. *J. Am. Chem. Soc.* **2001**, *123*, 1275.

65. You, C. -C.; De, M.; Han, G.; Rotello V. M. Tunable inhibition and denaturation of α-chymotrypsin with amino acid-functionalized gold nanoparticles. *J. Am. Chem. Soc.* **2005**, *127*, 12873.

66. Gestwicki, J. E.; Cairo, C. W.; Strong, L. E.; Oetjen, K. A.; Kiessling, L. L. Influencing receptor-ligand binding mechanisms with multivalent ligand architecture. *J. Am. Chem. Soc.* **2002**, *124*, 14922.

67. Mammen, M.; Chio, S. -K.; Whitesides, G. M. Polyvalent interactions in biological systems: implications for design and use of multivalent ligands and inhibitors. *Angew. Chem. Int. Ed.* **1998**, *37*, 2755.

68. Ilhan, F.; Galow, T. H.; Gray, M.; Clavier, G.; Rotello, V. M. Giant vesicle formation through self-assembly of complementary random copolymers. *J. Am. Chem. Soc.* **2000**, *122*, 5895.

CHAPTER 4

Application 1: Raman Label and Ag Nanocluster Containing Dendrimers as Highly Fluorescent, Scaffold Specific Biological Labels

4.1 Abstract

In biological systems it would be important to develop tools to enable background free single molecule Raman spectroscopy and fluorescence imaging. This chapter describes the encapsulation of sub-nm Ag nanoclusters into dendrimers and preliminary Raman spectroscopy of the resulting materials as a potential imaging tool for biology. The bright fluorescence and Raman enhancing capabilities of noble metal nanoclusters allows for creation of biolabels for *in vivo* imaging with stronger emission than known fluorescent labels. The combination of strong dendrimer encapsulated Ag nanocluster fluorescence with Raman incorporated labels in PAMAM dendrimers, allows for creation of strongly absorbing and emitting fluorescent materials with unambiguous scaffold specific Raman information for the development of biological labels.

4.2 Introduction

Confinement of electrons within a metallic nanostructure at sizes comparable to the Fermi wavelength of the electron[1] leads to electronic energy states which exhibit molecule-like transitions as the density of these states is too low for reproducing bulk properties of metal. This results in discrete nanocluster energy levels and significantly modified optical properties.[2-4] Such nanostructures present new optical materials on the

single molecule level with controllable size-dependent properties.[5-6] Non toxic noble metal nanoclusters consisting of few atoms show a strong, discrete and size dependent emission,[7-10] at sizes much smaller than do either semiconductor quantum dots,[11-12] or Raman enhancing metal particles.[13-15] Hence, Ag and Au nanoclusters are attractive candidates for the development of smallest possible fluorescent labels, which are very bright and photostable and expand the reach of single molecule methods.

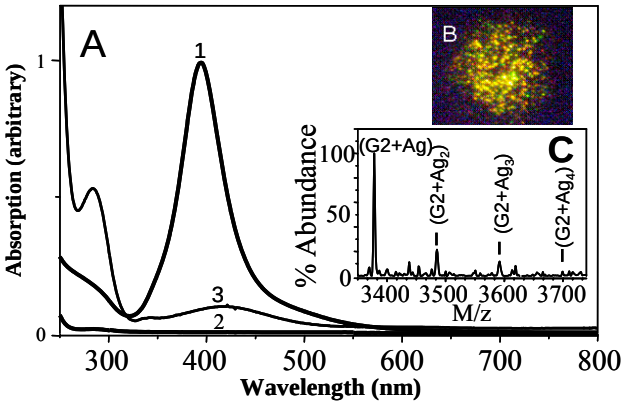

Figure 4.1 (A) UV-vis spectra of aqueous Ag/dendrimer solutions[16] (1) Strong plasmon absorption (398 nm) characteristic of large, nonfluorescent dendrimer encapsulated silver nanoparticles (2) absorption spectrum of non fluorescent (dendrimer:Ag) solution before photoactivation, (3) the same solution after photoactivation to yield highly fluorescent silver nanodots; (B) Fluorescence image;[16] (C) ESI-MS of photoactivated G2-OH PAMAM-$AgNO_3$ solution. Ag_n nanodot peaks are spaced by the Ag atomic mass (107.9)[16]

A new synthesis of noble metal clusters based on removal of metals from the solution into PAMAM dendrimers was reported first in 2002 by Dickson and coworkers.[16-18] Such dendrimer encapsulated and stabilized nanoclusters (< 1 nm in diameter), showed extremely strong, robust and size dependent single molecule fluorescence (Figure 4.1).[16] These dendrimer containing nanoclusters were generated by reduction of a solution of Au or Ag salt with PAMAM dendrimer using either

photoactivation with weak UV light or standard reducing agents, maintaining neutral pH. The reduced metal atoms aggregate within the dendrimers to form small nanoclusters and large nanoparticles, which are readily removed by centrifugation.[16] The resultant dendrimer encapsulated nanocluster exhibited two orders of magnitude stronger emission than any other known fluorescent label.

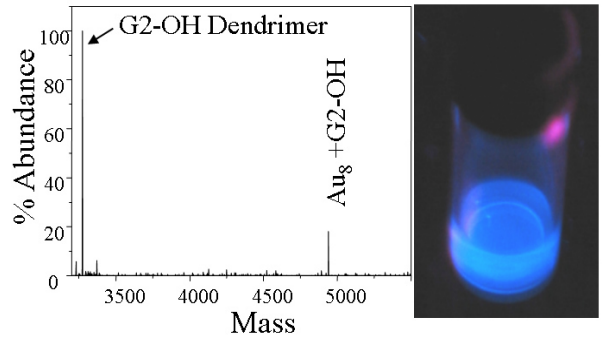

Figure 4.2 (A) Excitation and emission spectra of G4-OH PAMAM encapsulated gold nanodots. (B) Emission from Au nanodots under long-wavelength UV lamp irradiation[17]

Thereafter, Dickson and coworkers reported blue light-emitting PAMAM stabilized Au_8 nanoclusters (evident by the mass spectra in Figure 4.2) with high quantum yields.[17] Subsequently, by adjusting the initial concentration ratios, they could tune Au and Ag nanocluster excitation and emission spectra spanning the entire spectral range from the UV to the near-infrared,[18] as shown in Figure 4.3. The intense photoactivated emission of these dendrimer encapsulated Au or Ag nanoclusters with very long life before photobleaching make these materials attractive new nanomaterials for studying biological systems.

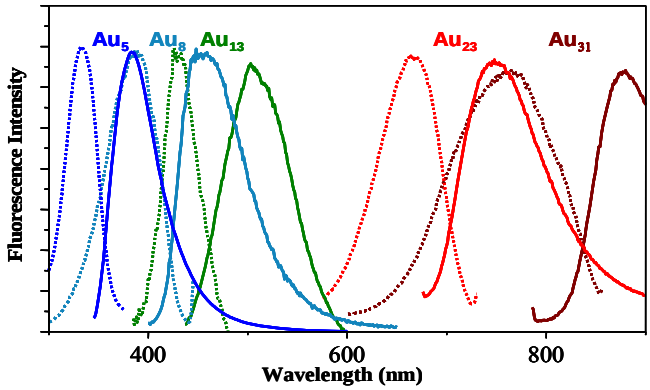

Figure 4.3 Excitation and emission spectra of different strongly fluorescent Au nanodot solutions spanning through visible and near-IR region[18]

Based on these findings by Dickson and coworkers, the objective of the science described in this chapter is to develop PAMAM based dendrimers containing Raman tags in their core for the development of ultra-bright biolabels with single molecule fluorescence (from noble metal nanocluster encapsulation) and background free, scaffold specific Raman imaging (from incorporated Raman labels). While the single nanocluster fluorescence is already brighter than other labels, the advantages offered by Raman over fluorescence include extremely high emission rates due to shorter lifetime, no photobleaching and narrow emission to reduce noise by reducing spectral bandwidth. A variety of Raman active functional groups including carbon-deuterium (C-D) and triple bonds (C≡N,C≡C, C≡O) have vibrational frequencies outside the fingerprint and hydrogen stretching regions in the nearly background free (1900-2300 cm^{-1}) spectral region. Incorporation of such functional groups 'or Raman tags' in the core of the dendrimers allows for background free Raman imaging and characterization of these dendrimers. By choosing proper excitation wavelength and time gated detection, single molecule Raman imaging of these dendrimers could offer scaffold specific information in a background free spectral window.

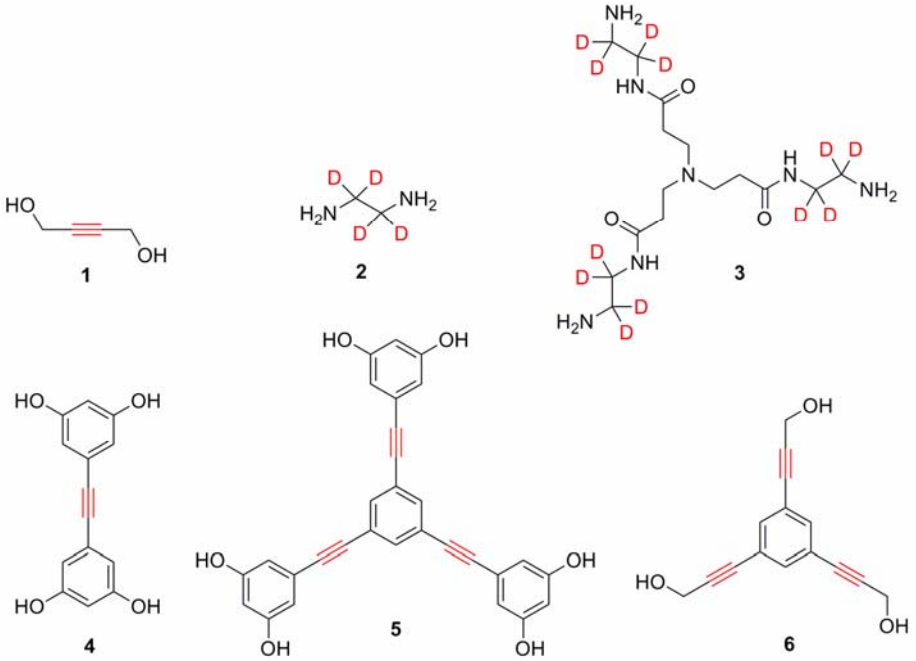

Figure 4.4 Dendrimer cores containing triple bonds and carbon-deuterium bonds as Raman tags

Figure 4.4 outlines the cores that were used for the synthesis of PAMAM based dendrimers incorporating such Raman tags. Cores **2** and **3** contain deuterium instead of hydrogen and are based on the original PAMAM core while cores **1**, **4**, **5** and **6** contain one or more carbon-carbon triple bonds. These cores were designed to increase systematically the amount of carbon-carbon triple bonds in the core to enable the optimal C≡C concentration for the Raman imaging. The synthesis of the dendrimers containing these Raman tags were done in collaboration with Dr. Kunsang Yoon.

4.3 Results and Discussion

Cores **1** and **2** were commercially available while cores **4**, **5** and **6** were synthesized using standard palladium catalyzed couplings. In general, the corresponding aryl halides and TMS-acetylene were coupled under Sonogashira coupling[20-21]

conditions using diphosphine-palladium chloride as palladium source with a copper co-catalyst and an amine base. The TMS groups were then removed using a mild base and the terminal alkyne was coupled to another aryl molecule using the aforementioned coupling conditions to afford a core molecule as shown in Scheme 4.2 for synthesis of core **5**. All cores were fully characterized by ^{1}H, ^{13}C NMR as well as mass spectroscopies and elemental analysis.

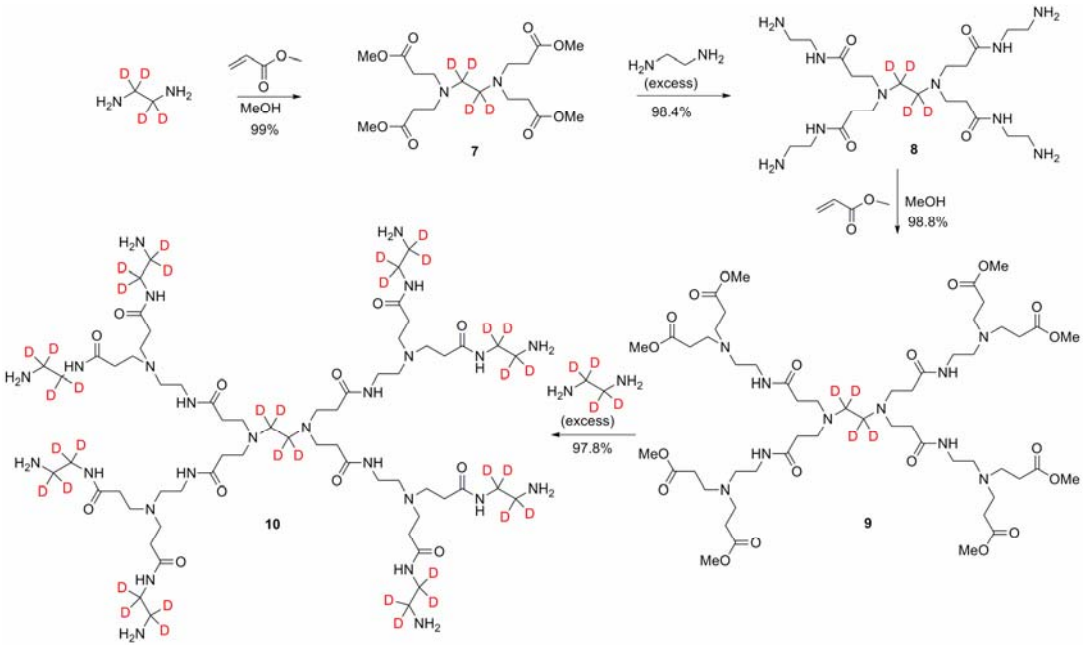

Scheme 4.1 Synthesis of G-2 PAMAM based dendrimer **10**

After the successful synthesis of the cores, the dendrimers were synthesized using a divergent synthesis approach. The synthesis was carried out in close analogy to literature procedures[19] with consecutive Michael additions. Reaction of the core molecules **1** and **2** with methacrylate under Michael addition conditions gave the alkylated dendrimer **7** as shown in Scheme 4.1. The amidation of this molecule with excess ethylene diamine resulted in the increased generation dendrimer **8**. Iteration of

these additions on the dendrimer molecule and using excess of deuterated-ethylene diamine in the final reaction step afforded the second generation deuterated dendrimer **10**.

Dendrimer **17** was synthesized similarly by using core **1** and carrying out consecutive Michael additions with methacrylate and amidations with excess ethylene diamine to afford the second generation dendrimer. Conjugated core dendrimers **16**, **18** and **19** were obtained after synthesizing cores **4**, **5**, and **6** by Sonogashira coupling[20-21] outlined earlier and as shown in Scheme 4.2 for the synthesis of **5**. Reaction of core molecule **5** with methyl bromo-acetate gave the half generation dendrimer **13** and its amidation with excess ethylene diamine and Michael addition using methacrylate followed by another amidation with ethylene diamine afforded second generation dendrimer **16**.

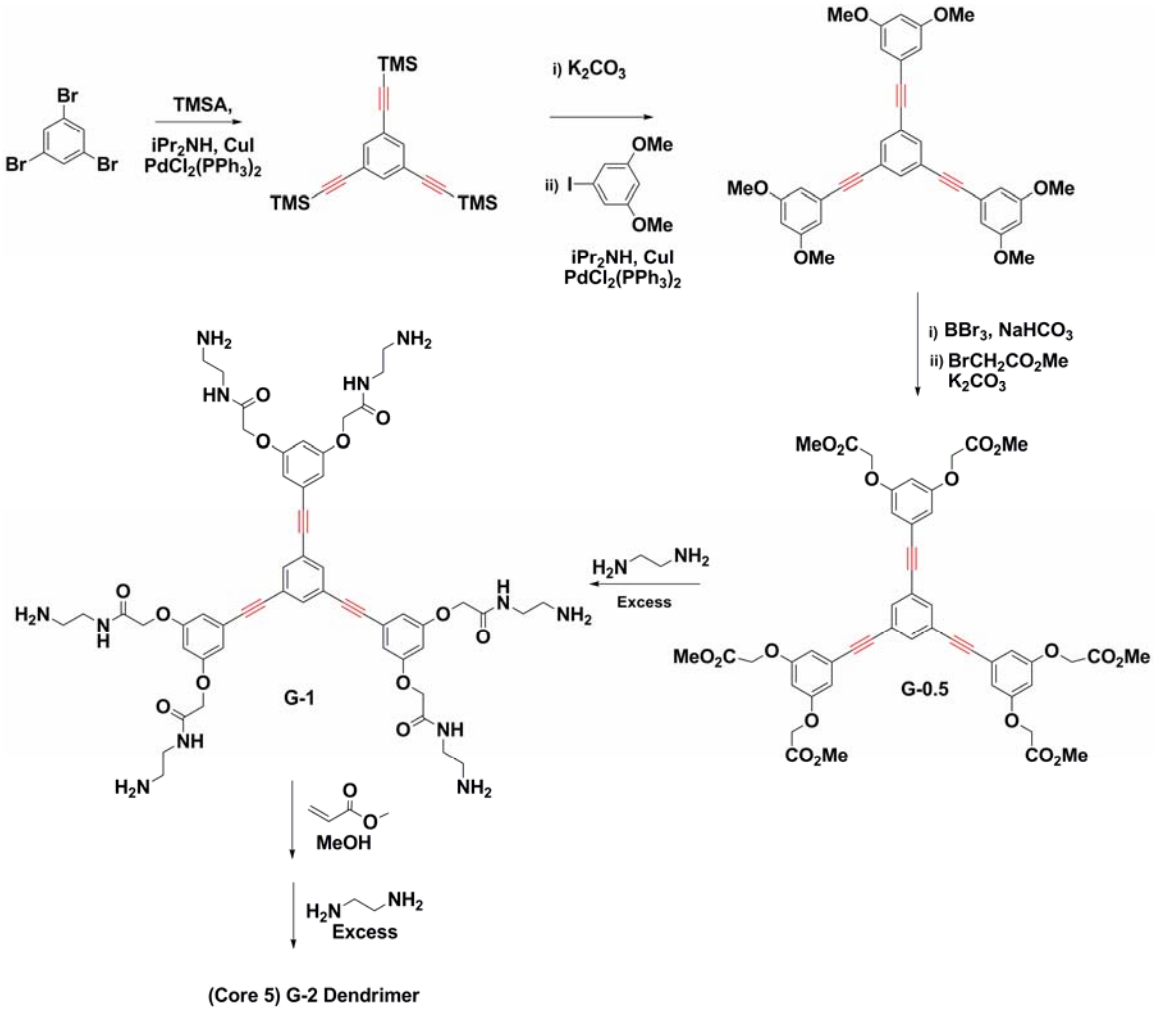

Scheme 4.2 Synthesis of G-2 PAMAM based dendrimer **16**

Other conjugated dendrimers **18** and **19** were synthesized similarly using first Sonogashira couplings for synthesis of cores **4** and **6**, followed by alternating Michael addition reaction with methacrylate and amidation reaction using ethylene diamine until generation two dendrimers were obtained.

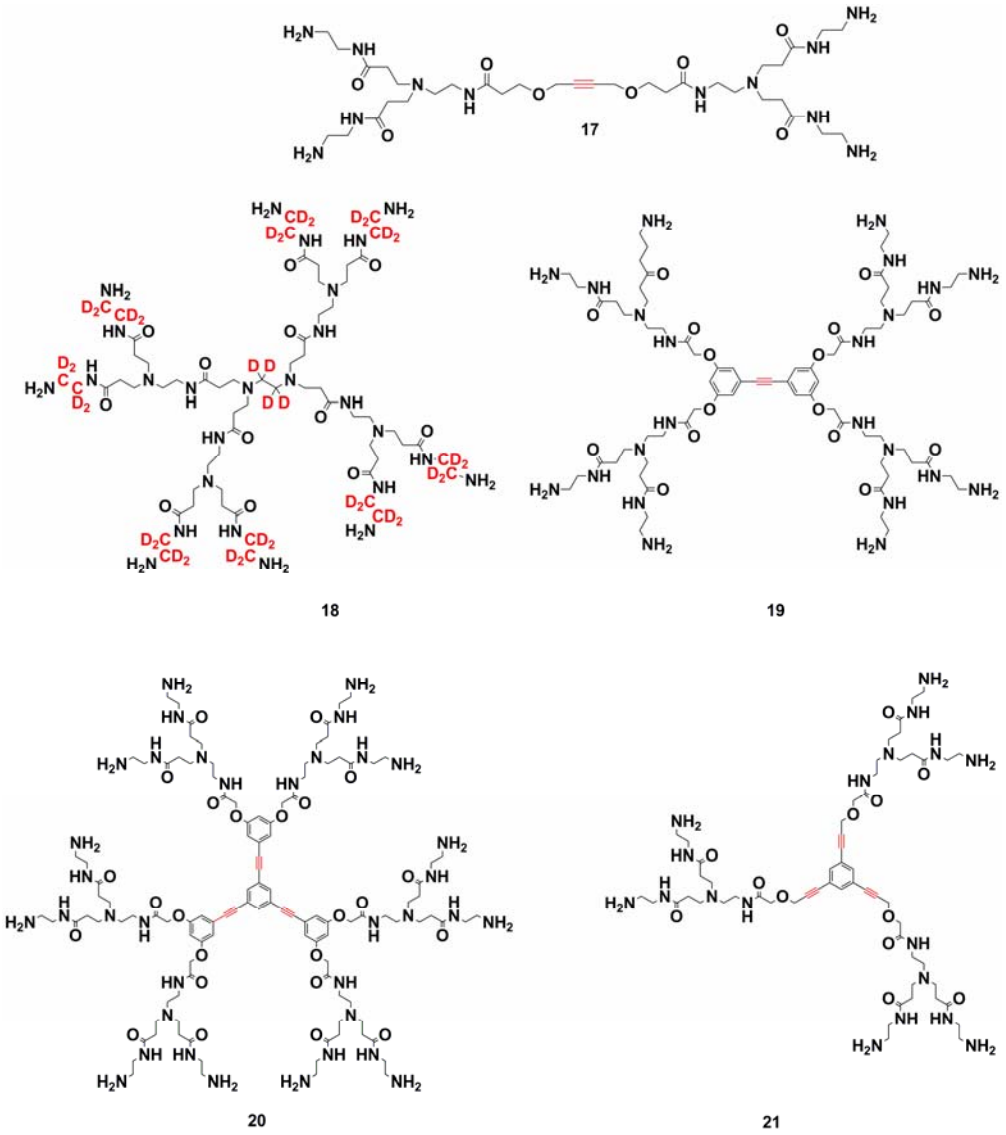

Figure 4.5 Synthesized G-2 PAMAM based dendrimers containing Raman tags

All the synthesized dendrimers as shown in Figure 4.5, were submitted to Dr. Dickson's group for single molecule imaging studies which were performed by Dr. Dulal Senapati.

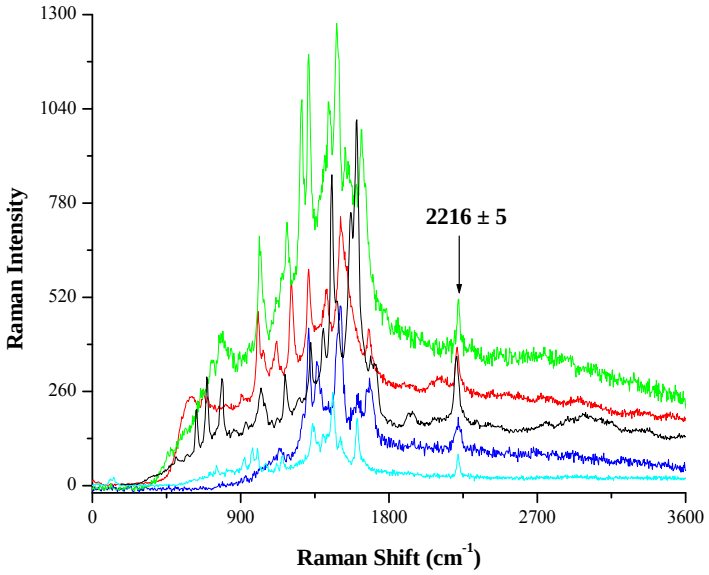

Figure 4.6 Single molecule Raman spectra of dendrimer **9** encapsulated Ag_n at different excitation wavelength (458 nm, 476 nm, 488 nm, 514.5 nm and 530 nm). Peak at 2216 cm^{-1} corresponds to the C-D Raman stretch[22]

For the single molecule studies, the dendrimer encapsulated Ag nanoclusters are produced in water by *in-situ* photoreduction of a solution of a 10^{-6} M dendrimer with around 10 fold excess of $AgNO_3$ in 18-MΩ water. The resulting solutions are centrifuged and decanted solution is used to ensure absence of nanoparticles. Raman spectra of encapsulated Ag nanoclusters are collected under Ar^+ laser excitation (514.5 nm laser line) in an epifluorescent configuration. Rapidly photoreduced at 458-530 nm, the individual spots emit bright fluorescence and Raman for hours.[22]

As observed in the single molecule Raman studies done by Dickson Group,[22] the Raman spectra (see Figure 4.6 for single molecule Raman spectra of dendrimer **9**) of dendrimers with Raman tags encapsulated few atom Ag-nanoclusters show three types of emission. These emissions are (1) Sharp Raman lines in the 0-3000 cm^{-1} spectral window,

independent of excitation wavelength but dependent upon the encapsulating dendrimer scaffold (2) Fluorescence background in 0-3000 cm^{-1} spectral window, with a constant background under sharp Raman lines which varies in intensity, shape and time and is dependent both on nanocluster and encapsulating scaffold, (3) broad intense fluorescence beyond Raman window and independent of excitation wavelength. This broad emission is from different clusters showing different fluorescence emission and accounts for multi-colored emission from the same dendrimer encapsulated nanoclusters.

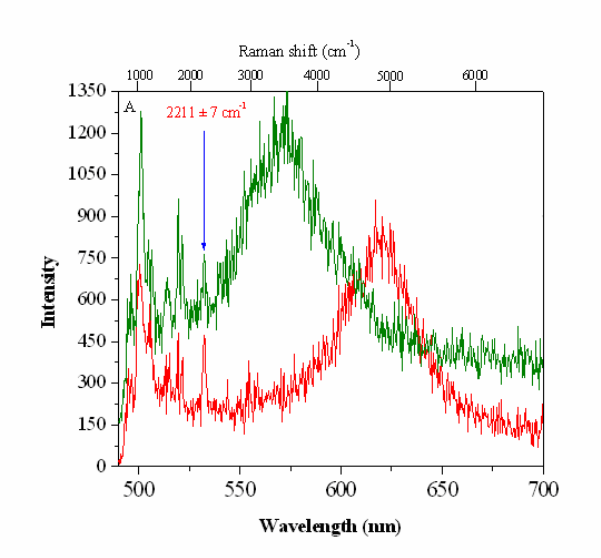

Figure 4.7 Spectrally separated Raman and fluorescence from two different PAMAM dendrimer **9** encapsulated Ag nanoclusters using 476 nm excitation.[22] The sharp peak at 532 nm (2211 cm^{-1}) is the C-D stretch of dendrimer scaffold **9** and the peak between 550-650 nm is the fluorescence peak from two different Ag nanoclusters in dendrimer **9**. The peaks before 525 nm are from dendrimer scaffold **9**

Based on the studies by Dickson group,[22] a maximum diameter of single molecule Raman enhancing Ag nanocluster is determined to be 1.6 nm, consistent with species that are too small to support plasmon scattering, but sufficient to yield strong fluorescence. The strong Raman transitions of the alkyne (C≡C) and carbon-deuterated (C-D) functionalities appear in the unobscured spectral windows, with frequencies

characteristic of only the scaffold as seen in Figure 4.7. Additionally, the strong Ag nanocluster fluorescence is spectrally separate from the identifiable Raman features, suggesting competing pathways in the nanocluster excited states leading to Raman enhancement. (Figure 4.7)

4.4 Conclusion

Five set of dendrimers, incorporating Raman tags (carbon-carbons triple bonds or carbon-deuterium bonds) were synthesized and submitted to Dr. Dickson's group for single molecule Raman enhancement and Ag – nanocluster encapsulated fluorescence studies. All these dendrimers show chemically specific and distinct signals in the single molecule Raman spectra (in a background free spectral window from 1900-2500 cm^{-1}) corresponding to C-D and/or a C≡C stretches. In addition, the dendrimer encapsulated Ag_n nanoclusters showed bright and spectrally separated fluorescence. Ongoing studies on these Raman tag containing and Ag nanocluster encapsulating dendrimers at Dickson group would pave the way for use of these molecules as extremely bright, photostable and scaffold specific biological labels.

4.5 Experimental

Materials and General Procedures

All reactions were carried out under an Argon atmosphere. Tetrahydrofuran was distilled over sodium/benzophenone and methanol over Mg coupled with iodine. Ethylene diamine and methyl acrylate were distilled over calcium hydride and stored in Schlenk-flasks under argon. All other reagents were purchased from commercial sources and used as received unless otherwise noted. Separations of amine-terminated dendrimers were performed by column chromatography using technical grade silica gel (60 Å, 40-63 μm) or Alumina. NMR spectra were acquired with a Varian Mercury 400 (^{1}H, 400.0 MHz; ^{13}C, 100.6 MHz) or aVarian Mercury 300 (^{1}H, 300.0 MHz; ^{13}C, 75.5 MHz) spectrometers. Chemical shifts are reported in ppm and referenced to the residual nuclei in the corresponding deuterated solvents. Mass spectra were recorded with a VG 7070 EQ-HF hybrid tandem mass spectrometer. Single molecule studies were carried out in Dr. Dickson's group.[22]

[Core 1] G-0.5:

2-Butyne-1,4 diol or core **1** (5g, 0.058 mol) was dissolved in 50 ml of THF and the solution was cooled to 0 ºC. To this stirred solution, *n*-butyl lithium (3ml, 0.012 mol) was added dropwise and the reaction mixture was allowed to warm up to room temperature. Methyl acrylate (12.5g, 0.116 mol) was added dropwise to the reaction and the reaction mixture was stirred at room temperature overnight. All volatiles were removed under reduced pressure and the residue was dissolved in diethyl ether and washed twice with 2M HCl, water and brine. The combined ether layers were dried over magnesium sulfate, filtered and evaporated. The crude product was purified by column

chromatography (SiO_2, EtOAc/Hexanes = 1: 5) to yield 10 g product (66 %) as a colorless oil. ^{1}H NMR ($CDCl_3$): δ = 2.75 (t, 4H, *J* = 6.2 Hz), 3.56 (s, 6H), 3.74 (t, 4H, *J* = 5.62), 4.25 (s, 4H). ^{13}C NMR ($CDCl_3$): δ = 173.0, 83.3, 66.2, 54.5, 51.5, 34.9. MS (ESI) m/z (100%) = 258.11 (M^+, calcd 258.11).

[Core 1] G-1:

Ethylene diamine (120 g, 2 mol) was mixed with 30 ml methanol and cooled to 0 ºC. To this solution, a 50% (w/w) methanol solution of **[Core 1]** G-0.5 (10g, 0.038 mol) was added and the reaction was stirred at room temperature for 3 days. The excess of ethylene diamine and methanol were removed by distillation followed by an azeotropic distillation using a 3/1 toluene/methanol solvent mixture. The crude product was purified by column chromatography (Alumina, EtOAc/MeOH = 10:1) to yield 11.9 g (98%) of the target compound as a colorless oil. ^{1}H NMR ($CDCl_3$): δ = 2.35 (t, 4H, *J* = 6.2 Hz), 2.87 (distorted t, 4H), 3.31 (t, 4H, *J* = 6.7 Hz), 3.66 (t, 4H, *J* = 5.62 Hz), 4.29 (s, 4H). ^{13}C NMR ($CDCl_3$): δ = 166.1, 83.3, 65.3, 54.1, 42.6, 40.9, 33.1. MS (ESI) m/z (100%) = 314.21 (M^+, calcd 314.20).

[Core 1] G-1.5

To a 50 wt% methanol solution of methyl acrylate (6g, 0.06 mol) was added dropwise, with stirring, over a 30-min period a 50-75 wt% methanol solution of **[Core 1] G-1** (5g, 0.014 mol). The reaction was stirred under argon atmosphere at room temperature for 4 days followed by heating at 40ºC for 30 min. Then the excess methyl acrylate and methanol were removed by rotary evaporation yielding the light yellow product which was dried under vacuum (12.3 g, 98%). ^{1}H NMR ($CDCl_3$): δ = 2.33 (m, 12H), 2.42 (m,

4H), 2.54 (m, 8H), 3.25 (t, 4H, *J* = 6.7 Hz), 3.55 (s, 12H), 3.71 (t, 4H, *J* = 5.81 Hz), 4.29 (s, 4H, C-CH_2-O-). ^{13}C NMR ($CDCl_3$): δ = 173.8, 168.7, 83.3, 65.3, 54.1, 52.3, 51.4, 49.2, 42.7, 38.2, 32.0. Anal Calcd for $C_{30}H_{50}N_4O_{12}$: C, 54.70; H, 7.65; N, 8.51. Found: C, 54.20; H, 7.98; N, 8.31.

[Core 1] G-2 or **17:**

Ethylene diamine (160 g, 2.6 mol) was mixed with 40 ml of methanol and cooled to 5 ºC. To this cooled solution was added a 50% (w/w) methanol solution of **[Core 1] G-1.5** (4.5g, 0.006 mol). The reaction was run at 5 ºC for 3 days and then heated to 40ºC for 30 min. Then, the excess ethylene diamine and methanol were removed by rotary evaporation and the product was dried under vacuum (5.15 g, 99%). ^{1}H NMR ($CDCl_3$): δ = 2.33 (m, 8H), 2.42 (m, 4H), 2.54 (distorted t, 4H), 2.75 (m, 16H), 3.25 (m, 12H), 3.71 (t, 4H, *J* = 5.81 Hz), 4.29 (s, 4H). ^{13}C NMR ($CDCl_3$): δ = 168.3, 165.5, 83.3, 65.3, 54.1, 53.5, 49.5, 42.6, 41.7, 38.0, 33.1, 31.2. MS (ESI) m/z (100%) = 770.39 (M^+, calcd 770.39).

[Core 2] G-0.5 or **7:**

A round bottom flask equipped with a stir bar was charged with ethylene-d_4-diamine (50 mg, 0.779 mmol in methanol (1 ml)). To this solution, methyl acrylate (0.41 ml, 4.6 mmol) was added dropwise at 0 ºC. The reaction mixture was stirred at room temperature for three days with additional additions of methyl acrylate (0.41 ml) every 24 hrs and the conversions were monitored by TLC. The excess methyl acrylate and methanol were removed under reduced pressure and the product was dried on high vacuum (315 mg, 99%). ^{1}H NMR ($CDCl_3$): δ = 2.34 (t, 8H, *J* = 6.56 Hz), 2.61 (t, 8H, *J* =

5.31 Hz), 3.71 (s, 12H). ^{13}C NMR ($CDCl_3$): δ = 174, 51.4, 49.2, 32.6. MS (ESI) m/z (100%) = 408.23 (M^+, calcd 408.24).

[Core2] G-1 or **8:**

Ethylene diamine (7g, 0.11 mol) was mixed with 1 ml methanol and stirred at room temperature. To this solution was added a methanol solution of **[Core 2] G-1** (215 mg, 0.526 mmol). The reaction mixture was stirred at room temperature for 3 days. Excess ethylene diamine and methanol were removed by distillation and the product was dried under vacuum at 50º C to yield 270 mg of the product (98.4%). ^1H NMR ($CDCl_3$): δ = 2.35 (t, 8H, *J* = 6.56 Hz), 2.55 (m, 16H), 3.27 (t, 8H, *J* = 6.64 Hz). ^{13}C NMR ($CDCl_3$): δ = 169.3, 53.5, 45.7, 42.6, 32.6, 32.5. MS (ESI) m/z (100%) = 520.41 (M^+, calcd 520.41). Anal Calcd for $C_{22}H_{44}$ $D_4N_{10}O_4$: C, 50.75; H, 10.06; N, 26.90. Found: C, 49.80; H, 10.20; N, 26.70.

[Core 2] G-1.5 or **9:**

To a stirred solution of **[Core 2] G-1** (270 mg, 0.519 mmol) in methanol (2 ml), was added methyl acrylate (0.59 ml, 6.2 mmol) dropwise at 0 ºC. The reaction mixture was stirred at room temperature for four days with additional additions of methyl acrylate (0.59 ml) every 24 hrs and the conversion were monitored by TLC. The excess methyl acrylate and methanol were removed under reduced pressure and the product dried under vacuum to yield 620 mg (98.8%) of product. ^1H NMR ($CDCl_3$): δ = 2.38 (t, 8H, *J* = 6.56 Hz), 2.48 (m,16H), 2.55 (t, 8H, *J* = 5.42 Hz), 2.79 (m, 24H), 3.25 (t, 8H, *J* = 6.64 Hz), 3.71 (s, 24H). ^{13}C NMR ($CDCl_3$): δ = 174, 165.3, 53.5, 52.3, 51.4, 49.2, 42.4, 33.1, 32.6, 32.4. MS (ESI) m/z (100%) = 1208.70 (M^+, calcd 1208.70). Anal Calcd for $C_{54}H_{92}$ $D_4N_{10}O_{20}$: C, 53.63; H, 8.33; N, 11.58. Found: C, 53.35; H, 8.66; N, 11.25.

[Core 2] G-2 or **10:**

Ethylene-d_4-diamine (250 mg, 3.91 mmol) was mixed with 0.5 ml methanol and stirred at room temperature. To this solution was added a methanol solution of **[Core 2] G-1.5** (24 mg, 0.019 mmol) and the reaction mixture was stirred at room temperature for 4 days. The excess of ethylene-d_4-diamine was removed under reduced pressures. 26.4 mg of product (97.8%) was obtained after drying under vacuum. ^{1}H NMR ($CDCl_3$): δ = 2.35 (br, 24H), 2.61 (t, 8H, *J* = 5.41 Hz), 2.82 (m, 24H), 3.25 (t, 8H, *J* = 6.7 Hz). ^{13}C NMR ($CDCl_3$): δ = 169.2, 164.3, 53.5, 49.5, 42.4, 40.6, 33.1, 32.2, 32.0, 30.4, 27.3.

1,3,5-Tris[(trimethylsilyl)ethynyl]benzene or **11:** (Synthesis done by Dr. Yoon)

A solution of 1,3,5-tribromobenzene (10.00 g, 31.8 mmol), $PdCl_2(PPh_3)_2$ (223 mg, 0.318 mmol), and CuI (303 mg, 1.59 mmol) in *i*-Pr_2NH was purged with argon for 15 minutes, and trimethylsilylacetylene (14.8 mL, 105 mmol) was added slowly at room temperature via a syringe. The reaction mixture was stirred for 48 hours at 60 °C. The mixture was cooled to room temperature, quenched with an aqueous solution of 5% HCl, and extracted with diethyl ether twice. The combined organic layers were washed with brine, dried over Na_2SO_4, filtered, concentrated *in vacuo*, and purified by silica gel column chromatography eluting with hexanes to give 8.87 g of title compound as a yellow solid in 76% yield. ^{1}H NMR ($CDCl_3$, 300 MHz): δ 0.21 (s, 27H), 7.47 (s, 3H). ^{13}C NMR ($CDCl_3$, 75.5 MHz): δ -0.1, 95.5, 103.1, 123.5, 134.8.

1,3,5-Triethynylbenzene: (Synthesis done by Dr. Yoon)

To a solution of 1,3,5-tris[(trimethylsilyl)ethynyl]benzene (6.92 g, 18.9 mmol) in a mixture of THF (60 mL) and MeOH (60 mL) was added K_2CO_3 as a solid. After stirring

for 18 hours at room temperature, the mixture was quenched with water and extracted twice with diethyl ether. The combined organic layers were washed with brine, dried over $MgSO_4$, and then filtered. Most of the volatiles were removed using a rotary evaporator. The crude product was further purified by silica gel column chromatography to give 2.63 g of the title compound as a yellow solid in 93% yield. ^{1}H NMR ($CDCl_3$, 300 MHz): δ 3.11 (s, 3H), 7.56 (s, 3H). ^{13}C NMR ($CDCl_3$, 75.5 MHz): δ 78.7, 81.6, 122.8, 135.5.

1-Iodo-3,5-dimethoxybenzene: (Synthesis done by Dr. Yoon)

3,5-dimethoxyaniline (15.00 g, 0.0979 mol) was added to a reaction flask containing HCl (100 mL) and ice-cooled water (100 mL) at 0 °C. A solution of $NaNO_2$ (8.11 g, 0.117 mol) in water (40 mL) was added dropwise *via* an addition funnel to give a dark red solution. After stirring for 1 hour, the water/ice bath was removed and a solution of KI (65.0 g, 0.392 mol) in water (150 mL) was added slowly. After stirring for 18 hours at room temperature, the mixture was extracted with diethyl ether (200 mL × 4). The combined organic layers were washed with brine (200 mL × 2) and an aqueous saturated $Na_2S_2O_3$ solution (200 mL × 2), dried over $MgSO_4$, filtered, and concentrated to a small volume. Silica was added and all the volatiles were removed to dryness. This preloaded silica gel was placed on a pad of silica gel and eluted with petroleum ether (3 L) to give 16.11 g of title compound as a white solid in 62% yield. ^{1}H NMR ($CDCl_3$, 400 MHz): δ 3.76 (s, 6H), 6.40 (t, J = 2.4 Hz, 1H), 6.86 (d, J = 2.4 Hz, 2H). ^{13}C NMR ($CDCl_3$, 100 MHz): δ 55.4, 94.0, 100.5, 115.6, 160.7.

1,3,5-Tris[(3,5-dimethoxyphenyl)ethynyl]benzene or **12:** (Synthesis done by Dr. Yoon)

A solution of 1,3,5-triethynylbenzene (0.158 g, 1.06 mmol) and 1-iodo-3,5-dimethoxybenzene (0.878 g, 3.32 mmol) in *i*-Pr_2NH was purged with argon for 15 minutes, and $PdCl_2(PPh_3)_2$ (14.8 mg, 0.0211 mmol) and CuI (20.1 mg, 0.106 mmol) were then added quickly. After stirring for 18 hours at room temperature, the reaction mixture was filtered and the filtrate was concentrated *in vacuo*, and purified by silica gel column chromatography to give 0.499 g of title compound as an orange solid in 85% yield. ^{1}H NMR ($CDCl_3$, 300 MHz): δ 3.81 (s, 18H), 6.49 (t, *J* = 2.4 Hz, 3H), 6.69 (d, *J* = 2.4 Hz, 6H), 7.66 (s, 3H). ^{13}C NMR ($CDCl_3$, 75.5 MHz): δ 55.5, 87.3, 90.5, 109.4, 123.8, 123.9, 128.0, 134.1, 160.4. HRMS EI: $[M]^+$ calcd for $C_{36}H_{30}O_6$, 558.2042; found, 558.1988.

1,3,5-Tris[(3,5-dihydroxyphenyl)ethynyl]benzene or **[Core 5]:** (Synthesis done by Dr. Yoon)

To a solution of 1,3,5-tris[(3,5-dimethoxyphenyl)ethynyl]benzene (0.395 g, 0.707 mmol) in dry CH_2Cl_2 (10 mL) was added BBr_3 dropwise at –10 °C. After the stirring for an additional 20 minutes at –10 °C, the mixture was allowed to stir for 24 hours at room temperature. The mixture was then poured into ice-water and then a saturated aqueous $NaHCO_3$ solution was added slowly to adjust the pH of the mixture to 7-8. The mixture was extracted with ethyl acetate four times. The combined organic layers were washed with brine and dried over $MgSO_4$. After the filtration, all the volatiles were removed *in vacuo,* and the crude product was further purified by silica gel column chromatography eluting with EtOAc/petroleum ether (1:1) to give 0.319 g of the title compound in 95% yield. ^{1}H NMR (acetone-d_6, 300 MHz): δ 6.43 (t, *J* = 2.1 Hz, 3H), 6.58 (d, *J* = 2.1 Hz, 6H), 7.63 (s, 3H), 8.20 (bs, 6H). ^{13}C NMR (acetone-d_6, 75.5 MHz): δ 87.0, 91.7, 110.9,

124.5, 125.0, 134.3, 159.2, 207.5. LRMS MALDI-TOF: $[M + H]^+$ calcd for $C_{30}H_{19}O_6$, 475.1; found, 475.1.

[Core 5] G-0.5 or **13:** (Synthesis done by Dr. Yoon)
To a solution of 1,3,5-tris[(3,5-dihydroxyphenyl)ethynyl]benzene (0.082 g, 0.173 mmol) and methyl bromoacetate (0.49 mL, 5.18 mmol) in acetone (17 mL) was added K_2CO_3 (0.573 g, 4.15 mmol). After stirring for 18 hours at 60 °C, the mixture was cooled down to room temperature, and water (30 mL) was added to give a white precipitate which was filtered and dried *in vacuo* to provide 0.125 g of the title compound as a white solid in 80% yield. ^{1}H NMR ($CDCl_3$, 300 MHz): δ 3.82 (s, 18H), 4.64 (s, 12H), 6.54 (t, J = 2.4 Hz, 3H), 6.70 (d, J = 2.4 Hz, 6H), 7.63 (s, 3H). ^{13}C NMR ($CDCl_3$, 75.5 MHz): δ 52.4, 65.3, 87.8, 90.0, 103.4, 110.9, 123.6, 124.4, 134.2, 158.6, 168.7. LRMS MALDI-TOF: $[M + H]^+$ calcd for $C_{48}H_{43}O_{18}$, 907.2; found, 907.2.

[Core 5] G-1 or **14:** (Synthesis done by Dr. Yoon)
To a solution of **[Core 5] G-0.5** (0.090 g, 0.0992 mmol) in a mixture of MeOH and THF (1:1, 5 mL) was added ethylene diamine (0.99 mL, 14.9 mmol) at 0 °C. After the mixture was stirred for 24 hours at room temperature, all the volatiles including the excess amount of ethylene diamine were removed *in vacuo* to give 0.103 g of the title compound as a yellow solid in 97 % yield. ^{1}H NMR (DMSO-d_6, 300 MHz): δ 2.59 (t, J = 6.3 Hz, 12H), 3.12 (t, J = 6.0 Hz, 12H), 4.52 (s, 12H), 6.69 (s, 3H), 6.81 (s, 6H), 7.76 (s, 3H), 8.08 (bs, 6H). LRMS MALDI-TOF: $[M + H]^+$ calcd for $C_{54}H_{67}N_{12}O_{12}$, 1075.5; found, 1075.5.

[Core 5] G-1.5 or **15:** (Synthesis done by Dr. Yoon)

To a solution of **[Core 5] G-1** (0.062 g, 0.0576 mmol) in MeOH (3 mL) was added methyl acrylate (0.12 mL, 1.38 mmol) and the reaction was stirred for 3 days. Additional portions of methyl acrylate (0.1 mL each) were added into the reaction mixture every 24 hours. After 3 days, all the volatiles were removed *in vacuo* and the crude product was further purified by silica gel column chromatography to give 0.105 g of the title compound as a clear yellow thick oil in 86% yield. ^{1}H NMR ($CDCl_3$, 300 MHz): δ 2.40 (t, *J* = 6.6 Hz, 24H), 2.55 (t, *J* = 5.6 Hz, 12H), 2.72 (t, *J* = 6.6 Hz, 24H), 3.42 (q, *J* = 5.4 Hz, 12H), 3.62 (s, 36H), 4.49 (s, 12H), 6.70 (t, *J* = 2.1 Hz, 3H), 6.78 (d, *J* = 2.1 Hz, 6H), 7.17 (t, *J* = 5.4 Hz, 6H), 7.62 (s, 3H). ^{13}C NMR ($CDCl_3$, 75.5 MHz): δ 32.5, 36.5, 48.9, 51.6, 52.7, 67.4, 87.8, 89.8, 103.4, 111.2, 123.7, 124.5, 134.2, 158.5, 167.5, 172.8. HRMS MALDI-TOF: $[M + H]^+$ calcd for $C_{102}H_{139}N_{12}O_{36}$, 2107.9415; found, 2107.9381.

[Core-5] G-2 or **16:** (Synthesis done by Dr. Yoon)

To a solution of **[Core-5] G-1.5** (0.0972 g, 0.0461 mmol) in a mixture of MeOH and THF (1:1, 5 mL) was added ethylene diamine (0.92 mL, 13.8 mmol) at 0 °C. After the mixture was stirred for 24 hours at room temperature, all the volatiles including excess amount of ethylene diamine were removed *in vacuo* to give 0.110 g of the title compound as a yellow solid in 98 % yield. ^{1}H NMR (DMSO-d_6, 300 MHz): δ 2.18 (bs, 24H), 2.48 (m, 36H), 2.64 (bs, 24H), 3.02 (t, *J* = 6.6 Hz, 24H), 3.19 (d, *J* = 4.5 Hz, 12H), 4.51 (bs, 12H), 6.69 (bs, 3H), 6.81 (bs, 6H), 7.74 (bs, 3H), 7.90 (bs, 12H), 8.08 (bs, 6H). HRMS MALDI-TOF: $[M + H]^+$ calcd for $C_{114}H_{187}N_{36}O_{24}$, 2444.4519; found, 2444.4473.

Methyl (2-propynyloxy)acetate: (Synthesis done by Dr. Yoon)

To a suspension of sodium hydride (3.65 g, 152 mmol) in tetrahydrofuran (150 mL) at 0 °C under argon was added dropwise propargyl alcohol (9.00 mL, 152 mmol). After stirring for 1 hour at 0 °C, methyl bromoacetate (15.9 mL, 168 mmol) was added and the reaction mixture was stirred for 30 minutes at 0 °C, stirred at room temperature for 2 hours, and then treated with 20 ml of 5% aquous HCl. The organic layer was isolated and the aqueous layer was extracted with ether (2 × 100 mL). The combined organic layers were washed with brine, dried over Na_2SO_4, filtered, concentrated *in vacuo*, and purified by silica gel column chromatography eluting with methylene chloride to give 12.10 g of title compound as a colorless clear oil in 62% yield. ^{1}H NMR ($CDCl_3$, 300 MHz): δ 2.48 (t, J = 2.5 Hz, 1H), 3.77 (s, 3H), 4.21 (s, 2H), 4.31 (d, J = 2.5 Hz, 2H). ^{13}C NMR ($CDCl_3$, 75.5 MHz): δ 51.9, 58.2, 66.0, 75.6, 78.3, 170.3.

[Core 6] G-0.5: (Synthesis done by Dr. Yoon)

A solution of 1,3,5-triiodobenzene (0.295 g, 0.646 mmol), $PdCl_2(PPh_3)_2$ (9.10 mg, 0.0129 mmol), and CuI (12.3 mg, 0.0646 mmol) in THF (3 mL) and Et_3N (3 mL) was purged with argon for 15 minutes, and a solution of methyl(2-propynyloxy)acetate (0.257 g, 2.00 mmol) in THF (1 mL) was then added slowly at room temperature via syringe. The reaction mixture was stirred for 24 hours at 40 °C. The mixture was cooled to room temperature, quenched with an aqueous solution of 5% HCl, and extracted with diethyl ether twice. The combined organic layers were washed with brine, dried over Na_2SO_4, filtered, concentrated *in vacuo*, and purified by silica gel column chromatography eluting with EtOAc/petroleum ether (1:1) to give 0.260 g of title compound as a yellow solid in 88% yield. ^{1}H NMR ($CDCl_3$, 300 MHz): δ 3.78 (s, 9H), 4.26 (s, 6H), 4.52 (s, 6H), 7.45

(s, 3H). ^{13}C NMR ($CDCl_3$, 75.5 MHz): δ 52.0, 58.9, 66.3, 85.4, 99.9, 123.1, 134.8, 170.1. HRMS MALDI-TOF: $[M + H]^+$ calcd for $C_{24}H_{25}O_9$, 457.1499; found, 457.1701.

[Core 6] G-1: (Synthesis done by Dr. Yoon)

To a solution of **[Core 6] G-0.5** (0.625 g, 1.37 mmol) in MeOH (7 mL) was added ethylene diamine (6.87 mL, 102.7 mmol) at 0 °C. After the mixture was stirred for 24 hours at room temperature, all the volatiles including excess amount of ethylene diamine were removed *in vacuo* to give 0.728 g of the title compound in 98 % yield. ^{1}H NMR (CD_3OD, 300 MHz): δ 3.22 (m, 12H), 4.02 (s, 6H), 4.42 (s, 6H), 7.41 (s, 3H).

[Core 6] G-1.5: (Synthesis done by Dr. Yoon)

To a solution of **[Core 6] G-1** (0.92 g, 1.70 mmol) in MeOH (10 mL) was added methyl acrylate (1.10 mL, 12.2 mmol). After stirring for 3 days (additional portions of methyl acrylate (1.0 mL each) were added into the reaction mixture every 24 hours), all the volatiles were removed *in vacuo* and the crude product was further purified by silica gel column chromatography eluting with EtOH/EtOAc (1:4) to give 0.84 g of the title compound as a clear yellow thick oil in 47% yield. ^{1}H NMR ($CDCl_3$, 300 MHz): δ 2.40 (t, J = 5.0 Hz, 12H), 2.51 (t, J = 4.5 Hz, 6H), 2.71 (t, J = 5.1 Hz, 12H), 3.35 (q, J = 4.2 Hz, 6H), 3.63 (s, 18H), 4.06 (s, 6H), 4.41 (s, 6H), 6.05 (bm, 3H), 7.40 (s, 3H). ^{13}C NMR ($CDCl_3$, 75.5 MHz): δ 32.5, 36.3, 48.9, 51.5, 52.8, 59.0, 68.9, 85.0, 85.3, 122.8, 134.4, 168.7, 172.5. LRMS MALDI-TOF: $[M + H]^+$ calcd for $C_{51}H_{73}N_6O_{18}$, 1057.5; found, 1057.6.

[Core 6] G-2 or **19:** (Synthesis done by Dr. Yoon)

To a solution of **[Core 6] G-1.5** (0.120 g, 0.114 mmol) in MeOH (5 mL) was added ethylene diamine (2.28 mL, 34.1 mmol) at 0 °C. After the mixture was stirred for 24 hours at room temperature, all the volatiles including excess ethylene diamine were removed *in vacuo* to give 0.130 g of the title compound in 94 % yield. ^{1}H NMR (CD_3OD, 300 MHz): δ 2.35 (t, *J* = 7.8 Hz, 18H), 2.57 (t, *J* = 7.7 Hz, 12H), *3*.25 (m, 18H), 3.28 (m, 12H), 4.09 (s, 6H), 4.51 (s, 6H), 7.51 (s, 3H). ^{13}C NMR (DMSO-d_6, 75.5 MHz): δ 33.3, 41.1, 41.9, 42.9, 49.6, 52.2, 58.3, 68.6, 84.3, 87.2, 123.1, 134.3, 168.4, 171.5. HRMS MALDI-TOF: $[M + H]^+$ calcd for $C_{57}H_{97}N_{18}O_{12}$, 1225.7533; found, 1225.7417.

4.6 References

1. Xie, R. H.; Bryant, G. W.; Zhao, J. J.; Kar, T.; Smith, V. H. Tunable optical properties of icosahedral, dodecahedral, and tetrahedral clusters. *Phys. Rev. B* **2005**, *71*, 125422.

2. Empedocles, S.; Bawendi, M. Spectroscopy of single CdSe nanocrystallites. *Acc. Chem. Res.* **1999**, *32*, 389.

3. El-Sayed, M. A. Some interesting properties of metals confined in time and nanometer space of different shapes. *Acc. Chem. Res.* **2001**, *34*, 257.

4. Link, S.; El-Sayed, M. A. Shape and size dependence of radiative, non-radiative and photothermal properties of gold nanocrystals. *Int. Rev. Phys. Chem.* **2000**, *19*, 409.

5. Peyser, L. A.; Vinson, A. E.; Bartko, A. P.; Dickson, R. M. Photoactivated fluorescence from individual silver nanoclusters. *Science* **2001**, *291*, 103.

6. Lee, T. H.; Gonzalez, J. I.; Zheng, J.; Dickson, R. M. Single-molecule optoelectronics. *Acc. Chem. Res.* **2005**, *38*, 534.

7. Wilcoxon, J. P.; Martin, J. E.; Parsapour, F.; Wiedenman, B.; Kelly, D. F. Photoluminescence from nanosize gold clusters. *J. Chem. Phys.* **1998**, *108*, 9137.

8. Rabin, I.; Schulze, W.; Ertl, G. Absorption spectra of small silver clusters Agn (n>=3). *Chem. Phys. Lett.* **1999**, *312*, 394.

9. Mostafavi, M.; Keghouche, N.; Delcourt, M. O.; Belloni, J. Ultraslow aggregation process for silver clusters of a few atoms in solution. *Chem. Phys. Lett.* **1990**, *167*, 193.

10. Bigioni, T. P.; Whetten, R. L.; Dag, O. Near-infrared luminescence from small gold nanocrystals. *J. Phys. Chem. B* **2000**, *104*, 6983.

11. Bruchez, M.; Moronne, M.; Gin, P.; Weiss, S.; Alivisatos, A. P. Semiconductor nanocrystals as fluorescent biological labels. *Science* **1998**, *281*, 2013.

12. Chan, W. C. W.; Nie, S. M. Quantum dot bioconjugates for ultrasensitive nonisotopic detection. *Science* **1998**, *281*, 2016.

13. Kneipp, K.; Wang, Y.; Kneipp, H.; Perelman, L. T.; Itzkan, I.; Dasari, R.; Feld, M. S. Single molecule detection using surface-enhanced Raman scattering (SERS). *Phys. Rev. Lett.* **1997**, *78*, 1667.

14. Nie, S. M.; Emory, S. R. Probing single molecules and single nanoparticles by

surface-enhanced Raman scattering. *Science* **1997**, *275*, 1102.

15. Michaels, A. M.; Nirmal, M.; Brus, L. E. Surface enhanced Raman spectroscopy of individual rhodamine 6G molecules on large Ag nanocrystals. *J. Am. Chem. Soc.* **1999**, *121*, 9932.

16. Zheng, J.; Dickson, R. M. Individual water-soluble dendrimer-encapsulated silver nanodot fluorescence. *J. Am. Chem. Soc.* **2002**, *124*, 13982.

17. Zheng, J.; Petty, J. T.; Dickson, R. M. High quantum yield blue emission from water-soluble Au8 nanodots. *J. Am. Chem. Soc.* **2003**, *125*, 7780.

18. Zheng, J.; Nicovich, P. R.; Dickson, R. M. Highly fluorescent noble-metal quantum dots. *Annu. Rev. Phys. Chem.* **2007**, *58*, 409.

19. Tomalia, D. A.; Huang, B.; Swanson, D. R.; Brothers, H.M.; Klimash, J.W. Structure control within poly(amidoamine) dendrimers: size, shape and regio-chemical mimicry of globular proteins. *Tetrahedron* **2003**, *59*, 3799.

20. Tykwinski, R. R. Evolution in the palladium-catalyzed cross-coupling of sp- and sp2-hybridized carbon atoms. *Angew. Chem., Int. Ed.* **2003**, *42*, 1566.

21. Thorand, S.; Krause; N. Improved procedures from the palladium-catalyzed coupling of terminal alkynes with aryl bromides (Sonogashira coupling). *J. Org. Chem.* **1998**, *63*, 8551.

22. Dulal, S.; Goyal, P.; Yoon, K.; Zheng, J.; Weck, M.; Dickson, R. M. Plasmon free single molecule Raman spectroscopy from dendrimer encapsulated fluorescent Ag-nanocluster. *In Submission*.

CHAPTER 5

Application 2: Development of Dendritic Molecular Transporters for studying Molecular-weight Dependence on Cellular Uptake

5.1 Abstract

The dependence of surface functionality of dendritic molecules on the cellular uptake has been studied in literature as outlined in this chapter. This project aims to understand the molecular weight dependence of dendritic molecular transporters on the cellular uptake behavior. For this purpose, a dendritic molecular transporter bearing a fluorescent core, a maleimide unit for conjugation to a cell penetrating peptide and containing a dendronized molecular-weight variable framework was synthesized. The dendronized framework was obtained by the synthesis of a dendron coupled to small ether terminated molecules. The molecular weight of this framework can be varied by simply using higher molecular weight ether terminated oligomers. This dendronized framework was then coupled to a fluorescent core which was earlier conjugated to the maleimide unit. The next phase for this research is to submit this target molecule to our collaborator, Dr. Farhni at Georgia Tech, who will do the *in vitro* cell studies to study the uptake of this dendritic molecule.

5.2 Introduction

The development of novel approaches that facilitate cellular uptake of a variety of physiologically and therapeutically active agents relies on the elucidation of new

molecular transporter/translocator molecules and methodologies. The identification of molecular transporters that enable or enhance cellular uptake of drug candidates and probes is a challenge of great significance in chemistry, biology and medicine.[1-4] In the past several years, strategies to overcome the limiting uptake of the plasma membrane have included the use of cell permeable peptide (CPP) vectors,[5-7] such as the Tat peptide and other various arginine-rich oligopeptides.[8-12] HIV-Tat peptide and its arginine-rich oligo-derivatives have been given much attention, primarily due to their high efficiency, short sequence, and capabilities of transporting various types of molecular structures, such as small molecular weight compounds, oligonucleotides, magnetic beads, plasmid DNA, and even a 129 kDa protein, across the membranes of most cell types.[13-18] While the number of arginines in an oligomer influences the uptake to a point, 8-mers (RRRRRRRR) offer the best match of performance.[8-12] D-oligomers of arginine work as well or better than L-isomers due presumably to protease resistance.[19]

The goal of the research presented in this chapter was to identify and elucidate molecular transport methodology for cellular uptake of dendritic molecules coupled to a cell permeable octa-arginine. The effect of surface charge [20-26] of dendrimers on cellular uptake and localization has been studied and reported extensively. Several studies reporting the effect of surface charge on dendrimers over their cellular uptake have demonstrated that dendrimers with NH_2 and OH end functionality enter cells faster than carboxyl terminated, acetamide and PEG terminated dendrimers by either non specific charge based adsorption or endocytosis.[20-26] In one study, PAMAM G-5 amine and acetamide terminated dendrimers were used to study cell binding and uptake.[21] The uptake of G-5 amine terminated PAMAM dendrimers into Rat2 cells was seen in 1 h

while no uptake of G-5 acetamide terminated PAMAM dendrimers was seen during this duration.[21] (Figure 5.1)

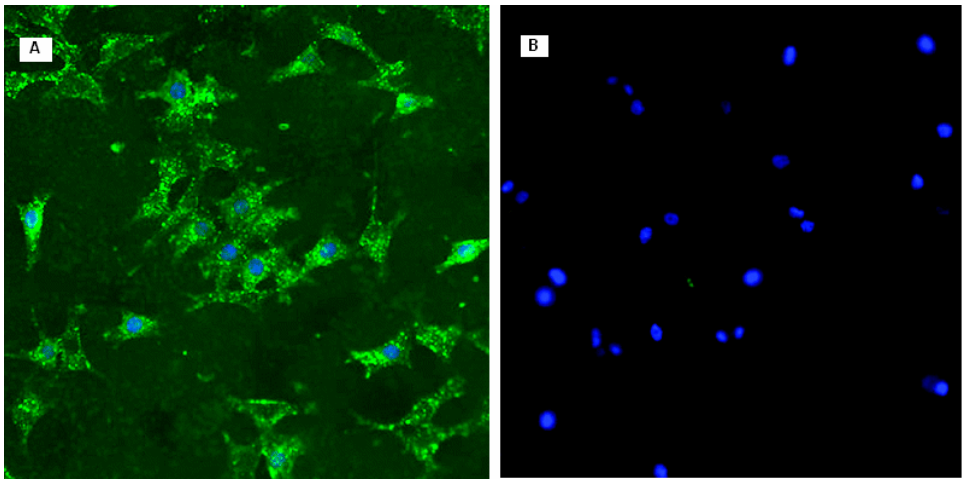

Figure 5.1 Fluorescence microscopy of[21] (A) Rat2 cells incubated with PAMAM G5-NH_2-FITC at 37 ˚C for 1h, (B) Rat2 cells incubated with PAMAM G5-Ac-FITC at 37 ˚C for 1h. Blue spots represent the nucleus stained by DAPI and green spots are dendrimer-FITC conjugate[21] (Adapted figure)

In another study, the binding of KB cells to G-5 carboxy terminated, acetamide terminated and hydroxyl terminated dendrimers each coupled to the tumor targeting group folic acid was studied.[20] Flow cytometry studies showed that the efficiency of internalization of the carboxyl terminated dendrimers was markedly lower than the one of hydroxyl and acetamide dendrimers.[20]

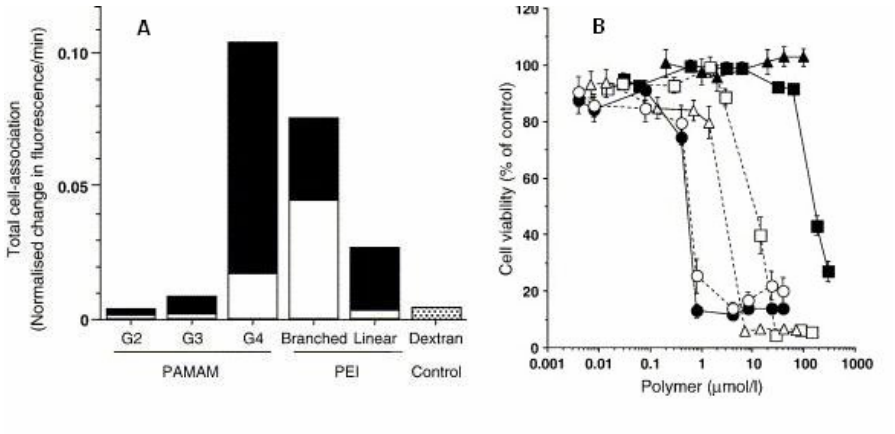

Figure 5.2 (A) Comparison of the rates of cellular association and internalization for PEI and PAMAM dendrimers.[27] Black corresponds to the rate of polymer internalization and white represents the binding (cell association at 4 ˚C) related to the total rate of cellular accumulation. For cationic polymers exocytosis was negligible. FITC-dextran is showed as a control. (B) Cytotoxicity of cationic polymers and dextran in B16F10 cells.[27] Incubation period 72 h. Plot symbols are as follows: PAMAM G-2 (□), PAMAM G-3 (○), PAMAM G-4 (Δ), branched PEI (●), linear PEI (■) and dextran (▲) (Adapted figure)

Few generation dependent studies have been carried out on the cellular uptake of dendrimers, keeping other parameters such as the nature of surface functionality constant.[27-28] In one study,[27] generation dependent uptake investigated using linear and branched poly(etheleneimine)s (PEI) and poly(amidoamine) dendrimers (PAMAM) showed that all the cationic polymers were internalized by adsorptive endocytosis with maximum uptake seen for PAMAM G-4 >> branched PEI > linear PEI > PAMAM G-3 > PAMAM G-2 as seen in Figure 5.2A. However, all the cationic polymers displayed cytotoxicity that was concentration and generation dependent with PAMAM G4 being the most toxic[27] (Figure 5.2B).

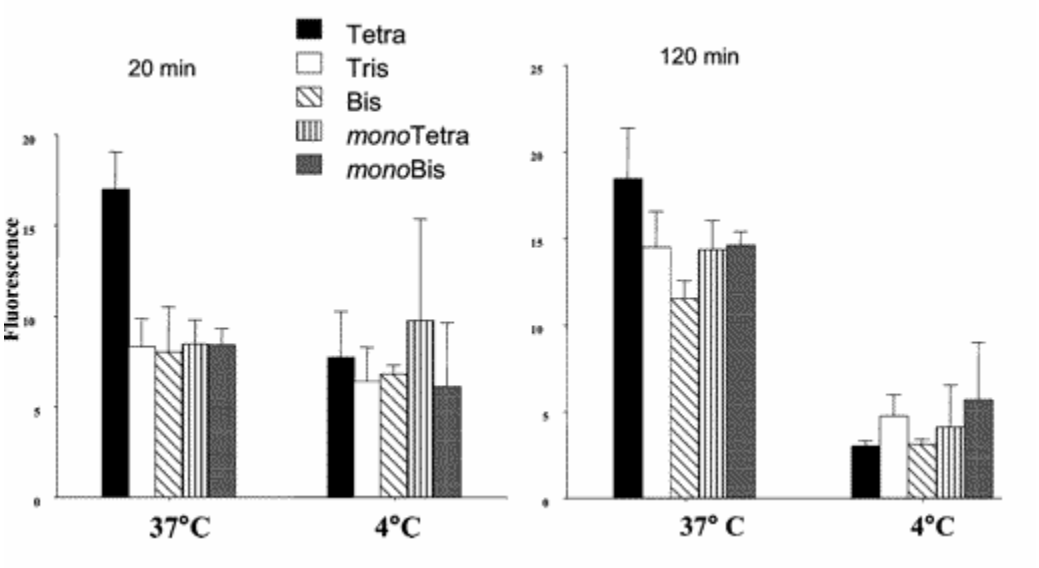

Figure 5.3 Cell association of OG-labeled PEG dendrons with ECV304 cells over time at 37 and 4 ˚C, by flow cytometry[29] (Adapted figure)

Dendron structures have been recognized to be ideal building blocks for biomedical applications because of their monodispersity, high loading capacity and bioconjugation capability.[30] In contrast to the effect of surface charge and dendrimer generation on cell uptake as described above, only two studies have investigated solely the effect of molecular weight of dendritic molecules on cellular uptake and localization.[29-30] In a study by Veronese and coworkers,[29] five PEG-based dendrons were synthesized and labeled with an orgenon green (OG) dye. The five dendrons were: (i) diamino,bisPEG (M_w = 1300), (ii) triamino,tris PEG (M_w = 1946), (iii) tetraamino,tetraPEG(M_w = 3956), (iv) monocarboxy,diamino,bisPEG (M_w = 1346) and (v) monocarboxy,tetraamino,tetraPEG (M_w = 3999). All dendrons had either NH_2 or NH_2 and COOH terminal groups and were nontoxic to endothelial cell (line EVC304) at concentrations up to 4 mg/ mL. At 37 ˚C, all the OG-labeled PEG dendrons showed progressive uptake by EVC304 cells. The tetraamino,tetraPEG dendron showed the

greatest rate of internalization over first 20 min(Figure 5.3). At 4 ˚C, cellular uptake was inhibited and PEG dendron localization to perinuclear vesicles was confirmed by fluorescence microscopy (Figure 5.4).[29]

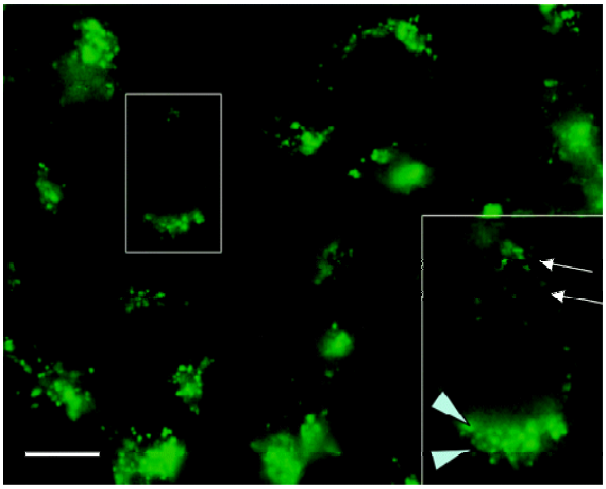

Figure 5.4 Fluorescence microscopy of trisaminotris-PEG-OG dendron in ECV304 cells.[29] The perinuclear region is shown to be enriched by fluorescence. The enlarged image shows fluorescence positive vesicular structures in the perinuclear (arrowhead) and peripheral regions (arrows) (Adapted figure)

In a recent study by Harth and coworkers,[30] two dendrons (M_w = 3898 and M_w = 4404) each having nine arginines attached to their branches as the cell penetrating vector with a fluorescein dye attached at the focal point were used for cell uptake studies with NIH-3T3 fibroblasts cells.[30] The authors reported that the lower molecular weight dendron localized in nucleus while the higher molecular weight dendron concentrated in cytosol (Figure 5.5). They also observed that the two dendron conjugates were able to internalize into cells not only at 37 ˚C but also at 4 ˚C, with no significant decrease in fluorescence.

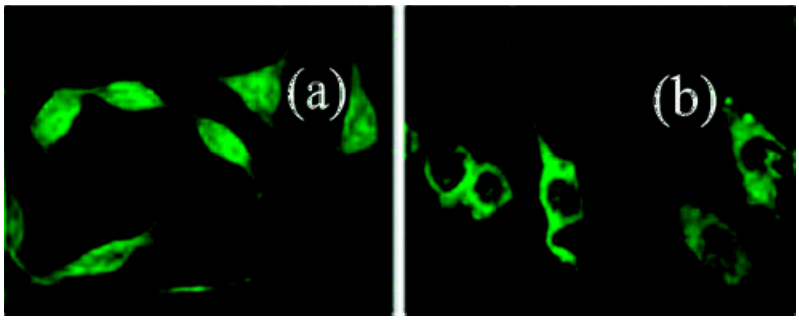

Figure 5.5 Confocal microscopy of[30] (a) M_w = 3898 dendron and (b) M_w = 4404 dendron unto unfixed cells at 37˚C (Adapted figure)

Both these aforementioned studies[29-30] indicate a molecular weight dependence over cellular uptake and localization. However, no systematic study using a neutral surface charge on dendritic molecules while being attached to a cell penetrating vector, and the molecular weight dependence of their cellular uptake has been reported. Our goal is to develop and elucidate the molecular weight dependence of dendrimers on cell uptake and cellular localization to enable delivery to intracellular sites such as nucleus or cytosol while keeping nonspecific effects such as surface charge to a minimum. Our first step towards this goal is to exploit dendrons having methyl ethers as terminating groups to reduce surface charge effects and to simply vary the lengths of oligomeric spacers. Our research design includes a highly fluorescent core of p-phenylene ethynylene derivatives with an emission in the visible region to follow the cell uptake and a terminal maleimide group for the attachment of cell penetrating peptide (CPP) vector to this dendronized scaffold using thiol chemistry (Figure 5.6).

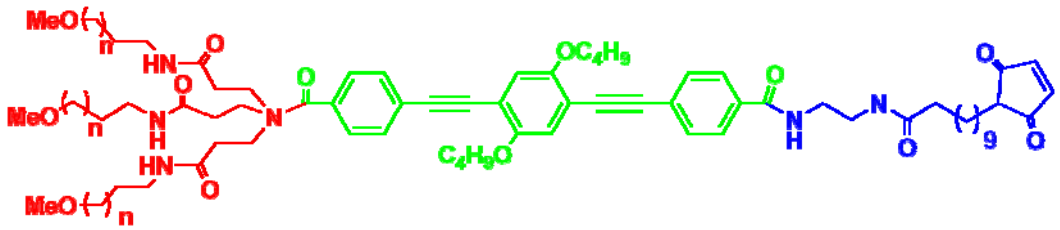

Figure 5.6 Target molecule: Molecular weight variable dendronized molecule bearing a maleimide unit for CPP attachment and a fluorescent core

5.3 Results and Discussion

The synthesis of the molecular weight variable framework was attempted first by the conjugation of synthesized amine terminated poly(ethylene glycol) as the termination unit to the dendron **7**. Amine terminated poly(ethylene glycol) was synthesized following a literature procedure[31] for the synthesis of α-(p-Toulene-sulfonyl)-ω-methoxypenta(oxyethylene) or **4** as shown in Scheme 5.1. Compound **4** was then reacted with sodium azide in DMF at 80˚C for 2 days to obtain the PEG-Azide **5**.

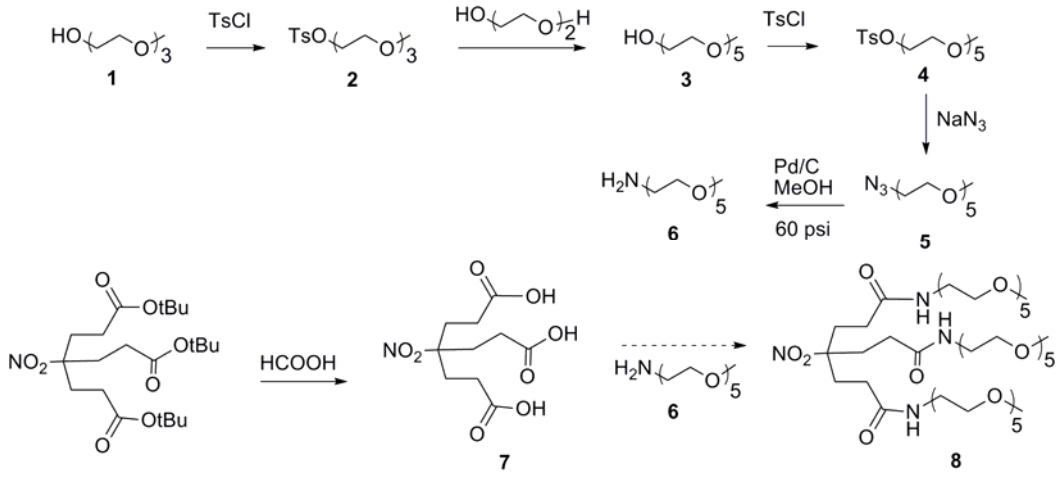

Scheme 5.1 Synthesis of amine terminated-PEG **6**

The reduction of the azide to the amine on **5** was then attempted through various literature procedures. Reduction with triphenyl phosphine in THF and water or in MeOH showed product in the crude sample but several attempts to isolate the product through cation exchange chromatography failed. Other reducing agents such as Zn with Nickel (II) chloride, sodium amalgam in MeOH showed very low conversions. Finally, using Pd/C in MeOH for the reduction of PEG-Azide **5** into PEG-Amine **6** showed near quantitative reduction after 2 days at 60 psi H_2 atmosphere. The synthesized PEG-Amine **6** was then attempted to couple to dendron **7**[35] using standard acid, amine coupling conditions such as DCC and HOBt or EDCI and HOBt. Both coupling reactions failed to yield the product. The acid dendron **7** was also converted to the acid chloride for coupling to **6**, but decomposition was observed in this case. The PEG-Amine molecule route was then abandoned. Instead, the use of commercial methoxy propyl amine as the termination unit for coupling to dendron **7** was investigated.

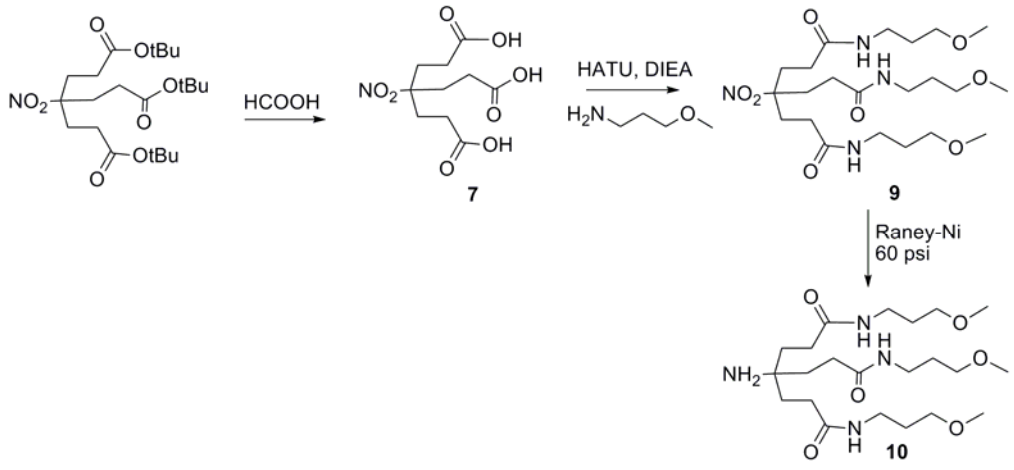

Scheme 5.2 Synthesis of dendron scaffold **10**

Using the aforementioned acid-amine couplings conditions like DCC-HOBt, EDCI-HOBt, DCC-DMAP gave the tri-substituted product **9** in very low yields while using acid chloride conversion of dendron acid **7** showed again decomposition of the starting material. Finally, using the strong coupling agent HATU with diisopropylethylamine yielded the coupled product **9** in 52 % yield. The product was the reduced to give compound **10** in 96 % yields (Scheme 5.2).

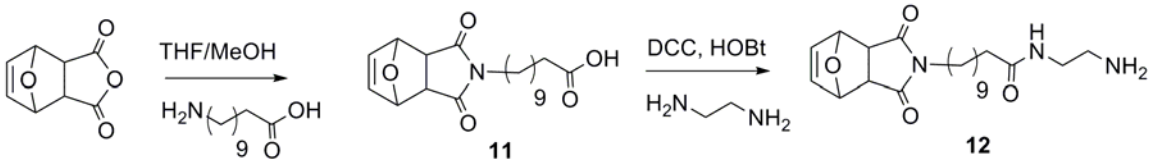

Scheme 5.3 Synthesis of maleimide-containing compound **12**

The furan-protected maleimide functional unit **12** was synthesized as shown in Scheme 5.3. 7-Oxabicyclo[2.2.1]-5-heptene-2,3 dicarboxylic anhydride was reacted with 11-amino undecanoic acid using 1:1 volume of THF and MeOH. The obtained product **11**, after column chromatography, was reacted with an excess of ethylene diamine using DCC and HOBt coupling conditions to yield the protected maleimide product **12**.

The fluorescent core **15** was synthesized as shown in Scheme 5.4. Compound **13** was obtained as described in literature procedures.[32] **14** was obtained thereafter following Sonogashira-Heck type coupling according to published reports by Bunz and coworkers.[33-34] Deprotection of the methyl ester groups on **14** using KOH in ethanol gave the fluorescent diacid **15**.

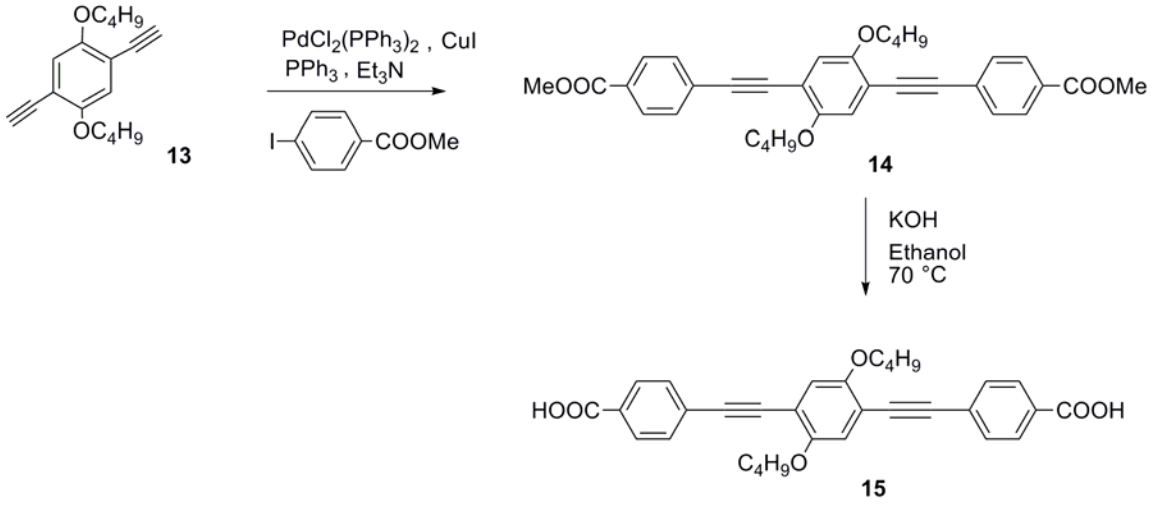

Scheme 5.4 Synthesis of the fluorescent core **15**

For the coupling to the diacid core **15** to the protected maleimide unit **12**, DCC and HOBt were used as coupling agents with two equivalents of diacid **15** and one equivalent of maleimide molecule **12**. The product was a mixture of mono and disubstitutions on **15**, which was difficult to separate due to the close R_fs of both products. Subsequently, this was purified by repeated silica gel column chromatography to obtain pure product **16** as a bright yellow solid. **16** was then coupled to dendron **10** using DIEA, HATU coupling reagents to obtain the final target product **17**, the purification for which is currently underway in our laboratory. **17** is submitted to and will be investigated by our collaborators for cell uptake studies.

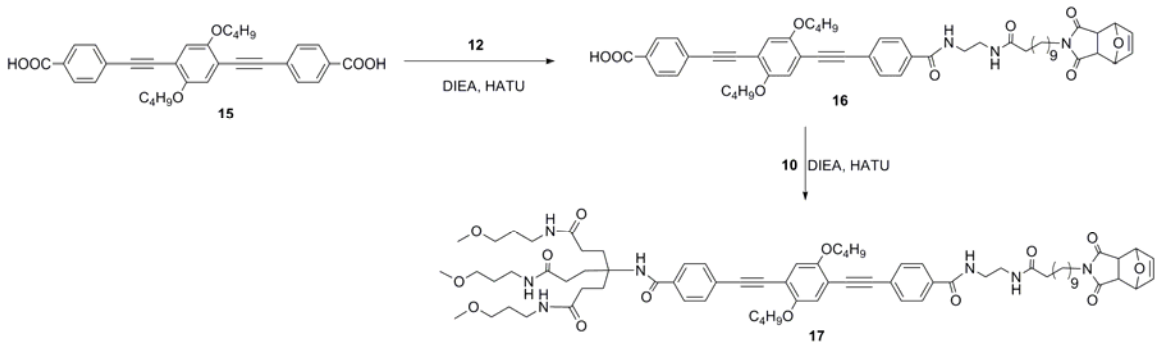

Scheme 5.5 Synthesis of dendritic molecule **17**

5.4 Conclusion

A dendritic molecule with a framework amenable for creating molecular weight variable dendrons through simple attachment of long or short length oligomers terminating in neutral charged methoxy units was conceived and synthesized. A fluorescent core based on a phenylethnylene moiety was synthesized and coupled to a maleimide moiety (for later attachment to a cell penentrating vector) and subsequently to the dendronized framework. This molecule was designed for studying the molecular weight dependence of cellular uptake and localization of dendron-containing delivery materials and will be submitted to and analyzed in detail by our collaborators in Dr. Fahrni's research group.

5.5 Experimental

Materials and General Procedures

All reagents were purchased from commercial sources and used as received unless otherwise noted. Tetrahydrofuran was distilled over sodium/benzophenone and methanol over Mg coupled with iodine. All air- or moisture-sensitive reactions were performed using oven-dried or flame-dried glassware under an inert atmosphere of dry argon or

nitrogen. Dichloromethane was dried by passing through columns of activated copper and alumina successively. DMF was purchased anhydrous and dried further using 5 Å molecular sieves. Analytical thin layer chromatography (TLC) was performed using Silica XHL pre-coated (250 μm thickness) glass backed TLC plates from Sorbent Technologies. Compounds were visualized using UV light or phosphomolybdic acid stains. Flash column chromatography was performed using silica gel 60 Å (230 - 400 mesh) from Sorbent Technologies. NMR spectra were acquired with a Bruker AV-400 (^{1}H, 400.0 Hz; ^{13}C, 100.5 MHz) spectrometer. Chemical shifts are reported in ppm and referenced to the residual nuclei in the corresponding deuterated solvents. Abbreviations used include singlet (s), doublet (d), triplet (t), quartet (q), and unresolved multiplet (m). Mass spectral analyses were obtained using either LC-MS on Agilent 1100 series LC/MSD (XCT) electrospray trap or on ABI 4700 Proteomics Analyzer for matrix assisted laser desorption ionization (MALDI) tandem time-of-flight (TOF).

Compound 9: (Synthesis done by Dr. Ornelas)

To a mixture of **7** (0.163 g, 0.590 mmol) and distilled 3-methoxy-propanamine (0.205 g, 2.3 mmol) and HATU (0.989 g, 2.6 mmol) in dry DMF (10 ml) was added DIEA (1 ml) under argon atmosphere. The reaction mixture was stirred at rt for 16 h and then concentrated *in vacuo*. The reaction mixture was re-dissolved in ethyl acetate and washed with H_2O and brine, dried over $MgSO_4$, and filtered. The resulting crude product was purified by silica gel column chromatography to yield the product **9** as yellow oil in 52 % yield. ^{1}H NMR (400 MHz, [D]$CHCl_3$, TMS): δ = 1.73 (m, 6H), 1.89-2.40 (m, 12H), 2.99 (s, 9H), 3.32-3.61 (m, 12H), 6.62(s, 3H). ^{13}C NMR (100.5 MHz, $CDCl_3$,

TMS): δ = 29.0, 30.5, 30.9, 37.4, 39.6, 44.5, 58.5, 70.8, 93.4, 161.5, 171.3. LC-MS: [M + H] $^{+}$ calcd for $C_{22}H_{43}N_4O_8$, 491.3; Found, 491.2.

Compound 10: To a solution of **9** (150 mg, 0.305 mmol) in absolute EtOH (10 mL) was added Raney-Ni (100 mg). The reaction mixture was stirred under 60 psi of H_2 for 48 hours at 51 °C. The catalyst was removed by filtration on celite and the filtrate was concentrated *in vacuo* to afford amine dendron **10** (135 mg, 96%). ^{1}H NMR (400 MHz, [D]$CHCl_3$, TMS): δ = 1.73 (m, 6H), 1.89-2.40 (m, 12H), 2.99 (s, 9H), 3.32-3.61 (m, 12H), 6.59 (s, 3H). ^{13}C NMR (100.5 MHz, $CDCl_3$, TMS): δ = 28.5, 30.7, 30.9, 37.4, 39.6, 44.5, 53.4, 58.5, 70.8, 161.5, 171.3. LC-MS: [M + H] $^{+}$ calcd for $C_{22}H_{45}N_4O_6$, 461.3; Found, 461.2.

Compound 11: To a solution of exo-3,6-(Epoxy-1,2,3,6-tetrahydropthalic anhydride) (2.16 g, 0.013 mol) in MeOH (25 ml) and THF (25 ml) was added 11-amino-undecanoic acid (2.62 g, 0.013 mol). The reaction mixture was refluxed at 65 ˚C for 2 days. The reaction was then concentrated *in vacuo*, the residue re-dissolved in CH_2Cl_2 and washed with H_2O and brine, dried over $MgSO_4$, and filtered. The crude product was purified by silica gel column chromatography eluting with CH_2Cl_2, EtOAc (1:1) to afford the pure product **11** as a white solid (1 g, 23% yield). ^{1}H NMR (400 MHz, [D]$CHCl_3$, TMS): δ = 1.31-1.72 (m, 16H), 2.34 (t, *J* = 7.2 Hz, 2H), 2.83 (s, 2H), 3.51(t, *J = 8.6 Hz*, 2H), 5.28 (s, 2H), 6.53 (s, 2H). ^{13}C NMR (100.5 MHz, $CDCl_3$, TMS): δ = 24.6, 26.6, 27.5, 29.1, 29.2, 33.9, 39.0, 47.3, 80.9, 136.5, 176.3, 179.4. LC-MS: [M + H] $^{+}$ calcd for $C_{19}H_{28}NO_5$, 350.2; Found, 350.2.

Compound 12: To a solution of **11** (0.5 g, 0.0014 mol) in THF (20 ml) was added DCC (0.354 g, 0.0017 mol) and HOBt (0.232 g, 0.0017 mol) and the reaction mixture was stirred at rt for 1 h. To this reaction mixture, ethylene diamine (1 ml, 0.014 mol) was added and the reaction mixture was stirred at rt for 4 days. The solvent was removed *in vacuo* and the excess ethylene diamine was removed under high vacuum. The reaction mixture was re-dissolved in CH_2Cl_2 and washed with H_2O and brine, dried over $MgSO_4$, and filtered. The crude product was purified by silica gel column chromatography eluting with EA, Hexane (2:1) and thereafter with 5 % MeOH to afford the pure product **12** as a white solid (200 mg, 36 % yield). ^{1}H NMR (400 MHz, [D]$CHCl_3$, TMS): δ = 1.18-1.68 (m, 16H), 2.11 (t, *J= 6.4 Hz*, 2H), 2.28 (t, *7.6 Hz*, 2H), 2.79 (s, 2H), 3.31 (m, 2H), 3.48(t, *J=6.6 Hz*, 2H), 5.21 (s, 2H), 6.32 (s, 1H), 6.47 (s, 2H). ^{13}C NMR (100.5 MHz, $CDCl_3$, TMS): δ = 23.1, 25.6, 26.5, 27.5, 29.1, 36.6, 39.0, 39.8, 40.3, 47.3, 81.1, 136.5, 171.4, 176.3. MALDI-TOF: $[M + K]^+$ calcd for $C_{21}H_{33}N_3O_4K$, 430.2; Found, 430.4

Compound 14: A solution of **13** (270.3 mg, 1mmol) and methyl-4-iodobenzoate (262.0 mg, 1mmol) in piperidine and THF were purged with argon for 15 minutes. The $PdCl_2(PPh_3)_2$ (14.8 mg, 0.0211 mmol) and CuI (20.1 mg, 0.106 mmol) were added quickly at room temperature. After stirring for 18 hours at room temperature, the reaction mixture was filtered and the filtrate was concentrated *in vacuo*, and purified by silica gel column chromatography to yield **14** as an orange solid in 88% yield. ^{1}H NMR (400 MHz, [D]$CHCl_3$, TMS): δ = 0.98 (t, *J= 6.8 Hz*, 6H), 1.61 (m, 4H), 1.87 (m, 4H),

3.92 (s, 6H), 4.06 (t, *J=7.2 Hz*, 4H), 7.02 (s, 2H), 7.56 (d, *J=8 Hz*, 4H), 8.02 (d, *J= 8 Hz*, 2H). ^{13}C NMR (100.5 MHz, $CDCl_3$, TMS): δ = 14.1, 19.5, 31.5, 52.4, 69.5, 89.1, 94.5, 114.1, 117.0, 128.3, 129.7, 131.6, 154.0, 166.8

Compound 15: To a solution of KOH (3 g) in ethanol (100 ml) and water (100 ml) was added **14** (1.65 g, 0.003 mol). The reaction mixture was stirred at 70 ˚C for 3 days, neutralized by the addition of 10% HCl (50 ml), filtered and dried on high vacuum to collect the product **15** as bright yellow solid (1.06 g, 67.8% yield). ^{1}H NMR (400 MHz, [D]$CHCl_3$, TMS): δ = 0.98 (t, *J=6.8 Hz*, 6H), 1.51 (m, 4H), 1.75 (m, 4H), 4.11 (m, 4H), 7.24 (m, 2H), 7.65 (d, *J=8 Hz*, 4H), 8.01 (d, *J= 8.2 Hz*, 4H). ^{13}C NMR (100.5 MHz, $CDCl_3$, TMS): δ = 13.6, 18.7, 24.4, 25.2, 30.7, 33.3, 68.6, 88.7, 113.1, 116.7, 126.7, 129.6, 130.5, 131.2, 153.2, 166.6

Compound 16: To a mixture of **15** (74.8 mg, 0.191 mmol) and **10** (195 mg, 0.382 mmol) was added DCC (39.4 mg, 0.191 mmol) and HOBt (25.8 mg, 0.191 mmol) in dry DMF (10 ml) under argon atmosphere. The reaction mixture was stirred at rt for 2 days and then concentrated *in vacuo*. The resulting crude product was purified by repeated silica gel column chromatography to yield the product **16** as bright yellow solid. ^{1}H NMR (400 MHz, [D]$CHCl_3$, TMS): δ = 0.84(m, 6H), 0.94-1.41(m, 10H), 1.52(m, 8H), 1.98 (m, 4H), 2.29 (t, *J = 6.6 Hz*, 2H), 2.75 (s, 2H), 3.4 (t, *J = 6.4 Hz*, 4H), 3.98 (t, *J =6.4 Hz*, 4H), 4.64 (m, 2H), 5.2 (s, 2H), 6.42 (s, 2H), 6.92(s, 2H), 7.53 (m, 6H), 7.71 (d, *J= 7.4 Hz*, 2H), 8.0 (d, *J= 7.2 Hz*, 2H). ^{13}C NMR (100.5 MHz, $CDCl_3$, TMS): δ = 12.8, 13.1, 18.2, 21.6, 22.1, 23.6, 25.5, 26.5, 27.9, 28.1, 28.2, 28.3, 28.6, 29.1, 31.8, 32.1, 36.0, 36.3, 38.0, 46.3,

68.3, 79.8, 87.1, 88.3, 93.3, 106.2, 113.1, 115.8, 125.4, 127.5, 129.0, 130.5, 133.3, 152.7, 164.9, 169.1, 175.3, 177.2

Compound 17: (Purification done by Dr. Ornelas)

To a mixture of **16** (13 mg, 0.014 mmol) and **12** (12.8 mg, 0.028 mmol) and HATU (12.5 mg, 0.033 mmol) in dry DMF (5 ml) was added DIEA (10 μL) at rt under argon atmosphere. The reaction mixture was stirred at rt for two days and then concentrated *in vacuo*. The reaction mixture was re-dissolved in ethyl acetate and washed with H_2O and brine, dried over $MgSO_4$, and filtered. The crude reaction mixture was purified by silica gel column chromatography to yield product as a bright yellow solid. ^{1}H NMR (400 MHz, [D]$CHCl_3$, TMS): δ = 1.02 (m, 2H), 1.31(m, 10H), 1.63-1.98 (m, 18H), 1.99-2.42 (m, 8H**)**, 2.85 (s, 10H), 3.26-3.59 (m, 13H), 3.98 (m, *J* = 4H), 5.31 (s, 2H), 6.32 (s, 4H), 6.52 (s, 2H), 7.01(s, 2H), 7.19 (d, *J = 7.2 Hz*, 2H), 7.33 (m, 4H), 7.54 (d, *J = 7.4 Hz*, 2H), 7.89 (d, *J= 7.2 Hz*, 2H), 8.21 (s, 2H).

5.6 References

1. Snyder, E. L.; Dowdy, S. F. Recent advances in the use of protein transduction domains for the delivery of peptides, proteins and nucleic acids in vivo. *Expert Opin. Drug Del.* **2005**, *2*, 43.

2. Frankel, A. D.; Pabo, C. O. Cellular uptake of the tat protein from human immunodeficiency virus. *Cell* **1988**, *55*, 1189.

3. Langel, Ü. *Cell-Penetrating Peptides*, CRC Press LLC, Boca Raton, FL, **2002**.

4. Futaki, S.; Suzuki, T.; Ohashi, W.; Yagami, T.; Tanaka, S.; Ueda, K.; Sugiura, Y. Arginine-rich peptides: an abundant source of membrane-permeable peptides having potential as carriers for intracellular protein delivery. *J. Biol. Chem.* **2001**, *276*, 5836.

5. Lindsay, M. A. Peptide-mediated cell delivery: application in protein target validation. *Curr. Opin. Pharmacol.* **2002**, *2*, 587.

6. Bennet, R. P.; Dalby, B. Protein delivery using VP22. *Nat. Biotechnol.* **2002**, 20, 20.

7. Derossi, D.; Joliot, A. H.; Chassaing, G.; Prochiantz, A. The 3rd helix of the antennapedia homeodomain translocates through biological-membranes. *J. Biol. Chem.* **1994**, *269*, 10444.

8. Joliot, A.; Prochiantz, A. Transduction peptides: from technology to physiology. *Nat. Cell Biol.* **2004**, *6*, 189.

9. Futaki, S. Oligoargine vectors for intracellular delivery: design and cellular-uptake mechanisms. *Biopolymers* **2006**, *84*, 241.

10. Rothbard, J. B.; Jessop, T. C.; Wender, P. A. Adaptive translocation: the role of hydrogen bonding and membrane potential in the uptake of guanidinium-rich transporters into cells. *Adv. Drug. Delivery Rev.* **2005**, *57*, 495.

11. Brooks, H.; Lebleu, B.; Vives, E. Tat peptide-mediated cellular delivery: back to basics. *Adv. Drug Delivery Rev.* **2005**, *57*, 559.

12. Snyder, E. L.; Dowdy, S. F. Cell penetrating peptides in drug delivery. *Pharm Res.* **2004**, *21*, 389.

13. Wadia, J. S.; Stan, R. V.; Dowdy, S. F. Transducible TAT-HA fusogenic peptide enhances escape of TAT-fusion proteins after lipid raft macropinocytosis. *Nat. Med.* **2004**, *10*, 310.

14. Wender, P. A.; Mitchell, D. J.; Pattabiraman, K.; Pelkey, E. T.; Steinman, L.; Rothbard, J. B. The design, synthesis, and evaluation of molecules that enable or enhance cellular uptake: peptoid molecular transporters. *Proc. Natl. Acad. Sci. U.S.A.* **2000**, *97*, 13003.

15. Zhao, M.; Weissleder, R. Intracellular cargo delivery using tat peptide and derivatives. *Med. Res. Rev.* **2004**, *24*, 1.

16. Vives, E.; Brodin, P.; Lebleu, B. A truncated HIV-1 Tat protein basic domain rapidly translocates through the plasma membrane and accumulates in the cell nucleus. *J.Biol. Chem.* **1997**, *272*, 16010.

17. Fischer, P. M.; Krausz, E.; Lane, D. P. Cellular delivery of impermeable effector molecules in the form of conjugates with peptides capable of mediating membrane translocation. *Bioconjugate Chem.* **2001**, *12*, 825.

18. de la Fuente, J. M.; Berry, C. C. Tat peptide as an efficient molecule to translocate gold nanoparticles into the cell nucleus. *Bioconjugate Chem.* **2005**, *16*, 1176.

19. Wender, P. A.; Kreider, E.; Pelkey, E. T.; Rothbard, J.; VanDeusen, C. L. Dendrimeric molecular transporters: synthesis and evaluation of tunable polyguanidino dendrimers that facilitate cellular uptake. *Org. Lett.* **2005**, *7*, 4815.

20. Quintana, A.; Raczka, E.; Piehler, L.; Lee, I.; Myc, A.; Majoros, I.; Patri, A. K.; Thomas, T.; Mule, J.; Baker Jr., J. R. Design and function of a dendrimer-based therapeutic nanodevice targeted to tumor cells through the folate receptor. *Pharm. Res.* **2002**, *19*, 1310.

21. Hong, S.; Bielinska, A. U.; Mecke, A.; Keszler, B.; Beals, J. L.; Shi, X.; Balogh, L.; Orr, B. G.; Baker Jr.; J. R.; Holl, M. M. B. Interaction of polyamidoamine dendrimers with supported lipid bilayers and cells: hole formation and the relation to transport. *Bioconjugate Chem.* **2004**, *15*, 774.

22. Kannan, S.; Kolhe, P.; Raykova, V.; Glibatec, M.; Kannan, R. M.; Lieh-Lai, M.; Bassett, D. Dynamics of cellular entry and drug delivery by dendritic polymers into human lung epithelial carcinoma cells. *J. Biomater. Sci. Polymer Ed.* **2004**, *15*, 311.

23. Jevprasesphant, R.; Penny, J.; Attwood, D.; D'Emanuele, A. Transport of dendrimer nanocarriers through epithelial cells via the transcellular route. *J. Controlled Release* **2004**, *97*, 259.

24. El-Sayed, M.; Rhodes, C. A.; Ginski, M.; Ghandehari, H. Transport mechanisms of polyamidoamine dendrimers across Caco-2 cell monolayers. *Int. J. Pharm.* **2003**, *265*, 151.

25. Kolhe, P.; Khandare, J.; Pillai, O.; Kannan, S.; Lieh-Lai, M.; Kannan, R. M. Preparation, cellular transport, and activity of polyamidoamine-based dendritic nanodevices with a high drug payload. *Biomaterials* **2006**, *27*, 660.

26. Kang, H.; DeLong, R.; Fisher, M. H.; Juliano, R. L. Tat-conjugated PAMAM dendrimers as delivery agents for antisense and siRNA oligonucleotides. *Pharm. Res.* **2005**, *22*, 2099.

27. Seib, F. P.; Jones, A. T.; Duncan, R. Comparison of the endocytic properties of linear and branched PEIs, and cationic PAMAM dendrimers in B16f10 melanoma cells. *J. Controlled Release* **2007**, *117*, 291.

28. Hollins, A. J.; Benboubetra, M.; Omidi, Y.; Zinselmeyer, B. H.; Schatzlein, A. G.; Uchegbu, I. F.; Akhtar, S. Evaluation of generation 2 and 3 poly(propylenimine) dendrimers for the potential cellular delivery of antisense oligonucleotides targeting the epidermal growth factor receptor. *Pharm. Res.* **2004**, *21*, 458.

29. Berna, M.; Dalzoppo, D.; Pasut, G.; Manunta, M.; Izzo, L.; Jones, A. T.; Duncan, R.; Veronese, F. M. Novel monodisperse PEG-dendrons as new tools for targeted drug delivery: synthesis, characterization and cellular uptake. *Biomacromolecules* **2006**, *7*, 146.

30. Huang, K; Voss, B.; Kumar, D.; Hamm, H. E.; Harth, E. Dendritic molecular transporters provide control of delivery to intracellular compartments. *Bioconjugate Chem.* **2007**, *18*, 403.

31. Lauter, U.; Meyer, W. H.; Wegner, G. Molecular composites from rigid-rod poly(p-phenylene)s with oligo(oxyethylene) side chains as novel polymer electrolytes. *Macromolecules* **1997**, *30*, 2092.

32. Kobayashi, N.; Kijima, M. Microporous materials derived from two- and three-dimensional hyperbranched conjugated polymers by thermal elimination of substituents. *J. Mater. Chem.* **2007**, *17*, 4289.

33. Ricks, H. L.; Shimizu, L. S.; Smith, M. D.; Bunz, U. H. F.; Shimizu, K. D. An N, N'-diaryl urea based conjugate polymer model system. *Tetrahedron Lett.* **2004**, *45*, 3229.

34. Bunz, U. H. F. Synthesis and structure of PAEs. *Adv. Polym. Sci.* **2005**, *177*, 1.

35. Goyal, P.; Yoon, K.; Weck, M. Multifunctionalization of dendrimers through orthogonal transformations. *Chem. Eur. J.* **2007**, *13*, 8801.

CHAPTER 6

Poly(styrene) Resin Supported Dendronized Catalysts for Enhanced Cooperativity in Heterogeneous Bimetallic Catalysis

6.1 Abstract

Excellent enantioselectivities and isolated yields have been achieved for the hydrolytic kinetic resolution of epoxides using a resin-supported dendronized R,R-(salen)Co catalyst with catalyst loadings as low as 0.04 mol%, the lowest metal loadings of any heterogeneous resin supported (salen)Co catalyst reported in the literature. In addition, the supported catalysts can be recycled and reused with comparable enantioselectivities. It is hypothesized that the high catalytic activity can be attributed to the flexible linker and the dendronized framework supporting the (salen)Co moieties on the resin thereby promoting cooperativity between two metal centers. The work presented in this chapter opens up new opportunities for the design of highly active resin supported catalysts that catalyze transformations through a bimetallic pathway.

6.2 Introduction

One of the secondary goals of this thesis is use the dendritic framework and molecules for enhanced functional utility and activity in catalysis. Of the many areas of chemistry and material sciences explored with dendritic molecules, catalysis is one of the most popular. Since the last decade, many catalytic dendritic systems have been reported which have catalytic units in the core or along the branches of interior or decorating the periphery of dendrimers.[1-5] A few reported dendritic catalytic systems are heterogeneous by design.[6-7] Heterogeneous dendronized catalysts are prepared by grafting dendrons and growing them stepwise on insoluble organic or inorganic solids.[8,9] The use of dendrons on a heterogeneous system adds an additional level of control, with increased number of sites available for attachment of catalyst on the insoluble material.

The advantages of heterogeneous catalysts include easy separation of the metal catalysts from the products, easy recyclability of the oftentimes expensive metal catalysts by simple filtration, as well as the potential use of solid supported catalysts in continuous flow processes.[10-11] One major limitation to the use of solid-supported catalysts is the limited tunability of the supported catalysts in regard to activity and selectivity. In most cases, solid-supported catalysts are less active and selective than their homogeneous counterparts.[12-15] Therefore, new strategies to immobilize catalysts on insoluble organic and inorganic supports that allow for the tuning of catalytic activity and enantioselectivity as well as for easy recyclability of the catalyst for repeated re-use are warranted.

The study of dendritic catalysts, both homogeneous and heterogeneous have revealed a phenomenon in which the dendritic architecture leads to an improvement in the catalytic performance per catalytic unit (increased conversion and selectivity), and

named as positive dendritic effect.[8,16] Such effects have been observed for many metallic and nonmetallic catalytic systems.[17-21] The direct grafting and synthesis of heterogeneous dendronized catalysts on solid resin (shown in Figure 6.1) are characterized by high conversions due to large excess of soluble reagents and by ease of separation and purification.[8]

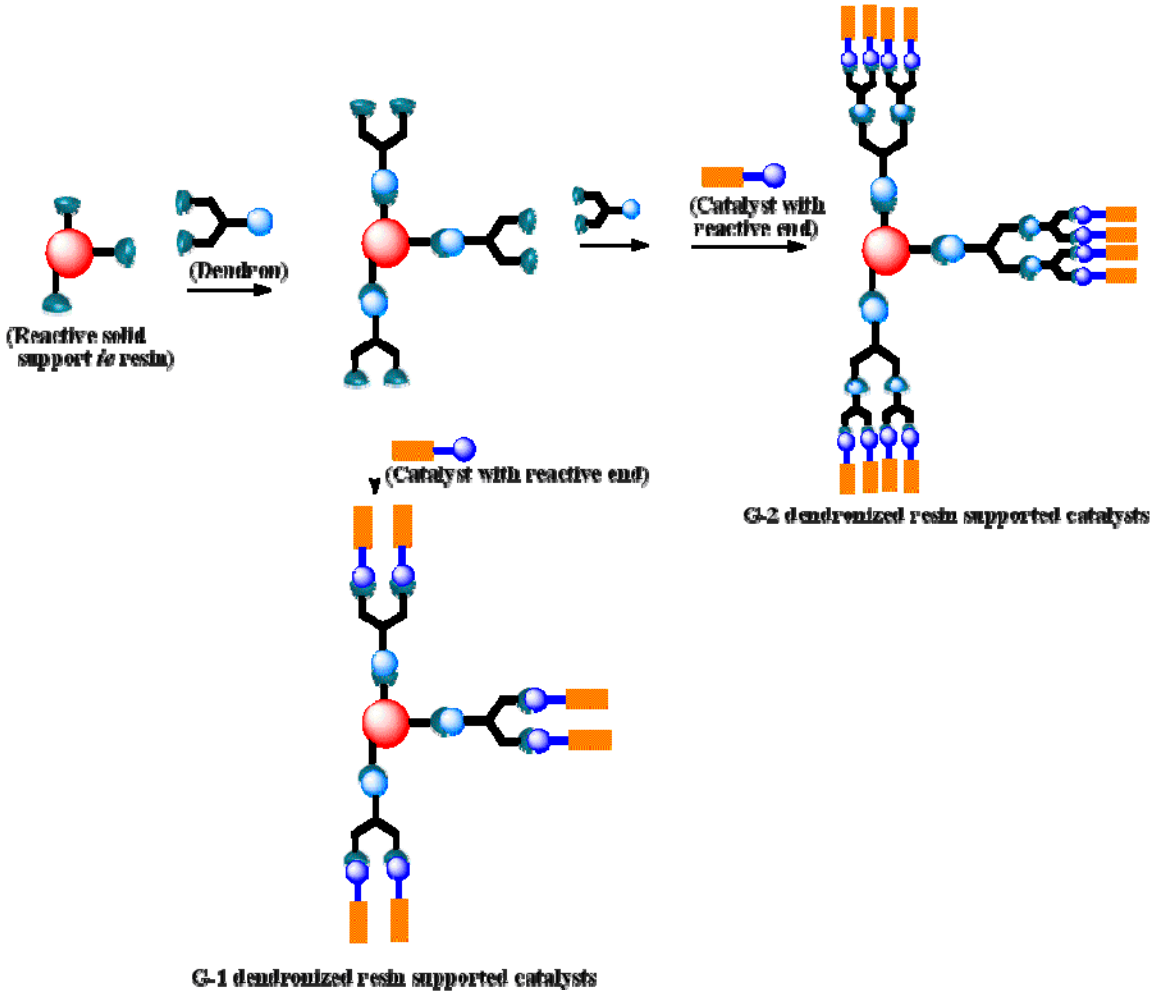

Figure 6.1 Solid phase synthesis of dendronized catalysts on a resin.

The early use of heterogeneous dendritic solid supported catalysts have been reported for the hydroformylation to convert terminal olefins into aldehydes,[22-26] Pd catalyzed Heck reaction[27-28] and Suzuki cross-couplings reactions,[29] olefin epoxidation[30] and Co-catalyzed Pauson-Khand cycloaddition reactions.[31] In most of these catalysis, there is an increase in activity of catalytic systems using solid supported catalysts. Enantioselective reactions with ligands immobilized on solid dendronized supports were the next step towards complexity. Towards this goal, Rhee and coworkers[32] used G1-G5 PAMAM dendron on silica functionalized with a chiral amino alcohol ephedrine, and catalyzed the enantioselective addition of diethyl zinc to benzaldehydes (Scheme 6.1). A dependence on the dendron generation and general loading on silica was observed. With low initial loadings of 0.24 mmol g^{-1} on silica, increased catalytic activities with increasing dendron generations were observed (except in case of G-5 which showed deterioration). Higher initial loading of 0.9 mmol g^{-1} on silica resulted in lowered catalytic activity with increasing dendron generation.

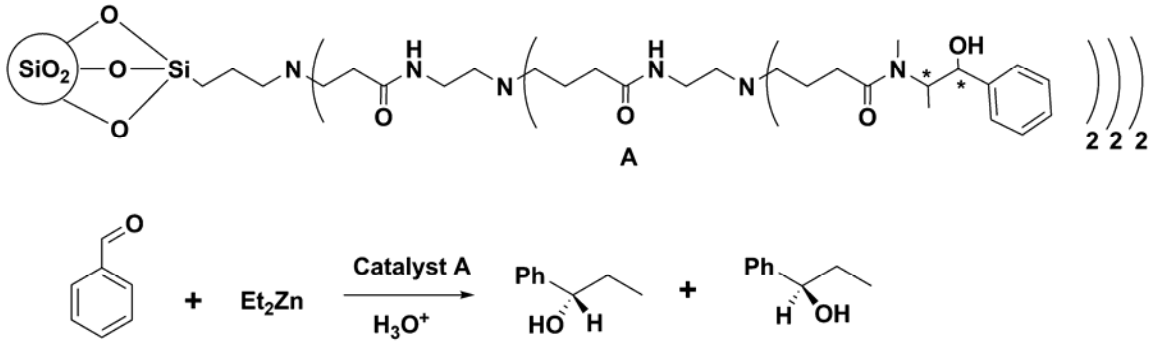

Scheme 6.1 Enantioselective addition of diethyl zinc to benzaldehyde catalyzed by silica supported dendritic amino alcohol ligands[32] (Adapted figure)

The research presented in this chapter is the first study to our knowledge, of enantioselective reactions using dendronized-supported catalysts on poly(styrene) resin. We envision our system as a model for catalytic reactions involving cooperative interactions. More fully understood and optimized, the developed system may be used for design of recyclable catalysts with high catalytic activity for continuous flow reactors and in fine chemical industry.

The chiral salen catalyst was chosen since chiral metallosalen catalysts[33-37] have emerged as a powerful and ubiquitous family of catalysts for numerous asymmetric organic transformations including the epoxidation of olefins,[38-39] the hydrolytic kinetic resolution of epoxides,[40-46] other epoxide ring-opening reactions,[47] hetero Diels-Alder reactions,[48] and conjugate addition reactions.[49-50] In this study, we specifically investigated the hydrolytic kinetic resolution (HKR) of racemic epoxides by (salen)Co catalysts, since the obtained enantiopure epoxides are versatile intermediates for asymmetric organic syntheses in the pharmaceutical and fine chemical industries.

Currently, only two reported[51-52] uses of resins as supports for HKR have been described. In both these studies, the salen ligand was covalently attached to polymers as shown in Figure 6.2 for Jacobsen's resin supported catalyst system. However, these resin-supported catalysts required high catalyst loadings in HKR when compared to other reported optimized recyclable systems.[44, 53]

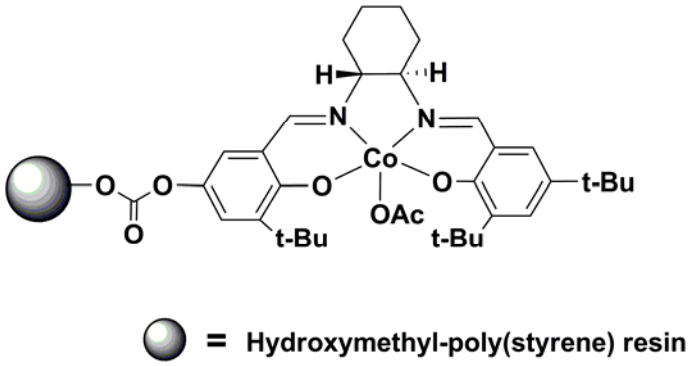

Figure 6.2 Poly(styrene) resin supported (salen)-Co catalysts reported by Jacobsen.[51]

It has been postulated that the HKR of epoxides using (salen)Co catalysts follows a bimetallic pathway where two catalytic centers with proper proximity are needed for the catalysis to occur.[54-58] Examples of promoting high local concentrations of (salen)Co for beneficial effects on catalytic activity for HKR have been shown prior on dendrimers,[17] polymers[34,43-44,59-61] and silica.[56] In contrast to soluble supports, it is more difficult to generate cooperative activation on a solid material due to the absence of elaborate control over the proper proximity and relative conformation of active centers on a surface, porous material or insoluble polymer.[56] This chapter presents a new strategy to address these shortcomings by employing a dendron to immobilize (salen)Co catalysts on the resin (Figure 6.3).

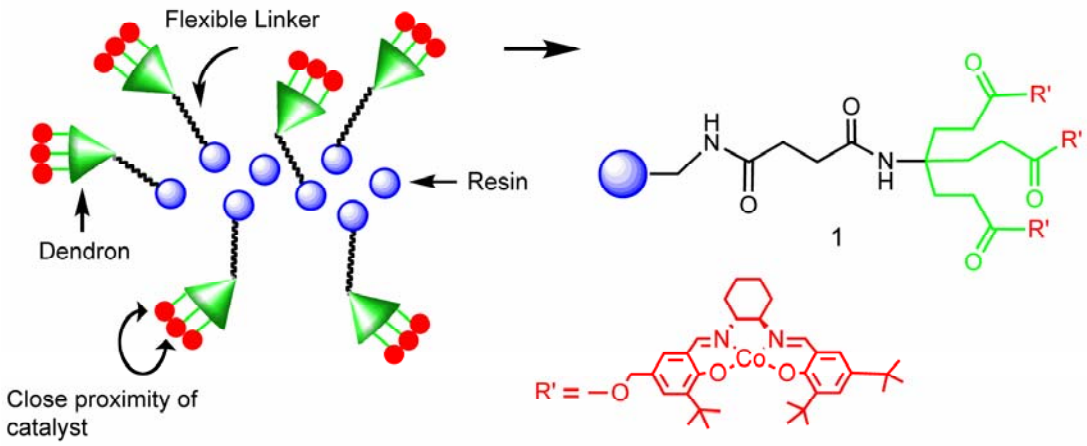

Figure 6.3 Schematic representation of the resin-supported catalyst design and structure.

The three components of the system are: a cross-linked poly(styrene) resin, a dendron based linker and a (salen)Co catalyst. Poly(styrene) resin was an attractive choice for the backbone owing to its ease of commercial availability and its chemical inertness. Commercially available generation one dendron[63] exhibits a branched structure and allows for the covalent attachment of up to three catalytic moieties along the dendron periphery, forcing them in close proximity to each other thereby promoting cooperative interactions between them. The resulting catalytic system upon activation shows high activities and enantioselectivities in the HKR of a variety of terminal epoxides with catalyst loadings as low as 0.04 mol% and allows for easy catalyst separation from product mixtures by simple filtration. The recovered catalysts are demonstrated to retain their activity and enantioselectivity upon recycling.

6.3 Results and Discussion

The first step towards the synthesis of the resin-supported catalysts involved a one-pot synthesis of unsymmetrical salen ligand **2**, using a procedure developed by the

Weck group.[62] Resin catalyst **1** was then synthesized following the synthetic protocol outlined in Scheme 1. Acid terminated dendron **3** was synthesized in 74% yield by reacting an aminotriester dendron[63] with succinic anhydride using pyridine as the solvent. This step was carried out to create a long spacer between the dendron branch points and the resin surface thereby installing a higher degree of flexibility to the systems. Dendron linker **3** was then reacted with pentafluorophenol and DCC to obtain the activated ester dendron **4** in 56% yields which was then coupled with aminomethylated poly(styrene) resin (1.4 mmol g^{-1} of amine loading) to obtain the dendron linker immobilized poly(styrene) resin **5**. The immobilization was also supported by the appearance of a new signal in ^{13}C solid-state NMR spectrum at 27 ppm, corresponding to the primary methyl carbons, and at 80 ppm corresponding to the *t*-butyl tertiary carbon. The *t*-butyl ester groups on **5** were then hydrolyzed by stirring the resin in formic acid for 20 hrs. The complete removal of protecting groups was identified by the disappearance of the signal at 80 ppm in the ^{13}C solid-state NMR spectrum and at 27.4 ppm corresponding to the primary methyl carbons. Elemental analysis of the oxygen content on **6** showed that 0.899 mmol g^{-1} of the hydrolyzed dendron linker was attached to the resin. Resin **6** was then coupled to salen ligand **2** using DCC and DMAP coupling conditions to yield **7**.

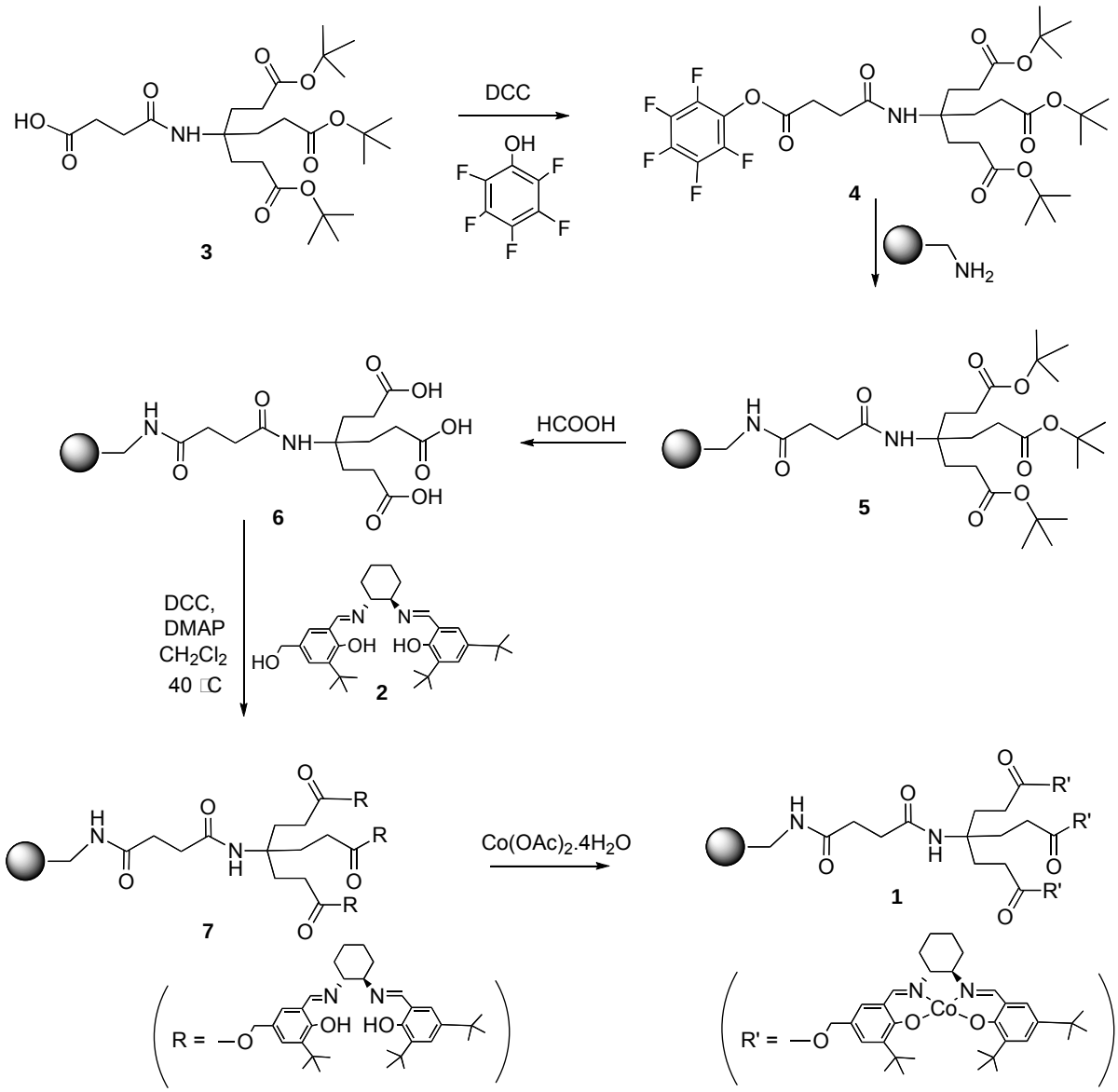

Scheme 6.2 Synthesis of poly(styrene) resin-supported dendronized (salen)Co complexes.

Formation of the product was supported by the appearance of a new signal in the ^{13}C solid state NMR spectrum at 119 ppm corresponding to the aromatic carbon next to the imine (*C*-CH_2-N=) and a broad signal between 63 ppm -79 ppm corresponding to the overlap of signals of the cyclohexane carbon attached to the nitrogen (-*C*-N) and the benzyl carbon (-*C*H_2-O). Elemental analysis of oxygen content corresponded to an

estimated 90.1 % of salen ligands coupled to the terminal acid sites of the dendron on the resin **7**. Resin **7** was then metallated with cobalt (II) acetate tetrahydrate in methanol to yield target resin **1**. The loading of cobalt on resin **1** was determined by elemental analysis of cobalt content to be 0.561 mmol g^{-1}.

With resin catalyst **1** in hand, its catalytic activity in the hydrolytic kinetic resolution (HKR) of a small library of epoxides (Table 1) was investigated. Prior to the catalysis, the Co^{II} centers were oxidized to the corresponding Co^{III} active species under air through the addition of excessive acetic acid. The oxidation process was followed by a color change from deep red to dark brown which is well documented in the literature.[43] We investigated the HKR of the following structurally diverse racemic epoxide substrates: (*rac*)-epichlorohydrin, (*rac*)-allyl glycidyl ether, (*rac*)-1,2-epoxyhexane and (*rac*)-styrene oxide (Table 1). The resolution of (*rac*)-epichlorohydrin was complete within 3 hours at ambient temperature using 0.04 mol% cobalt loading of **1**, affording the (S)-enantiomer in >99% *ee* and 46% isolated yield. Using the same catalyst loading, (*rac*)-allyl glycidyl ether was resolved in 7 hours to give the remaining enantiomer in >99% *ee* and 45% isolated yields. The resolution of (*rac*)-1,2-epoxyhexane was complete in 2 hours with the enantiomeric excess of the remaining epoxide higher than 99% and 47% isolated yield. The resolution of the conjugate epoxide, (*rac*)-styrene oxide, took nearly 22 h and a catalyst loading of 0.06 mol% for completion. While we still obtained the remaining epoxide with *ee*'s above 99% we isolated the enantiopure epoxide with lower yields (40%) when compared to the other substrates (Table 6.1).

Table 6.1 HKR of racemic terminal epoxides.

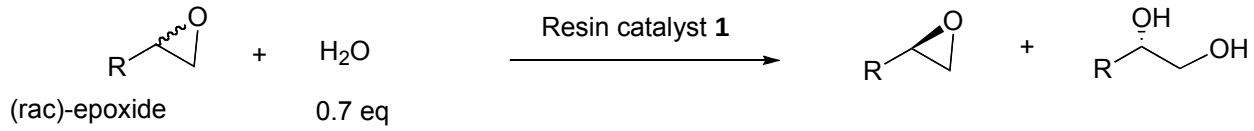

Entry	R	Catalyst Loading [mol%][a]	Time[h]	*ee* [%][b]	Yield [%][c]
1	CH_2Cl	0.04	3	>99	46
2	*n*-Bu	0.04	2	>99	47
3	$CH_2OAllyl$	0.04	7	>99	45
4	Ph	0.06	22	>99	40

[a]Catalyst loadings are reported on a per cobalt basis relative to racemic epoxide; [b]Enantiomeric excess of the remaining epoxide was determined by GC analysis using a Chiraldex G-TA column; [c]Isolated yield based on racemic epoxides; theoretical maximum yield = 50%.

A key motivation to develop the resin immobilized salen complex lies in its potential for easy recovery and reuse for subsequent reactions. Therefore, the recyclability of **1** for the HKR reaction of (*rac*)-1,2 epoxyhexane was investigated. The HKR was carried out using the reaction conditions described above. After complete conversion of the *S*-epoxide to the corresponding diol, we separated and purified the resin easily from the reaction mixture by simple filtration and washing with dichloromethane. The collected resin catalyst **1** was reactivated with acetic acid and then reused under strictly identical conditions as for the first cycle. Using this protocol, we reused **1** in five consecutive catalyses. The results of the recycling experiment are shown in Table 6.2.

While, the enantioselectivity of the re-used catalyst remained almost the same after 5 cycles, the catalytic activity fell marginally. The reaction time had to be extended to 3.5 hours for the fifth cycle to obtain an *ee* of 98%. This result clearly demonstrates the high recyclability of the resin supported dendronized catalyst **1** for the HKR of racemic epoxides.

Table 6.2 Recycling of resin catalyst **1** in the HKR of (*rac*)-1,2 epoxyhexane.

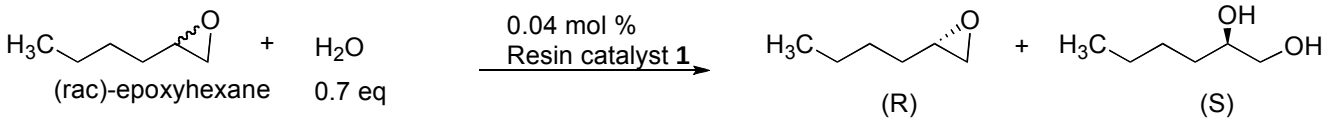

Cycle	Reaction Time [h]	Yield [%][a]	*ee* [%][b]
1	2	47	>99
2	2	45	>99
3	2	45	>99
4	3	42	98
5	3.5	44	98

[a]Isolated yield based on racemic epoxides; theoretical maximum yield = 50%; [b]Determined by GC analysis using a chiraldex G-TA column.

In order to gain a better understanding of the catalytic properties of the activated resin catalyst **1**, we investigated the kinetics of recycling of **1** for the HKR of (*rac*)-1,2-epoxyhexane for the 1st, 3rd and 5th cycle. The kinetic experiments were carried out at

room temperature with 0.7 eq of water and a catalyst loading of 0.04 mol %. The kinetic plot of *ee* versus the reaction time is presented in Figure 6.4. Chiral GC analysis showed that the reaction proceeded to completion in 2 hours in the presence of resin-supported catalyst **1** for the 1st cycle. While the catalytic activity of the third recycle is comparable to the first cycle, it fell significantly for the fifth cycle. For the fifth cycle, the resolution took about 3.5 h to be completed with 98% *ee* of the remaining epoxide. These results demonstrate that the resin-supported catalyst can be recycled with comparable activities several times. Multiple recycling events start to lower the activity of the supported catalysts. Nevertheless, even after 5 catalytic cycles does **1** retain its excellent selectivity. To investigate whether the lower activities are a result of cobalt leaching off the resin into the solvent, we measured the cobalt loading of the resin before the first (cobalt loading 3.31%) and after the fifth catalytic cycle (cobalt loading 3.28%) using elemental analysis. The resin loadings for both experiments are identical within experimental errors suggesting that cobalt leaching is not the source of the decreased catalyst activity.

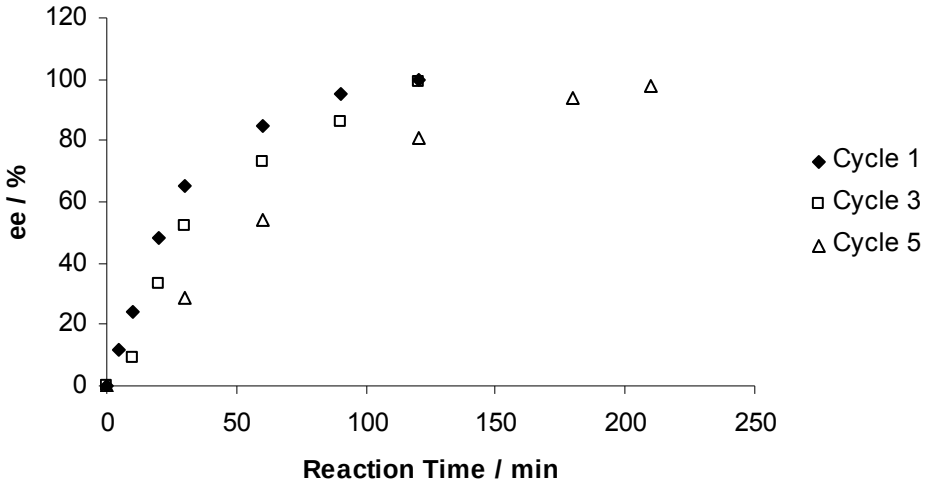

Figure 6.4 Plot of *ee* vs. reaction time in the hydrolytic kinetic resolution of *rac*-1,2 epoxyhexane

The aforementioned data sufficiently demonstrates that the new resin catalyst **1** possesses high activity, enantioselectivity and reusability in the HKR of epoxides. As outlined in the introduction, two earlier reports have investigated the HKR of terminal epoxides with resin supported (salen)Co catalysts.[51, 52] In comparison to these known resin-supported (salen)Co complexes, **1** is significantly more active. Prior to this work, the best resin supported Co-salen catalyst for the HKR was a system reported by Jacobsen and coworkers.[52] Their system is based on the direct immobilization of Co(salen) complexes onto poly(styrene) resins. In comparison to the reported study, the HKR using catalyst **1** proceeds in significantly (up to 80%) lower catalyst loadings (routinely 0.04 mol % were used in this study while the lowest catalyst loadings reported in the literature was 0.25 mol% catalyst) and with shortened or equally fast resolution time for the HKR of terminal epoxides. HKR of epichlorohydrin took around 3 h with both, the Jacobsen's catalyst[52] and our system, while the HKR of 1,2 epoxy hexane took only 2 h with our catalyst **1** whereas the literature reported 4 h.[52] We suggest that the enhanced activities of our resin supported dendronized catalyst **1** as evidenced by the lower catalyst loadings and/or shortened reaction times can be attributed to the dendronized framework that potentially provides a favorable geometry for the two metal centers to interact with each other by increasing the local catalyst concentration and facilitating the intramolecular bimetallic transition state.

6.4 Conclusion

This chapter describes the development of a poly(styrene) resin supported R,R-(salen)Co catalyst for the hydrolytic kinetic resolution of terminal epoxides. The resin

supported dendronized catalyst shows high catalytic activities and enantioselectivities for the HKR of a library of terminal epoxides. Catalyst loadings as low as 0.04 mol% for the HKR resulted in *ee's* often above 99% with outstanding isolated yields. Such low catalyst loadings, high *ee's*, and excellent yields have not been achieved before using any resin supported (salen)Co catalyst. It is hypothesized that the high catalyst activity stems from the unique dendron design that allows for close proximity of two catalytic sites to each other. A second advantage of the resin supported catalysts is that it can be recycled easily by filtration. This work opens new opportunity for the design of efficient insoluble polymer supported catalysts for reactions that involve bimolecular transition state or cooperative interactions between catalytic centers and might potentially allow for the employment of such catalysts in continuous flow reaction chambers.

Hence by developing and studying these dendronized constructs for catalysis, the present strategy allows for the design and synthesis of heterogeneous catalysts with tunable catalytic activity using the dendronized linker. This approach circumvents problems such as low catalyst activity (especially for those requiring cooperative interactions between metal centers for catalysis) associated with catalysts supported on traditional insoluble polymers. The dendronized linker is amenable to use on other support systems such as silica and soluble polymers giving us a large pool of supports to investigate and exploit in future studies.

6.5 Experimental

Materials and methods

All starting materials were obtained from commercial suppliers and used without further purification unless otherwise stated. Aminomethylated poly(styrene) resin with 50-100 mesh and 1.4 mmol g^{-1} loading was purchased from Novabiochem. All air- or moisture-sensitive reactions were performed using oven-dried or flame-dried glassware under an inert atmosphere of dry argon or nitrogen. Dichloromethane was dried by passing through columns of activated copper and alumina successively. Chlorobenzene was distilled under an atmosphere of argon prior to use. DMF was purchased anhydrous and dried further using 5 Å molecular sieves. Analytical thin layer chromatography (TLC) was performed using Silica XHL pre-coated (250 μm thickness) glass backed TLC plates from Sorbent Technologies. Compounds were visualized using UV light or phosphomolybdic acid stains. Flash column chromatography was performed using silica gel 60 Å (230 - 400 mesh) from Sorbent Technologies. All NMR spectra were acquired on a Varian Mercury 400 MHz spectrometer (^{1}H, 400.0 MHz; ^{13}C, 100.6 MHz). Chemical shifts are expressed in parts per million (δ), coupling constants (*J*) are reported in Hertz (Hz), and splitting patterns are reported as singlet (s), doublet (d), triplet (t), quartet (q), multiplet (m), or broad (br). Mass spectra were recorded with a VG 7070 EQ-HF hybrid tandem mass spectrometer. Cross-polarization magic angle spinning (CP-MAS) ^{13}C solid-state NMR spectra, were collected on a Bruker DSX-500 MHz instrument. Samples were packed in 7-mm zirconia rotors and spun at 12.5 kHz. Typical ^{13}C CP-MAS parameters were 4000 scans, a 90° pulse length of 5μs and a recycle time of 5 s. Enantiomeric excesses (*ee*) were determined by capillary gas-phase chromatography

(GC) analysis on a Shimadzu GC 14 A instrument equipped with a FID detector and a Chiraldex G-TA column (30 m × 0.25 mm) with helium as a carrier gas.

Synthesis of Dendron (2): To a round-bottomed flask equipped with a magnetic stir bar was added aminotriester[63] (10 g, 0.024 mol), succinic anhydride (3.61 g, 0.036 mol) and pyridine (48 ml). The reaction was stirred for 3 days following by the removal of pyridine *in vacuo*. The reaction mixture was redissolved in methylene chloride and washed with water and brine. The collected organic layers were then dried with $MgSO_4$ and the solvent was removed *in vacuo*. The product was purified by flash column chromatography (1:1 CH_2Cl_2/EtOAc) to afford the product as a white solid (9.2 g, 74.1%). ^{1}H NMR (400 MHz, $CDCl_3$) δ = 1.44 (s, 27H), 1.97 (t, 6H, *J* = 5.4 Hz), 2.22 (t, 6H, *J* = 5.3 Hz), 2.49 (t, 2H, *J* = 4.6 Hz), 2.67 (t, 2H, *J* = 4.8 Hz), 6.63 (br s, 1H). ^{13}C NMR (400 MHz, $CDCl_3$) δ = 27.5, 29.7, 29.9, 30.2, 58.9, 80.9, 163.5, 171.9, 172.4. HRMS (ESI +) [M+1] calcd for $C_{26}H_{45}NO_9$: 515.31 (100.0%), found: 516.31. Anal. Calcd for $C_{26}H_{45}NO_9$: C, 60.56; H, 8.80; N, 2.72; Found: C, 60.52; H, 8.85; N, 2.70.

Synthesis of Dendron (3): To a round-bottomed flask equipped with a magnetic stir bar and a reflux condenser was added **2** (2 g, 0.0038 mol), DCC (1.03 g, 0.0050 mol) and pentafluorophenol (1.71 g, 0.0093 mol) in DMF (30 mL). The reaction mixture was stirred at room temperature for 16 h, during which a precipitate formed. The precipitate was filtered off and the DMF was removed *in vacuo* at 55 °C to afford a crude mixture. The product was then subjected to flash column chromatography (9:1 hexane/EtOAc) to afford **3** as a white solid (1.50 g, 56.8%). ^{1}H NMR (400 MHz, $CDCl_3$) δ = 1.44 (s, 27H),

1.97 (t, 6H, J = 5.4 Hz), 2.22 (t, 6H, J = 5.7 Hz), 2.56 (t, 2H, J = 4.5 Hz), 3.10 (t, 2H, J = 4.8 Hz), 6.23 (s, 1H). ^{13}C NMR (400 MHz, $CDCl_3$) δ = 27.5, 29.7, 29.9, 30.2, 58.9, 80.9, 138.1, 140.1, 142.4, 143.4, 163.5, 171.9, 172.4. HRMS (ESI +) [M+1] calcd for $C_{32}H_{44}F_5NO_9$: 681.29 (100.0%), found: 682.30. Anal. Calcd for $C_{32}H_{44}F_5NO_9$: C, 56.38; H, 6.51; N, 2.05; Found: C, 56.42; H, 6.49; N 2.01.

Synthesis of Resin (5): Aminomethylated poly(styrene) HL (Novabiochem, 1.4 mmol g^{-1}, 300 mg, 0.42 mmol), **2** (572.2 mg, 0.84 mmol) and anhydrous DMF (10 ml) were charged to a Schlenk flask and stirred at 100 °C in an Ar atmosphere for 20 h. Filtration and rinsing with anhydrous DMF and CH_2Cl_2 followed by drying under high vacuum overnight yielded the orange colored resin **4**. Resin **4** (378 mg) was suspended in 95% HCOOH (12 ml) and stirred at room temperature for 20 h. The reaction mixture was then filtered though a frit and washed with DMF and CH_2Cl_2. The solid was dried on high vacuum to yield the orange resin **5**. Elemental analysis of oxygen showed that 0.899 mmol g^{-1} hydrolyzed dendron was immobilized on the resin.

Synthesis of Resin (6): Resin **5** (87 mg, 0.078 mmol of dendron) and CH_2Cl_2 (15 mL) were added under an atmosphere of argon to a flame dried round bottomed flask equipped with a magnetic stir bar. Then, the salen ligand[62] (306.2 mg, 0.588 mmol), DCC (242.6 mg, 1.176 mmol) and DMAP (86.2 mg, 0.705 mmol) were added to the reaction mixture. The reaction mixture was allowed to reflux for 3 days. The solvent was removed *in vacuo*. The resin was suspended in DMF and centrifuged for multiple times, each time removing the supernatant and re-suspending the resin in a fresh DMF

solution to remove the urea adducts and excess reagents. The resin was then filtered through a medium coarseness frit and washed with excess dichloromethane, DMF and methanol. The yellow solid was collected and dried on high vacuum for 2 days to give resin material **6**. Elemental analysis of oxygen content showed that 0.890 mmol g^{-1} of dendron was immobilized on the resin.

Synthesis of Resin (1): Resin **6** (66.5 mg) was dissolved in CH_2Cl_2 (2ml) in a vial and stirred under an argon atmosphere (in glove box). A solution of cobalt (II) acetate tetrahydrate (15.69 mg, 0.063 mmol) in methanol (2ml) was added to the mixture and the reaction mixture was stirred at room temperature for 2-3 days. The color of the resin changed from yellow to deep red. The reaction was then diluted with methanol, stirred for 4-5 mins and suction filtered on a frit washing continuously with methanol. The washed red resin material was collected in a vial and dried over high vacuum to give resin **1**. Elemental analysis of cobalt showed that 0.561 mmol g^{-1} Co was loaded on the resin.

General procedure for HKR of terminal epoxides: Resin catalyst **1** (3.56 mg, 0.002 mmol on basis of cobalt, 0.04 mol %) was dissolved in CH_2Cl_2 (1ml) in a vial and stirred. To this, 0.1 ml glacial acetic acid was added to activate the catalyst and the reaction mixture was stirred in open air for 30 minutes. The reaction mixture was then evacuated *in vacuo* to remove excess acetic acid and dichloromethane and then pumped on high vacuum for 5 minutes. To the resulting resin, the desired racemic epoxide (5 mmol) was added along with chlorobenzene (50 µl, internal standard) and the vial was immersed in a

water bath at room temperature. Water (0.7 eq, 63 μl) was then injected to start the reaction. Samples (4 μl) were removed from the reaction mixture at each designated time interval and diluted with anhydrous diethyl ether (3ml) and passed through a plug of silica gel in a pasteur pipet to remove water and the resin catalyst. The conversion and the enantiomeric excesses were calculated by the GC analysis.

6.6 References

1. Berger, A.; Gebbink, R. J. M. K.; van Koten, G. Transition metal dendrimer catalysts. *Top. Organomet. Chem.* **2006**, *20*, 1.

2. Reek, J. N. H.; Arevalo, S.; Van Heerbeek, R.; Kamer, P. C. J.; Van Leeuwen, P. W.N. M. Dendrimers in catalysis. *Adv. Catal.* **2006**, *49*, 71.

3. Helms, B.; Fréchet, J. M. J. The dendrimer effect in homogeneous catalysis. Adv. *Synth. Catal.* **2006**, *348*, 1125.

4. Liang, C.; Fréchet, J. M. J. Applying key concepts from nature: transition state stabilization, pre-concentration and cooperativity effects in dendritic biomimetics. *Prog. Polym. Sci.* **2005**, *30*, 385.

5. Van Heerbeek, R.; Kamer, P. C. J.; Van Leeuwen, P. W. N. M.; Reek, J. N. H. Dendrimers as support for recoverable catalysts and reagents. *Chem. Rev.* **2002**, *102*, 3717.

6. Bourrier, O.; Kakkar, A. K. Metallodendritic materials for heterogenized homogeneous catalysis. *Macromol. Symp.* **2004**, *209*, 97.

7. Rheiner, P. B.; Seebach, D. High-molecular weight and polymer-bound dendritic TADDOLs for membrane reactors and heterogeneous enantioselective lewis acid catalysis. *Polym. Mater. Sci. Eng.* **1997**, *77*, 130.

8. Dahan, A.; Portnoy, M. Dendrons and dendritic catalysts immobilized on solid support: synthesis and dendritic effects in catalysis. *J. Polym. Sci., Part A.: Polym. Chem.* **2005**, *43*, 235.

9. King, A. S. H.; Twyman, L. J. Heterogeneous and solid supported dendrimer catalysts. *J. Chem. Soc., Perkin Trans. 1.* **2002**, *20*, 2209.

10. Mizuno, N.; Misono, M. Heterogeneous Catalysis *Chem. Rev.* **1998**, *98*, 199.

11. Hagen, J. *Industrial Catalysis: A practical approach*, Wiley-VCH: Weinheim Germany, **1999**

12. Choudary, B. M.; Ramani, T.; Maheswaran, H.; Prashant, L.; Ranganath, K. V. S.; Kumar, K. V. Catalytic asymmetric epoxidation of unfunctionalized olefins using silica, LDH and resin-supported sulfonate-Mn(salen) complex. *Adv. Synth. Catal.* **2006**, *348*, 493.

13. Fan, Q-H.; Li, Y-W.; Chan, A. S. C. Recoverable catalysts for asymmetric organic synthesis. *Chem. Rev.* **2002**, *102*, 3385.

14. Baleizao, C.; Garcia, H. Chiral salen complexes: an overview to recoverable and reusable homogeneous and heterogeneous catalysts. *Chem. Rev.* **2006**, *106*, 3987.

15. Angelino, M. D.; Laibinis, P. E. Synthesis and characterization of a polymer-supported salen ligand for enantioselective epoxidation. *Macromolecules* **1998**, *31*, 7581.

16. Kehat, T.; Goren, K.; Portnoy, M. Dendrons on insoluble supports: synthesis and applications. *New J. Chem.* **2007**, *31*, 1218.

17. Breinbauer, R.; Jacobsen, E. N. Cooperative asymmetric catalysis with dendrimeric [Co(salen)] complexes. *Angew. Chem. Int. Ed.* **2000**, *39*, 3604.

18. Ropartz, L.; Morris, R. E.; Foster, D. F.; Cole-Hamilton, D. J. Increased selectivity in hydroformylation reactions using dendrimer based catalysts; a positive dendrimer effect. *Chem. Commun.* **2001**, *4*, 361.

19. Reetz, M. T.; Lohmer, G.; Schwickardi, R. Synthesis and catalytic activity of dendritic diphosphane metal complexes. *Angew. Chem. Int. Ed.* **1997**, *36*, 1526.

20. Francavilla, C.; Drake, M. D.; Bright, F. V.; Detty, M. R. Dendrimeric organochalcogen catalysts for the activation of hydrogen peroxide: improved catalytic activity through statistical effects and cooperativity in successive generations. *J. Am. Chem. Soc.* **2001**, *123*, 57.

21. Ribourdouille, Y.; Engel, G. D.; Richard-Plouet, M.; Gade, L. H. A strongly positive dendrimer effect in asymmetric catalysis: allylic aminations with Pyrphos-palladium functionalized PPI and PAMAM dendrimers. *Chem. Commun.* **2003**, *11*, 1228.

22. Bourque, S. C.; Maltais, F.; Xiao, W-J.; Tardiff, O.; Alper, H.; Arya, P.; Manzer, L.E. Hydroformylation reactions with rhodium-complexed dendrimers on silica. *J. Am. Chem. Soc.* **1999**, *121*, 3035.

23. Bourque, S. C.; Alper, H.; Manzer, L. E.; Arya, P. Hydroformylation reactions using recyclable rhodium-complexed dendrimers on silica. *J. Am. Chem. Soc.* **2000**, *122*, 956.

24. Arya, P.; Rao, N. R.; Singkhonrat, J.; Alper, H.; Bourque, S. C.; Manzer, L. E. A divergent, solid-phase approach to dendritic ligands on beads. Heterogeneous catalysis for hydroformylation reactions. *J. Org. Chem.* **2000**, *65*, 1881.

25. Alper, H.; Arya, P.; Bourque, S. C.; Jefferson, G. R.; Manzer, L. E. Solid-phase catalysis: a biomimetic approach towards ligands on dendritic arms to explore recyclable hydroformylation reactions. *J. Am. Chem. Soc.* **2001**, *123*, 2889.

26. Lu, S-M.; Alper, H. Carbonylative ring expansion of aziridines to β-lactams with Rhodium-complexed dendrimers on resin. *J. Org. Chem.* **2004**, *69*, 3558.

27. Dahan, A.; Portnoy, M. Remarkable dendritic effect in the polymer-supported catalysis of the heck arylation of olefins. *Org. Lett.* **2003**, *5*, 1197.

28. Dahan, A.; Portnoy, M. Pd catalysis on dendronized solid support: generation effects and the influence of the backbone structure. *J. Am. Chem. Soc.* **2007**, *129*, 5860.

29. Mansour, A.; Portnoy, M. Synthesis of a diverse set of phosphorous ligands on solid support and their screening in the Heck reaction. *Tetrahedron Lett.* **2003**, *44*, 2195.

30. Bu, J.; Judeh, Z. M. A.; Ching, C. B.; Kawi, S. Epoxidation of olefins catalyzed by Mn(II) salen complex anchored on PAMAM-SiO_2 dendrimer. *Catal. Lett.* **2003**, *85*, 183.

31. Dahan, A.; Portnoy, M. Dendritic effect in polymer-supported catalysis of the intramolecular Pauson-Khand reaction. *Chem. Commun.* **2002**, *22*, 2700.

32. Chung, Y-M.; Rhee, H-K. Dendritic chiral auxiliaries on silica: a new heterogeneous catalyst for enantioselective addition of diethylzinc to benzaldehyde. *Chem. Commun.* **2002**, 238.

33. Doyle, A. G.; Jacobsen, E. N. Enantioselective alkylations of tributyltin enolates catalyzed by Cr(salen)Cl: access to enantiomerically enriched all-carbon quaternary centers. *J. Am. Chem. Soc.* **2005**, *127*, 62.

34. Ready, J. M.; Jacobsen, E. N. Highly active oligomeric (salen)Co catalysts for asymmetric epoxide ring-opening reactions. *J. Am. Chem. Soc.* **2001**, *123*, 2687.

35. Taylor, M. S.; Jacobsen, E. N.; Asymmetric catalysis in complex target synthesis. *Proc. Natl. Acad. Sci. U. S. A.* **2004**, *101*, 5368.

36. Irie, R.; Noda, K.; Ito, Y.; Katsuki, T. Enantioselective epoxidation of unfunctionalized olefins using chiral (salen) manganese (III) complexes. *Tetrahedron Lett.* **1991**, *32,* 1055.

37. Jacobsen, E. N.; Zhang, W.; Muci, A. R.; Ecker, J. R.; Deng, L. Highly enantioselective epoxidation catalysts derived from 1,2-diaminocyclohexane. *J. Am. Chem. Soc.* **1991**, *113*, 7063.

38. Zhang, W.; Loebach, J. L.; Wilson, S. R.; Jacobsen, E. N. Enantioselective epoxidation of unfunctionalized olefins catalyzed by salen manganese complexes. *J. Am. Chem. Soc.* **1990**, *112*, 2801.

39. Irie, R.; Noda, K.; Ito, Y.; Matsumoto, N.; Katsuki, T. Catalytic asymmetric epoxidation of unfunctionalized olefins. *Tetrahedron Lett.* **1990**, *31*, 7345.

40. A. E.; Keith, J. M.; Larrow, J. F.; Jacobsen, E. N. Practical considerations in kinetic resolution reactions. *Adv. Synth. Catal.* **2001**, *343*, 5.

41. Schaus, S. E.; Brandes, B. D.; Larrow, J. F.; Tokunaga, M.; Hansen, K. B.; Gould, A. E.; Furrow, M. E.; Jacobsen, E. N. Highly selective hydrolytic kinetic resolution of terminal epoxides catalyzed by chiral (salen) CoIII complexes. Practical synthesis of enantioenriched terminal epoxides and 1,2-diols. *J. Am. Chem. Soc.* **2002**, *124*, 1307.

42. Tokunaga, M.; Larrow, J. F.; Kakiuchi, F.; Jacobsen, E. N. Asymmetric catalysis with water: efficient kinetic resolution of terminal epoxides by means of catalytic hydrolysis. *Science* **1997**, *277*, 936.

43. Zheng, X.; Jones, C. W.; Weck, M. Poly(styrene)-supported Co-Salen complexes as efficient recyclable catalysts for the hydrolytic kinetic resolution of epichlorohydrin. *Chem.- Eur. J.* **2006**, *12*, 576.

44. Zheng, X.; Jones, C. W.; Weck, M. Ring-expanding olefin metathesis: a route to highly active unsymmetrical macrocyclic oligomeric Co-Salen catalysts for the hydrolytic kinetic resolution of epoxides. *J. Am. Chem. Soc.* **2007**, *129*, 1105.

45. Holbach, M.; Weck, M. A practical one-pot synthesis of enantiopure unsymmetrical salen ligands. *J. Org. Chem.* **2006**, *71*, 1825.

46. Zheng, X.; Jones, C. W.; Weck, M. Engineering polymer-enhanced bimetallic cooperative interactions in the hydrolytic kinetic resolution of epoxides. *Adv. Synth. Catal.* **2008**, *350*, 255.

47. Martinez, L. E.; Leighton, J. L.; Carsten, D. H.; Jacobsen, E. N. Enantioselective ring opening of epoxides catalyzed by Salen Cr(III) complexes. *J. Am. Chem. Soc.* **1995**, *117*, 5897.

48. Schaus, S. E.; Brnalt, J.; Jacobsen, E. N. Asymmetric hetero-Diels-Alder reactions catalyzed by chiral Salen chromium (III) complexes. *J. Org. Chem.* **1998**, *63*, 403.

49. Sammis, G. M.; Jacobsen, E. N. Highly enantioselective, catalytic conjugate addition of cyanide to α,β-unsaturated imides. *J. Am. Chem. Soc.* **2003**, *125*, 4442.

50. Madhavan, N.; Weck, M. Highly active polymer-supported (Salen)Al catalysts for the enantioselective addition of cyanide to α,β-unsaturated imides. *Adv. Synth. Catal.* **2008**, *350*, 419.

51. Solodenko, W.; Jas, G.; Kunz, U.; Kirschning, A. Continuous enantioselective

kinetic resolution of terminal epoxides using immobilized chiral cobalt-Salen complexes. *Synthesis* **2007**, 583.

52. Annis, D. A.; Jacobsen, E. N. Polymer-supported chiral Co(Salen) complexes: synthetic applications and mechanistic investigations in the hydrolytic kinetic resolution of terminal epoxides. *J. Am. Chem. Soc.* **1999**, *121*, 4147.

53. Rossbach, B. M.; Leopold, K.; Weberskirch, R. Self-assembled nanoreactors as highly active catalysts in the hydrolytic kinetic resolution (HKR) of epoxides in water. *Angew. Chem. Int. Ed.* **2006**, *45*, 1309.

54. Sammis, G. M.; Danjo, H.; Jacobsen, E. N. Cooperative dual catalysis: application to the highly enantioselective conjugate cyanation of unsaturated imides. *J. Am. Chem. Soc.* **2004**, *126*, 9928.

55. Ma, J.-A. Cahard, D. Towards perfect catalytic asymmetric synthesis: dual activation of the electrophile and the nucleophile. *Angew. Chem. Int. Ed.* **2004**, *43*, 4566.

56. Yang, H.; Zhang, L.; Zhong, L.; Yang, Q.; Li, C. Enhanced cooperative activation effect in the hydrolytic kinetic resolution of epoxides on [Co(Salen)] catalysts confined in nanocages. *Angew. Chem. Int. Ed.* **2007**, *46*, 6861.

57. Hansen, K. B.; Leighton, J. L.; Jacobsen, E. N. On the mechanism of asymmetric nucleophilic ring-opening of epoxides catalyzed by (Salen) CrIII complexes. *J. Am. Chem. Soc.* **1996**, *118*, 10924.

58. Nielsen, L. P. C.; Stevenson, C. P.; Blackmond, D. G.; Jacobsen, E. N. Mechanistic investigation leads to a synthetic improvement in the hydrolytic kinetic resolution of terminal epoxides. *J. Am. Chem. Soc.* **2004**, *126*, 1360.

59. Song, Y.; Yao, X.; Chen, H.; Bai, C.; Hu, X.; Zheng, Z. Highly enantioselective resolution of terminal epoxides using polymeric catalysts. *Tetrahedron Lett.* **2002**, *43*, 6625.

60. Ready, J. M.; Jacobsen, E. N. A practical oligomeric [(salen)Co] catalyst for asymmetric epoxide ring-opening reactions. *Angew. Chem. Int. Ed.* **2002**, *41*, 1374.

61. Song, Y.; Chen, H.; Hu, X.; Bai, C.; Zheng, Z. Highly enantioselective resolution of terminal epoxides with cross-linked polymeric salen-Co(III) complexes. *Tetrahedron Lett.* **2003**, *44*, 7081.

62. Holbach, M.; Zheng, X.; Burd, C.; Jones, C. W.; Weck, M. Modular approach for the development of supported, monofunctionalized, Salen catalysts. *J. Org. Chem.* **2006**, *71*, 2903.

63. Available commercially from Frontier Scientific

CHAPTER 7

Dendritic Architectures: Present System and Potential Future Applications

7.1 Abstract

This chapter summarizes the objective of the research presented in this thesis and the accomplishments which have brought us closer to the goal of tunable dendritic architectures for biological and catalytic applications. However, many of the exciting applications and potential impact of these systems have yet to be realized. This chapter reviews the current status of dendritic structures and puts forth optimization methods and strategies using our dendritic structures that should be investigated in the future to enable this research to flourish and progress toward our continued goal of contributions to biological and catalysis sciences.

7.2 Current Status of Dendritic Architectures

The overall goal of this thesis is to create dendritic architectures which are biologically relevant and contributing to, ultimate development of scaffolds for cellular imaging at single molecule level as *in vivo* labels, and of novel scaffolds that allow for tunable attachment of biological molecules on their periphery for targeting and delivery of therapeutic cargo. We chose to work with dendrimers, due to their structural uniqueness and function (as outlined in Chapter 2), suitable for biological applications and synthetic techniques amenable to the creation of functionally tunable molecules. At the commencement of this thesis research, synthetic methodologies for the creation of

dendrimers with unique sites for surface functionalization were very few and limited.[1-4] Existing scaffolds that are amenable to post-synthetic manipulations, suffered from non-quantitative deprotection steps or the lack of robust orthogonal groups.[1-4] The creation of dendrimers with robust, reactive and distinct orthogonal functional groups on its periphery with perfect specificity and selectivity for its complementary group was an unfulfilled goal.

Furthermore, prior to the work described in this dissertation, the field of dendrimers in biological sciences suffered from few major deficiencies: (i) inefficient routes to dendrimers containing selective functional handles, (ii) non-orthogonal functional handles and strategies for post-synthetic manipulations, which limited the scope of biomaterials preparation, and (iii) the absence of quantitative post-synthetic manipulations. With the introduction of mono- and bi-functionalized dendrimers described in chapter 3,[5-6] many of these problems have been overcome. These dendrimers have not only provided for the realization of orthogonal multifunctionalization strategies, but have provided post-synthetic routes for future covalent and chemoselective attachment to desirable ligands, antibodies or target receptor proteins, thereby allowing for modular surface modification for creation of targeted delivery vehicles.

Another area of biological science affected by this thesis is single molecule imaging. The creation and extension of highly fluorescent and photostable labels inside dendritic scaffolds reported by Dickson and coworkers,[7-9] to contain scaffold specific chemical information is highly desirable for the advancement of live cell imaging methods. Most fluorescent labels suffer from photobleaching and low signal to

background on single molecule level, that limits both their *in vitro* and *in vivo* applications. With the development of Raman label containing dendrimers described in chapter 4,[10] some of those problems have been addressed. This work lays out the basic methodology for the eventual creation of ultrabright, scaffold specific information containing biological labels to follow single cell dynamics in living systems.

Additionally, as a secondary application, the use of dendritic frameworks in heterogeneous solid supported catalysis for reactions involving bimetallic intermediates was explored and applied. Prior to this thesis work, heterogeneous resin supported catalysts for HKR reactions suffered from high catalyst loadings and low enantioselectivities induced by the solid support.[11-12] With the use of flexible linker and dendron framework supporting the catalysts, both of these problems were addressed.[13] This work opens up new routes for the creation of high performance heterogeneous catalysts which employ a bimetallic transition state.

The future of dendrimers for biological and catalytic applications is promising and has matured to the possibility of addressing advanced problems in both fields. In the following section, some of the ongoing and possible future applications using the dendritic structures developed in this thesis are outlined.

7.3 Future Work Towards Dendritic Architectures

The ultimate goal of this work is to develop engineered dendrimers and dendritic molecules for biological applications such as targeted delivery, imaging, therapeutics and for catalytic applications such as catalyst-supported dendronized (soluble and insoluble)

polymers. This section will suggest potential implementations of the current dendritic systems developed in this thesis, to improve and expand their utility.

7.3.1 In vitro and in vivo self assembly of dendritic nanoparticles

The foremost application of our tunable dendrimers and dendritic nanoparticles should involve the utilization of multivalency of dendritic molecules as well as the selective attachment chemistry of our developed systems for addressing biological problem. A chemical self assembly approach utilizing dendritic multivalent particles can be used to improve the sensitivity and biodistribution of targeted MRI contrast agents. In order to exploit the favorable biodistribution characteristics of small agents, self assembly of smaller dendritic particles at the receptor site can be utilized (Figure 7.1).

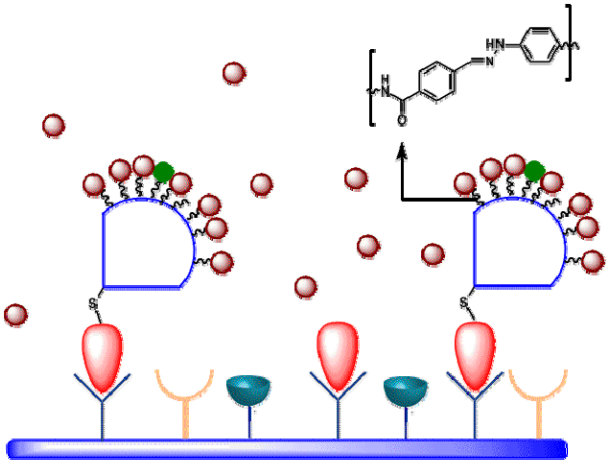

Figure 7.1 Self assembly of smaller dendritic particles at receptor sites to larger dendrimers carrying Gd chelates utilizing aldehyde-hydrazine interactions

This ongoing collaborative project with the Canary group is an extension of our present expertise on the synthesis of tunable multivalent dendritic molecules. It proposes to utilize our monofunctional dendron nanoparticle for the creation of a primary dendritic nanoparticle which is coupled to (i) an antibody for targeting to receptor units on tumor, (ii) a near-infrared (NIR) fluorescent tag for tracking, and (iii) eight aldehyde functional

handles (Figure 7.2) for *in vivo* reaction with hydrazine units on a secondary dendrimer nanoparticle carrying multiple reporter groups such as Gadolinium chelates for MRI imaging. The self-assembly of the secondary nanoparticle around the first by the reaction between hyrazines and aldehydes respectively, would enable the delivery of hundreds of contrast agents to the tumor receptor site.

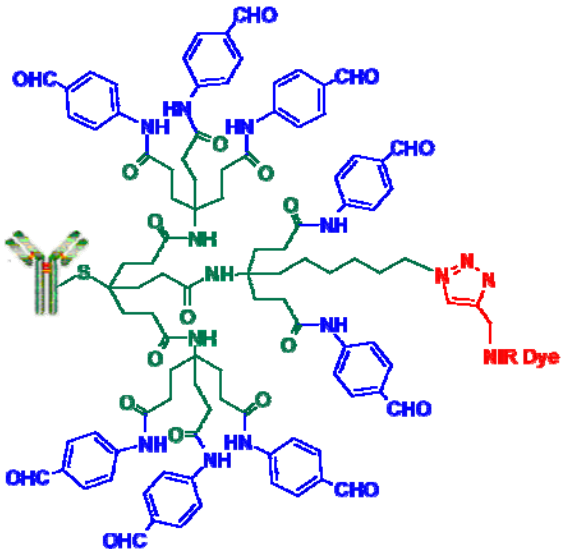

Figure 7.2 Dendritic nanoparticle carrying a NIR dye, eight aldehyde functionalities (for *in vivo* self assembly to hydrazine carrying Gd coupled dendrimer) and an antibody for targeting

Optimizations on the architecture of dendritic nanoparticle could include using longer linker for the attachment of the aldehyde functionality to the dendritic nanoparticle, in order to extend it more into the solvent environment. This could aid the self-assembly between aldehyde units on the primary nanoparticle and hydrazine units on the secondary nanoparticle. Once the pharmokinetic properties of the primary nanoparticle are established, *in vivo* murine trials will begin to assess the degree of

assembly at the tumor site. The ultimate goal of this project would seek to overcome the sensitivity problems[14] that have thwarted the development of targeted MRI contrast agents for early breast cancer detection, while exploiting the favorable biodistribution characteristics of smaller agents. Assembly of this nanomodular system should result in a large amplification of MR signal at the site due to higher concentration of contrast agent, and an increase in the rotational correlation time of the assembled system, allowing for earlier detection of abnormalities.

7.3.2 Dendronized norbornene polymers for targeted delivery devices

Implementation of our unique dendritic architectures with selective functional handles to dendronized polymers can bring about novel drug delivery devices.

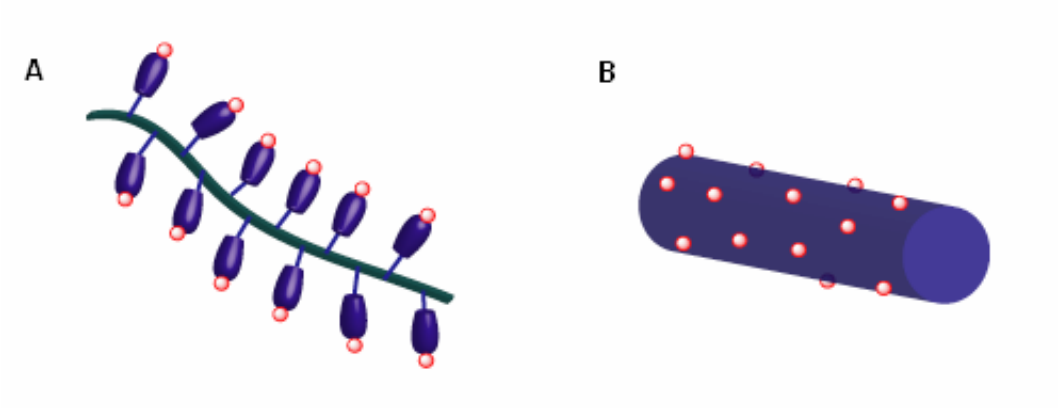

Figure 7.3 Dendronized norbornene polymers (A) stretched backbone by dendronization (B) self-assembled structure in water resulting in the formation of cylinders

For example, a poly(norbornene) dendronized polymer employing our dendrons with selective handles (Figure 7.3A), would likely self-assemble in water to form cylindrical nanostructures decorated with orthogonal functional handles on its surface, as shown in Figure 7.3B. The cylindrical structure can be used to encapsulate drugs much like dendrimers, and the orthogonal handles can be functionalized with targeting agents

for targeted delivery applications. It is known that due to their elongated shape and flow capabilities, cylindrical micelles are excellent candidates for drug delivery vehicles.[15-17] The majority of studies have used block copolymers for this purposes. Morphologies of dendronized polymers have been extensively studies by Percec and coworkers as discussed in Chapter 1.[24-26] However, few studies[18-19] have been reported on water soluble dendronized polymers and studies with selective orthogonal handles decorated dendronized polymers are non-existent.

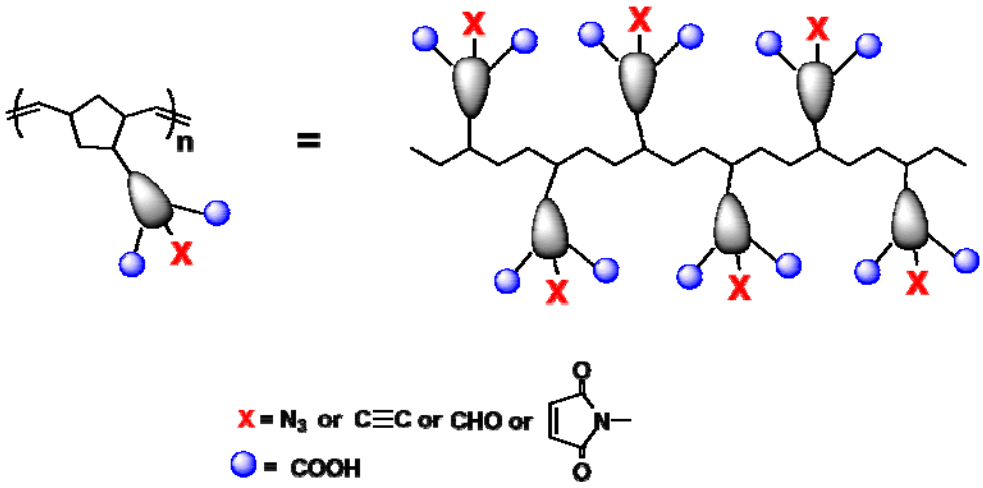

Figure 7.4 Dendronized norbornene polymer carrying a monofunctional dendron at every repeat unit each bearing an orthogonal handle (azide, alkyne, aldehyde or maleimide unit)

In our case, we could use poly(norbornene) as the polymer backbone with dendritic side-chains. Advantages of poly(norbornene) include well-defined polymers with low polydispersities, highly functional group tolerant polymerization methodology – ROMP and increased main chain rigidity when compared to vinyl based polymers.[21-23] We can synthesize our dendronized poly(norbornene) polymers shown in Figure 7.4 by the attachment of our dendrons carrying selective orthogonal handles (such as azide,

aldehyde, alkynes or maleimide) and containing protected acid functional groups to the norbornene monomer and its subsequent polymerization. The deprotection to the free acid on the dendronized polymer would likely yield a water soluble dendronized polymer (Figure 7.4). We could characterize these novel dendronized polymers in water as a function of temperature, pH and concentration. Detailed characterization of these dendronized polymers (which are likely to be cylindrical in shape due to their molecular architecture) using small angle x-ray scattering (SAXS) can help design well-defined materials. We could eventually aim to functionalize these materials using the orthogonal handles present on their periphery with biological moieties such as cell recognition units and antibodies for targeting or with imaging agents.

Additional optimizations later could include coupling poly(ethylene glycol) units to the dendritic side-chains for biocompatibility and the copolymerization with a monomer carrying pH or temperature sensitive side-chains such as acrylamides for devising a pH or temperature dependent drug release at tumor site.

7.3.3 Dendronized polymers as highly active recyclable catalysts

Metallated salen catalysts are among the most versatile catalysts for a diverse set of organic transformation and for the enantioselective synthesis of organic compounds, as detailed in Chapter 6. As reported in chapter 6,[13] the dendronization of insoluble resin supported cobalt-salen catalysts leads to higher catalytic activity evidenced by lower catalyst loading and faster reaction time when compared to directly immobilized catalysts. The enhanced reactivity was contributed to the high local concentration of catalysts immobilized on the dendron which facilitated the intermediate bimetallic transition state. Hence, it would be logical to extend the benefits of dendronization to

soluble polymer systems such as poly(norbornene), which has been extensively investigated by our group for development of metal-salen supported recyclable catalysts.[20-22]

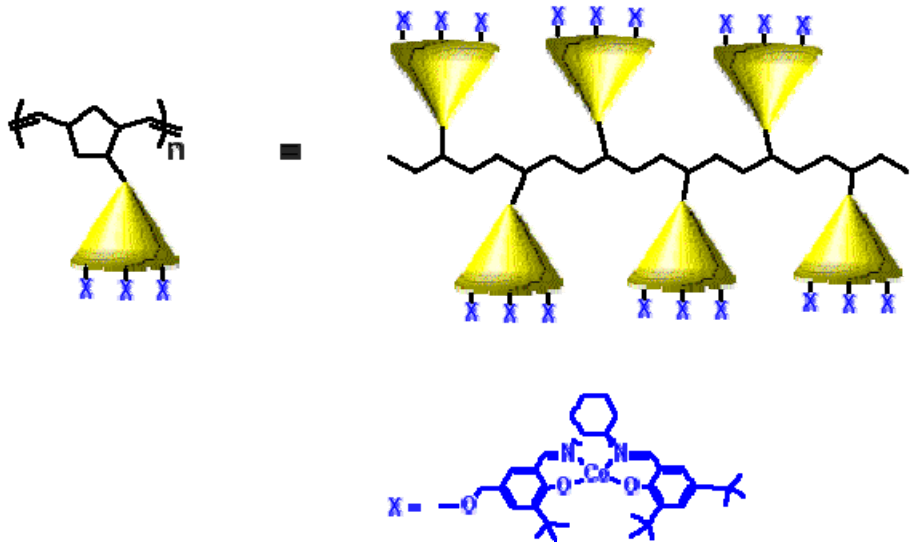

Figure 7.5 Poly(norbornene) dendronized Co-Salen supported catalysts

The extension of the dendronization to soluble polymer system should enable the development of highly efficient catalysts in terms of activity and reactivity. This can be achieved by attaching the G-1 dendron used in resin catalysis studies to the norbornene monomer followed by coupling of the salen moieties to the dendronized monomer and its polymerization. Metallation of salen centers with cobalt would result in dendronized salen catalysts, as shown in Figure 7.5. The catalytic activity and recyclability of the dendronized polymers for the hydrolytic kinetic resolution (HKR) of terminal epoxides could be monitored by chiral GC or HPLC analysis. If high catalytic activity is observed as expected from such dendronization compared to existing directly supported polymer

catalysts, this concept could be extended to other metal salen catalysts such as aluminum salen and to those catalytic reactions which utilize a bimetallic transition state.

7.3.4 Scaffold specific Raman information containing dendrimers as highly fluorescent and targeted biolabels for tumor imaging

The achievements of this thesis in defining methodology for the creation of dendrimers with selective orthogonal handles on their periphery as discussed in Chapter 3, in combination to the development of highly fluorescent dendrimers containing Raman labels for unambiguous scaffold specific information as discussed in Chapter 4, should be combined to enable the development of highly fluorescent, scaffold specific and antibody targeted biolabels for tumor imaging, as shown in Figure 7.6.

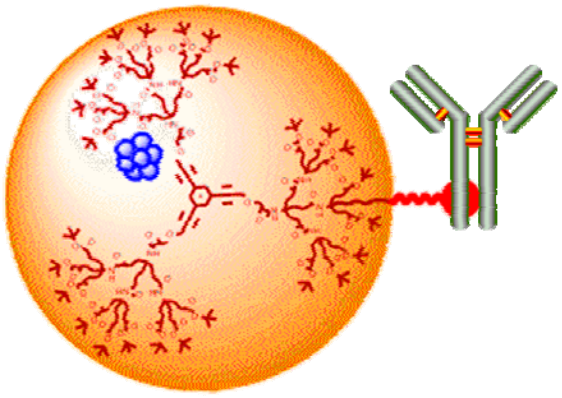

Figure 7.6 Scaffold specific Raman label and Ag nanodot containing dendrimers, as highly fluorescent biolabels coupled to an antibody specific to tumor receptor

This could be achieved by coupling one G-2 monofunctional dendron containing an orthogonal handle on its periphery (Chapter 3) and two G-2 nonfunctional dendron units to the aromatic core containing triple bonds (Chapter 4), to obtain a Raman label and a selective orthogonal handle containing dendrimer. This dendrimer could then be coupled to a screened monoclonal antibody using the complementary orthogonal

functional handle present on the dendrimer surface. The antibodies could be screened to different human carcinomas such as Cetuximab which targets the epidermal growth factor receptor (EGFR) over-expressed in many cancers or BrE3 which binds to glycosylated MUCI receptor, common in many epithelial cancers. This could then be followed by *in vitro* cell studies and flow cytometry studies to study the binding of the targeted dendrimer to tumor receptors and compared to a negative control. Ultimately, this could be monitored and studied in *in vivo* systems.

In conclusion, the work accomplished in the thesis has the potential to be applied for and overcome current drawbacks in many areas, particularly as shown for the field of biological sciences and catalysis. Continuing advances will further bolster the field of dendritic molecules, while realization of its full potential will be dependent upon its continued evolution. Based on the contributions made in this thesis, a variety of interesting future use of the methodologies and concepts developed here could be envisaged and remain to be seen.

7.4 References

1. Zhang, W.; Simanek, E. E. Dendrimers based on Melamine. Divergent and orthogonal, convergent syntheses of a G3 dendrimer. *Org. Lett.* **2000**, *2*, 643.

2. Bo, Z.; Schäefer, A.; Franke, P.; Schlüter, A. D. A facile synthetic route to a third generation dendrimer with generation-specific functional aryl bromides. *Org. Lett.* **2000**, *2*, 1645-1648.

3. Hawker, C. J.; Fréchet, J. M. J. Control of surface functionality in the synthesis of dendritic macromolecules using the convergent-growth approach. *Macromolecules* **1990**, *23*, 4726-4729.

4. Ganesh, R. N.; Shraberg, J.; Sheridan P. G.; Thayumanavan, S. Synthesis of difunctionalized dendrimers: an approach to main-chain poly(dendrimers). *Tetrahedron Lett.* **2002**, *43*, 7217.

5. Yoon, K.; Goyal, P.; Weck, M. Monofunctionalization of dendrimers with use of microwave-assisted 1,3-dipolar cycloadditions. *Org. Lett.* **2007**, *9*, 2051.

6. Goyal, P.; Yoon, K.; Weck, M. Multifunctionalization of dendrimers through orthogonal transformations. *Chem Eur. J.* **2007**, *13*, 8801.

7. Zheng, J.; Dickson, R. M. Individual water-soluble dendrimer-encapsulated silver nanodot fluorescence.*J. Am. Chem. Soc.* **2002**, *124*, 13982.

8. Zheng, J.; Dickson, R. M. High quantum yield blue emission from water-soluble Au8 nanodots. *J. Am. Chem. Soc.* **2003**, *125*, 7780.

9. Zheng, J.; Nicovich, P. R.; Dickson, R. M. Highly fluorescent noble-metal quantum dots. *Annu. Rev. Phys. Chem.* **2007**, *58*, 409.

10. Dulal, S.; Goyal, P.; Yoon, K.; Zheng, J.; Weck, M.; Dickson, R. M. Plasmon free single molecule Raman spectroscopy from dendrimer encapsulated fluorescent Ag-nanocluster. *Manuscript in Preparation.*

11. Annis, D. A.; Jacobsen, E. N. Polymer-supported chiral Co(Salen) complexes: synthetic applications and mechanistic investigations in the hydrolytic kinetic resolution of terminal epoxides. *J. Am. Chem. Soc.* **1999**, *121*, 4147.

12. Baleizao, C.; Garcia, H. Chiral salen complexes: an overview to recoverable and reusable homogeneous and heterogeneous catalysts. *Chem. Rev.* **2006**, *106*, 3987.

13. Goyal, P.; Zheng, X.; Weck, M. Enhanced cooperativity in hydrolytic kinetic resolution of epoxides using poly(styrene) resin-supported dendronized Co-(Salen) catalysts. *Adv. Synth. Catal.* Submitted.

14. Aref, M.; Brechbiel, M.; Wiener, E. C. Identifying tumor vascular permeability heterogeneity with magnetic resonance imaging contrast agents. *Investigative Radiol*. **2002**, *37*, 178.

15. Wang, X.; Guerin, G.; Wang, H.; Wang, Y.; Manners, I.; Winnik, M. A. Cylindrical block copolymer micelles and co-micelles of controlled length and architecture. *Science* **2007**, *317*, 644.

16. Lee, C. C.; Yoshinda, M.; Fréchet, J. M. J.; Dy, E. E.; Szoka, F. C. In vitro and in vivo evaluation of hydrophilic dendronized linear polymers. ***Bioconjugate Chem.*** **2005***, 16*, 535.

17. Li, W.; Zhang, A.; Schlueter, A. D. Efficient synthesis of first and second generation, water soluble dendronized polymers. *Macromolecules* **2008**, *41*, 43.

18. Zhu, B.; Han, Y.; Sun, M.; Bo, Z. Water soluble dendronized polyfluorenes with an extremely high quantum yield in water. *Macromolecules* **2007**, *40*, 4494.

19. Zhang, Z-B.; Teng, Y-H.; Freas, W.; Mohanty, D. K. Unimolecular amphiphilic nanocontainers based on dendronized linear polymers. *Macromol. Rapid Commun.* **2006**, *27*, 626.

20. Zheng, X.; Jones, C. W.; Weck, M. Engineering polymer-enhanced bimetallic cooperative interactions in the hydrolytic kinetic resolution of epoxides. *Adv. Synth. Catal.* **2008**, *350*, 255.

21. Madhavan, N.; Weck, M. Highly active polymer-supported (Salen)Al catalysts for the enantioselective addition of cyanide to α,β-unsaturated imides. *Adv. Synth. Catal.* **2008**, *350*, 419.

22. Holbach, M.; Zheng, X.; Burd, C.; Jones, C. W.; Weck, M. Modular approach for the development of supported, monofunctionalized, Salen catalysts. *J. Org. Chem.* **2006**, *71*, 2903.

23. Zheng, X.; Jones, C. W.; Weck, M. Ring-expanding olefin metathesis: a route to highly active unsymmetrical macrocyclic oligomeric Co-Salen catalysts for the hydrolytic kinetic resolution of epoxides. *J. Am. Chem. Soc.* **2007**, *129*, 1105.

24. Percec, V.; Ahn, C. H.; Cho, W. D.; Jamieson, A. M.; Kim, J.; Leman, T.; Schmidt, M.; Gerle, M.; Moeller, M.; Prokhorova, S. A.; Sheiko, S. S.; Cheng, S. Z. D.; Zhang, A.; Ungar, G.; Yeardley, D. J. P. Visualizable cylindrical macromolecules with controlled stiffness from backbones containing libraries of self-assembling dendritic side groups. *J. Am. Chem. Soc.* **1998**, *120*, 8619.

25. Percec, V.; Cho, W. D.; Mosier, P. E.; Ungar, G.; Yeardley, D. J. P. Structural analysis of cylindrical and spherical supramolecular dendrimers quantifies the concept of monodendron shape control by generation number. *J. Am. Chem. Soc.* **1998**, *120*, 11061.

26. Percec, V.; Ahn, C. H.; Ungar, G.; Yeardley, D. J. P.; Moller, M.; Sheiko, S. S. Controlling polymer shape through the self-assembly of dendritic side-groups. *Nature* **1998**, *391*, 161.